Sorptive separation of phenolic compounds from wastewater

by

Shuixiu Lai

A thesis

presented to University of Waterloo

in fulfilment of the

thesis requirement for the degree of

Doctor of Philosophy

in

Chemical Engineering

Waterloo, Ontario, Canada, 2017

Examining Committee Membership

The following served on the Examining Committee for this thesis. The decision of the Examining Committee is by majority vote.

External Examiner	Dr. Shafiq Alam Associate Professor
Supervisor	Dr. Xianshe Feng Professor
Internal Member	Dr. Ali Elkamel Professor
	Dr. Yuning Li Associate Professor
Internal-external Member	Dr. Sigrid Peldszus Research Associate Professor

AUTHOR'S DECLARATION

I hereby declare that I am the sole author of this thesis. This is a true copy of the thesis, including any required final revisions, as accepted by my examiners.

I understand that my thesis may be made electronically available to the public.

Abstract

This study explores the potential of using PEBA as a sorbent for removing phenolic compounds from wastewater. The sorption isotherms of phenol, 4-chlorophenol (4-CP), 4-nitrophenol (4-NP), 4-methylphenol (4-MP) and catechol from their respective single solute solutions were studied based on the Linear, Langmuir and Freundlich models. The Freundlich model was shown to be suitable to represent the equilibrium sorption of all the phenolic compounds in the PEBA sorbent, and the sorption capacity of these phenolic compounds in PEBA is in the order: catechol<phenol<4-MP<4-NP<4-CP. Thermodynamic analysis revealed that phenol sorption in PEBA was a spontaneous exothermic process.

The sorption kinetics was studied using PEBA sorbent in the form of a flat membrane with well-defined dimensions to help identify the mechanism and rate controlling step of the sorption process. The kinetic data were fitted with the pseudo-first and -second order models as well as the diffusion model. The pseudo-second order model was shown to fit the experimental data better than the pseudo-first order model, and an oversight in the model fitting with regard to equilibrium sorption capacity in prior work was discussed and corrected. Sorption of phenol, 4-CP, 4-NP, 4-MP and catechol in PEBA was represented by the pseudo-second order model, while mass diffusion inside the sorbent was not negligible for thick membranes.

Multi-solute sorption isotherms and kinetics were determined for binary and quinary solute systems. The competitive Freundlich model and the IAST model were fitted to the equilibrium data. It was found that the competitive Freundlich model was adequate to represent isotherms for all binary solute systems studied; however, there was a considerable deviation between the model predictions and the experimental data in the quinary solute

system. Strongly sorbed solutes tended to inhibit the sorption of weakly sorbed solutes. The sorption competition was shown to affect the sorption kinetics of individual solutes, and such effect was found to be related to the molecular size of the sorbate component and its affinity to the sorbent.

Chemical elution, thermal regeneration and vacuum-assisted thermal regeneration were proposed and studied for regeneration of PEBA sorbent exhausted with the phenolic compounds. Ethanol, methanol and NaOH solution were all effective regenerants for the sorbent, and no significant change in the sorption characteristics was observed for a number of sorption-regeneration cycles. Thermal regeneration (90°C for 2 h) was also effective for regenerating PEBA exhausted with phenol and 4-MP. When exhausted with 4-MP, the PEBA sorbent could be regenerated using vacuum-assisted thermal regeneration (80°C for 3 h at a vacuum pressure of 5 kPa), and highly concentrated solutions ($\approx$70,000 ppm) of 4-MP were collected.

PEBA fibres were prepared and immobilized in a packed-bed for column sorption studies. The effects of inlet feed concentration, flow rate, fibre diameter and flow interruption on the breakthrough were evaluated. The BDST, Clark and Yoon-Nelson models were fitted to the experimental data. It was shown that the BDST model described the breakthrough curve adequately when the solute in the effluent was at lower concentrations ($0<C/C_0<0.15$); while over a broader range of effluent concentration ($0<C/C_0<0.90$), the Clark model fitted the breakthrough curve better than Yoon-Nelson model. The sorption capacities of phenolic compounds in the column were found to be comparable to those determined in batch sorption studies. Complete regeneration of the exhausted column was achieved using NaOH and there was no change in breakthrough characteristics after column regeneration.

Acknowledgements

First and foremost I want to thank my supervisor Dr. Xianshe Feng. I could not have accomplished this tough journey without his help. I appreciate all his contributions of time, ideas, and funding to this study. I gained insight into many fundamental theories about thermodynamics and kinetics in this thesis through numerous discussions with him. His guidance, patience and immense knowledge helped me in the research and in writing this thesis. I would like to express my sincere appreciation to him for enlightening me the way of critical thinking and the attitude of "steady and slow" during research. This is not only beneficial to my academic life but will also be beneficial to my personal life in the future. Thanks again for his continuous support and encouragement during the past four years, and I could not have imagined having a better supervisor for my PhD study.

Besides my supervisor, I would like to thank my committee members of this thesis: Dr. Shafiq Alam, Dr. Sigrid Peldszus, Dr. Yuning Li and Dr. Ali Elkamel, for their valuable advices, insightful comments and challenging questions which motivated me to explore my research from different perspectives.

My sincere thanks also goes to Dr. Gil Francis, who did some preliminary work relating to this project; to Dr. Prodip Kundu, who helped me with the FORTRAN programming in Chapter 4; to Mr. Ralph Dickhout, who provided enormous help in the operation of the High Performance Liquid Chromatography.

I would like to extend my thanks to my fellow lab mates Dihua Wu, Boya Zhang, Yifeng Huang, Yijie Hu, Ying Zhang, Muhammad Usman Farooq, Bo Qiu, Aoran Gao and Jingjing Zhang for their company and emotional support. Thanks for their help in some of my experimental setups, and for the inspirational discussions we had over the past four years.

We were working together as colleagues, but we also had a lot of fun together as friends. I feel lucky to have the opportunity to work in such a friendly lab.

Last but not least, I thank for my dearest parents, my younger brother and friends I met in Canada, who support me through thick and thin during the past few years. Their unconditional love is my strength when I am weak. PhD study is a long and tough journey, without their support it would not be possible for me to conduct this research and complete this thesis. This thesis is dedicated to them.

Table of Contents

Chapter 3

Equilibrium study of sorption of phenolic compounds in PEBA: single-solute systems..62

Chapter 4

Kinetic study of sorption of phenolic compounds in PEBA: single-solute systems 85

List of Figures

List of Tables

List of Symbols

a_{ij}	The competitive effect of solute component j on i
A	The model parameter in the Clark model
C	Boundary layer (mmol/g)
C_0	Initial concentration of sorbate in solution (mmol/L)
C_{ad}	Concentration of the sorbate in the solid phase at equilibrium (mmol/L)
C_b	The sorbate concentration in the effluent (mmol/L)
C_e	Concentration of sorbate in the solution at equilibrium (mmol/L)
C_e'	Instantaneous solute concentration
C_i	The liquid phase concentration of solute i in the multi-solute system
$C_i{}^0$	The liquid phase concentration of solute i in the single solute system
C_s	Concentration of the standard reference solution (mmol/L)
C_t	Concentration of sorbate in solution at time t (mmol/L)
D_c	Intraparticle diffusivity (m^2/min)
D_z	Dispersion coefficient (cm^2/min)
D	The diameter of the fibre diameter (μm)
E_a	Activation energy (J/mol)
F	The volumetric flow rate of the feed solution (mL/min)
k_1	Pseudo-first order rate constant (min^{-1})
k_2	Pseudo-second order rate constant ($g \cdot mmol^{-1} \cdot min^{-1}$)
k_a	Rate constant of adsorption
k_d	Rate constant of desorption

k_i	Intraparticle diffusion constant (mmol·g^{-1}·min$^{-1/2}$)
k_{BD}	The kinetic rate constant of the BDST model (L·mg^{-1}·min^{-1})
k_{Th}	The kinetic rate constant of the Thomas model (L·mg^{-1}·min^{-1})
k_{YN}	The kinetic rate constant of the Yoon-Nelson model (min^{-1})
K_d	Distribution constant
K_F	Freundlich constant($(mol)^{1-1/n}.g^{-1}.L^{1/n}$)
K_H	Henry's sorption constant (L/g)
K_L	Langmuir constant (L/mmol)
l	Thickness of the membrane (m)
M	The mass of the sorbent (g)
$1/n$	Heterogeneity factor in the Freundlich model
N_0	The sorption capacity of the sorbate in a column bed (mg/L)
Q_T	The total uptake of solute by the solid phase in the multi-solute system
Q_e	The amount of sorbate sorbed per mass sorbent at equilibrium (mmol/g)
Q_i	The sorption uptake of solute component i in the multi-solute system
$Q_i{}^0$	The sorption uptake of solute component i in the single-solute system
Q_m	The maximum sorption capacity (mmol/g)
Q_t	The amount of sorbate sorbed per mass sorbent at time t (mmol/g)
r	Model parameter in the Clark model
R	Universal gas constant (J·mol^{-1}·K^{-1})
t	Time (min)
T	Temperature (K)

u	The superficial velocity (cm/min)
V_{total}	The total volume of the effluent (L)
$x_i\,^{(eq)}_{(I)}$	Mole fraction of substance (i) in phase (I)
$x_i\,^{(eq)}_{(II)}$	Mole fraction of substance (i) in phase (II)
z_i	The mole fraction of solute component i in the sorbent phase
Z	The distance to the column inlet (cm)
α_e	Activity of sorbate in the solution at equilibrium
α_s	Activity of adsorbed sorbate in the sorbent at equilibrium
γ_e	Activity coefficient of sorbate in solution at equilibrium
γ_s	Activity coefficient of sorbed sorbate in the sorbent at equilibrium
ΔG^0	Standard Gibbs free energy change (J/mol)
ΔH^0	Standard Enthalpy change (J/mol)
ΔS^0	Standard Entropy change (J·mol^{-1}·K^{-1})
θ	Fraction of adsorption sites covered by adsorbate molecules
τ	The time required to obtain 50% breakthrough (min)
π	The spreading pressure (J/cm^2)

Chapter 1

Introduction

1.1 Background

Phenols and substituted phenols are common pollutants in wastewater. They can cause unpleasant taste and odour in drinking water. In addition, they are harmful to human health due to their toxicity and carcinogenicity [1]. Therefore, effective methods must be developed for economical removal of these compounds from wastewater.

Numerous technologies have been employed to remove phenol and its derivatives from wastewater, including the conventional methods of distillation and extraction [2], chemical oxidation [3], biodegradation [4], and membrane separation [5]. Of these methods, sorption appears to be a suitable process based on overall separation performance. It is effective for removing a large variety of compounds, and has the advantages of easy operation and high efficiency to treat low-concentration pollutants. Moreover, sorption is generally reversible, and the adsorbent can be regenerated for reuse.

Accordingly research has been undertaken to explore suitable adsorbents for phenolic compounds. Activated carbon has been widely used as an adsorbent because of its known effectiveness. However, the high regeneration cost of activated carbon has motivated research to seek other better adsorbents for phenolic compounds. Polymeric adsorbents have attracted a lot of attention in recent years due to its good regeneration performance. Poly (ether block amide) (PEBA) is a copolymer used as membrane materials in pervaporation separation and shows excellent selectivity to phenol [6, 7]. PEBA 2533 (short D hardness 25)

has a polyether content as high as 80 wt.%, which has been proven to have good selectivity to phenol [5]. Examining the good pervaporative performance of PEBA membranes for phenol separation revealed that PEBA 2533 has excellent affinity to phenol, and it is thus expected to be an effective adsorbent for phenolic compounds.

The evaluation of the sorbent performance is typically based on the equilibrium sorption capacity, sorption rate and regeneration properties. Equilibrium sorption capacity, indicating the affinity of the solute to the sorbent, is of particular interest in the fixed-bed operation design. Numerous studies have examined the equilibrium adsorption from a thermodynamic point of view, but many isotherm studies ignored its connection to the sorption kinetics [8-11]. Apart from sorption capacity, sorption kinetics of a given sorbent is also of great importance in the sorption system design. In addition, the analysis of the sorption kinetics can help understand sorption mechanism and the rate-controlling step of the sorption process, which will provide an insight into sorption performance. Tien [12] pointed out many articles on adsorption over the past few decades have just focused on applying conventional models to fit the experimental data but failed to interpret the equilibrium data or kinetic data obtained with sorbent characteristics and sorption mechanism. As a result, the "good data fit" does not have much significance.

Sorption can either be a surface-based process (i.e., adsorption) or involve the bulk of the sorbent phase (i.e., absorption). The surface-based physical forces of interfacial imbalance and attraction (e.g., van der Waals) may play an important role in the adsorption process. However, after sorbate molecules are bound to the surface, they may gradually penetrate the solid phase to reach the interior uniformly, forming a solid "solution" [13].

Thus sorption is a complicated process and it is significantive to identify the sorption mechanism by appropriate experimental design.

There are much fewer studies about sorptive behaviour of phenolic compounds in multi-solute systems than that in single-solute systems. It is because compared with the single-solute isotherms, the multi-solute isotherm data require a tedious and time consuming procedure to obtain experimentally [14]. In the latter case, one phenolic compound is removed in the presence of other compounds. Thus it is important to investigate the competitive sorption behaviour among the phenolic compounds in multi-solute systems. The presence of one species is expected to affect both the equilibrium uptake capacity and the uptake rate of other species. In addition, the competitive sorption behaviour in multi-component systems is also related to the sorption behaviour in their single-solute systems. Thus, the study of multi-component system is expected to provide an insight into the sorption process that is impossible to get in single-solute systems.

The regeneration property of a sorbent is of particular interest from an economic point of view. One popular method for regeneration of sorbents spent by phenolic compounds is chemical elution. The eluting reagent can either be an organic solvent (e.g., acetone [15, 16] , methanol [15-18], and ethanol [16, 17, 19, 20]) or reactive reagents (e.g., sodium hydroxide [15, 16, 18, 21, 22]). Chemical regeneration has an advantage of in-situ operation (i.e., no need for transporting sorbents), but it ends up with a solution consisting of the eluting reagent and desorbed sorbate. An alternative method is thermal regeneration where no extra chemical are produced, but the high temperatures ($>500^0$C) required are often a problem for thermal regeneration of activated carbon exhausted by phenolic compounds [23-25]. The high regeneration temperature not only increases the operating cost but also

causes damages to the surface structure of the sorbent, resulting in a decrease in the sorption capacity of the regenerated sorbent. Therefore, it would be a great asset of the sorbent if low regeneration temperature is technically feasible in the thermal regeneration process.

Compared with the batch sorption studies, fixed-bed operation can provide additional information for industrial applications. Dynamic adsorption of phenolic compounds in a fixed-bed has been studied extensively, but only in very few cases were the results of column studies interpreted with sorption kinetics and sorption mechanism obtained from batch studies. In addition, the assumptions in the model development were often ignored in the fixed-bed sorption modelling (e.g., concentration range).

1.2 Research objectives

The objective of this study was to explore the potential use of PEBA 2533 as a new sorbent for phenolic compounds by evaluating the sorptive behaviour of phenol, 4-chlorophenol (4-CP), 4-nitrophenol (4-NP), 4-methylphenol (4-MP) and catechol in PEBA 2533. The research consisted of the following tasks:

(1) To conduct batch sorption studies to investigate the sorption isotherm and sorption kinetics in single-solute systems (aqueous solutions containing one phenolic compound).

(2) To conduct sorption of phenolic compounds by PEBA 2533 in multi-solute systems to investigate the effects of solute-solute interactions on the sorption isotherms and kinetics.

(3) To examine the regeneration performance of the PEBA sorbent by regenerating the exhausted sorbent via different means, including solvent elution, chemical elution, and thermal regeneration.

(4) To perform sorption of phenolic compounds in a fixed bed configuration and to investigate the effects of experimental conditions (i.e., inlet concentration, flow rate, and sorbent size) on the breakthrough of the column.

1.3 Thesis structure

This thesis consists of eight chapters and they are organized as follows:

Chapter 1 presents the background of this study, including an overview of research that has been done in the field, and additional work that should be investigated further. The research objectives of this study are also presented.

The literature review is provided in Chapter 2. It provides an introduction of the development of technologies on removing phenolic compounds from wastewater, and a review of sorbent development for phenolic compound removal. Basic sorption characteristics (e.g., single-solute sorption isotherm, multi-solute sorption isotherm, sorption kinetics in single-and multi-solute systems) and fixed-bed sorption behaviour are briefly introduced together with modelling work for the various aspects. The regeneration methods of sorbents exhausted by phenolic compounds have also been discussed.

In Chapter 3, equilibrium sorption studies were carried out to determine the sorption isotherms of phenol, 4-CP, 4-NP, 4-MP and catechol in PEBA 2533 in single-solute systems. The isotherm data was analyzed by the Linear, Langmuir and Freundlich models. In addition, thermodynamic parameters such as standard Gibbs free energy change, enthalpy change and entropy change were determined to reveal the nature of the sorption system.

In Chapter 4, sorption kinetics was investigated for the single-solute systems. In order to identify the sorption mechanism, sorption kinetics was compared between two series of

PEBA membranes: one series with the same surface area but different thicknesses, and the other series with the same weight but different surface areas. The kinetics data were fitted to the pseudo-first and second order models and diffusion model, and a modified approach in determining the kinetic parameters was used to correct an oversight in data fitting that has been used commonly in the literature.

Chapter 5 presents the results of equilibrium and kinetic studies in multi-solute systems. The competitive effects among the solutes on sorption capacity and sorption rate were investigated. The multi-solute sorption data were fitted to the competitive Freundlich model and ideal adsorbed solution theory (IAST) model. The kinetic data were fitted to the modified pseudo-second order model and diffusion model for the multi-solute systems.

Chapter 6 presents the regeneration performance of PEBA 2533 exhausted by phenolic compounds. The spent sorbent was regenerated by elution with methanol, ethanol, and 0.15 mol/L sodium hydroxide solutions, respectively. In addition, thermal regeneration and vacuum-assisted thermal regeneration method were also applied to regenerate the spent PEBA sorbent. The efficiency of the regeneration was evaluated by comparing the sorption isotherms of phenolic compounds in pristine and regenerated PEBA sorbent.

The fixed-bed sorption of phenolic compounds in PEBA 2533 was studied in Chapter 7. The effects of inlet concentration, inlet flow rate, sorbent size and feed interruption on the sorption breakthrough were investigated, and the BDST, Clark and Yoon-Nelson models were employed to analyze the experimental data. Continuous sorption-regeneration runs were carried out to evaluate the performance of column regeneration.

General conclusions and original contributions of this research are summarized in Chapter 8, where recommendations for future work are also proposed. Figure 1.1 shows the organization of this thesis.
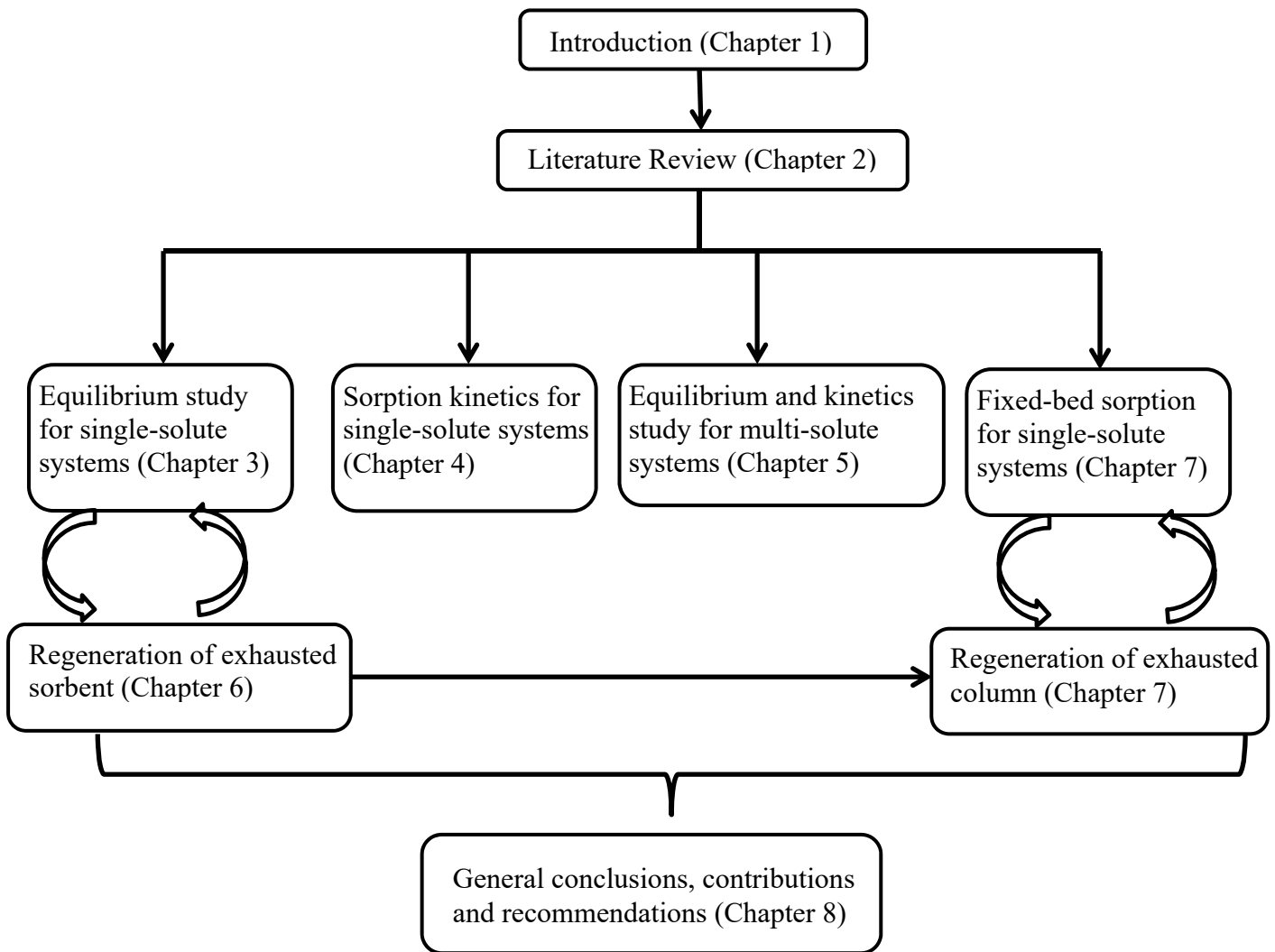
Figure 1.1 Thesis structure in terms of chapters and content relevance

Chapter 2

Literature review

2.1 Removal of phenolic compounds from wastewater

Phenols and their derivatives constitute a very large group of organic pollutants in the environment. Phenolic compounds discharged to aqueous systems produce unpleasant taste and odour. In addition, most phenolic compounds are carcinogens. Due to their toxicity at low concentrations, many phenolic compounds have been designated as priority pollutants by the US Environmental Protection Agency and European Union Drinking Water Directive 80/778/EC [26]. Because of the negative effect of phenolic compounds on human health, there are stringent regulations on the discharge of phenol-containing wastewater.

Industrial sources of phenolic compounds include oil refineries, petrochemical units, and chemical plants that are producing phenolic resins, including phenol-formaldehyde resin, a low-cost thermosetting resin widely used in plywood adhesive, construction, automotive and appliance industries [27]. Phenolic derivatives are also widely used as intermediates in the synthesis of insecticides, herbicides and some medical products [1]. Thus phenol and its derivatives are among the most prevalent organic pollutants in the industrial wastewater [28].

Due to widespread uses in many industries, phenolic wastewater has become a great concern in environment. Many methods have been employed to remove phenolic compounds from aqueous solutions.

2.1.1 Destruction technologies for removal of phenolic compounds

One process to degrade phenolic compounds is oxidation, including chemical oxidation, electro-oxidation and photo-oxidation.

In chemical oxidation, chemical oxidants such as ozone [29, 30] and hydrogen peroxide [31] may be used to oxidize phenolic compounds. The high generation cost of ozone and its low solubility in water limit the wide application of the ozonation process. Thus ozonation is usually used as a pretreatment to biodegrade phenolic compounds [32]. H_2O_2 is more cost effective than ozone, but the oxizability of H_2O_2 is relatively low, and the fenton reagent [31] or heterogeneous fenton-like heterogeneous catalysts [33] are often employed to enhance the kinetics by introducing hydroxyl radicals, which can effectively oxidize organic compounds. Recent studies show that the presence of catalysts and the use of a combination of different oxidation methods can improve the removal efficiency of phenolic compounds [34, 35].

Electro-oxidations include direct anodic electro-oxidation and indirect electro-oxidation. In direct anodic electro-oxidation, hydroxyl radicals are produced in the oxide anode and then used to degrade the phenolic compounds [36]. In an indirect electro-oxidation process, chemical oxidants (e.g., ozone, chlorine, and hydrogen peroxide) are electrically generated and then used to destroy organic compounds. For instance, in the electro-fenton process [37], hydrogen peroxide is generated from dissolved oxygen in aqueous solutions, and Fe (II) is added as catalyst to oxidize the organic pollutants.

In a photo-oxidation process, UV irradiation in the presence of a photocatalyst induces the generation of various oxygen-containing radicals, which can effectively decompose the organic compounds. The combination of photo-oxidation and chemical

oxidation can enhance the oxidizability. Dixit et al. [38] reported the maximum degradation of phenol and 4-chlorophenol is 74.6% and 79.8%, respectively, using a combined $UV/H_2O_2/TiO_2$ system.

Besides oxidation, another destruction technology for phenolic compounds is biodegradation. Due to the toxicity of phenolic compounds to micro-organisms, it is difficult to apply the biodegradation process to industrial wastewater streams containing high concentrations of phenolic compounds. However, phenolic compounds can be converted to less harmful or harmless compounds by microorganisms at low concentrations. Tobajas et al. [4] used comamonas testosterone to biodegrade phenol (80-240 mg/L) and 4-chlorophenol (15-30 mg/L).

A potential practical problem with oxidization is the high operating cost, because either expensive chemicals or reactors are required in oxidation processes. Biodegradation is cost effective, but the toxicity of phenolic compounds limits its wide application. In addition, phenolic compounds cannot be recovered in oxidation processes, and secondary pollution is also possible in some cases.

2.1.2 Separation technologies for removal of phenolic compounds

An alternate process is to separate phenolic compounds from wastewater, including distillation, extraction, adsorption and membrane separation processes. Steam distillation is a traditional method based on the volatility of phenolic compounds [27]. Phenol-water solutions have a minimum azeotrope, at 9.21% phenol (w/w), corresponding to a molar fraction of 0.019, T_{eb} 94.5°C at 1 atm. [27]. Tumakaka et al. [39] reported the liquid-vapour-solid phase diagram for water-phenol system. Ghizellaoui and Meniai [40] compared the equilibrium curve for phenol-water system with and without the presence of salts. An

advantage of steam distillation for phenol recovery is that no other contaminants will be generated, but the energy consumption in this process is relatively high. Therefore, it is useful mainly for the treatment of phenolic wastewater at high concentrations.

Another widely used method to treat high concentration phenolic water is extraction. Effective extractant for phenolic compounds include kerosene [2], alcohols [41], tributyl phosphate [26], trialkylphosphine oxide [42] and trialkylphosphine sulphide [43]. The extraction process is advantageous for treating high concentration phenolic wastewater (over 3000 mg/L) [41]. Phenolic compounds are first recovered by organic solvents, and then the residual low concentrated phenolic stream can be treated by the biological process [27]. The main problem with the extraction process is the recovery of the organic extractant. In recent years, membrane extraction technique is shown to be an attractive alternative to conventional liquid-liquid extraction process because the analytes can be isolated in a continuous fashion [1]. For instance, supported liquid membranes combine extraction, diffusion, stripping and regeneration in one single step [26]. When an emulsion liquid membrane is used, the extraction and stripping occur simultaneously in the same stage. Park et al. [44] used a novel emulsion liquid membrane to extract phenol and substituted phenols at relatively high concentrations (1000 ppm).

Membrane pervaporation is recently developed to remove phenolic compounds from wastewater [45]. Generally, the pervaporation process is carried out at vacuum at permeate side, and the permeated vapour is collected by a cold trap. Polymers such as ethylene-propene-diene terpolymer [46], polyurethane [47], PEBA and polydimethysiloxane [48] have been extensively used for membrane materials. Of these membranes, PEBA membranes have shown good phenol permeability [5, 49, 50].

2.2 Sorption of phenolic compounds from wastewater

Sorption is another method to separate organic pollutants from wastewater. Compared to other processes, sorption has the advantages of easy operation, high efficiency, and no secondary pollution. Sorption is especially useful to treat dilute streams.

2.2.1 Sorption of phenolic compounds by activated carbon

Due to its porous structure which results in a large specific surface area, activated carbon has a high capacity to adsorb phenolic compounds. In addition, activated carbon is easy to modify to improve its property, and thus activated carbon is one of the most effective adsorbents for water purification. Typical activated carbons possess high surface area in the range of 600-2000 m^2/g [51].

Commercially available activated carbons are usually derived from relatively expensive materials such as coconut shell, wood or coal [52]. In order to reduce the production cost, cheaper waste materials including straw [51], sawdust [53], rice husk [54] and sewage sludge [55] have also been used to produce activated carbon. Aygün et al. [56] produced activated carbon from four different kinds of agricultural wastes, and the attrition rate of the carbon was reported to be 10%. In addition, the regeneration process of saturated carbon is usually difficult, incomplete, and results in a substantial loss of the adsorbent, especially for powdered activated carbon. Thus saturated carbons are usually disposed of or burnt in furnaces. The high generation cost and unsatisfactory regeneration property of activated carbon has motivated many researchers to search for alternative economic sorbents. Table 2.1 lists some studies about the adsorption of phenolic compounds on activated carbons.

2.2.2 Sorption of phenolic compounds by minerals

Clay materials possess a layered structure, high surface area and porosity. Bentonite, montmorillonite, kaolinite and diatomite have attracted attention because of their abundance, low prices and their potential for ion-exchange. The market price of montmorillonite is considered to be 20 times cheaper than that of activated carbon [57]. Because of their surface characteristics, clay minerals can be chemically modified to improve their physical and chemical properties. Wu et al. [58] used both inorganic and organic-pillared montmorillionite to adsorb phenol, and they found that the adsorption capacity depended on the micropore structure and surface components of montmorillionite and that using the modified clay with surfactant can improve its adsorption capacity significantly. Organophilic bentonites can be produced by exchange of inorganic cations (e.g., Na^+, Ca^{2+} and Mg^{2+}) which are naturally present in the mineral surface of bentonite with organic cations (i.e., NH^{4+}) [59, 60].

Zeolites have a three dimensional framework with negatively charged lattices. Although their phenol removal efficiency may not be as good as that of clay minerals, the advantages of zeolites include the lower price and selectivity to certain pollutants because of the rigid porous structure [52]. It was reported that zeolites must be hydrophobic and have a high Si/Al ratio in order to selectively adsorb phenol from water [61]. Su et al. [62] studied the adsorption of phenol using zeolite-templated carbon with different pores and surface structures. The adsorption capacity was increased after thermal treatment under nitrogen because of the carboxylic group. Kuleyin [63] studied the adsorption behaviour of phenol and 4-chlorophenol on zeolite modified by hexadecyltrimethyl ammonium bromide and benzyltetradecyl ammonium bromide.

Siliceous minerals (i.e., alunite, perlite, and dolomite) are also used as adsorbent for phenolic compounds. Dolomite has an ideal formula of $CaMg(CO_3)_2$. Although the adsorption properties of the raw dolomites are not significant, they can be used as effective adsorbents for phenolic compounds after thermal treatment [64]. Alunite is one mineral of the jarosite group and contains approximately 50% SiO_2 [52]. Raw alunite doesn't have good adsorption properties either, but calcined alunite has been shown to be effective for adsorption of organic pollutants. Perlite is an organic siliceous volcanic glassy rock with an amorphous structure. The adsorption of phenol and 4-chlorophenol on chitosan-coated perlite was investigated by Kumar et al. [65] The adsorption of pentachlorophenol on dolomite was studied by Marouf et al. [64] via batch processes.

A summary of the studies using minerals as adsorbents for capturing phenolic compounds is listed in Table 2.2.

2.2.3 Sorption of phenolic compounds by biological materials

Agricultural wastes (e.g., sawdust, rice husk, and bark) are used as adsorbents to remove phenolic compounds from wastewater. Mohamed et al. [66] used sawdust to prepare activated carbon by chemical activation with sulfuric acid. These carbons were used to remove phenol, catechol, resorcinol and hydroquinone from waster. It was reported that their adsorption capacity followed the order of phenol>hydroquinone>resorcinol>catechol. Dutta et al. [67] treated sawdust with phosphoric acid, and the sawdust was then charred in a muffle furnace at 500^0C, followed by cooling and washing with dilute NH_3 solution to neutralize the acid. The charred saw dust was used to adsorb 4-nitrophenol. Kalderis et al. [54] impregnated rice husk with $ZnCl_2$ and carbonized the rice husk at 700^0C to be used as an adsorbent for

phenol. Vazquez et al. [68] treated pinus pinaster barks with formaldehyde in an acid medium at 50°C to remove phenol from water.

Industrial wastes (e.g., fly ash, red mud and sludge) have also been considered as adsorbents for organic pollutants because of their availability and low cost. Chaudhary and Balomajumder [69] treated coal fly ash with H_2SO_4 and impregnated with aluminum sulphate at 70°C and pH=5, and the fly ash was then used to remove phenol from water. Tor et al. [70, 71] compared the adsorption capacity of phenol on neutralized and acidic activated red mud, and it was found that the acid activated red mud had a larger adsorption capacity for phenol. Monsalvo et al. [55, 72] produced different activated carbons from sewage sludge to remove phenol from wastewater.

Agricultural and industrial wastes are readily available in large quantities. Although the cost of raw materials is very low, chemicals and the high operating temperature required in the treatment process increase the process cost and limit its application.

Biological materials such as chitin, chitosan, peat and other biomass can be used as chelating agents to remove phenolic compounds from aqueous solution. Bioadsorbents contain functional groups (e.g., hydroxyl, carboxyl, and amino groups) which can form complexes with phenolic compounds. Li et al. [73] chemically modified chitosan with salicylaldehyde and β-cyclodextrin to adsorb phenol, 4-nitrophenol and 4-chlorophenol. Compared with raw chitosan, the β-cyclodextrin modified chitosan exhibited specific selectivity to 4-chlorophenol. Biosorption of phenolic compounds by biomasses (e.g., seaweeds [74], fungus [75-77], and alga [78]) have been extensively studied in recent years. Antizar and Galil [79] used biomass grown on agar plates and biomass collected from a

simulated aquifer to remove phenol and chlorophenols from wastewater. Table 2.3 lists some studies about the adsorption of phenolic compounds by biological materials.

2.2.4 Sorption of phenolic compounds by polymeric adsorbents

In the past few decades, polymeric adsorbents have been emerging as a potential alternative to activated carbon in terms of adsorption-regeneration properties, mechanical strength and adjustable surface properties. Al-Muhtaseb et al. [80] used poly(methyl methacrylate) (PMMA) to remove phenol from wastewater. The adsorption of phenol on PMMA was shown to be governed by film diffusion. The equilibrium data were best described by the Freundlich and Redlich–Peterson isotherm models.

Amberlite XAD-4 resin is the most widely used polymeric adsorbent for the removal of phenolic compounds from wastewater. Amberlite XAD-4 resin is a macroporous styrene-divinylbezene copolymer. The adsorption properties of phenol [81] , 4-CP [82], 4-NP [21], 4-MP [81] on Amberlite XAD-4 resin have been studied. The main problem with XAD-4 resin is its poor contact with aqueous solutions because of its extremely hydrophobic surface. Activation solvents (i.e., methanol, acetone, and acetonitrile) are usually needed in the pre-treatment process to increase the water wettability [81]. Another problem is its much lower adsorption capacity compared with activated carbon.

Recently, hyper-cross-linked polymeric adsorbent has attracted increasing attention due to its adjustable matrix and pore structure. Pan et al. [21] prepared a hyper-cross-linked polymer from the styrene–divinylbenzene copolymer, followed by a chromethylation and post cross-linking. The synthesized polymer exhibited a significantly high capacity to adsorb 4-NP than XAD-4. Li et al. [83] studied the adsorption of phenol, 4-CP, 4-NP and 4-MP on a hypercorsslinked polymer. Compared to the commercial XAD-4, the polymeric sorbent can

be easily wetted by water and had a high adsorption capacity towards phenolic compounds. The increased capacity may be attributed to the microporous structure and partial polarity of the network. Sun et al. [84] modified the hypercrosslinked polymer by introducing tertiary amino groups. It was found that the aminated hypercrosslinked polymer had a higher adsorption capacity due to Lewis acid-base interaction between phenolic compounds and the amino groups on the polymer matrix.

The adsorption capacities of phenolic compounds by some polymeric adsorbents are listed in Table 2.4.

2.3 Adsorption isotherms

For a given sorbate-sorbent system, the amount of sorbate taken by the sorbent at a given temperature and concentration is characterized by the adsorption equilibrium:

$$Q_e = f\,(C_e, T) \tag{2.1}$$

where Q_e refers to the amount of adsorbate adsorbed per unit mass of adsorbent, commonly expressed by moles of adsorbate per gram of adsorbent. At a given temperature, the amount of adsorption at equilibrium may be considered as:

$$Q_e = f\,(C_e) \tag{2.2}$$

This means the equilibrium uptake is a function of solute concentration at equilibrium, and this relationship is commonly referred to as the adsorption isotherm. Different isotherm models are used to represent the equilibrium data. The parameters in these models can be determined from experiments to provide an insight into the adsorption capacity and probable adsorption mechanism.

2.3.1 Equilibrium models of adsorption

2.3.1.1 The linear model

The linear isotherm model is the simplest model, and it is sometimes called Henry's adsorption isotherm. It can be expressed by

$$Q_e = K_H C_e \qquad (2.3)$$

where K_H is Henry's adsorption constant. The linear isotherm model can be used to describe the initial part of many practical isotherms when the solute concentration in the solution is low.

2.3.1.2 The Langmuir model

The Langmuir model is by far the most widely used expression for physical adsorption (or even chemisorption) from liquid solutions. The model was developed by Langmuir [85] in 1916. The adsorption process is expressed as

$$A + B \underset{K_d}{\overset{K_a}{\rightleftharpoons}} AB \qquad (2.4)$$

where A represents free adsorbate molecules in solution, B represents vacant sites on the adsorbent, and AB represents the occupied sites. K_a is the rate constant of adsorption, and K_d is the rate constant of desorption. The Langmuir model assumes the following [86]:

a. Adsorption of adsorbate molecules takes place at well-defined localized states.

b. All the adsorption sites are identical, and each site accommodates one adsorbate molecule only.

c. There are no lateral interactions.

Let θ represent the fraction covered by adsorbate molecules, then vacant sites on the adsorbents is $(1-\theta)$. The adsorption and desorption rates are:

Rate of adsorption: $K_a C_e (1 - \theta)$,

Rate of desorption: $K_d \theta$.

At equilibrium, the rate of adsorption should be equal to the rate of desorption

$$K_a C_e (1 - \theta) = K_d \theta \tag{2.5}$$

Rearranging:

$$\theta = \frac{K_a C_e}{K_d + K_a C_e} = \frac{\left(\frac{k_a}{k_d}\right) C_e}{1 + \left(\frac{K_a}{K_d}\right) C_e} \tag{2.6}$$

Based on the definition of θ, one has:

$$\theta = \frac{Q_e}{Q_m} \tag{2.7}$$

Comparing Eq. (2.6) with Eq. (2.7), we have:

$$\theta = \frac{Q_e}{Q_m} = \frac{\left(\frac{k_a}{k_d}\right) C_e}{1 + \left(\frac{K_a}{K_d}\right) C_e} = \frac{K_L C_e}{1 + K_L C_e} \tag{2.8}$$

where K_L is defined as $K_L = K_a / K_d$.

Eq. (2.8) can be rearranged as:

$$\frac{1}{Q_e} = \frac{1}{Q_m} + \frac{1}{Q_m K_L} \frac{1}{C_e} \tag{2.9}$$

which is the linearized form of the Langmuir model. In this equation, Q_m refers to theoretical maximum adsorption capacity (mmol/g), K_L represents the Langmuir constant (L/mmol). Parameters Q_m and K_L can be obtained from plots of $1/Q_e$ vs. $1/C_e$.

2.3.1.3 The Freundlich model

Zeldowitsch assumed an exponentially decaying function of site density with respect to uptake capacity and obtained an empirical isotherm in 1934 [86], which is expressed as:

$$Q_e = K_F C_e^{1/n}$$

(2.10)

It has a linear form:

$$\ln Q_e = \ln K_F + \frac{1}{n} \ln C_e$$

(2.11)

In this expression, Q_e is the adsorption uptake at equilibrium (mmol/g), C_e is the solute concentration at equilibrium (mmol/L), K_F is the Freundlich constant and has a unit of $(\text{mol})^{1-1/n}.\text{g}^{-1}.\text{L}^{1/n}$ and $1/n$ is the heterogeneity factor. Parameters K_F and $1/n$, which can be calculated from the slope and intercept of the linear $\ln Q_e$ vs. $\ln C_e$ plots, are related to the adsorption capacity and adsorption intensity, respectively.

The Freundlich isotherm model, in many ways, is a simple way to represent experimental data. It is a useful empirical equation widely applied to describe a heterogeneous system.

Tables 2.1-2.4 present various adsorbent-adsorbate systems for the adsorption of phenolic compounds. Equilibrium models applied in these systems and corresponding model parameters (e.g., K_F, n, K_L and Q_m) are also presented.

Table 2.1 Adsorption of phenolic compounds by activated carbon

Adsorbent	Solute	T (°C)	Model	Parameters	Ref.
Granular activated carbon	Phenol	30	Freundlich	K_F=1.18, n=4.08	[87]
Granular activated carbon	4-NP	30	Freundlich	K_F=1.39, n=5.88	[87]
Granular activated carbon	4-NP	30	Freundlich	K_F=1.58, n=4.52	[21]
Powered activated carbon	2-CP	25	Freundlich	K_F=1.73, n=5.13	[88]
Powered activated carbon	2-CP	25	Freundlich	K_F=0.760, n=2.46	[88]
Granular activated carbon	2-CP	25	Freundlich	K_F=1.41, n=4.41	[88]
Granular activated carbon	2-CP	25	Freundlich	K_F=0.935, n=1.81	[88]
Granular activated carbon	Resorcinol	30	Freundlich	K_F=0.933, n=4.35	[89]
Granular activated carbon	Catechol	30	Freundlich	K_F=1.01, n=4.88	[89]
Granular activated carbon	4-MP	28	Langmuir	Q_m=1.62, K_L=0.130	[90]
Granular activated carbon	4-NP	28	Langmuir	Q_m=1.39, K_L=0.030	[90]
Activated carbon	4-MP	-	Langmuir	Q_m=0.795, K_L=36.8	[91]
Activated carbon	4-MP	-	Langmuir	Q_m=0.851, K_L=71.4	[91]
Activated carbon	4-MP	-	Langmuir	Q_m=0.703, K_L=16.2	[91]

K_F: (mmol/g) (L/mmol)$^{1/n}$ K_L: L/mmol Q_m: mmol/g

Table 2.2 Adsorption of phenolic compounds by minerals

Adsorbent	Solute	T (°C)	Model	Parameters	Ref.
Organophilic bentonite	Catechol	30	Langmuir	Q_m=0.507, K_L=0.257	[60]
Diatomite/carbon KC1	4-MP	-	Langmuir	Q_m=0.268, K_L=10.8	[91]
Diatomite/carbon KC3	4-MP	-	Langmuir	Q_m=0.758, K_L=21.6	[91]
Bentonite	Phenol	20	Langmuir	Q_m=0.009, K_L=1.49	[92]
Modified bentonite	4-NP	30	Langmuir	Q_m=0.773, K_L=1.99	[59]
Modified bentonite	4-NP	30	Langmuir	Q_m=1.75, K_L=0.835	[59]
Bentonite	4-CP	20	Freundlich	K_F=0.142, n =1.35	[93]
Perlite	4-CP	20	Freundlich	K_F=0.0712, n =1.43	[93]
Zeolite CS-1	Phenol	30	Langmuir	Q_m=1.48, K_L=5.647	[62]
Zeolite CS-1N	Phenol	30	Langmuir	Q_m=2.21, K_L=10.5	[62]
Zeolite CS-2	Phenol	30	Langmuir	Q_m=1.36, K_L=6.59	[62]
Zeolite CS-2N	Phenol	30	Langmuir	Q_m=2.04, K_L=14.2	[62]
Zeolite CF-1	Phenol	30	Langmuir	Q_m=2.13, K_L=2.16	[62]
Zeolite CF-1N	Phenol	30	Langmuir	Q_m=3.43, K_L=4.71	[62]
HDTMA-zeolite	Phenol	20	Freundlich	K_F=0.0174, n =1.37	[63]
BDTBA-zeolite	Phenol	20	Freundlich	K_F=0.0261, n =1.19	[63]
HDTMA-zeolite	4-CP	20	Freundlich	K_F=0.0225, n =1.23	[63]
BDTBA-zeolite	4-CP	20	Freundlich	K_F=0.126, n =1.60	[63]
Chitosan-coated perlite	Phenol	-	Langmuir	Q_m=2.04, K_L=0.376	[65]
Chitosan-coated perlite	4-CP	-	Langmuir	Q_m=2.50, K_L=0.643	[65]

K_F: (mmol/g) (L/mmol)$^{1/n}$ K_L: L/mmol Q_m: mmol/g

Table 2.3 Adsorption of phenolic compounds by biological materials

Adsorbent	Solute	T (^{o}C)	Model	Parameters	Ref.
Sawdust	Phenol	22	Freundlich	K_F=0.044, n =43.7	[94]
Sawdust	4-CP	28	Langmuir	Q_m=1.47, K_L=41.2	[53]
Charred saw dust	4-NP	20	Langmuir	Q_m=1.06, K_L=14.3	[67]
Rice husk	Phenol	-	Langmuir	Q_m=0.207, K_L=173	[54]
Rice husk	Phenol	-	Freundlich	K_F=0.00306, n =2.32	[54]
Pinus pinaster bark	Phenol	25	Freundlich	K_F=0.0588, n =2.00	[68]
Acid activated red mud	Phenol	25	Langmuir	Q_m=0.0870, K_L=9.51	[71]
Neutralized red mud	Phenol	25	Langmuir	Q_m=0.0440, K_L=4.80	[70]
Chitosan	Phenol	30	Langmuir	Q_m=0.021, K_L=0.191	[73]
Chitosan	4-CP	30	Langmuir	Q_m=0.0200, K_L=0.192	[73]
Chitosan	4-NP	30	Langmuir	Q_m=0.0140, K_L=0.282	[73]
Chitosan	Phenol	30	Freundlich	K_F=0.0110, n =1.02	[73]
Chitosan	4-CP	30	Freundlich	K_F=0.0555, n =1.05	[73]
Chitosan	4-NP	30	Freundlich	K_F=0.0623, n =1.07	[73]
Biomass 1	Phenol	-	Freundlich	K_F=0.111, n =0.840	[79]
Biomass 2	Phenol	-	Freundlich	K_F=0.0675, n =0.826	[79]
Biomass	4-CP	-	Freundlich	K_F=0.00848, n =2.381	[79]

K_F: (mmol/g) (L/mmol)$^{1/n}$ K_L: L/mmol Q_m: mmol/g

Table 2.4 Adsorption of phenolic compounds by polymeric adsorbents

Adsorbent	Solute	T (°C)	Model	Parameter	Ref.
PMMA	Phenol	25	Freundlich	K_F=0.571, n =2.81	[80]
NDA-701	4-NP	30	Freundlich	K_F=1.38, n =2.82	[21]
XAD-4	4-NP	30	Freundlich	K_F=0.490, n =1.68	[21]
XAD-4	4-CP	25	Langmuir	Q_m=0.217, K_L=24.4	[82]
XAD-4	Phenol	30	Freundlich	K_F=0.259, n =1.639	[81]
XAD-4	4-MP	30	Freundlich	K_F=0.656, n =2.38	[81]
XAD-4	4-CP	30	Freundlich	K_F=0.802, n =2.41	[81]
XAD-4	4-NP	30	Freundlich	K_F=0.526, n =1.69	[81]
NDA-100	Catechol	10	Freundlich	K_F=0.511, n =2.21	[84]
AH-1	Catechol	10	Freundlich	K_F=1.02, n =3.25	[84]
AH-2	Catechol	10	Freundlich	K_F=1.15, n =3.36	[84]
AH-3	Catechol	10	Freundlich	K_F=1.02, n =3.00	[84]
HJ-1	Phenol	20	Langmuir	Q_m=1.78, K_L=0.889	[95]
HJ-1	4-MP	20	Langmuir	Q_m=2.17, K_L=1.93	[95]

K_F: (mmol/g) (L/mmol)$^{1/n}$ K_L: L/mmol Q_m: mmol/g

2.3.2 Calculations of the thermodynamic parameters in adsorption

Thermodynamic parameters such as standard Gibbs free energy change (ΔG^0), entropy change (ΔS^0), and enthalpy change (ΔH^0) can provide helpful information for the adsorption type and mechanism of the adsorption process [96]. The free energy change ΔG^0 can be calculated from:

$$\Delta G^0 = -RTlnK_0 \qquad (2.12)$$

where R ($J \cdot mol^{-1} \cdot K^{-1}$) is the universal gas constant, T is the temperature in Kelvin, K_0 is the equilibrium constant of the adsorption process.

The change in the standard enthalpy ΔH^0 and the change in the standard entropy can be calculated using the Van't Hoff equation:

$$lnK_0 = \frac{\Delta S^0}{R} - \frac{\Delta H^0}{RT} \qquad (2.13)$$

Eq. 2.12 and Eq. 2.13 suggest that the correct calculation of thermodynamic parameters depends on how the thermodynamic equilibrium constant K_0 is determined. However, K_0 has been obtained in different ways in the literature, and there have been inconsistencies in the determination of K_0.

2.3.2.1 Determination of K_0 from isotherm constants
a. Determination of K_0 if Langmuir isotherm applies

For the adsorption process [96]:

Free adsorptive molecules + vacant sites $\rightleftharpoons$ occupied sites
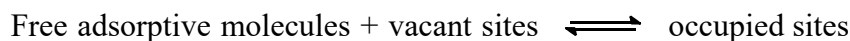
According to the definition of equilibrium constant, the thermodynamic equilibrium constant K_0 for the adsorption process can be written as:

$$K_0 = \frac{activity\ of\ occupied\ sites}{(activity\ of\ vaccant\ sites)(activity\ of\ adsorbate\ moledules\ in\ solution)} \qquad (2.14)$$

Let θ represent the fraction of occupied sites. Assuming the activity coefficients of occupied and unoccupied sites are the same, the above equation becomes:

$$K_0 = \frac{\theta}{(1-\theta)a_e} \qquad (2.15)$$

where a_e is the activity of adsorbate in solution at equilibrium.

Comparing Eq. 2.15 with the Langmuir model Eq. 2.8, we have:

$$K_0 = \frac{\theta}{(1-\theta)a_e} = \frac{K_L C_e}{a_e} \qquad (2.16)$$

The activity of a substance is related to its concentration by the following formula:

$$a_e = \gamma_e \frac{C_e}{C_s} \qquad (2.17)$$

where γ_e is the activity coefficient at the equilibrium, C_s is the standard concentration of the reference solution, which is equal to 1 mol/L in this case. Substituting Eq. 2.17 to Eq. 2.16 gives

$$K_0 = \frac{K_L C_e}{\gamma_e \frac{C_e}{C_s}} = \frac{K_L}{\gamma_e} \times 1\ mol/L \qquad (2.18)$$

Therefore, K_0 is numerically equal to K_L when γ_e equals unity [96].

In some studies [97-100], K_0 values were directly replaced by Langmuir constant K_L. According to Eq. 2.12, the equilibrium constant K_0 should be dimensionless. However, the Langmuir constant K_L is dimensional (e.g., L/mmol). Obviously K_0 and K_L are not directly interchangeable.

Liu [96] concluded from Eq. 2.18 that for neutral adsorbates or adsorbates with weak charges, K_L can be numerically equal to K_0 . This treatment was used in many studies [8,

101-105]. However, the activity coefficient γ_e is not only related to the charges carried by the solute but also to the ionic strength of the solution. This conclusion is valid only if the solute concentration at equilibrium is very small. Another problem with this approach is that the concentration of the standard reference solution is defined to be 1 mol/L, but in the adsorption study the unit of concentration is often expressed in either mg/L or mmol/L. It is obvious that the numerical value of K_L will change with its unit used. It should be noted that the conclusion that K_0 and K_L are numerically equal should be based on the condition that the unit of K_L is in L/mol.

Milonjić [106] proposed that the Langmuir constant could be converted to the proper dimensionless equilibrium constant by multiplying it with 55.5 mol H_2O/L when K_L is in the unit of L/mol. K_0 was calculated this way in some studies [107-109]. Zhou et al. [110] calculated K_0 by multiplying K_L (L/mg) with 10^6 mg H_2O/L in a similar way. If K_L is in the unit of L/mg, it should be modified accordingly since density of the solution is considered to be 1 g/mL. These approaches attempt to convert the unit of K_L based on the properties of the dilute solution. However, this method seems to lack the basis for changing the units of K_L based on properties of the solvent. Liu [96] pointed out that the previous treatment was resulted from misunderstanding of chemical activity.

b. Determination of K_0 if Freundlich isotherm applies

Unlike the Langmuir isotherm, the Freundlich isotherm is an empirical model for heterogeneous systems. Thus the Freundlich constant K_F has no clear physical meaning, and it is thus difficult to derive the proper equilibrium constant K_0 from K_F. Milonjić [106] put forward a correction for calculations of free energy from the Freundlich constant K_F by using a unit of L/g for K_F so as to get a dimensionless K_0 by multiplying K_F with 1000 g/L,

which is based on the fact the density of water is 1 kg/L. Otero et al. [111] calculated K_0 in this way. However, the unit of K_F is L/g only when n=1, and one cannot get a dimensionless K_0 when n is not equal to 1 if such a treatment is used.

2.3.2.2 Determination of K_0 from Q_e/C_e vs. C_e plots

Biggar and Cheung [112] defined the equilibrium constant for adsorption as:

$$K_0 = \frac{a_s}{a_e} = \frac{\gamma_s C_s}{\gamma_e C_e} \tag{2.19}$$

where a_s represents the activity of the adsorbed solute, a_e represents the activity of the solute in the solution at equilibrium. C_s is mmol of solute adsorbed per L of solvent in contact with the adsorbent surface, C_e is mmol of solute per L of solvent in the solution at equilibrium. γ_s is the activity coefficient of the adsorbed solute, and γ_e is the activity coefficient of the solute in the solution at equilibrium.

C_s is calculated according to the following equation:

$$C_s = \frac{(\rho_1/M_1)A_1 N Q_e}{s} \tag{2.20}$$

where ρ_1 is the density of solvent (g/ml), M_1 is the molecular weight of the solvent (g/mol), A_1 is the cross-sectional area of the solvent molecule (cm^2/molecules), N is Avogadro's number (6.02×10^{23} molecules/mol), s is the surface area of the adsorbent (cm^2/g), and Q_e is the amount of solute adsorbed by adsorbent at equilibrium (mmol/g).

When C_e approaches zero, the activity coefficient approaches unity, and thus Eq. 2.19 may be written as:

$$K_0 = \lim_{Q_e, C_e \to 0} \frac{C_s}{C_e} \tag{2.21}$$

28

Thus K_0 is obtained by plotting C_s/C_e vs. C_s and extrapolating to zero C_s. This approach assumes that the solute is adsorbed on the surface of the adsorbent, so the solute concentration in the adsorbent can be converted to concentration in the solvent using Eq. (2.20), and K_0 obtained by this approach is dimensionless. However, this method is only valid for surface adsorption which is not really suitable for our study.

C_s is not easy to calculate in some cases using Eq. (2.20). We noticed that in many studies, C_s in Eq. (2.21) is replaced with Q_e (mmol/g) the amount of solute adsorbed per mass of adsorbent. Thus K_0 is derived by plotting Q_e/C_e vs. Q_e and extrapolating to zero Q_e. However, it is worth noting that K_0 obtained in this way has a unit of L/g. Liu [96] also pointed out that it is difficult to understand the theoretical basis of this approach, in spite that it has been used in many studies [113-116].

2.3.2.3 Determination of K_0 based on distribution constant

For the adsorption process, assuming solute *(i)* is distributed in two different phases *I* (i.e., the solvent) and *II* (i.e., the adsorbent), and the distribution constant K_d may be defined as:

$$K_d = \frac{a_i \, ^{(eq)}_{(I)}}{a_i \, ^{(eq)}_{(II)}} \tag{2.22}$$

where $a_i \, ^{(eq)}_{(I)}$ and $a_i \, ^{(eq)}_{(II)}$ represents the activity of substance (i) in phases *I* and *II* at equilibrium respectively.

Liu [96] proposed that K_d equals to equilibrium constant K_0 when θ_e is small (i.e., the adsorption capacity of the adsorbent is much higher than the amount of adsorbate to be removed). This assumption is valid for dilute solutions.

According to the IUPAC, the concentration of stationary phase is expressed per unit volume of the phase. As such, the distribution constant may be defined as:

$$K_d = \frac{C_{ad}}{C_e} \tag{2.23}$$

where C_{ad} is the concentration of the solute in the adsorbent (mmol/L), C_e is the concentration of the solute in the solution at equilibrium (mmol/L). Considering the effect of the activity coefficient, K_0 is expressed as

$$K_0 = \lim_{C_{ad} \to 0, C_e \to 0} \frac{C_{ad}}{C_e} \tag{2.24}$$

where K_0 can be obtained by plotting C_{ad}/C_e versus C_{ad} and extrapolating to zero C_{ad}. In some studies [117-120], K_0 was calculated by this approach when Langmuir constant K_L was unavailable. In our study, K_0 values were calculated this way. However, C_{ad}, usually denoted by mmol/g, is converted to mmol/L using the density of the sorbent. Strictly speaking, K_d is not dimensionless since the units of C_{ad} and C_e are from two different phases and thus cannot be simply cancelled out.

2.4 Kinetic models of adsorption

In the past decades, several mathematical models have been proposed to describe the sorption kinetics.

2.4.1 Pseudo-first order kinetic model

In 1898, Lagergren [121] presented the first-order rate equation in which adsorption rate was assumed to be proportional to the adsorption capacity available. It can be expressed as follows:

$$\frac{dQ}{dt} = k_1(Q_e - Q) \tag{2.25}$$

where Q_e and Q are the solute uptake (mmol/g) at equilibrium and time t (min), respectively, and k_1 is the pseudo-first order rate constant.

Integration of Eq. (2.25) gives:

$$\ln(Q_e - Q) = -k_1 t + \ln Q_e \tag{2.26}$$

Plotting $\ln(Q_e - Q)$ vs. time t, a straight line can be obtained with the slope of $-k_1$ and the intercept of $\ln Q_e$. This was called pseudo-first order equation to distinguish the kinetic equations based on adsorption capacity from that based on the solute concentration in the solution [122].

2.4.2 Pseudo-second order kinetic model

The Pseudo-second order kinetic model was proposed by Ho and Mckay [123] to describe the adsorption of divalent metal onto peat. It assumed that chemisorption occurred involving valence forces through sharing or exchange electrons between peat and divalent metal ions as covalent forces [122]. The rate expression is given by:

$$\frac{dQ}{dt} = k_2(Q_e - Q)^2 \tag{2.27}$$

where Q represents the amount of adsorption (mmol/g) at time t (min), and Q_e represents the amount of adsorption (mmol/g) at equilibrium, k_2 is the rate constant of adsorption (g·mmol^{-1}·min^{-1})

Integrating Eq. (2.27) and applying initial condition $t = 0, Q = 0$, gives:

$$\frac{1}{Q_e - Q} = k_2 t + \frac{1}{Q_e} \tag{2.28}$$

Rearranging:

$$\frac{t}{Q} = \frac{1}{k_2 Q_e{}^2} + \frac{1}{Q_e} t \qquad\qquad (2.29)$$

If we plot t/Q vs. t, a straight line can be obtained with a slope of $1/Q_e$ and the intercept of $(1/k_2 Q_e{}^2)$.

The main assumption of the pseudo-second order model is that the rate limiting step is chemical adsorption involving valent forces through sharing or exchange of electrons. Similar to the pseudo-first order model, the pseudo-second order model is also based on adsorption capacity and not on the solute concentration in the solution [122].

2.4.3 Diffusion model

The diffusion model was first proposed by Weber and Morris in 1962 [124]. They found that in many adsorption processes, solute uptake varies proportionally with $t^{1/2}$ in the initial stage of adsorption process. The linear form of this model can be expressed by the following equation:

$$Q = k_i \sqrt{t} + C \qquad\qquad (2.30)$$

where k_i is the intraparticle mass transfer constant (mmol·g^{-1}·min$^{-1/2}$), and the value of the intercept C (mmol/g) is indicative of the boundary layer effect. According to this model, plots of Q versus $\sqrt{t}$ should be linear if diffusion is dominant in the adsorption process. If the plots are linear and pass through the origin, diffusion is the only rate controlling step; if the plots are linear but do not pass through the origin, then the rate of adsorption may be controlled by intraparticle diffusion together with boundary layer effects.

2.5 Sorption in multi-solute systems

2.5.1 Sorption of phenolic compounds in multi-solute systems

In practical instances, multiple phenolic compounds are likely to coexist in industrial wastewater. Thus the sorption technique shall not be limited to the removal of a single solute and interactions among the solute components in multi-solute systems on sorption performance were also worth investigating. Some attempts have been made to investigate the competitive sorption of phenolic compounds in multi-component system over the past few decades.

Lu and Sorial [125] studied the sorption of phenol, 2-methylphenol and 2-ethylphenol in binary and ternary solute systems. It was observed that the equilibrium uptake capacity of 2-methylphenol in the binary solute system increased with an increase in its concentration, whereas the opposite was observed for phenol. This indicates competitive effect of 2-methylphenol on phenol adsorption. Similarly, competitive effects of 2-ethylphenol on adsorption of phenol and 2-methylphenol in ternary solute systems were also observed. Competitive sorption of phenol, 4-chlorophenol and 4-nitrophenol on activated carbon was studied by Mihalache et al. [126]. Sorption capacity of phenol, which was the weakest adsorbing compound, was greatly reduced by the presence of 4-nitrophenol, which was the strongest adsorbing compound. Significant competitive interactions were observed for ternary solute systems, where sorption capacity of one phenolic compound was significantly reduced by the presence of other solute compounds for all the three phenol compounds. Huh et al. [127] conducted competitive sorption of phenol, 4-methylphenol, 2,4-dimethylphenol and 4-ethylphenol on montmorillonite. And a comparison of sorption capacity of phenol in single and multi-solute systems showed that sorption capacity of phenol decreased in the

following order: phenol(single solute)>phenol/4-methylphenol (bisolute)>phenol/2,4-dimethylphenol (bisolute)>phenol/4-methyphenol/2,4-dimethylphenol (trisolute).

Competitive sorption between phenolic compounds was found to be related to their sorption capacities in single solute system in some cases. Srivastava and Tyagi [128] studied the competitive sorption of four phenolic compounds (2,4,6-trinitrophenol, 4-nitrophenol, 4-chlorophenol and resorcinol) in bisolute systems on activated carbon developed from the fertilizer waste slurry. They found that the sorption of 2,4,6-nitrophenol, which had the highest adsorptive capacity on the adsorbent among the four, was not affected by the presence of other three phenols, and resorcinol, which was the least absorbable among the four solutes, did not affect the sorption of the other three phenols. Mutual suppressions of sorption capacity were observed in other bisolute systems. Similar results were reported for the sorption of phenol and 4-chlorophenol from bisolute solutions by Abburi [129], and the supressing effect was more pronounced for 4-chlorophenol on phenol than phenol on 4-chlorophenol. Khan et al. [130] also reported similar results for the competitive sorption of phenol and 4-chlorophenol on activated carbon. It was found that phenol had no significant effect on the sorption of 4-chlorophenol, whereas 4-chlorophenol influenced strongly on the sorption of phenol. For 2-chlorophenol/4-chlorophenol binary solute system, no competitive sorption effect was observed since the adsorbent had no preferential selectivity to the sorption of either compound. For 4-chlorophenol/3-methylphenol binary solute system, mutual depressions of the sorption capacities was observed for the two solutes.

However, different competitive sorption behaviours among the solute compounds have been observed in other studies. Garcia-Araya et al. [131] showed that in single-solute solutions, the adsorption capacity was in the order of syringic acid>4-hydrobenzoic

acid>gallic acid. However, in the presence of gallic acid (which was a less sorbable solute), the sorption of syringic acid (which has a larger sorption capacity) was greatly suppressed, and 4-hydrobenzoic acid affected the gallic acid sorption more significantly than syringic acid did. Juang et al. [132] compared sorption of phenol, 3-nitrophenol, and 2-methylphenol on surfactant-modified montmorillonite in single solute systems and bi-solute systems. The sorption capacities of phenols on montmorilonite were in the order: 3-nitrophenol>2-methylphenol>phenol in single solute systems. However, the extent of reduction in the sorption capacity due to competitive sorption effects was in the order: phenol>3-nitrophenol>2-methylphenol in bi-solute systems.

In spite of the competitive adsorption among phenolic compounds commonly observed, mutually enhanced adsorption among phenolic compounds has been reported in some cases. Wei and Nakato [133] studied the sorption of multi-component phenols (phenol, 2-chlorophenol, and 2,4-dichlorophenol) on two modified niobates ($C_{12}N$-$K_4Nb_6O_{17}$ and $2C_{18}2MeN$-$K_4Nb_6O_{17}$), the phenol compounds showed different competitive behaviours. For sorbent $2C_{18}2MeN$-$K_4Nb_6O_{17}$, the uptake of one phenol compound at low concentration was enhanced by the presence other phenol compounds in binary and ternary solute systems. Garcia-Araya et al. [131] also observed enhanced sorption of phenolic compounds on activated carbon at low concentrations. A possible reason is that at low solute concentrations, the sorption sites available for sorption were abundant, and the good affinity and solubility among the phenolic compounds may have helped each other in being adsorbed on the sorbent.

2.5.2 Multi-component adsorption models

Compared to single-solute adsorption isotherm, multi-component adsorption isotherms are tedious to determine experimentally. Therefore, prediction of multi-solute

sorption isotherms based on single-solute isotherms is desirable. Several mathematical models have been developed, and they are described in the following section.

2.5.2.1 Competitive Langmuir model

The earliest attempt to describe competitive sorption was made by Butler and Ockrent in 1930 [134], who proposed a Langmuir model for competitive sorption for binary solute systems:

$$Q_{e1} = \frac{Q_{m1} k_{L1} C_1}{1 + k_{L1} C_1 + k_{L2} C_2} \tag{2.31}$$

$$Q_{e2} = \frac{Q_{m2} k_{L2} C_2}{1 + k_{L1} C_1 + k_{L2} C_2} \tag{2.32}$$

where Q_{m1}, Q_{m2}, k_{L1}, and k_{L2} are the Langmuir constants obtained from single-solute systems.

The Langmuir competitive model was modified by Jain and Snoeyink in 1973 [135], who assumed that not all adsorption sites are available to all components. The number of adsorption sites for non-competitive adsorption is given by the difference between the maximum loadings (Q_m) of the species. Suppose $Q_{m1} > Q_{m2}$ for a bisolute system, competition for sorption sites by the two solutes occurs only when the uptake $Q \leq Q_{m2}$, and the two solutes do not compete for the sorption sites corresponding to ($Q_{m1} - Q_{m2}$), The modified equations are:

$$Q_{e1} = \frac{(Q_{m1} - Q_{m2}) k_{L1} C_1}{1 + k_{L1} C_1} + \frac{Q_{m2} k_{L1} C_1}{1 + k_{L1} C_1 + k_{L2} C_2} \tag{2.33}$$

$$Q_{e2} = \frac{Q_{m2} k_{L2} C_2}{1 + k_{L1} C_1 + k_{L2} C_2} \tag{2.34}$$

where Q_{e1} and Q_{e2} are the equilibrium uptakes of solute 1 and 2 at equilibrium concentrations C_1 and C_2, respectively, in mixture solution. The first term on the right side of Eq. (2.33) represents the Langmuir expression for solute 1 which adsorbed on the adsorbent without competition, and the second term represents solute uptake of solute 1 in competition with solute 2.

2.5.2.2 Competitive Freundlich model

It is worth noting that the Langmuir competitive model and the modified version are only applicable when all solutes obey the Langmuir isotherm individually. In cases where all solutes obey the Freundlich isotherm instead of the Langmuir isotherm, a Freundlich-type isotherm for multisolute adsorption was proposed by Sheindorf et al. in 1980 [136]. It was based on the assumption that each solute component individually obeys the Freundlich isotherm. The isotherm is written in the form:

$$Q_i = K_{Fi} C_i \left(\sum_{j=1}^{N} a_{ij} C_j \right)^{\frac{1}{n_i} - 1} \tag{2.35}$$

where N is the number of solute components in the system, Q_i is the equilibrium uptake of solute component i in multicomponent solute system, C_i and C_j are the concentrations of component i and j at equilibrium in the solution. K_{Fi} and n_i are the Freundlich constants for the solute i , which are considered to be the same as those in a single-solute system. a_{ij} represents for the competitive sorption effect of component j on component i. By definition, $a_{ij} = 1$ when $i = j$. If the adsorption of component i is not supressed by the presence of solute component j, $a_{ij} = 0$; If the adsorption of component i is significantly reduced by the presence of solute component j, a large a_{ij} value will result.

For binary solute systems, the adsorption isotherm for each solute is given by:

$$Q_1 = K_{F1}C_1(C_1 + a_{12}C_2)^{\frac{1}{n_1}-1} \tag{2.36}$$

$$Q_2 = K_{F2}C_2(a_{21}C_1 + C_2)^{\frac{1}{n_2}-1} \tag{2.37}$$

For a quinary solute system, the adsorption isotherm for each solute is:

$$Q_1 = K_{F1}C_1(C_1 + a_{12}C_2 + a_{13}C_3 + a_{14}C_4 + a_{15}C_5)^{\frac{1}{n_1}-1} \tag{2.38}$$

$$Q_2 = K_{F2}C_2(a_{21}C_1 + C_2 + a_{23}C_3 + a_{24}C_4 + a_{25}C_5)^{\frac{1}{n_2}-1} \tag{2.39}$$

$$\vdots$$

$$Q_5 = K_{F5}C_5(a_{51}C_1 + a_{52}C_2 + a_{53}C_3 + a_{54}C_4 + C_5)^{\frac{1}{n_5}-1} \tag{2.40}$$

There is a problem with the competitive Freundlich model with regards to the competition coefficient a_{ij}. Sheindorf et al. [136] stated that the product of a_{ij} and a_{ji} should be unity based on the thermodynamic definition of competition coefficients. However, such a reciprocal relationship between a_{ij} and a_{ji} is not commonly obtained in competitive adsorptions [130, 137, 138]. On the other hand, if there is no competitive effect between the two solute components, the competition coefficients a_{ij} and a_{ji} should be zero, and obviously the product of the two will not be unity. Although the competitive Freundlich model has been applied in multi-solute sorption systems, its thermodynamic theoretical origin is somewhat questionable, and to the best it is only a semi-empirical model.

2.5.2.3 Ideal adsorbed solution theory model (IAST)

The ideal adsorbed solution theory (IAST), originally proposed by Myers and Prausnitz [139] for mixed-gas sorption, is regarded as a model with the most thermodynamically accepted foundation. Radke and Prausnitz [140] extended the IAST to

multi-solute sorption in dilute aqueous solutions on activated carbon. The theory was based on the following assumptions [141]:

(1) The sorbent is thermodynamically inert.

(2) The chemical potentials in both solid and liquid phases are equal for each solute at sorption equilibrium. Therefore, the spreading pressure should be constant for all solutes in the mixture.

(3) The adsorbed phase forms an ideal solution. Therefore, the solid/liquid equilibrium may be described in analogy with the Raoult's law for vapour/liquid equilibrium.

The basic equations for IAST model are:

$$z_i = \frac{Q_i}{\sum_{i=1}^{n} Q_i} \tag{2.41}$$

$$C_i^{0}(\pi) = \frac{C_i}{z_i} \quad (constant\ T, \pi) \tag{2.42}$$

$$\frac{1}{Q_T} = \sum_{i}^{N} \frac{z_i}{Q_i^{0}} \quad (constant\ T, \pi) \tag{2.43}$$

$$Q_i = Q_T z_i \tag{2.44}$$

$$\pi_1 = \pi_2 = \cdots = \pi_n \tag{2.45}$$

where π (J/cm^2) is the spreading pressure of each component in the mixture, which is defined as the difference between the interfacial tension of the pure solvent-solid interface and that of the solution-solid interphase at the same temperature; Q_T (mmol/g) is the total uptake of solute by the solid phase in the multi-solute system, Q_i^{0} (mmol/g) is the uptake of solute i in the single-component system at the same spreading pressure and temperature, C_i (mmol/L) is the liquid-phase equilibrium concentration of solute i in multi-solute system, $C_i^{0}(\pi)$ (mmol/L)

is the liquid-phase equilibrium concentration of solute i in the single-solute system at spreading pressure π. z_i is the mole fraction of solute i in the adsorbed-phase.

In order to use the above equations, the spreading pressure must be evaluated from the single-solute isotherm by:

$$\pi(C_i^0) = \frac{RT}{1000A} \int_0^{C_i^0} \frac{Q_i^0}{C_i^0} dC_i^0 \qquad (2.46)$$

where π (J/cm^2) is the spreading pressure, A stands for the specific area of the adsorbent (cm^2/g) . If we plot $\frac{Q_e}{C_e}$ vs. C_e by using the single-solute isotherm data, spreading pressure π can be determined by the area under the curve. Rearranging Eq. (2.46):

$$\varphi = \frac{1000\pi A}{RT} = \int_0^{C_i^0} \frac{Q_i^0}{C_i^0} dC_i^0 \qquad (2.47)$$

where φ (mmol/g) is related to the spreading pressure π. Therefore, φ should be constant for all the solutes in the mixture.

An advantage of the IAST model is that it is not limited to a specific isotherm, and it can incorporate different isotherm equations for calculation. For example, by using the Freundlich isotherm, the analytical solution for the IAST is illustrated as follows:

Firstly, values of C_i and Q_i are determined experimentally for each solute in multi-solute systems. Then z_i (i.e., mole fraction of solute i in the solid phase) can be obtained using Eq. (2.41), and $C_i^0(\pi)$ can be obtained from Eq. (2.42). $Q_i^0(\pi)$ can be calculated from the single-solute isotherms by:

$$Q_i^0 = K_F(C_i^0)^{1/n} \qquad (2.48)$$

Substituting Eq. (2.48) into Eq. (2.47):

$$\varphi = \int_0^{C_i^0} \frac{K_F(C_i^0)^{1/n}}{C_i^0} dC_i^0 = nQ_i^0 \qquad (2.49)$$

where K_F and n are Freundlich constants of solute i for its single-solute system. Since φ is the same for all the solute components in the mixture as indicated from Eq. (2.45), one can estimate Q_j^0 for other solute components using the following equation:

$$Q_j^0 = \frac{1}{n}\varphi \qquad (2.50)$$

Substituting Eq. (2.50) into (2.43), and the value of Q_T, which may be different that is determined experimentally, can be estimated. Then the predicted Q_i for each solute component in the multi-solute system can be estimated using Eq. (2.44).

Table 2.5 summarizes the isotherm models applied for the sorption of phenolic compounds in multi-solute systems.

Table 2.5 Adsorption of phenolic compounds in multi-solute systems

Multi-component system	Sorbent	Types of model applied	Ref.
Phenol, 4-chlorophenol	Amberlite XAD-16 resin	competitive Langmuir, IAST	[129]
Phenol, 2-chlorophenol, 2,4-dichlorophenol	Organically modified niobates	competitive Freundlich	[133]
Gallic acid, Syringic acid 4-hydroxybenzoic acid	Bituminous coal based activated carbon	N/A	[131]
2,4,6-trinitrophenol, 4-nitrophenol, 4-chlorophenol, resorcinol	Activated carbon developed from waste slurry	competitive Langmuir, Modified competitive Langmuir	[128]
Phenol, 2-,3-, and 4-chlorophenol, 3-methylphenol	Activated carbon	competitive Langmuir, empirical, competitive Freundlich, generalized model	[130]
Phenol, resorcinol	Activated carbon, wood charcoal and rice husk ash	artificial neutral network model	[142]
Phenol, 4-chlorophenol, 4-nitrophenol	Activated carbon	competitive Langmuir, competitive Freundlich-Langmuir, Fritz-Schlunder model	[126]
Phenol, 3-nitrophenol, 2-methylphenol	Surfactant-modified montomorillonite	competitive Langmuir	[132]
Phenol, 4-methylphenol, 2,4-dimethylphenol, 4-ethylphenol	Organically modified montomorillonite	competitive Langmuir, IAST competitive dual mode sorption,	[127]
Phenol, 2-methylphenol, 2-ethylphenol	Activated carbon	IAST	[125]
2-chlorophenol, 3-cynaophenol, 4-nitrophenol	Organically modified montorillonite	IAST and competitive Langmuir	[143]

2.6 Regeneration of spent adsorbents

In the sorption process, sorbents eventually become saturated. After exhaustion, the sorbents must be replaced with fresh ones or they must be regenerated. Sorbent regeneration is usually preferred because it is normally cheaper than replacement [16], and the sorbate can also be recovered. Since the regeneration cost of the exhausted sorbents is vital to the economic feasibility of the sorption process, it is necessary to develop proper regeneration processes for the spent sorbents. Thermal and chemical regeneration are two commonly used approaches.

2.6.1 Thermal regeneration

Thermal regeneration is the most commonly used regeneration technique for industrial applications. In thermal regeneration, the sorbates are desorbed by volatilization and/or oxidation at high temperatures. For example, activated carbon is often regenerated at high temperatures (>500°C). However, the use of a high generation temperature not only increases the fuel cost but also reduces the sorption capacity of the regenerated carbon [144].

An early study conducted by Magne and Walker [145] showed that in the thermal regeneration of phenol-saturated activated carbon, physisorbed phenol can become chemisorbed during the course of thermal treatment at a high temperature. Chemisorption occurred on the particle sites, which are modified upon heating at 1223 K, and then phenol was decomposed on the surface, with some surface pores closed, and thereby decreasing the surface area accessible to phenol and resulting in reduced sorption capacity. They pointed out that a lower thermal treatment temperature and shorter treatment time was favourable to avoid chemisorption of phenol. Moreno-Castilla et al. [146] also reported the transformation

of physisorbed phenol to chemisorbed phenol when activated carbon-phenol system was heated up to 1100 K in an inert gas flow. They conducted seven sorption-regeneration cycles and found that the sorption capacity of 4-nitrophenol on the sorbent decreased the most, with little sorption capacity left after seven cycles. The reduction in sorption capacity was 50% for 4-methylphenol and 80% for phenol and 3-aminophenol after seven cycles.

Torrents et al. [144], who used relatively low temperatures (110-400°C) to desorb aromatic compounds from activated carbon, found the presence of electron-withdrawing functional groups on the aromatic ring (e.g., $-NO_2$ and $-Cl$) would increase the activation energy and thus requires a higher temperature and longer time for the desorption process. Sabio et al. [147] tested three thermal regeneration methods of saturated activated carbon with 4-nitrophenol and concluded that thermal regeneration could be carried out in a single step of direct air-gasification to simplify the process and reduce the operating cost, although this approach could only achieve a 87% recovery of 4-nitrophenol sorption capacity on activated carbon. A study by Berenguer et al. [23] showed that the regeneration of phenol-saturated activated carbon obtained by thermal treatment in an inert atmosphere at 750°C was the most efficient, reaching 80-86% of the original sorption capacity. Ania et al. [24] compared the regeneration of activated carbon sorbed with phenol using microwave energy with the conventional thermal regeneration using an electric furnace at 1123 K. They evaluated the sorption capacity of the sorbent from breakthrough curves in the packed-bed adsorption process. The microwave treatment could reduce the heating time and preserve the porous structure to a great extent.

Lin and Cheng [148] conducted thermal regeneration of benonites exhausted by phenol and 3-chlorophenol at 200°C for two hours and little change in the phenol and 3-

chlorophenol removal efficiency was observed even after five adsorption-regeneration cycles. Alvarez et al. [25] carried out thermal regeneration of phenol-saturated activated carbon at 1123 K in N_2 (pyrolysis alone) or N_2 and CO_2 (pyrolysis plus oxidation). They found that less than 30% of phenol was physically sorbed onto activated carbon and at least 50% overall mass of phenol was not removed upon heating to 1100 K. Batch adsorption of phenol was tested for three sorption-regeneration cycles, and the sorption capacity of the regenerated adsorbent was found to be 79.2%, 79.4% and 68% after each regeneration cycle, respectively. Roostaei and Tezel [149] regenerated phenol exhausted zeolite sorbent Hisiv 1000 in air atmosphere at 360°C for 16 h in an electronic oven. Sorption isotherm was determined to see whether the sorption capacity has changed after each regeneration step. It was observed that there was no apparent change in sorption capacity of phenol on Hisiv 1000 after regeneration up to 14 cycles.

In summary, thermal regeneration is advantageous to desorb strongly adsorbed species and to recover the sorbates. However, it has three major disadvantages: (1) thermal energy is required, (2) high temperature may damage the surface structure of the sorbent thus decrease the sorption capacity, (3) thermal regeneration can hardly be done in situ, and unloading, transporting and repacking of the sorbent are involved, which increases sorbent attrition.

2.6.2 Chemical regeneration

As an alternative to thermal regeneration, chemical regeneration offers several advantages: (1) it is convenient to conduct the sorption-regeneration cycles with the same setup without sorbent transportation, (2) no damage to the sorbent surface structure due to higher temperature can occur, (3) with proper treatment, both the chemical and the sorbate

can be recovered [16]. The most commonly used regenerating chemicals can be categorized into two groups: (1) organic solvents that can extract the sorbates from the sorbent; b, inorganic chemicals which may react with the sorbate and strip it off the sorbent.

For sorbents saturated by phenolic compounds, such organic solvents as acetone [15, 16], methanol [15-18], ethanol [16, 17, 19, 20] have been used as regenerants. Cooney et al. [16] tested 19 solvents for desorption of phenol from activated carbon, and 3 of them (acetone, methanol and dimethylformamide) were found to be better than others. When tested in column regeneration, methanol was shown to be effective. In general, solvent temperature and flow rate were not as important as the solvent volume and type. Zeng et al. [19] used industrial alcohol to desorb phenol from PDM-2 resin column, and a nearly 100% regeneration efficiency was achieved with 3 bed volumes of alcohol at room temperature. They performed five sorption-regeneration cycles with the column and found that the breakthrough curve of the first cycle was almost identical to that of the fifth cycle, indicating that PDM-2 could be completely regenerated without significant capacity loss. Regeneration of activated carbon exhausted from phenolic compounds with solvents has been explored by Grant and King [17], who found that the regeneration efficiency with ethanol and methanol was 85.3% and 78.1% , respectively, among 12 solvents tested.

Among inorganic regenerating agents, sodium hydroxide has been found be the most effective in the regeneration of phenol-saturated sorbents. The main mechanism of regeneration was postulated based on two aspects [18]: (1) sodium hydroxide reacts with phenols to form sodium phenate, a soluble salt which facilitates the desorption of phenols from the sorbent surface; (2) the high pH arising from NaOH can change the surface polarity of the sorbent and thus reduce the attraction between phenol and the sorbent.

Pan et al. [21] used dilute NaOH solutions as regenerant for 4-NP saturated column of a synthesized polymeric adsorbent (NDA-701) and granular activated carbon, and a nearly complete regeneration was obtained with NDA-701, while only 75% sorption capacity was recovered with the granular activated carbon. 25 adsorption-regeneration runs were performed, and the superposition of breakthrough curves of the first and the 25th cycle indicated that NDA-701 can be fully regenerated with the NaOH solution without any capacity loss. Rengaraj et al. [150] used different concentrations of sodium hydroxide to desorb phenol from the activated carbon made from rubber seed coat and commercial activated carbon, and they found that NaOH solution at 0.1 and 0.14 mol/L were required for regenerating the two adsorbents, respectively. Özkaya et al. [22] also performed phenol desorption from spent carbons using NaOH at different concentrations, and it was found that 0.15 mol/L NaOH was needed for effective desorption.

Leng and Pinto [18] investigated the regeneration of activated carbon loaded with different sorbates (phenol, aniline, benzoic acid and nitrobenzene), and the chemical regeneration of activated carbon was shown to depend primarily on the solubility of the sorbate in the eluting reagents, sorption capacity of the solutes, and the charge characteristics of the sorbent surface. By comparing the regeneration performance with five different eluting reagents (methanol, micellar solutions, hydrochloric acid, formic acid, and sodium hydroxide), they found that the solubility of the sorbates in the eluting reagents could be enhanced by adjusting the pH, adding micelles, or using reactive regenerants that could produce soluble forms of the sorbate. Gupta et al. [15] carried out desorption of 2,4,6-trinitrophenol, 4-NP, 4-CP and 1,3-dihydroxybezene from activated carbon columns using acetone, methanol, ethanol propanol, formic acid, acetic acid and sodium hydroxide. The

47

results revealed that methanol and NaOH were more effective than other chemicals for the column regeneration.

A disadvantage of chemical regeneration is that the solvent desorption-water wash scheme will end up with two solutions that require further treatment: The eluting solution containing the desorbed solute, and the water wash solution containing a significant amount of the eluting chemicals plus a small amount of residual sorbate [16]. In addition, if the regenerating solvent itself cannot be recovered, it will add to the cost of the adsorbent regeneration process.

2.7 Sorption in packed-bed columns

2.7.1 Packed bed adsorption of phenolic compounds

Compared with batch sorption processes which are usually limited to treat a small amount of wastewater, fixed bed processes can continuously treat a large volume of water until the column is exhausted, and thus they are often used in practice. The performance of the packed bed can be described by the breakthrough curve that characterizes the concentration-time profile. The breakthrough point is the time when the column effluent reaches the maximum allowable solute concentration which may be determined by the process specifications such as discharge regulations. The shape of the breakthrough curve depends on both the property of the sorbate-sorbent system and the operating conditions of the column (e.g., feed flow rate, feed concentration, bed depth, and the sorbent size) [151].

Using commercially available Amerlite XAD-4, Li et al. investigated the sorption of phenolic compounds by polymeric sorbents in packed columns [81, 83]. Mini-column adsorption was conducted to compare the breakthrough characteristics and the total sorption capacity of phenolic compounds by the polymeric sorbents in the column. An et al. [152]

used a salicylic acid grafted polymeric adsorbent for sorption of phenol, 4-CP and 4-NP. Column studies were performed to obtain the breakthrough capacity and saturation capacity of the column. Sorption of phenol, 2-CP and 4-CP on chitosan-coated perlite beads in a packed column was studied by Kumar et al. [65].

Gupta et al. [15, 153] used carbon prepared from waste slurry in fertilizer plants as a low lost adsorbent for phenolic compounds. The sorption of phenol, 2-CP, 4-CP, 4-NP, catechol, and 2,4,6-trinitrophenol by the slurry carbon in a fixed bed was conducted, and parameters of the packed-bed adsorber were obtained from the breakthrough curves. It was found that column sorption capacity is higher than the capacity obtained in the batch experiments. Goud et al. [154] used activated carbon prepared from tamarind nutshell as a low cost sorbent for phenol sorption, and the effects of flow rate, phenol concentration and particle size on the breakthrough curve characteristics were investigated. It was shown that the breakpoint time and phenol removal decreased with an increase in the flow rate, phenol concentration and particle size. Column sorption of phenol has also been studied on other low cost adsorbents including sugar cane bagasse [155] and olive mill waste [156].

Sze and McKay [157] studied the sorption of 4-CP on stratified activated carbon in packed columns. Four different types of packed-bed adsorption columns were used and compared under the same operating conditions but different column geometries and activated carbon particle size stratification. A cylindrical column with particle stratification packing is found to be most efficient. Yoshida et al. [158] synthesized a monolithic carbon cryogel with a microhoneycomb structure and used it to adsorb phenol in continuous flow systems. It was reported that the straight channels in this new material can minimize the pressure drop and thin channel walls only causes minimal mass transfer resistance. The effects of temperature

and bed depth on the breakthrough curves have been investigated, and the column utilization was reported to increase with an increase in the temperature and bed depth. Hammache et al. [159] optimized the experimental conditions of phenol adsorption in an activation carbon packed-bed adsorber by using experimental design methodology. The effects of flow rate, carbon bed height, temperature and initial phenol concentration were investigated and the results showed that the temperature has a weak influence on the adsorption yield, and an increase in the flow rate has a positive effect on the percent removal of phenol.

The breakthrough curves in the above mentioned sorption systems were determined experimentally and no mathematical modelling of the process was attempted. Experimentation can provide a specific breakthrough curve under given operating conditions; however, it is usually laborious and time consuming especially for systems with a long residence time. Thus mathematical modeling of the adsorption is very essential for describing and predicting the breakthrough behaviour of packed column adsorption systems.

2.7.2 Adsorption modelling in packed-bed column system

The development of mathematical models for predicting the dynamic adsorption behaviour has attracted much attention in the past few decades. The mass conservation for a packed bed system is

| Rate of accumulation of sorbate mass within the control volume | = | Rate of net sorbate input into the control volume associated with the bulk flow | − | Rate of net sorbate efflux from the control volume |

In a packed bed mode, the control volume could be a small element of in the bed, as shown in Figure 2.1. The flow is assumed to be along the direction of the bed axis; D_z is a dispersion coefficient (cm^2/min) if axial dispersion is not ignored, U_s is the superficial

velocity (cm/min), which equals the volumetric flow rate divided by the cross-sectional area of the column; Z is the distance to the inlet (cm), H is the bed depth (cm). Q is the local phenol uptake in the solid phase (mmol/g) and C_b is the phenol concentration in the liquid phase (mmol/L) at time t (min). Then the following rate equations can be written:

Rate of accumulation of sorbate mass in the control volume: $\frac{\Delta Z \Delta C}{\Delta t}$

Rate of net sorbate input associated with mass flow: $(U_s C_b)_Z - (U_s C_b)_{Z+\Delta Z}$

Rate of sorbate efflux due to axial dispersion: $\left(D_Z \frac{\partial C}{\partial Z}\right)_Z - \left(D_Z \frac{\partial C}{\partial Z}\right)_{Z+\Delta Z}$

Rate of sorbate efflux due to adsorption: $\frac{\Delta Z \Delta q}{\Delta t}$

The mass conservation equation for the fixed-bed adsorption system is

$$\frac{\Delta Z \Delta C}{\Delta t} = (U_s C_b)_Z - (U_s C_b)_{Z+\Delta Z} - \left(D_Z \frac{\partial C}{\partial Z}\right)_Z + \left(D_Z \frac{\partial C}{\partial Z}\right)_{Z+\Delta Z} - \frac{\Delta Z \Delta Q}{\Delta t} \qquad (2.51)$$

Dividing by ΔZ on both sides and for the limiting situation $\Delta Z \to 0$, Eq. (2.51) becomes:

$$\lim_{\Delta Z \to 0} \frac{\Delta C}{\Delta t} = \lim_{\Delta Z \to 0} \frac{(U_s C_b)_Z - (U_s C_b)_{Z+\Delta Z}}{\Delta Z} + \lim_{\Delta Z \to 0} \frac{\left(D_Z \frac{\partial C}{\partial Z}\right)_{Z+\Delta Z} - \left(D_Z \frac{\partial C}{\partial Z}\right)_Z}{\Delta Z} - \lim_{\Delta Z \to 0} \frac{\Delta Q}{\Delta t} \qquad (2.52)$$

The differential equation could be written as [86, 160]:

$$\frac{\partial c}{\partial t} + \frac{\partial Q}{\partial t} + U_s \frac{\partial C}{\partial Z} = D_Z \frac{\partial^2 C}{\partial Z^2} \qquad (2.53)$$

where the initial and boundary conditions are:

$$At \ t = 0, C(z,t) = 0; Q(z,t) = 0;$$

$$At \ Z = 0, C(0,0) = 0, C(0,t) = C_{in};$$

$$At \ Z = H, \frac{\partial c}{\partial z} = 0;$$

where C_{in} is the initial solute concentration of the influent, and H is the bed height.
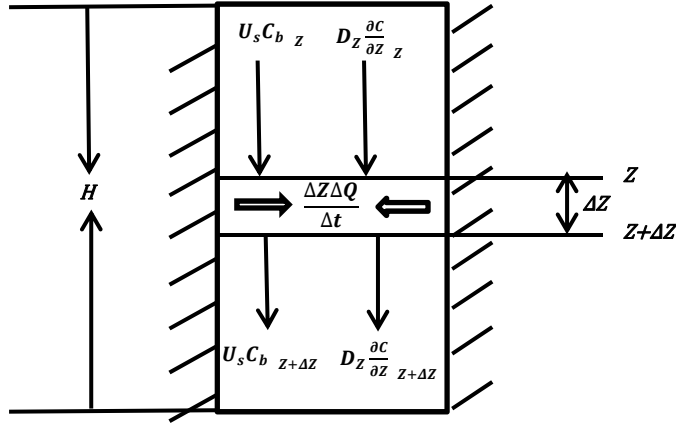
Figure 2.1 Control volume for mass balance considerations in fixed bed adsorption [86]

Eq. (2.53) is a general mass balance equation correlating the solid phase and the fluid phase in a packed-bed system. Together with the sorption rate and sorption isotherm equations, they form the governing equations for packed bed column sorption behaviour. Both sorption rate and sorption isotherm equations can be determined from the batch sorption studies [161]. The combination of these equations usually requires complex numerical methods to solve, and thus it is challenging to establish a general model for the packed-bed adsorption system. However, solutions are available for simplified models under some assumptions for certain circumstances. In the following section, a few widely used mathematical models for characterizing the column adsorption performance will be discussed in details.

2.7.2.1 The Adams-Bohart, Bed depth and service time (BDST), and Wolborska model

The fundamental equation describing the relationship between C/C_0 and t in a flow system was established by Adams and Bohart in 1920 when analyzing the typical chorine-charcoal transmission curve [162]. Assuming that the rate of "reaction" is proportional to

residual adsorption capacity of the sorbent and to the concentration of the sorbate in the solution, then following equations were obtained:

$$\frac{\partial Q}{\partial t} = -kQC \tag{2.54}$$

$$\frac{\partial c}{\partial z} = \frac{-kQC}{u} \tag{2.55}$$

where Q is the adsorption capacity available for taking up additional solute in the solution, C is the concentration of solute at a given distance, u is the linear flow rate and k is kinetic constant of the Adams-Bohart model.

By applying the boundary condition:

$$\begin{cases} t = 0, Q = Q_0 \\ z = 0, c = c_0 \end{cases}$$

The solution to the differential equations is:

$$\ln\left(\frac{C_0}{C} - 1\right) = \ln\left(e^{\frac{kQ_0Z}{u}} - 1\right) - kC_0t \tag{2.56}$$

It is reasonable to assume that the exponential term $e^{\frac{kQ_0Z}{v}}$ is much larger than 1, so Eq. (2.56) can be reduced to

$$\ln\left(\frac{C_0}{C} - 1\right) = \frac{kQ_0Z}{u} - kC_0t \tag{2.57}$$

Eq. (2.57) is the so called bed depth service time (BDST) model proposed by Huchins in 1973 [163]. The BDST model involves two variables for the sorption system: Z (the bed depth), and u (the linear flow rate). The BDST model has been widely used in predicting breakthrough curves in the fixed-bed sorption [164-167].

Ko et al. [168] pointed out that the BDST model ignored the intraparticle mass transfer resistance and the external film resistance such that the sorbate is considered to

adsorb onto the adsorbent surface directly. They proposed to modify the term bed sorption capacity Q_0 so that it would be a time-dependent quantity:

$$Q_t = Q_0(1 - \exp(-a\sqrt{t}))$$ (2.58)

where a is a rate parameter which depends on the mass transfer resistance.

Incorporating Eq. (2.58) into Eq. (2.57) gives:

$$\ln\left(\frac{C_0}{C} - 1\right) = \frac{kQ_0(1 - \exp(-a\sqrt{t})Z}{u} - kC_0t$$ (2.59)

Wolborska [169] studied the breakthrough behaviour in low-concentration range and made the following two assumptions: (1) the initial concentration distribution is translocated along the column at a constant velocity; (2) the low-concentration regions is characterized by constant kinetic coefficient and controlled by the external mass transfer. Then the following equations were formulated:

$$x = h - wt$$ (2.60)

where w is a constant velocity of the migration of the concentration fronts along the bed, and x is the bed height and h is the distance from the column inlet.

$$\frac{\partial Q}{\partial t} = \beta(c - c_i)$$ (2.61)

where β is the kinetic coefficient of the external mass transfer, c_i is the sorbate concentration at the interface and c is the sorbate concentration in the solution. With Eq. (2.60), (2.61) , and the mass balance equation Eq. (2.53), the breakthrough curve in low concentration range can be determined [169]:

$$ln\frac{c}{c_0} = \frac{\beta C_0 t}{Q_0} - \frac{\beta}{u}h$$ (2.62)

By comparing Eq. (2.62) with Eq. (2.57), we notice that the expression of Wolborska model is actually equivalent to the BDST model if β equals to $Q_0\ k_{AB}$ and $\ln\left(\frac{C_0}{C}-1\right)$ is approximated to $ln\frac{c}{c_0}$.

2.7.2.2 The Thomas model

The Thomas model is another widely used model for packed bed adsorption. It is based on the following assumptions [170, 171]:

(1) The axial diffusion is negligible so the mass balance can be simplified to:

$$\frac{\partial C}{\partial t}+\frac{\partial Q}{\partial t}+U_z\frac{\partial C}{\partial Z}=0 \tag{2.63}$$

(2) Film diffusion and internal diffusion are not rate-determining factors, and the rate of sorption is determined by chemical effects (i.e., surface reaction).

(3) The adsorption process complies with the Langmuir type isotherm at equilibrium and Langmuir kinetics.

Suppose the rate of adsorption is proportional to the product of the "concentration of empty holes" on the adsorbent and the concentration of solute in solution being adsorbed, and that the rate of desorption is first order with respect to the concentration of the adsorbed material. One can write:

$$\frac{\partial Q}{\partial t}=k_1(Q_0-Q)C-k_2Q \tag{2.64}$$

where k_1 and k_2 are the rate constants of the adsorption and desorption, respectively, and Q_0 is the initial adsorption capacity of the adsorbent.

By substituting Eq. (2.64) into Eq. (2.63), the following expression was obtained:

$$\ln\left(\frac{C_0}{C} - 1\right) = \frac{k_{Th}Q_0m}{F} - k_{Th}C_0t \tag{2.65}$$

where k_{Th} is the Thomas rate constant, m is the mass of adsorbent in the column, Q_0 is the maximum solid-phase concentration of the solute, and F is the volumetric flow rate.

It is worth noting that Eq. (2.63) is very similar to Eq. (2.53). One primary limitation of the Thomas model comes from neglecting the effect of external diffusion, and surface reaction kinetics is considered to be the only factor determining the sorption rate. Sorption process sometimes can be controlled or affected by diffusion and this discrepancy can lead deviations in model predictions.

2.7.2.3 The Clark model

In 1987, Clark [172] developed a model to predict the performance of system to adsorb organic compounds. The Clark model was derived based on the following [160]:

(1) The liquid-phase mass balance equation:

$$J = u\frac{dC}{dZ} \tag{2.66}$$

where J is the mass-transfer rate per unit reactor volume (mg of solute $h^{-1} \cdot cm^{-3}$), u is the linear flow rate (cm/h).

(2) The sorption isotherm obeys the Freundlich type:

$$Q_F = k_F(C_e)^{1/n} \tag{2.67}$$

(3) The adsorption rate is:

$$J = u\frac{dC}{dz} = k_T(C - C_e) \tag{2.68}$$

where k_T is the mass-transfer coefficient.

Defining:

56

$$r = \left(\frac{k_T}{u}\right)\frac{dZ}{dt}(n-1) \tag{2.69}$$

$$A = \left(\frac{C_0}{C} - 1\right)e^{rt} \tag{2.70}$$

The following equation is obtained:

$$C = \left(\frac{C_0{}^{n-1}}{1 + Ae^{-rt}}\right)^{\left(\frac{1}{n-1}\right)} \tag{2.71}$$

Based on Eq. (2.71), one can get parameters A and r through non-linear regression of the C vs. t data. Interestingly, neglecting two terms (i.e., $\frac{\partial c}{\partial t}$ and $D_Z\frac{\partial^2 c}{\partial Z^2}$) from Eq. (2.53) will yield Eq. (2.66). $\frac{\partial c}{\partial t}$ refers to the accumulation of sorbate concentration in a controlled volume and $D_Z\frac{\partial^2 c}{\partial Z^2}$ refers to flux due to axial diffusion. If one assumes uniformity of the control volume and neglects the molecular diffusion, then Eq. (2.53) can be converted to Eq. (2.66). The Clark model has successfully predicted a variety of adsorption systems, including some that even do not follow the assumptions used in the model derivation [160].

2.7.2.4 The Yoon-Nelson model

The Yoon-Nelson model proposed [173] is a relatively simple model for predicting the breakthrough curves. It is based on the assumption that the rate of decrease in the probability of adsorption for each molecule is proportional to q the probability for adsorption and p the probability for breakthrough:

$$-\frac{dQ}{dt} = k_{YN}pq = k_{YN}p(1-p) \tag{2.72}$$

Integration of Eq. (2.72) gives:

$$ln \frac{p}{1-p} = -k_{YN}(\tau - t) \tag{2.73}$$

Assuming $p = \frac{C_b}{C_0}$, one has:

$$ln \frac{C_b}{C_0 - C_b} = k_{YN}t - \tau k_{YN} \tag{2.74}$$

where k_{YN} is the kinetic rate constant of the Yoon-Nelson model and τ is the time required to obtain 50% breakthrough.

The Yoon-Nelson model is much simpler than others. It requires no detailed information about the bed height, flow rate, or the mass of the sorbate. On the other hand, limited by its simple form, it provides less valuable information for the dynamic adsorption system (e.g., the saturation bed capacity).

Chen et al. [174] and Huang et al. [175] investigated the adsorption of phenol on several modified XAD-4 resins packed in columns and used the Thomas model to fit the breakthrough curve. Adak and Pal [166] conducted the fixed bed sorption of phenol removal on surfactant-modified alumina. The effects of bed depth, flow rates and phenol inlet concentration on the sorption breakthrough were studied, and the column adsorption data was analyzed using the Adams and Bohart model. Sangeeta et al. [176] used a cross-linked starch based polymer to remove 4-NP, and the effects of initial solute concentration, bed height and flow rate on the breakthrough were investigated, The Yoon- Nelson model was fitted to the experimental data, and it was shown that the equilibrium adsorption capacity of 4-NP increased with an increase in the influent concentration and a decrease in the flow rate.

In some studies, more than one model may be used to describe the sorption in packed bed columns. Aksu and Gönen [165] used Adams-Bohart, Thomas, Clark and Yoon-Nelson models to predict the adsorption breakthrough of phenol using immobilized activated sludge

in a fixed bed. The Adams-Bohart model was shown to be valid for the low concentration range, the Clark model worked for higher flow rates and higher concentrations, and the Thomas model and the Yoon-Nelson model were able to describe breakthrough characteristics at a wider concentration range. Li et al. [177] used modified XAD-4 resins as adsorbent for phenol adsorption, four dynamic adsorption models (the Thomas, BDST, Clark, and Yoon-Nelson models) were used to characterize the dynamic adsorption data, all of the four models were reported to be suitable for representing the breakthrough curves. Srivastava et al. [164] studied the sorptive removal of phenol by Bagasse fly ash in a packed bed. Such operating conditions as the bed depth, flow rate, and phenol inlet concentration, and particle diameter of the adsorbent were examined. The experimental data were fitted by the Adam-Bohart, Wolborska, Thomas, Clark and Yoon-Nelson models. The bed depth service time (BDST) model at 50% breakthrough provided a good fit to the experimental data and the predicted column adsorption capacity is very close to that determined from the batch study. The Wolborska model is shown to work at low concentration range ($C/C_0 < 0.5$), and kinetic coefficient for mass transfer was determined by this model. The dynamic adsorption behaviour for the concentration range ($0.08 < C/C_0 < 0.99$) were well described by the Thomas, Clark and Yoon-Nelson models.

More recently, Garba et al. [178] studied phenol removal in a fixed bed packed with modified palm shell-based carbon. Breakthrough curves were obtained for different flow rates, bed depths and inlet concentrations. The Adam-Bohart, Thomas and Yoon-Nelson models were used to fit to the experimental data, but only the Yoon-Nelson model worked. Singh and Balomajumder [167] used modified rice husk as biosorbent for phenol and cyanide. The column performance was evaluated at different initial concentrations, flow rates and bed

depths. The Thomas, Adams-Bohart, Wolborska, and Yoon-Nelson models were fitted to the experimental data; while Thomas model was found to be the best for phenol, the Yoon–Nelson Model provided a good agreement with experimental data for both phenol and cyanide. Girish and Murty [179] used a forest waste to remove phenol in a fixed bed column. The effects of bed height, initial phenol concentration and feed flow rate on the performance of the column were studied. The experimental data were fitted to using the Thomas, Adams-Bohart, Yoon-Nelson, Modified dose-response, and linear driving force model. Both the Thomas model and the linear driving force model were found to be in good agreement with the experimental data.

Other models were also adopted to analyze the adsorption of phenolic compounds in fixed bed systems. For instances, the axial dispersion model has been used in the adsorption of phenol on activated carbon from date's stones [180] and pinus pinaster bark [181] packed in fixed beds. Constant-pattern wave approach was also used in some studies. Chern and Chien [182] used the constant-pattern wave approach with the Langmuir and Freundlich models to analyze the fixed bed adsorption of 4-NP on activated carbon. Juang et al. [183] also used the constant-pattern wave approach with Langmuir model to fit the sorption of phenol, 3-nitrophenol and 2-methylphenol on the surfactant-modified montmorillonite. Pan et al. [184] used the constant-pattern wave approach with Freundlich model to describe the fixed-bed adsorption of phenol and 4-NP on polymeric resin adsorbent. The homogeneous surface diffusion model (HSDM) [185] was also used to describe the dynamic adsorption of phenolic compounds in some cases.

Table 2.6 lists studies of packed-bed adsorption of phenolic compounds using various adsorbents.

Table 2.6 Fixed-bed adsorption of phenolic compounds by different sorbents

Adsorbent	Solute	Model	Ref
Immobilized activated sludge	Phenol	Adam-Bohart, Wolborska, Thomas, Clark, and Yoon-Nelson model	[165]
XAD-4 and modified resins	Phenol, 2-methoxyphenol	Thomas model	[174]
Modified XAD-4 resins	Phenol	Thomas model	[175]
Modified XAD-4 resins	Phenol	Thomas, BDST, Clark and Yoon-Nelson model	[177]
Activated carbon	4-CP	Homogeneous surface diffusion model	[157]
Cross-linked starch based polymer	4-NP	Yoon-Nelson model	[176]
Surface-modified alumina	Phenol	Adam-Bohart model	[166]
Activated charcoal	Catechol	Homogeneous surface diffusion model	[185]
Bagasse fly ash	Phenol	Thomas, Adam-Bhart, Clark, Yoon-Nelson, Wolborska	[164]
Activated carbon	Phenol	Axial dispersion model	[180]
Activated carbon	4-NP	Constant-pattern wave approach with the Langmuir and Freundlich models	[182]
Modified palm shell-based carbon	Phenol	Adam-Bohart, Thomas, and Yoon-Nelson model	[178]
Modified rice husk	Phenol	Adam-Bohart, Thomas, Wolborska and Yoon-Nelson model	[167]
Forest waste	Phenol	Adam-Bohart, Thomas, Yoon-Nelson, modified dose-response, and linear driving force model	[179]
Surfactant-modified montmorillonite	Phenol, 2-MP, 3-NP,	Constant-pattern wave approach with the Langmuir model	[183]
Pinus pinaster bark	Phenol	Axial dispersion model	[181]
Oil-palm-shell activated carbons	Phenol	Linear driving force model	[186]
Polymeric resin adsorbent	Phenol, 4-NP	Constant pattern wave approach with the Freundlich model	[184]

Chapter 3

Equilibrium study of sorption of phenolic compounds in PEBA: single-solute systems

3.1 Introduction

Poly(ether block amide) (PEBA) is a thermoplastic elastomer produced by polycondensation of a dicarboxylic polyamide and a polyether diol. It has good low temperature flexibility, high strength and toughness [187]. The general formula of PEBA is

$$\text{HO} \left[\overset{\overset{\displaystyle O}{\|}}{C} - PA - \overset{\overset{\displaystyle O}{\|}}{C} - O - PE - O \right]_n H$$
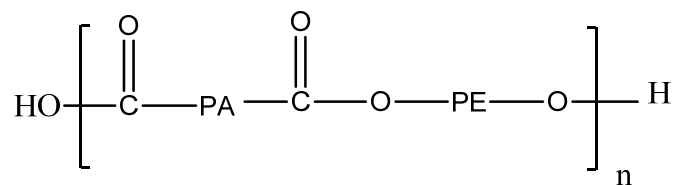
where PA represents polyamide and PE represents polyether. The combination of the rigid polyamide block and the flexible polyether block yields a block copolymer that exhibits a two-microphase structure: a crystalline phase due to the polyamide and an amorphous phase due to the polyether [187].

PEBA membranes have been widely used in pervaporation to remove phenolic compounds from aqueous solutions [7, 188]. Kujawski et al. [49] compared the separation properties of PEBA and poly(dimethylsiloxane) membranes in pervaporation of water-phenol mixtures and found that the PEBA membranes showed a better selectivity to phenol. Böddeker et al. [50] prepared PEBA membranes from different grades of PEBA (Shore D hardness 35, 40 and 55) for pervaporative separation of phenol from wastewater. In order to better understand the good selectivity of PEBA membrane to phenolic compounds, Groβ and

Heintz [188] studied the solubility and diffusivity of phenol, 2-chlorophenol and 4-nitrophenol in PEBA 4033 (Shore D hardness 40) membrane.

PEBA 2533 (Shore D hardness 25) comprises 20 wt.% nylon 12 as the amide segments and 80 wt.% poly(teteramethylene oxide) as the ether segments. The formula of PEBA 2533 can be expressed as：
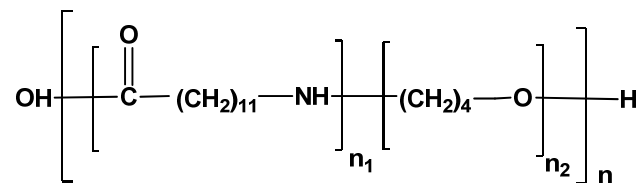
Compared with other grades, PEBA 2533 has a high polyether content (~80 wt.%) and excellent phenol selectivity [5, 189, 190]. The study of Hao et al. [5] showed that the good permselectivity of the PEBA 2533 membrane for phenol/water separation derived from the high solubility selectivity, revealing that PEBA 2533 has excellent affinity to phenol. PEBA 2533 is thus expected to be an effective sorbent for phenolic compounds. To our best knowledge, it has not been used as a sorbent for removal of phenolic compounds from wastewater.
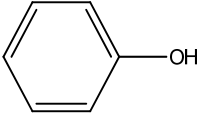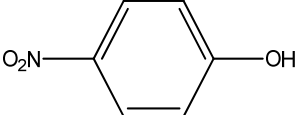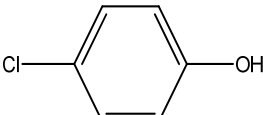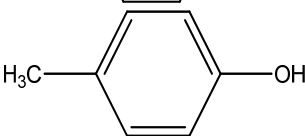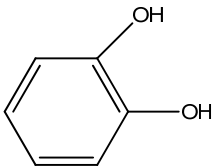
In this work, the sorption of phenolic compounds in PEBA was studied. The sorption isotherm can help understand the sorption mechanism. Three isotherm models (the Linear, Langmuir and Freundlich models) were used to analyze the experimental data. Based on the equilibrium sorption parameters, additional thermodynamic parameters can be determined to provide useful information about the type and the mechanism of the sorption process. The standard free energy change (ΔG^o) can be used to determine whether the adsorption process is spontaneous. The standard enthalpy change (ΔH^o) indicates if the adsorption process is

endothermic or exothermic. The standard entropy change (ΔS^o) reflects the change of randomness at the solid-solution interface during the adsorption.

3.2 Materials

PEBA 2533 was provided by Arkema Incooperated. N,N-dimethylacetamide (purity 99+%), 4-nitrophenol (purity 98%), 4-chlorophenol (purity 99+%), 4-methylphenol (purity 99+%), and catechol (purity 99+%) were purchased from Acros Organics Company. Phenol (purity 99%) was purchased from BDH Chemicals Ltd. Some physical properties of the sorbates used in this study are listed in Table 3.1.

Table 3.1 Physical properties of phenolic compounds used in this study

Compound	Molecular structure	Mol.wt (g/mol)	Solubility in water(g/100 mL at 20^0C)	λ_{max} (nm)	pK_a
Phenol		94.11	8.3	269	9.95
4-nitrophneol		139.11	1.16	317	7.15
4-chlorophenol		128.6	2.7	279	9.41
4-methylphenol		108.13	2.0	276	10.26
Catechol		110.1	43	274	9.48

λ_{max}: wavelength of the maximum sorption of light in a solution
pK_a: the negative decadic logarithm of the dissociation constant K_a of an acid

3.3 Experimental

In order to evaluate the sorption properties of PEBA, the PEBA membranes of known thicknesses and areas were used as the sorbent.

3.3.1 Preparation of PEBA membranes

Pellets of PEBA 2533 were dissolved in N,N-dimethylacetamide to form a 15 wt.% solution. The mixture was heated in water bath at $80^{o}C$ with vigorous mixing for two hours. The homogenous solution was allowed to stand for 24 hours to remove entrapped air bubbles. The membranes were prepared by pouring the solution into a Petri dish, followed by heating in an oven at $70^{o}C$ for 36 hours to evaporate the solvent. The membranes were washed several times with deionized water and dried in an oven at $50^{o}C$ for 8 h to ensure that all residual solvent was completely removed. In order to decrease the time required for the sorption equilibrium, thin membranes (thickness<300 μm) were used in equilibrium sorption studies. The thickness of the membrane was controlled by the amount of the polymer solution used in preparing the membrane and the membrane thickness was measured using a Starrett micrometer.

3.3.2 Sorption equilibrium study

Batch adsorption experiments were carried out in 125 mL glass bottles. Firstly, various solutions of phenolic compounds with known initial concentrations ranging from 50 to 10,000 ppm were prepared. Then PEBA membrane samples were weighed and immersed into the aqueous solutions of phenolic compounds. Preliminary experiments had shown that 24 hours were long enough for the adsorption process in membranes with thicknesses less

than 300 μm to reach equilibrium. Therefore, each adsorption measurement lasted for at least 24 hours at desired temperatures. The concentration of phenolic compounds was determined by a Shimadzu UV mini 1240 UV-Vis spectrophotometer. Calibration curves for determining the concentration of different phenolic compounds in water by spectrophotometry were attached in the Appendix. The equilibrium adsorption uptake Q_e (mmol/g) was calculated by

$$Q_e = \frac{V \times (C_0 - C_e)}{M}$$
(3.1)

where C_0 and C_e are the concentrations of solute in the solution at the beginning and at equilibrium (mmol/L), respectively, V is the volume of the solution (L), and M is the weight of the PEBA membrane sorbent (g). The sorption experiments were replicated, and the experimental error was found to be within 3%.

3.4 Results and discussion

3.4.1 Sorption isotherms

Figures 3.1(a)-(e) show the adsorption isotherms of phenol, 4-CP, 4-NP, 4-MP, and catechol in PEBA membrane at different temperatures. The equilibrium uptakes of phenolic compounds (mmol/g) were plotted against their equilibrium concentrations (mmol/L) at different temperatures. The reason for characterizing equilibrium uptake by mmol/g will be discussed in Chapter 4.

It is shown that the phenolic compounds have different sorption capacities in the PEBA sorbent. The sorption capacity of catechol is much lower than the sorption capacity of 4-CP at a given equilibrium concentration. In general, a lower temperature is favourable for the sorption of the compounds studied here. The equilibrium uptake decreases with an increase in temperature, which indicates that the sorption process is exothermic in nature.
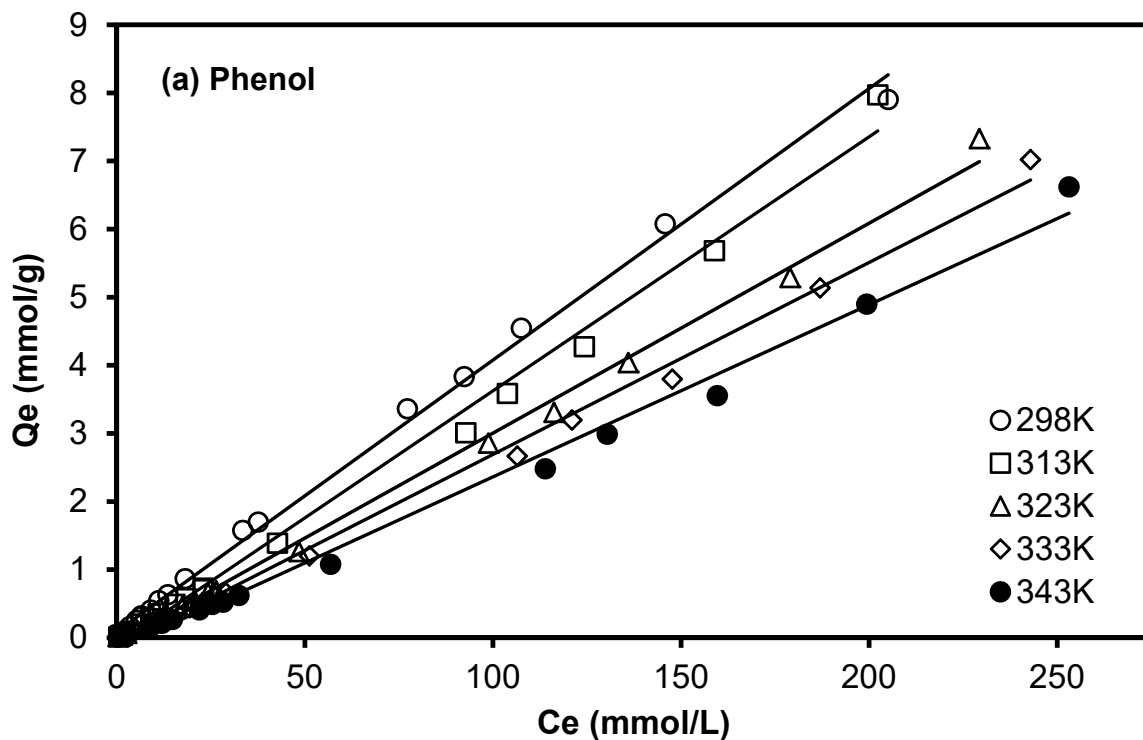
Figure 3.1(a) Sorption isotherms of phenol in PEBA at different temperatures
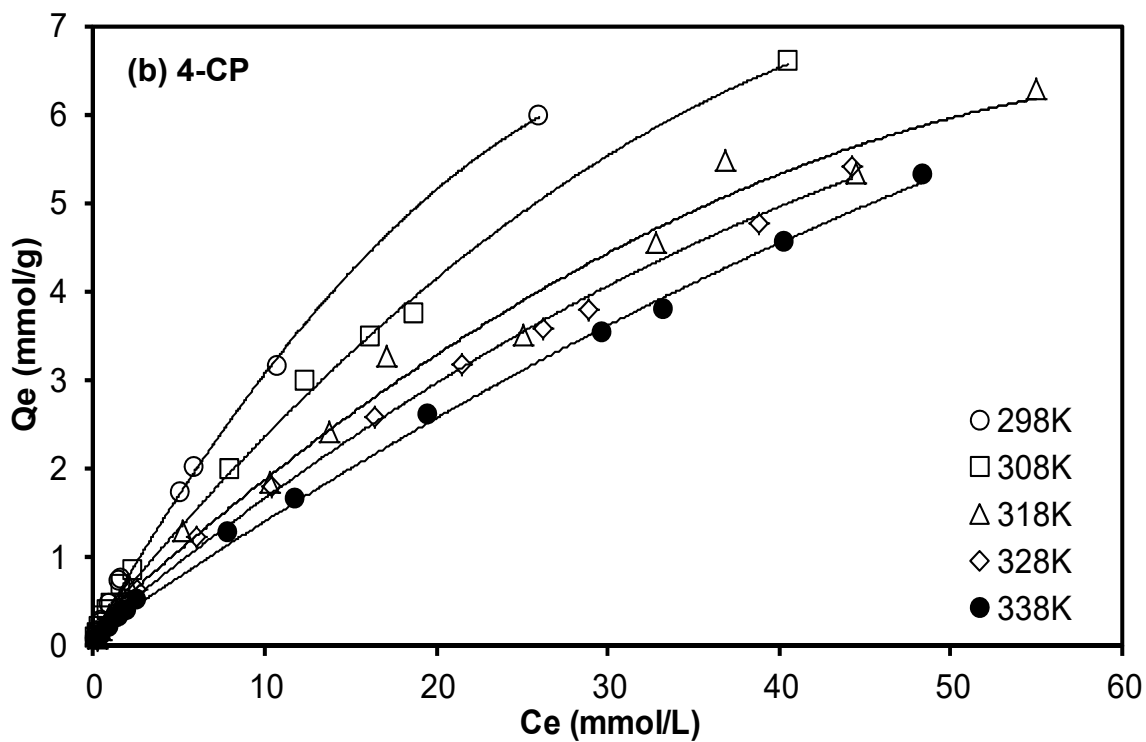
Figure 3.1(b) Sorption isotherms of 4-CP in PEBA at different temperatures

67
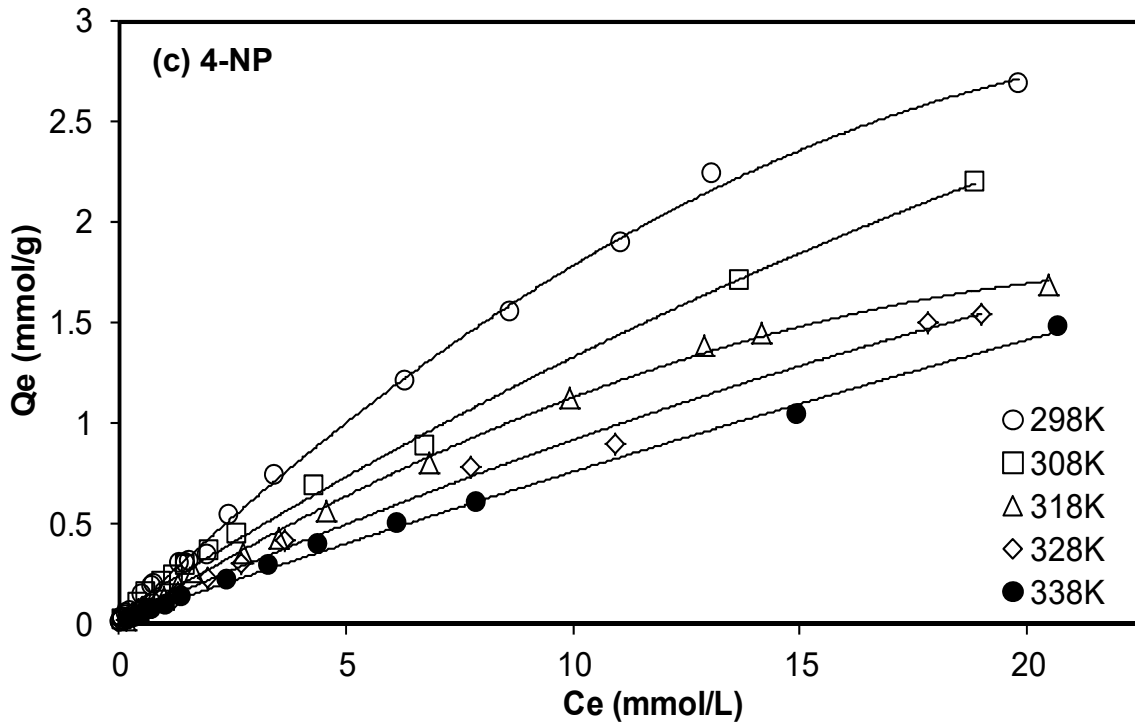
Figure 3.1(c) Sorption isotherms of 4-NP in PEBA at different temperatures
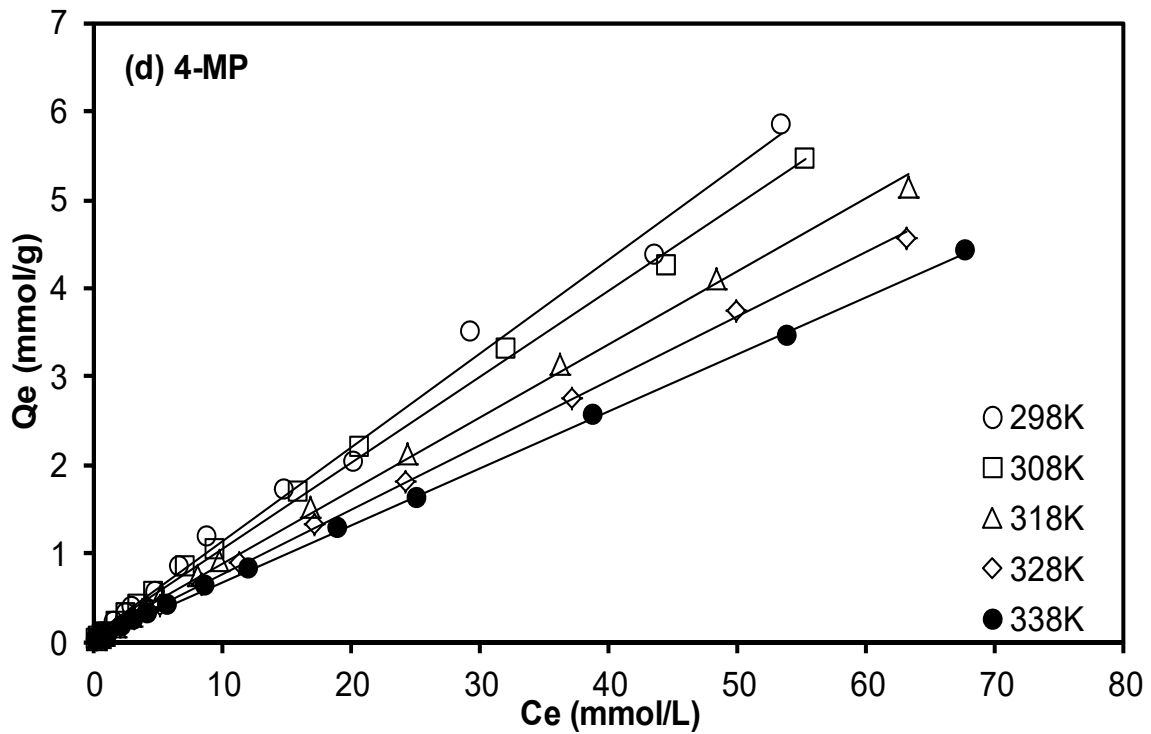
Figure 3.1(d) Sorption isotherms of 4-MP in PEBA at different temperatures
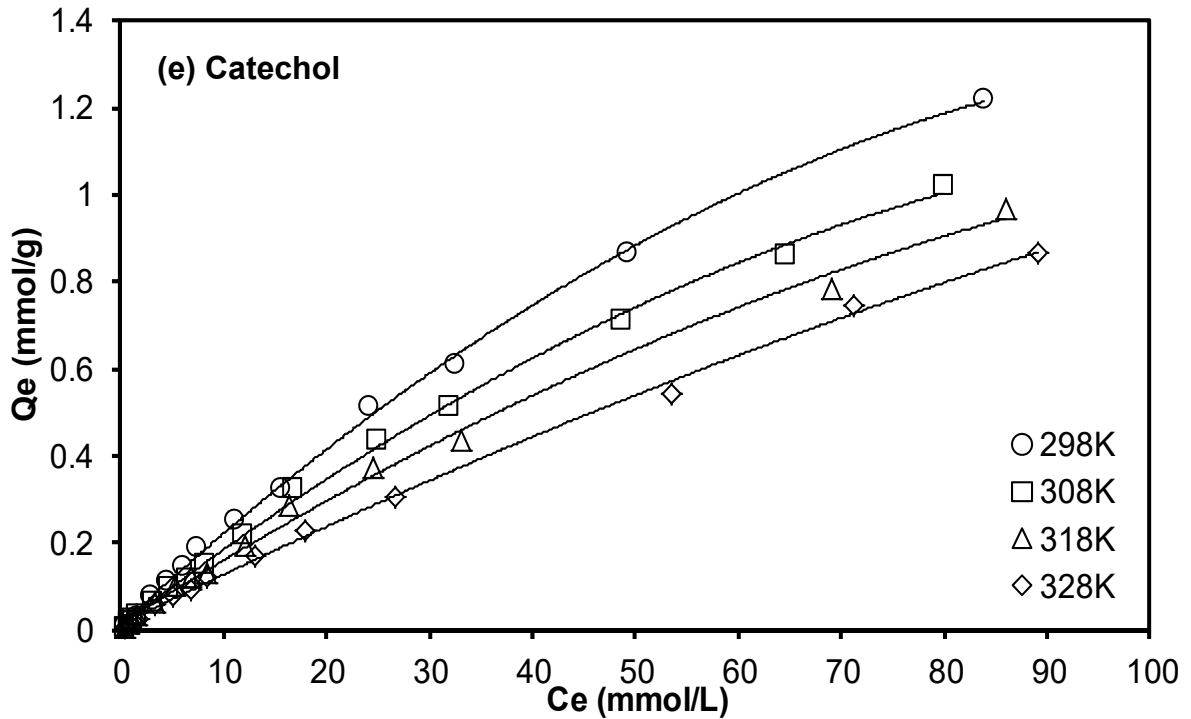
Figure 3.1(e) Sorption isotherms of catechol in PEBA at different temperatures

3.4.2 Equilibrium modeling

Three models were used to analyze the experimental data presented in Figures 3.1(a)-(e). The linear isotherm model was expressed by Eq. (2.3), and the linearized forms of the Langmuir and Freundlich isotherm models were represented by Eq. (2.9) and Eq. (2.11), respectively.

Q_e was plotted against C_e for the linear model; $1/Q_e$ was plotted against $1/C_e$ for the Langmuir model; Q_e was plotted against C_e in log scale for the Freundlich model. The sorption plots for the five phenolic compounds are shown in Figures 3.2-3.6, where the model parameters and correlation coefficient for each model are presented in Table 3.2.
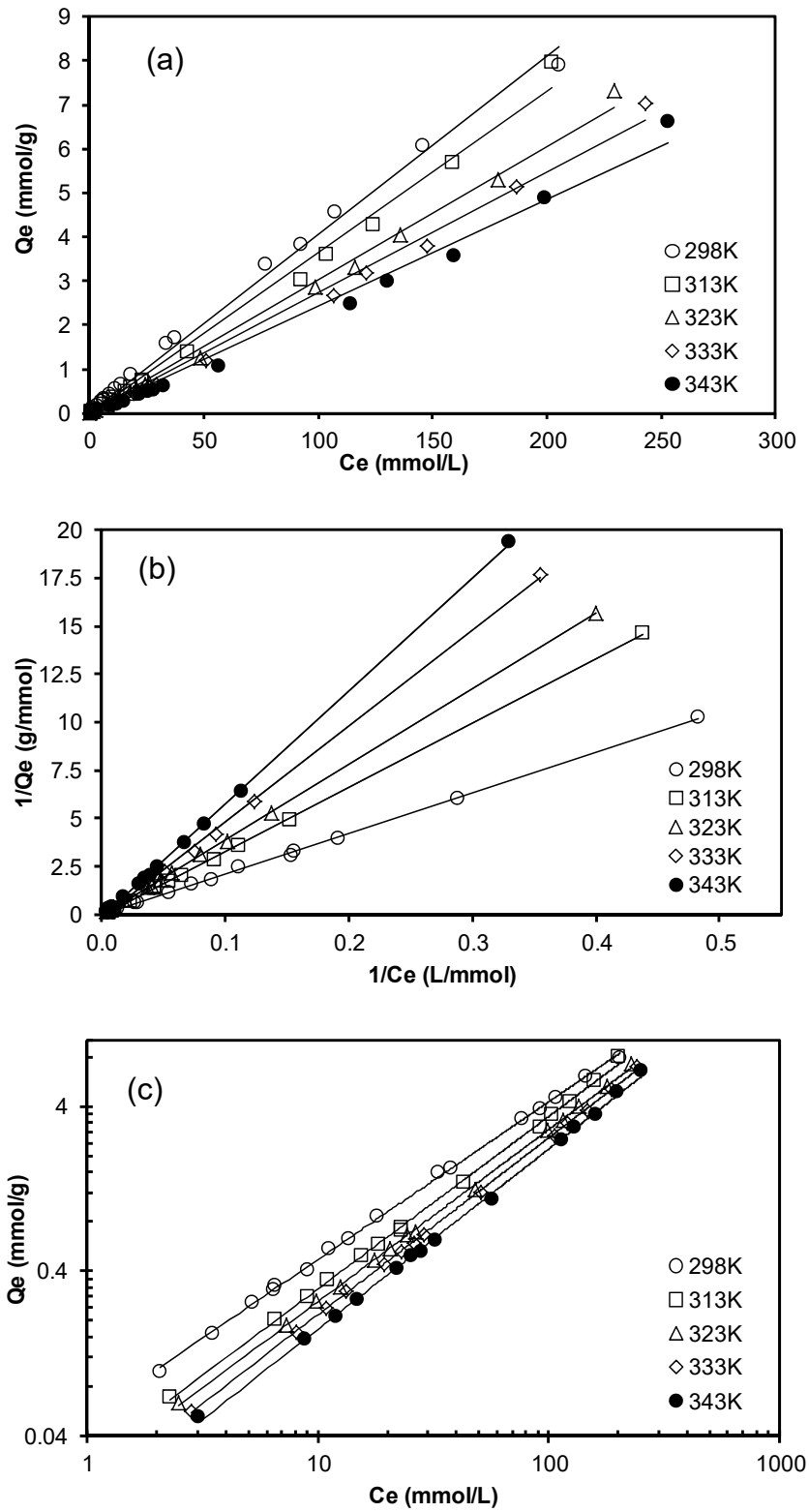
.Figure 3.2 The (a) linear, (b) Langmuir, and (c) Freundlich models of sorption of phenol in PEBA

70
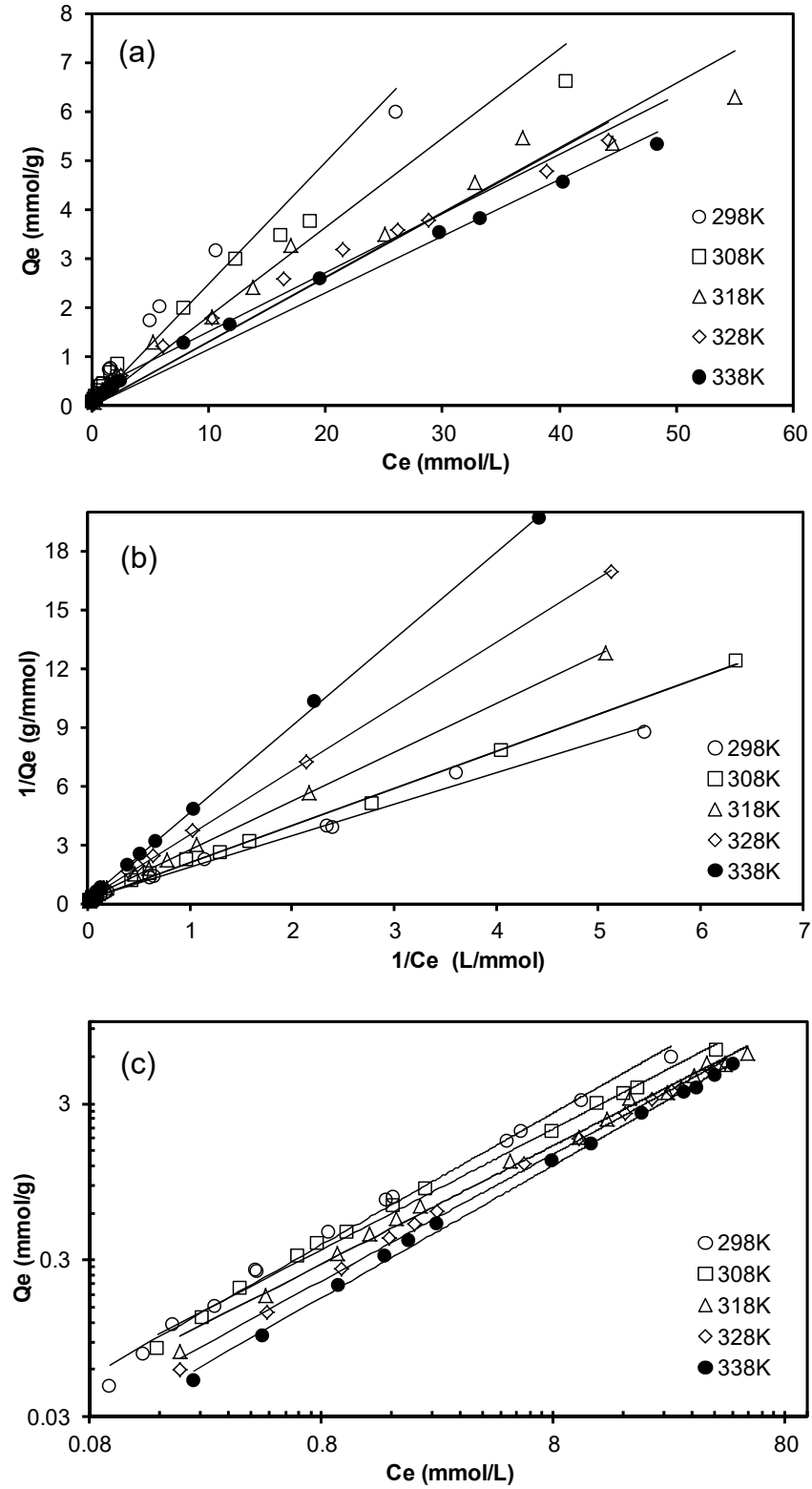
Figure 3.3 The (a) linear, (b) Langmuir, and (c) Freundlich models of sorption of 4-CP in PEBA
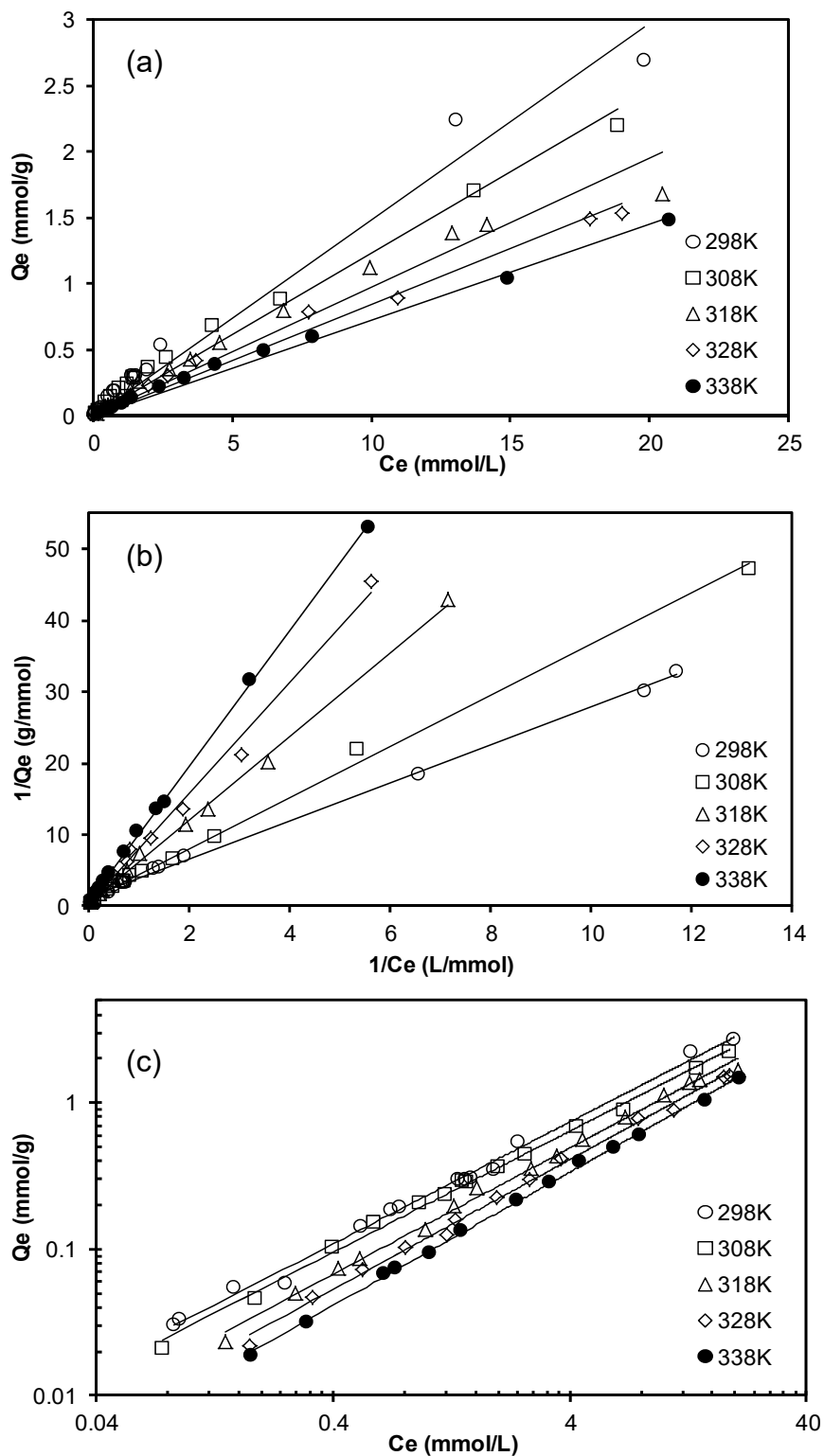
Figure 3.4 The (a) linear, (b) Langmuir, and (c) Freundlich models of sorption of 4-NP in PEBA
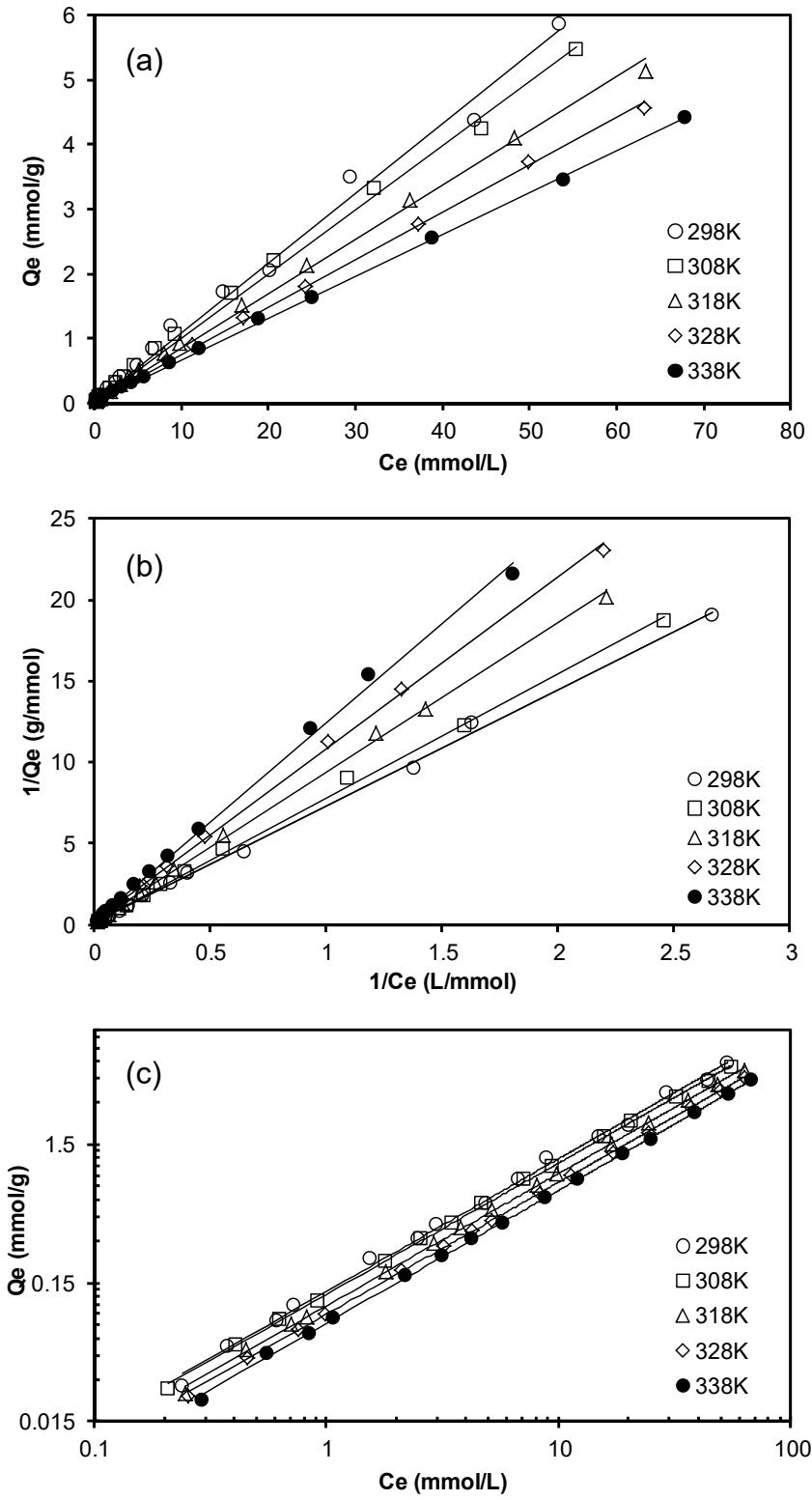
Figure 3.5 The (a) linear, (b) Langmuir, and (c) Freundlich models of sorption of 4-MP in PEBA
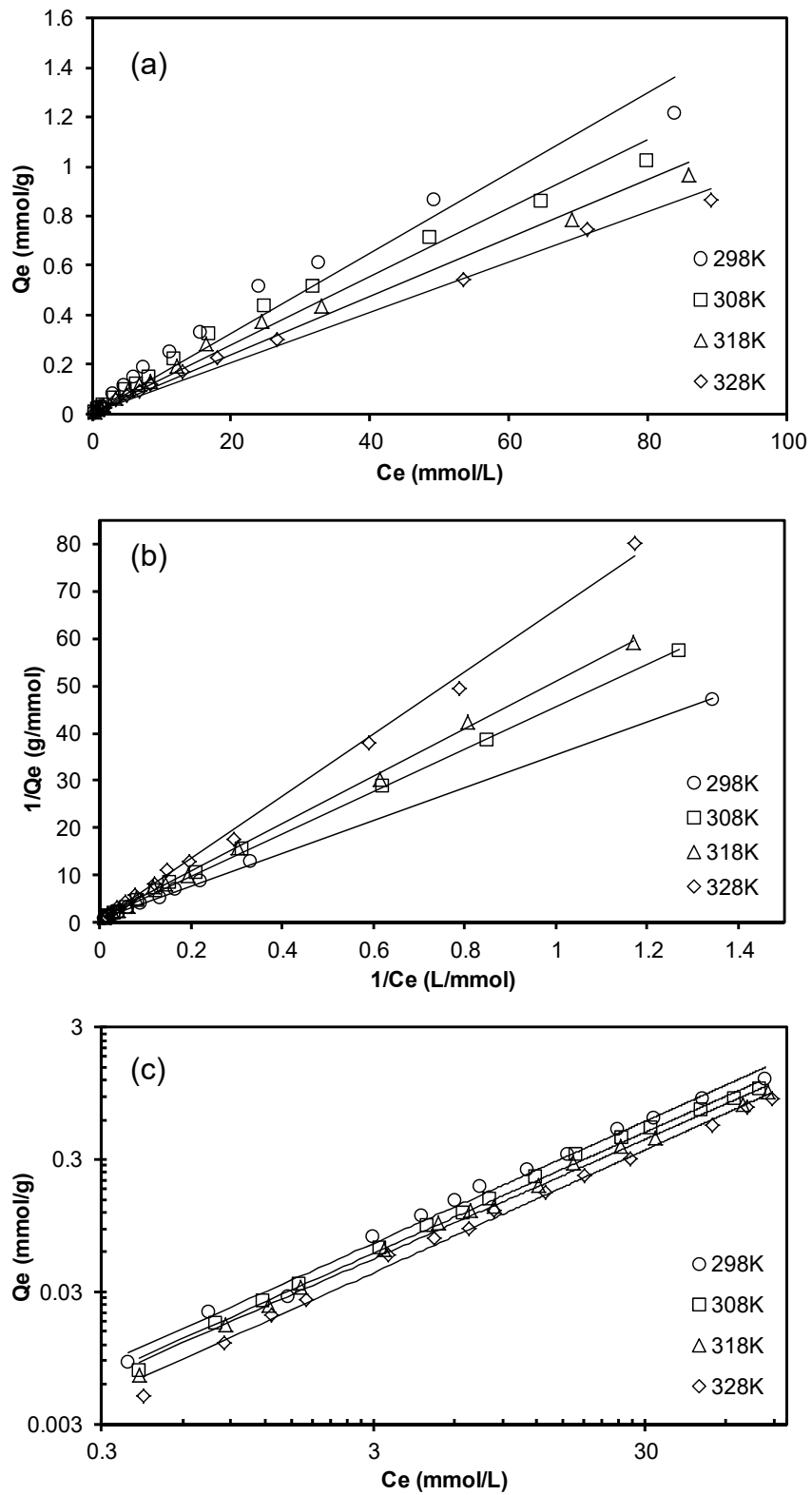
Figure 3.6 The (a) linear, (b) Langmuir, and (c) Freundlich models of sorption of catechol in PEBA

Table.3.2 Parameters of the linear, Langmuir and Freundlich models for the sorption of phenolic compounds in PEBA

	Linear isotherm		Langmuir isotherm			Freundlich isotherm		
	K_H (L/g)	R^2	Q_m (mmol/g)	K_L (L/mmol)	R^2	K_F $(mmol)^{1-\frac{1}{n}}(\frac{L}{g})^{1/n}$	$1/n$	R^2
Phenol								
298K	0.0406	0.996	-9.81	-0.00457	0.998	0.0518	0.957	0.999
313K	0.0365	0.992	-12.8	-0.00233	0.999	0.0279	1.04	0.999
323K	0.0303	0.996	-17.3	-0.00147	0.999	0.0234	1.05	0.999
333K	0.0273	0.994	-4.98	-0.00402	0.998	0.0182	1.08	0.999
343K	0.0242	0.989	-5.99	-0.00283	0.999	0.0142	1.09	0.998
4-CP								
298K	0.248	0.962	6.90	0.0845	0.993	0.452	0.842	0.991
308K	0.182	0.950	4.89	0.108	0.998	0.415	0.781	0.995
318K	0.131	0.939	4.36	0.0922	0.999	0.332	0.777	0.992
328K	0.131	0.973	4.31	0.0707	0.999	0.263	0.811	0.997
338K	0.115	0.988	5.43	0.0415	0.999	0.208	0.849	0.997
4-NP								
298K	0.149	0.977	0.845	0.443	0.997	0.238	0.823	0.996
308K	0.123	0.977	1.18	0.235	0.997	0.203	0.827	0.996
318K	0.0977	0.954	2.67	0.0640	0.998	0.149	0.862	0.996
328K	0.0846	0.986	5.32	0.0242	0.993	0.120	0.885	0.996
338K	0.0727	0.992	1.82	0.0577	0.999	0.0951	0.909	0.999
4-MP								
298K	0.108	0.992	8.83	0.0158	0.998	0.136	0.939	0.998
308K	0.0996	0.997	6.18	0.0211	0.999	0.126	0.941	0.999
318K	0.0841	0.998	5.99	0.0181	0.999	0.105	0.945	0.999
328K	0.0739	0.999	4.74	0.0199	0.999	0.0907	0.946	0.999
338K	0.0651	0.999	4.44	0.0184	0.998	0.0789	0.949	0.999
Catechol								
298K	0.0162	0.960	1.29	0.0205	0.999	0.0303	0.864	0.992
308K	0.0139	0.975	1.29	0.0173	0.999	0.0230	0.891	0.996
318K	0.0118	0.975	1.38	0.0144	0.999	0.0214	0.875	0.994
328K	0.0102	0.991	3.80	0.0040	0.997	0.0168	0.891	0.997

Figures 3.2-3.6 show that the linear model appears to be only suitable for representing the sorption of phenol and 4-MP in PEBA, but not suitable for 4-CP, 4-NP and catechol. For sorption of phenol in PEBA, the values of Langmuir model parameters were negative, as shown in Table 3.2, which indicates that the Langmuir model does not work for sorption of phenol in PEBA. For the sorption of 4-CP, 4-NP, 4-MP and catechol in PEBA in this study, both the Langmuir and Freundlich models fit the sorption data well. Many other studies showed similar results. Li et al. [73] studied the removal of phenol, 4-CP and 4-NP by chitosan and its modified products, and they found that the sorption isotherm of phenols can be described by both the Langmuir and Freundlich models. Koyuncu et al. [59] reported the sorption isotherm of 4-NP on modified bentonites can be described by both the Langmuir and Freundlich models. Koumanova et al. [93] found that the sorption of 4-CP in bentonite and perlite follows both the Langmuir and Freundlich models. Shakir et al. [60] reported that both the Langmuir and Freundlich models fit well to catechol sorption on bentonite at various temperatures.

Since the linear model is only suitable for sorption of phenol and 4-MP in PEBA and the Langmuir model is not suitable for phenol adsorption, whereas the Freundlich model can fit all the sorption data, it is reasonable to use the Freundlich model parameters to explain and compare the adsorption properties among different phenolic compounds in PEBA.

As shown by Table 3.2, the parameter K_F decreases with an increase in the temperature. This is because the sorption is exothermic. Table 3.2 also indicate that the sorption capacity (in terms of K_F values) at the room temperature (298 K) increases in the order: catechol<phenol<4-MP<4-NP<4-CP.

The different adsorption capacities among the phenolic compounds are due to many factors. Their solubility in the solution is an important factor that can affect sorption capacity. For instance, the sorption capacity of catechol in PEBA is the smallest among all the phenolic compounds studied here, which can be ascribed to the largest solubility of catechol in water (43 g/100 mL), as shown in Table 3.1. The large solubility of catechol in water means water would like to retain catechol molecules in the solution phase. On the other side, the sorption capacity of 4-CP in PEBA is found to be the largest. But the solubility of 4-CP in water is small (2.7 g/100 mL), and it seems that the hydrophobic PEBA has a good affinity to the hydrophobic 4-CP. Li et al. [83] also reported that 4-CP had the highest adsorption capacity among all the phenolic compounds they studied. This is in agreement with an earlier study [191] where a high hydrophobicity of an organic compound was found to favour its sorption onto non-polar and moderately polar polymeric sorbents from aqueous solutions.

Chemical properties of the solutes can also affect the sorption capacity. It was observed that phenols with the electron withdrawing groups (e.g., $-NO_2$ and $-Cl$) had a larger sorption capacity than phenols with electron donating groups (e.g., $-OH$ and $-CH_3$). Moreno-Castilla et al. [192] studied the sorption of substituted phenols on activated carbon, and found the sorption capacity was in the following order: amino phenol<methylphenol<nitrophenol< chlorophenol. Phenols with electron donating groups $-NH_2$ and $-CH_3$ had lower adsorption capacity than those with electron withdrawing groups $-NO_2$ and $-Cl$. Li et al. [81] studied the sorption capacity of phenol, 4-MP, 4-NP and 4-CP on polymeric adsorbent XAD-4, and the sorption capacity increased in the order phenol<4-MP<4-NP<4-CP, which is in agreement with the results of this study.

3.4.3 Sorption thermodynamics

Thermodynamic parameters involved in the sorption processes were calculated from the thermodynamic equilibrium constant K_0, which is a function of temperature. K_0 can be obtained from K_L if the sorption follows the Langmuir model, or it can be derived from the distribution coefficient K_d. In our study, however, the sorption of phenol in PEBA did not obey the Langmuir model. Thus K_0 was determined from K_d since this method is applicable to all the phenolic compounds studied. According to the definition of K_d in Eq. (2.23), C_{ad} is the concentration of the solute in the adsorbent (mmol/L), which was obtained from:

$$C_{ad} = Q_e \times \rho$$

where Q_e (mmol/g) is the sorption uptake of solute in the sorbent at equilibrium, ρ is the density of PEBA sorbent (1000 g/L). According to Eq. (2.24), if we plot $\frac{C_{ad}}{C_e}$ vs. C_{ad} and extrapolate C_{ad} to zero, K_0 can be obtained from $\lim_{C_e \to 0, C_{ad} \to 0} \frac{C_{ad}}{C_e}$ [96], as shown in Figures 3.7(a)-(e).
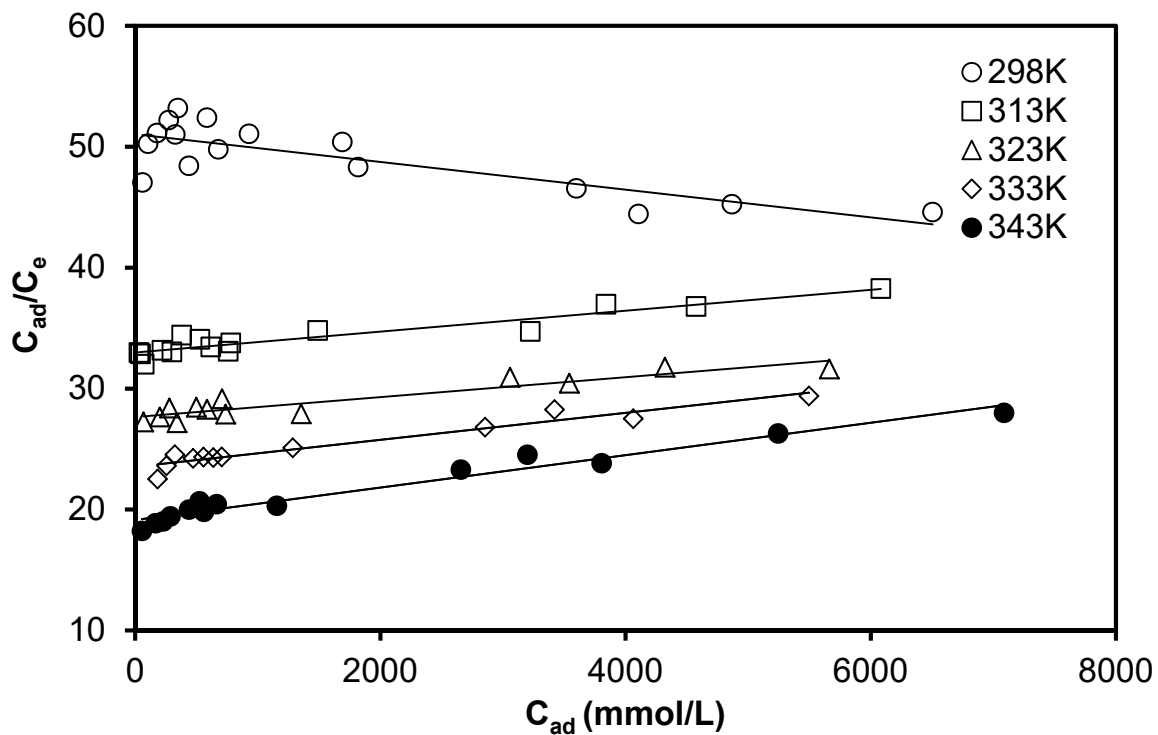
Figure 3.7(a) Plots of C_{ad}/C_e versus C_{ad} for phenol sorption in PEBA
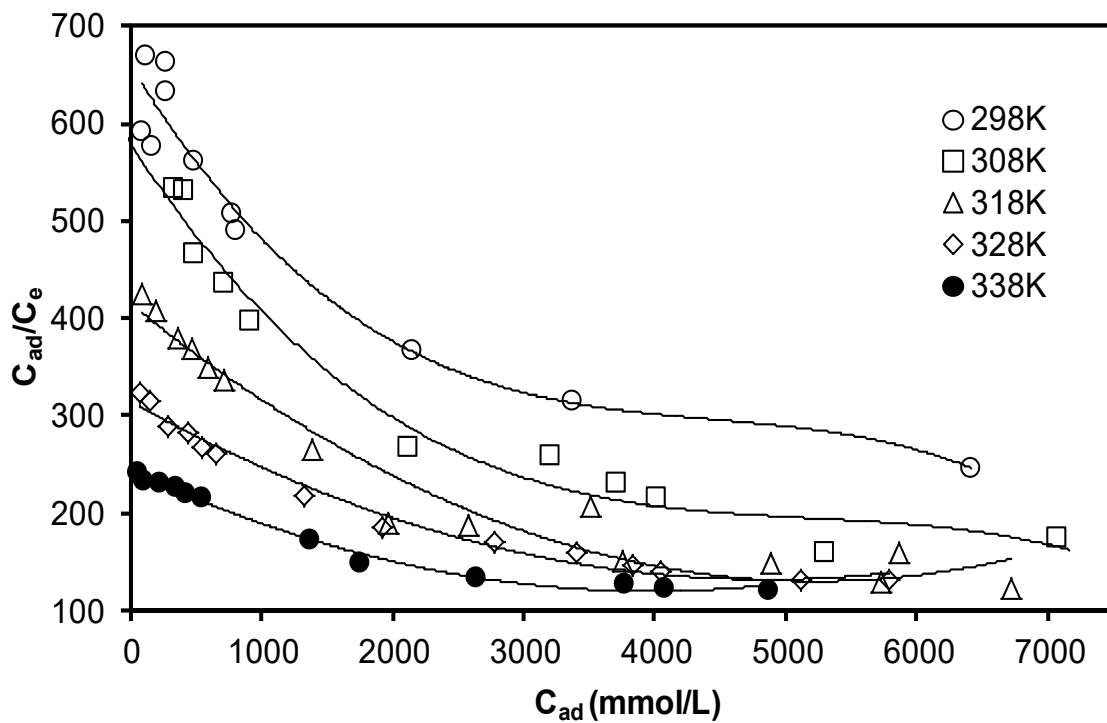
Figure 3.7(b) Plots of C_{ad}/C_e versus C_{ad} for 4-CP sorption in PEBA
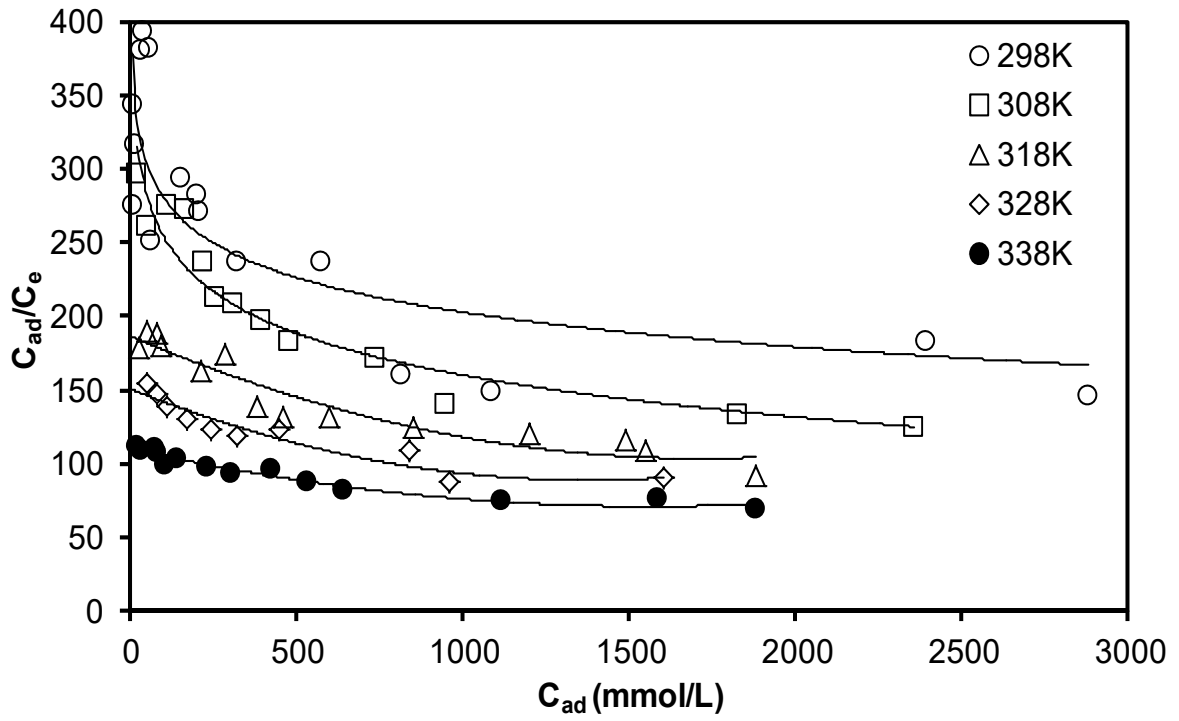
Figure 3.7(c) Plots of C_{ad}/C_e versus C_{ad} for 4-NP sorption in PEBA
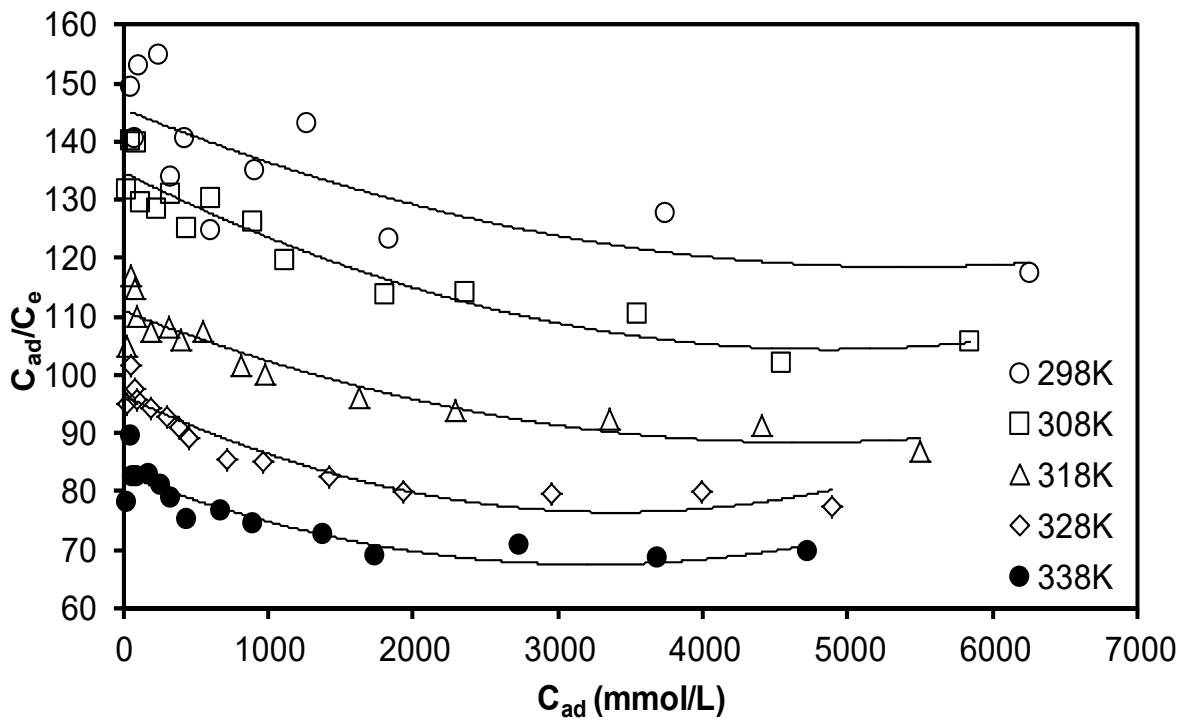
Figure 3.7(d) Plots of C_{ad}/C_e versus C_{ad} for 4-MP sorption in PEBA
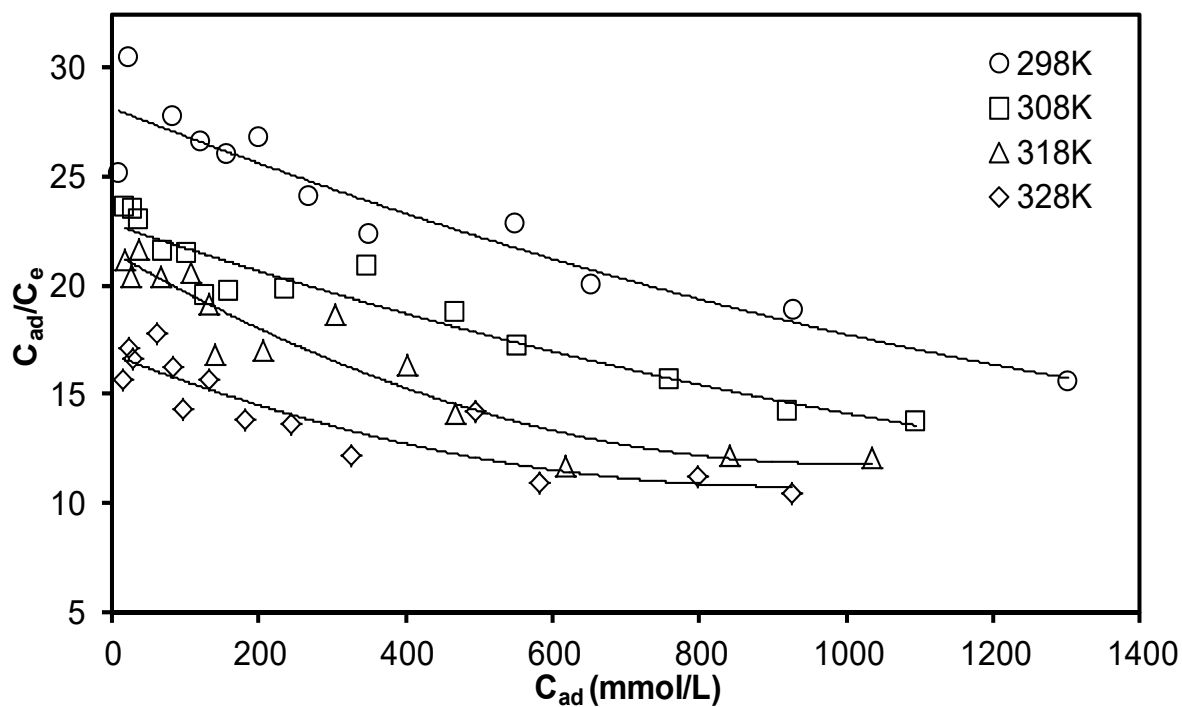
Figure 3.7(e) Plots of C_{ad}/C_e versus C_{ad} for catechol sorption in PEBA
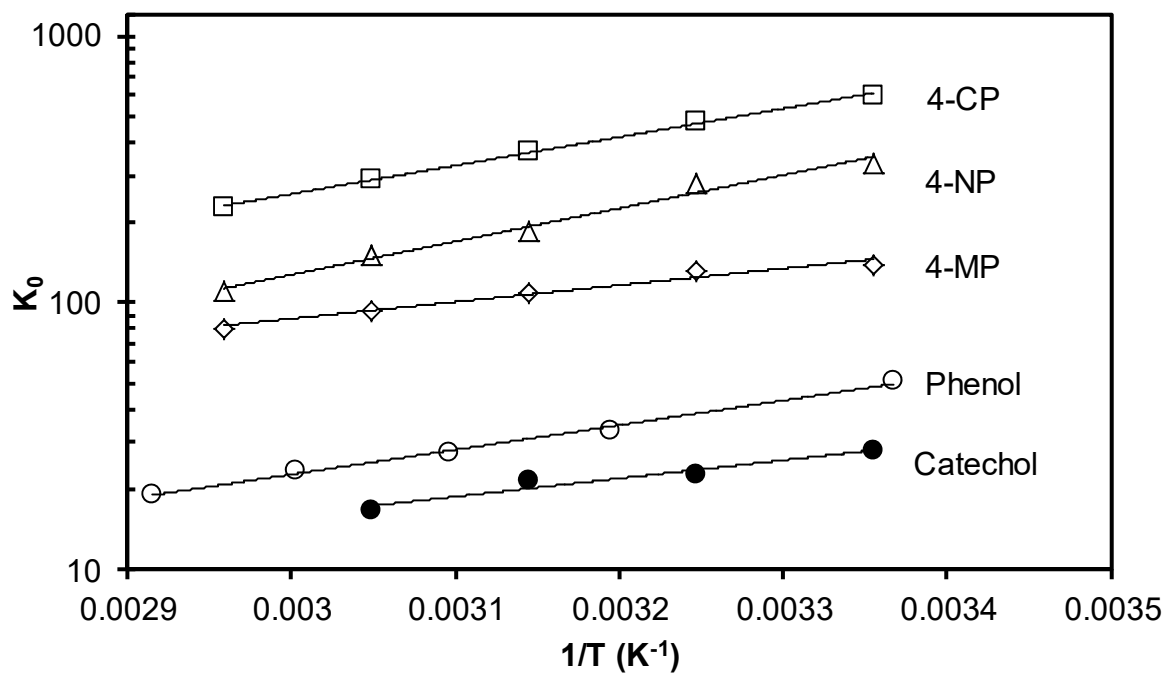
Figure 3.8 K_0 versus $1/T$ plots for phenolic compound sorption in PEBA

The estimated K_0 for different phenolic compounds at different temperatures were listed in Table 3.3. The change in the standard free energy ΔG^0 can be calculated from Eq. (2.12) and calculated ΔG^0 are presented at Table 3.3. The change in the standard enthalpy ΔH^0 and the change in the standard entropy ΔS^0 can be obtained from the slope and the intercept of $\ln K_0$ vs. $1/T$ plots according to Eq. (2.13). The K_0 vs. $1/T$ plots on a semi-log scale for all phenolic compounds are shown in Figure 3.8, and the calculated values of ΔH^0 and ΔS^0 are shown in Table 3.3.

As shown in Table 3.3, all the ΔG^0 values are negative, confirming that the sorption of phenol, 4-CP, 4-NP, 4-MP, and catechol in PEBA was spontaneous. The negative ΔH^o values suggest the sorption process was exothermic, which is supported by the observation that sorption capacities decreased with increasing temperature.

Table 3.3 Thermodynamic parameters for phenolic compound sorption in PEBA

	K_0	ΔG^0 (kJ·mol^{-1})	ΔH^0 (kJ·mol^{-1})	ΔS^0 (kJ·mol^{-1})
Phenol				
298K	51.0	-9.71		
313K	33.0	-9.10		
323K	27.7	-8.92	-17.7	-0.0270
333K	23.5	-8.74		
343K	19.1	-8.41		
4-CP				
298K	600	-15.8		
308K	479	-15.8		
318K	367	-15.6	-20.4	-0.0152
328K	290	-15.5		
338K	228	-15.3		
4-NP				
298K	334	-14.4		
308K	282	-14.4		
318K	187	-13.8	-23.8	-0.0310
328K	151	-13.7		
338K	110	-13.2		
4-MP				
298K	139	-12.2		
308K	132	-12.5		
318K	109	-12.4	-11.9	-0.00127
328K	93.5	-12.4		
338K	80.6	-12.3		
Catechol				
298K	28.2	-8.27		
308K	22.8	-8.00	-13.0	-0.0160
318K	21.6	-8.12		
328K	16.8	-7.69		

3.5 Conclusions

1. The linear model was suitable to describe the sorption of phenol and 4-MP in PEBA; the Langmuir model was suitable to represent the sorption of 4-CP, 4-NP, catechol and 4-MP in PEBA; the Freundlich model was suitable for the sorption of all phenolic compounds studied in PEBA.

2. The sorption capacity of the phenolic compounds in PEBA increases in the following order: catechol<phenol<4-MP<4-NP<4-CP. Phenolic compounds with electron-withdrawing groups have a larger sorption capacity in PEBA than those with electron-donating groups.

3. The sorption of phenol, 4-CP, 4-NP, 4-MP and catechol in PEBA was spontaneous, and it was an exothermic process.

Chapter 4

Kinetic study of sorption of phenolic compounds in PEBA: single-solute systems

4.1 Introduction

Apart from sorption capacity, sorption kinetics is also of great importance in the engineering design. In addition, the analysis of the sorption kinetics can help reveal the sorption mechanism and identify the rate controlling step of the sorption process. Thus sorption kinetics of phenol, 4-CP, 4-NP, 4-MP and catechol in PEBA was studied in this chapter.

Various kinetic models have been developed to investigate the sorption mechanisms, which can generally be categorised into two types: sorption reaction models and sorption diffusion models [193]. Sorption reaction models, including pseudo-first order model and pseudo-second order model, were originated from chemical reaction kinetics.

The pseudo-first order model was first proposed by Lagergren [194] to describe the adsorption of oxalic acid and malonic acid onto charcoal. Although it is widely applied to sorption data fitting, but there is no clear sorption mechanism related with this empirical equation [193]. More recently, Azizian [195] proposed a theoretical analysis of the pseudo-first order model based on the assumption of Langmuir sorption at a high initial solute concentration.

The pseudo-second order model was proposed by Ho et al. [196] to describe the adsorption of divalent metal ions onto peat. The main assumption is that the rate limiting step

may be chemical adsorption involving valent forces through sharing or the exchange of electrons between the peat and divalent metal ions. Azizian [195] derived the pseudo-second order model based on the Langmuir adsorption at low initial solute concentrations.

The diffusion models generally assume two or more consecutive steps involving in the sorption process: (1) transport of the solute across the liquid film surrounding the adsorbent (i.e., external diffusion); (2) diffusion of solute in the adsorbent (i.e., internal diffusion). The diffusion model is helpful to identify if the internal diffusion is the sole rate-limiting step of the sorption process, and the diffusion coefficient can be obtained from the initial stage of sorption when the external diffusion is negligible.

In theory, the sorption reaction models are suitable for chemisorption, and the sorption diffusion models are suitable for physical sorption processes. It should be noted that an agreement between the kinetic equations with experimental data cannot be accepted as proof for the sorption mechanism. However, in many studies, the sorption kinetic models are selected merely based on the correlation coefficient without considering the conditions under which the model applies. Ho and Mckay [123] suggested that the sorption system variables (i.e., agitation speed, sorbent size, temperature etc.) should be more extensively tested and that several kinetic models should be compared to confirm the sorption mechanism.

There are generally three steps involved in the sorption of phenolic compounds in PEBA membrane [197]:

1. Transport of phenolic compounds from the bulk solution to the exterior surface of the PEBA membrane;

2. Migration of the phenolic compounds across the solid-liquid interface and sorption onto external surface sites of the membrane;

3. Diffusion of phenolic molecules within the membrane.

Step (1) generally happens fast and is not the rate controlling step for sorption. If the surface reaction controls the overall sorption kinetics, then step (2) will be the rate controlling step. If diffusion within the PEBA membrane determines the overall sorption kinetics, then step (3) will be the rate controlling step for sorption.

The present investigation, therefore, used PEBA sorbent in a flat membrane form to reveal the sorption mechanism because of its well-defined area and thickness. Instead of using the correlation coefficient of the kinetic equation alone, the dependencies of rate constant and diffusion coefficient on the sorbent size were evaluated to shed light on the sorption mechanism involved. If the sorption process is solely controlled by the surface reaction between the solute and adsorbent, the rate constant should be independent of the thickness of PEBA membranes. If the sorption process is solely controlled by the internal diffusion, the diffusion coefficient should be independent of the thickness of PEBA membranes. In addition, the rate controlling step can be partly characterized by the activation energy for the sorption process [124], and thus the sorption kinetics was investigated at various temperatures to determine the activation energy.

4.2 Experimental

The thicknesses and weights of the PEBA membranes were measured, and then the membrane samples were immersed into a glass bottle containing 100 mL of the solution containing phenolic compounds. As the sorption proceeded, the concentration of phenolic compounds in the solution was monitored with a UV/Vis spectrometer. Q_t (mmol/g), the amount of sorption at time t, was calculated by:

$$Q_t = \frac{V \times (C_0 - C_t)}{M} \qquad (4.1)$$

where C_0 represents the initial solute concentration in the solution (mmol/L), C_t represents the solute concentration at time t (mmol/L), V is the volume of the solution (L), and M is the mass of the PEBA sorbent (g).

To identify the mechanism of sorption process, two series of membrane samples were prepared: one with the same surface area but different weights; and the other the same weight but different surface areas. The membranes were used to sorb phenolic compounds at 298K. In order to investigate the effect of temperature on the sorption process, PEBA membranes with the same weight and thickness were immersed into solutions with the same initial concentration at different temperatures.

4.3 Results and discussion

4.3.1 Sorption kinetics

In order to examine whether the sorption only occurs at the surface of the PEBA membrane or there is diffusion into the membrane, the sorption capacities are characterized by the sorbate amount sorbed per gram of PEBA membrane (mmol/g) and the sorbate amount sorbed per surface area of the PEBA membrane (mmol/cm^2). The sorption data for membranes having the same surface area but different weights (i.e., thicknesses) are shown in Figures 4.1(a)-(b). Clearly, the sorption uptake was not determined by the surface area of the PEBA sorbent, the equilibrium phenol uptake characterized by (mmol/cm^2) increased with an increase in the membrane thickness. If the sorption only took place on the surface, the equilibrium sorption uptake characterized by mmol/cm^2 would be the same for membranes with the same surface area.

Figure 4.1(a) shows that the equilibrium phenol uptake characterized by (mmol/g) decreased with an increase in the membrane thickness. This was because the membranes had different weights, resulting in different solute concentrations when sorption reached equilibrium since the initial solute concentration was the same. As the weight of the membrane increased, the solute concentration decreased due to sorption in PEBA. The lower equilibrium solute concentration led to a lower sorption uptake, which was in accordance with the results shown in Figure 3.1(a).
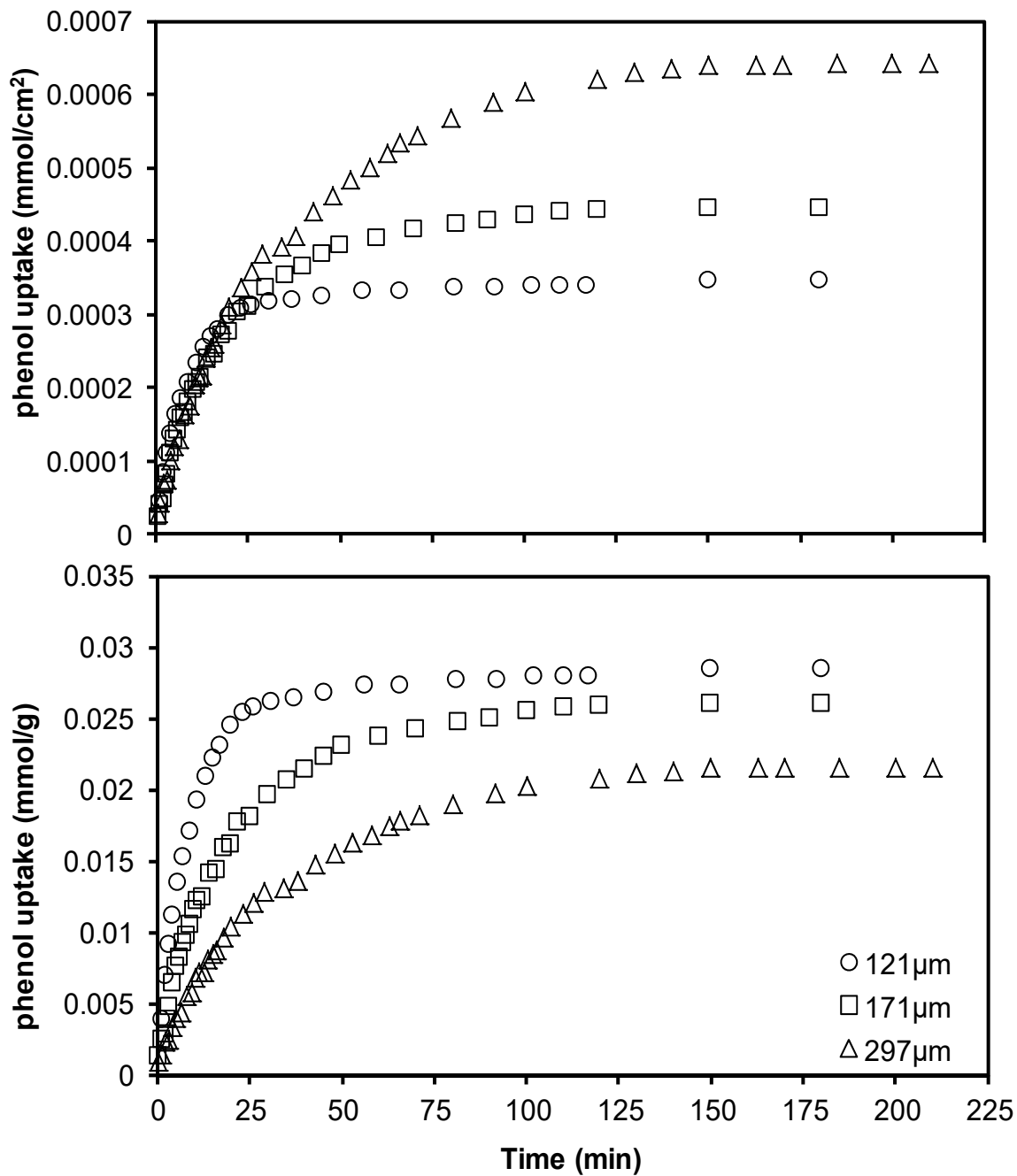
Figure 4.1(a) Kinetics of phenol sorption by PEBA membrane with same surface area but different thicknesses. *(membrane surface area=23.7 cm², the thickness of three membrane are 121 μm, 171 μm and 297 μm, respectively; temperature=298 K; initial concentration phenol=50 ppm)*
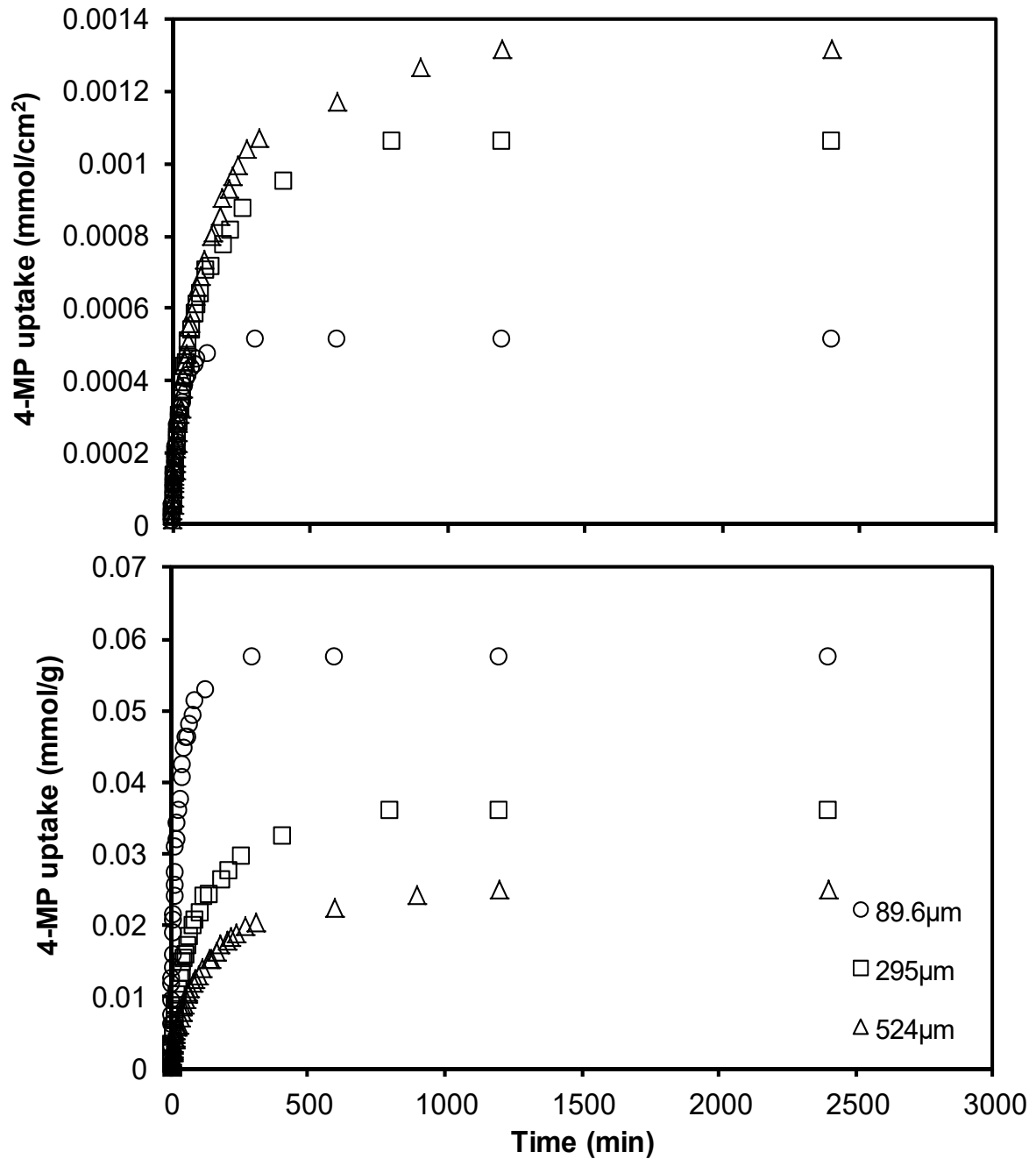
Figure 4.1(b) Kinetics of 4-MP sorption by PEBA membrane with same surface area but different thicknesses. *(membrane surface area=23.7 cm^2, the thickness of three membrane are 89.6 μm, 295 μm and 524 μm, respectively; temperature=298 K; initial concentration 4-MP=50 ppm)*

In order to confirm that solute diffusion into the membrane indeed occurred in the sorption process, the sorption kinetics for membranes having the same weight but different surface areas were also determined. Figures 4.2(a) and (b) show the sorption kinetics of phenol and 4-MP by the PEBA membranes. It is shown that the equilibrium phenol sorption uptake denoted by mmol/g was the same for membranes with the same weight but different thicknesses. This confirms that the sorption of phenol occurred not only on the surface, but mainly in the interior, and diffusion in the PEBA membrane was significant in the sorption process. Similar results were obtained for the sorption of 4-MP, 4-CP, 4-NP, and catechol by PEBA membrane, as shown in Figures 4.2(c)-(e). It can thus be concluded that the sorption uptake did not occur at the surface only, and the sorbate entered (i.e., diffusion) the solid bulk of the PEBA sorbent. In the following the sorption kinetics will be evaluated quantitatively based on uptake per sorbent mass.
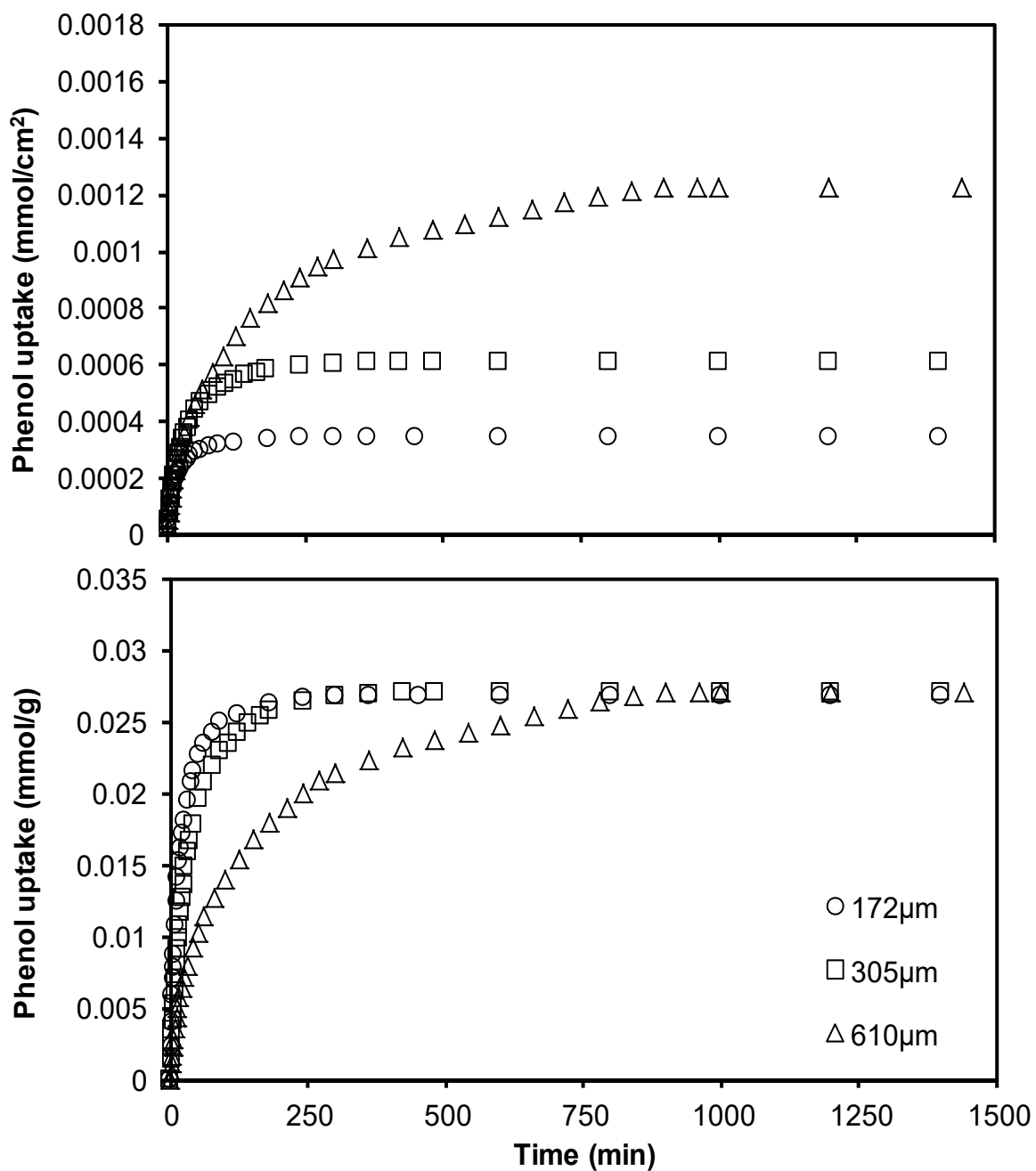
Figure 4.2(a) Kinetics of phenol sorption by PEBA membrane with same weight but different surface areas *(membrane weight=0.497 ±0.003 g, the thickness of three membrane are 172 μm, 305 μm and 610 μm respectively, temperature=298 K, initial concentration phenol =50 ppm)*
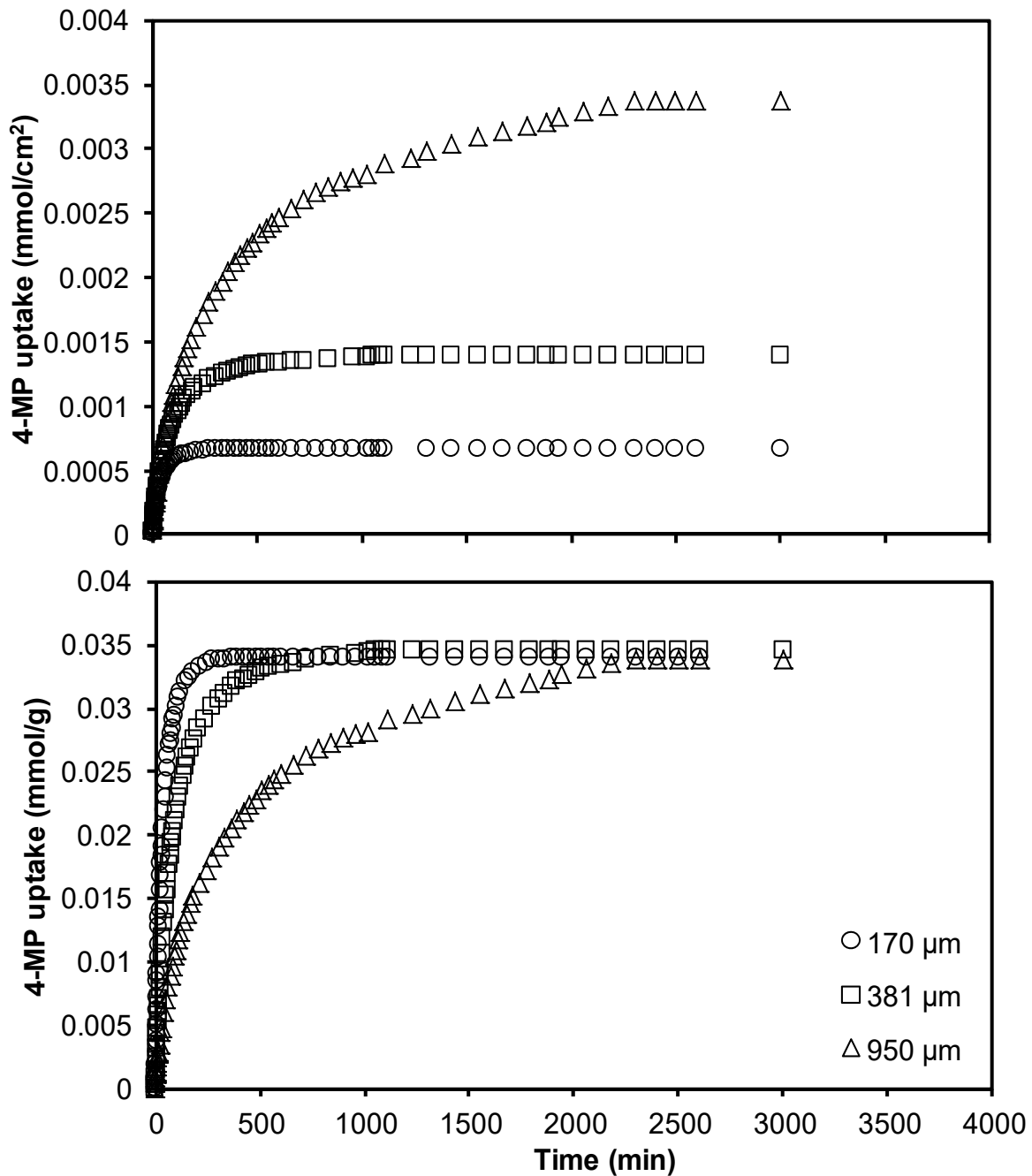
Figure 4.2(b) Kinetics of 4-MP sorption by PEBA membrane with same weight but different surface areas (*membrane weight=0.774 ±0.001g, the thickness of three membrane are 170 μm, 381 μm and 950 μm respectively, temperature=298 K, initial concentration 4-MP =50 ppm*)
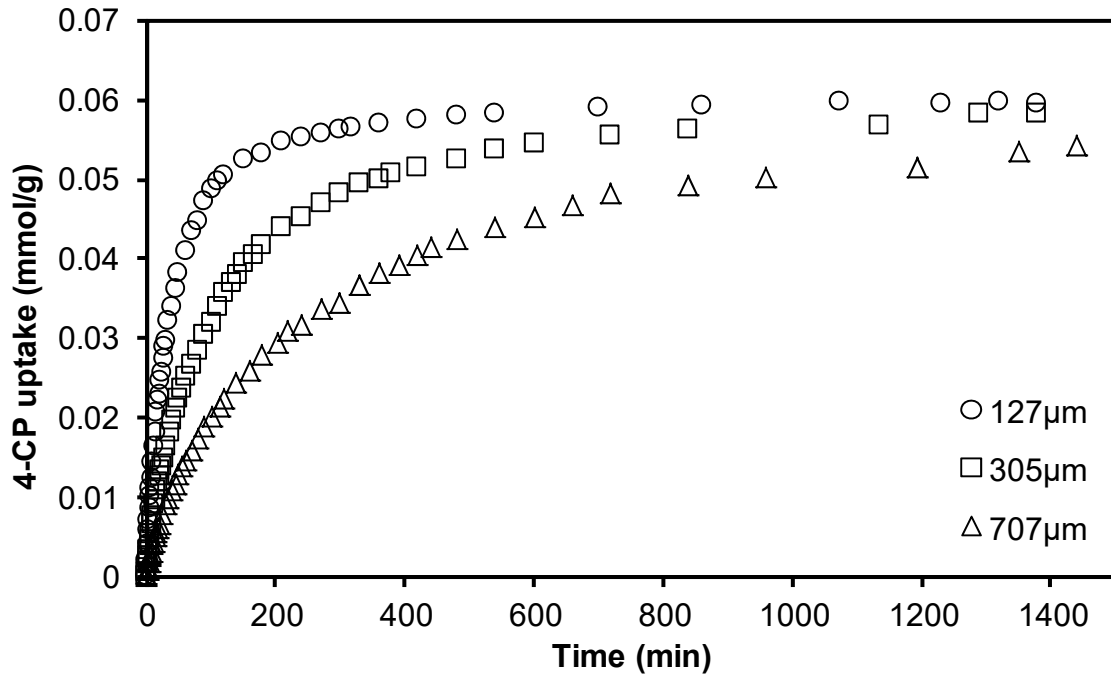
Figure 4.2(c) Kinetics of 4-CP sorption by PEBA membrane with the same weight but different thicknesses *(membrane weight=0.525 ±0.001 g, the thickness of three membrane are 127 μm, 305 μm and 707 μm respectively, temperature=298 K, initial concentration 4-CP =50 ppm)*
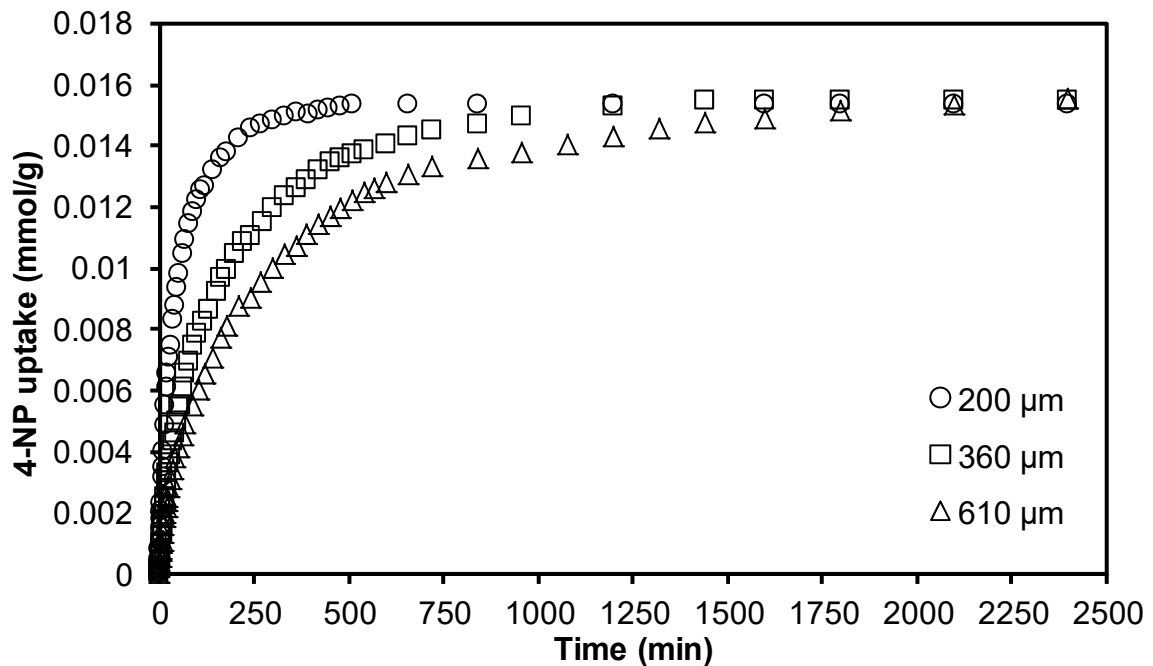
Figure 4.2(d) Kinetics of 4-NP sorption by PEBA membrane with the same weight but different thicknesses *(membrane weight=0.637 ±0.001 g, the thickness of three membrane are 200 μm, 360 μm and 610 μm respectively, temperature=298 K, initial concentration 4-NP =20 ppm)*
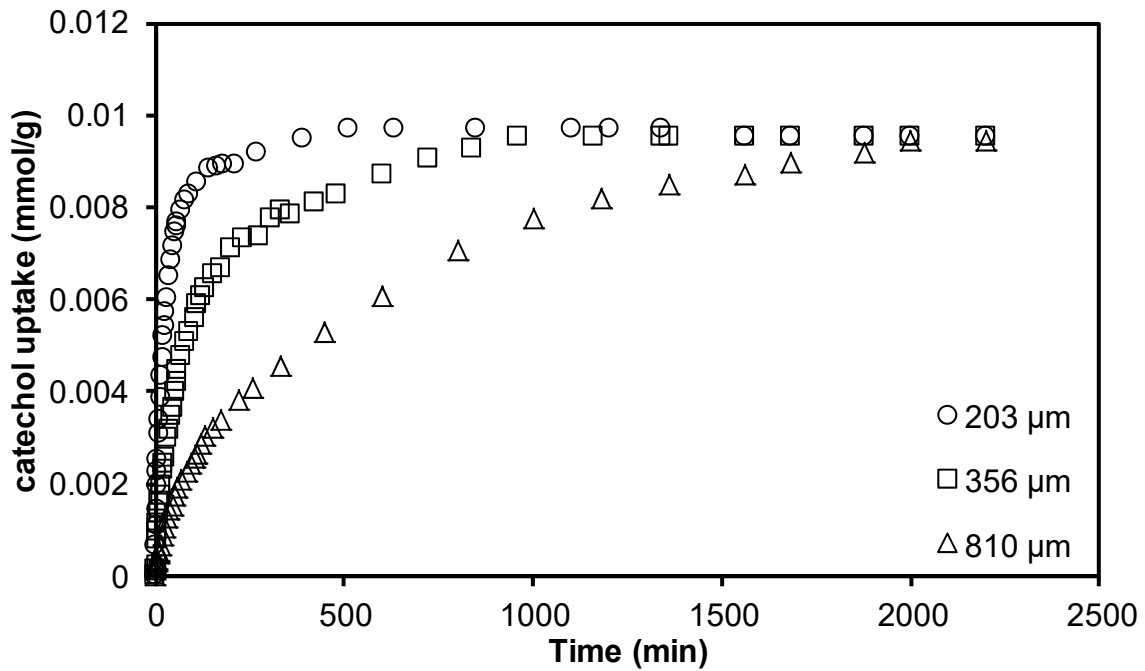
Figure 4.2(e) Kinetics of catechol sorption by PEBA membrane with the same weight but different thicknesses (*membrane weight=0.676 ±0.001 g, the thickness of three membrane are 203 μm, 356 μm and 810 μm respectively, temperature=298 K, initial concentration catechol=40 ppm*)

4.3.2 Kinetic models based on surface reaction

In order to see if the surface reaction is the rate determining step, reaction-based kinetic models including the pseudo-first order and pseudo-second order models, were fitted to the sorption kinetic data presented in Figures 4.2(a)-(e). If the pseudo-first order model applies, plotting $ln(Q_e - Q)$ against time t will produce a straight line with a slope of $-k_1$ and intercept of $ln\,Q_e$. If the pseudo-second order model applies, plotting t/Q against time t will yield a straight line. Figures 4.3(a)-(e) showed the plots. Based on the linearized forms of pseudo-first order and second order equations, the kinetic parameters involved in the models were obtained, and they are given in Table 4.1.
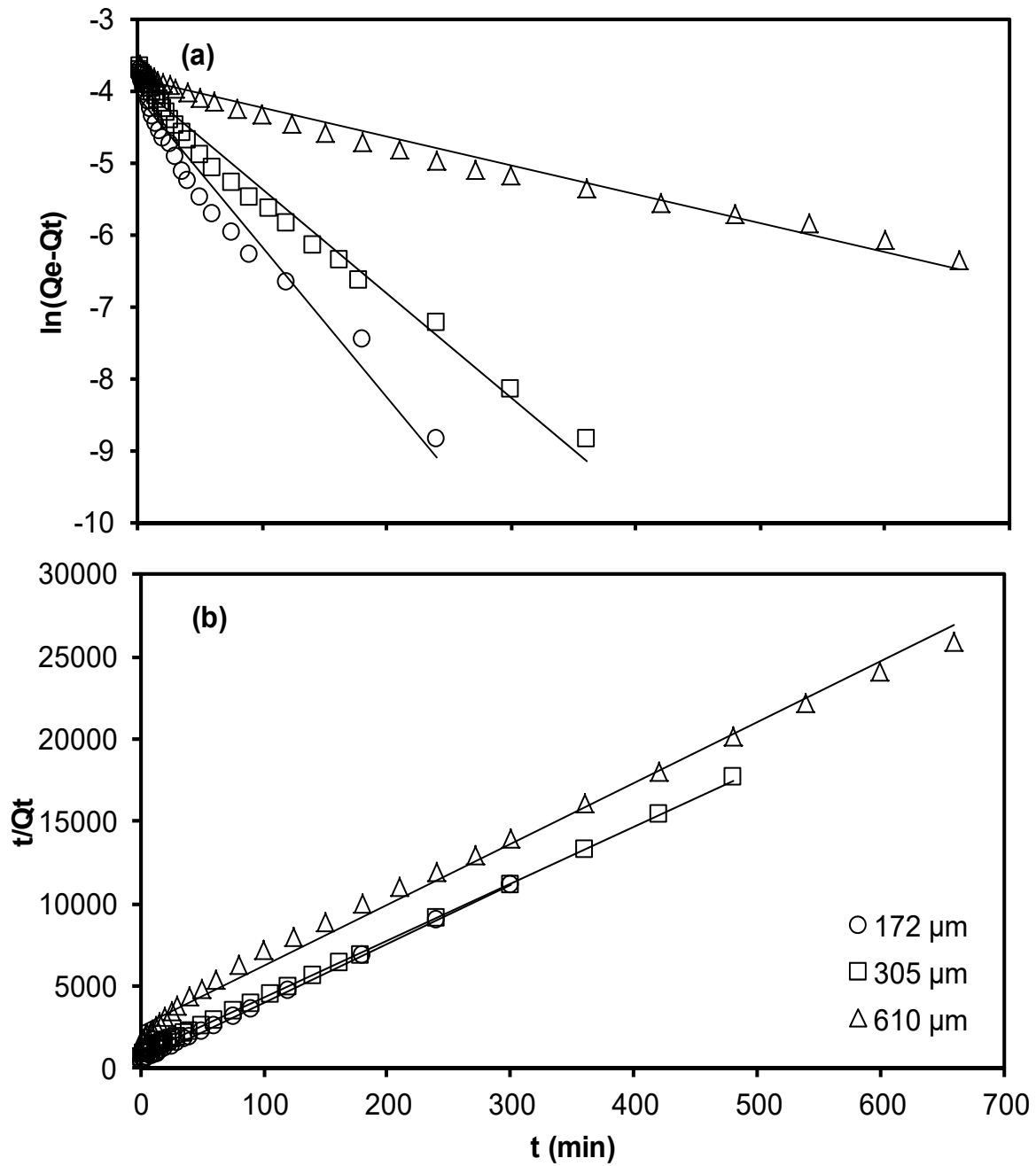
Figure 4.3 Sorption kinetic data plotted for linearized (a) pseudo-first order model, (b) pseudo-second order model, for phenol sorption in PEBA membrane *(experimental data from Figure 4.2(a))*
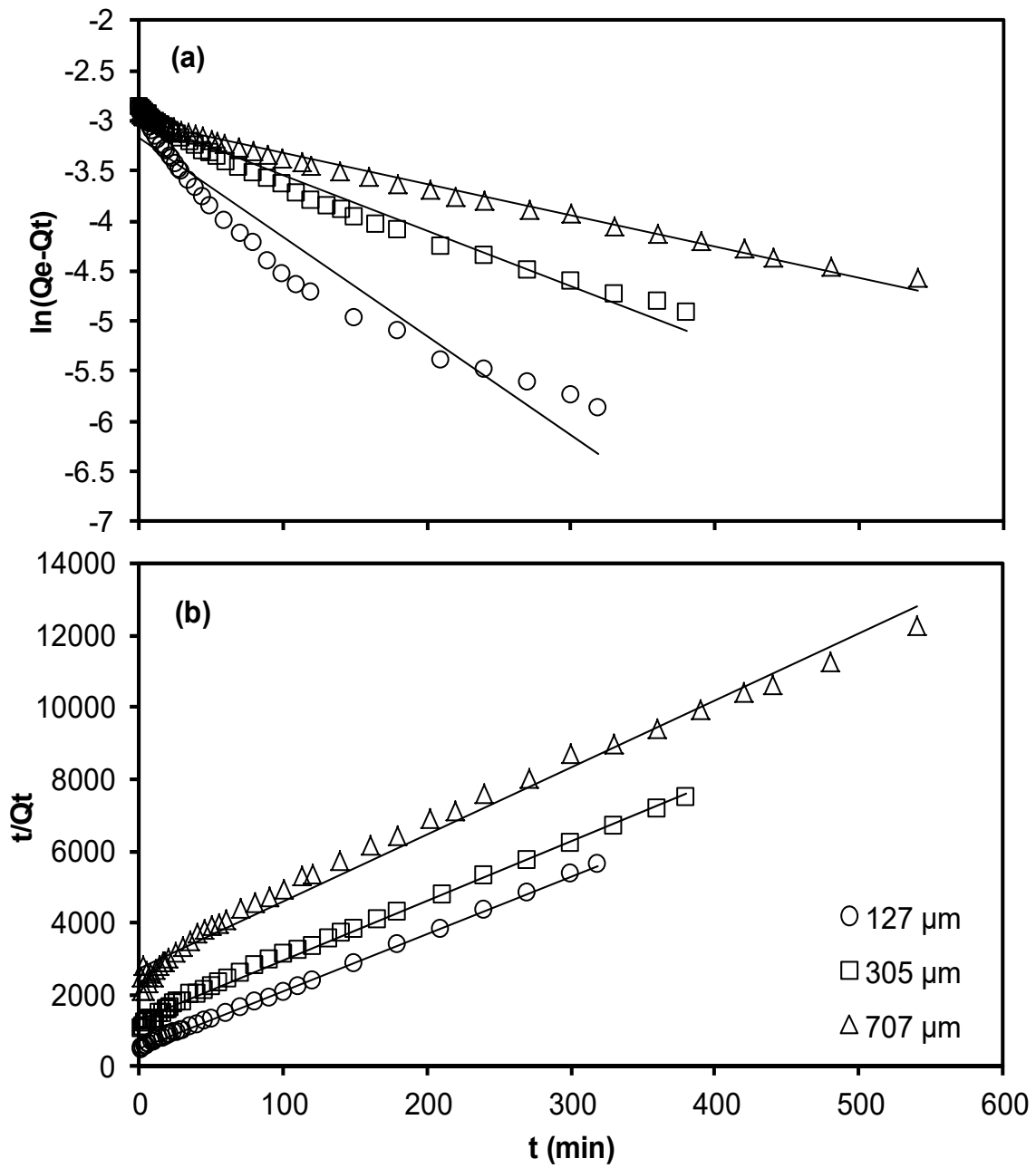
Figure 4.4 Sorption kinetic data plotted for linearized (a) pseudo-first order model, (b) pseudo-second order model, for 4-CP sorption in PEBA membrane *(experimental data from Figure 4.2(c))*
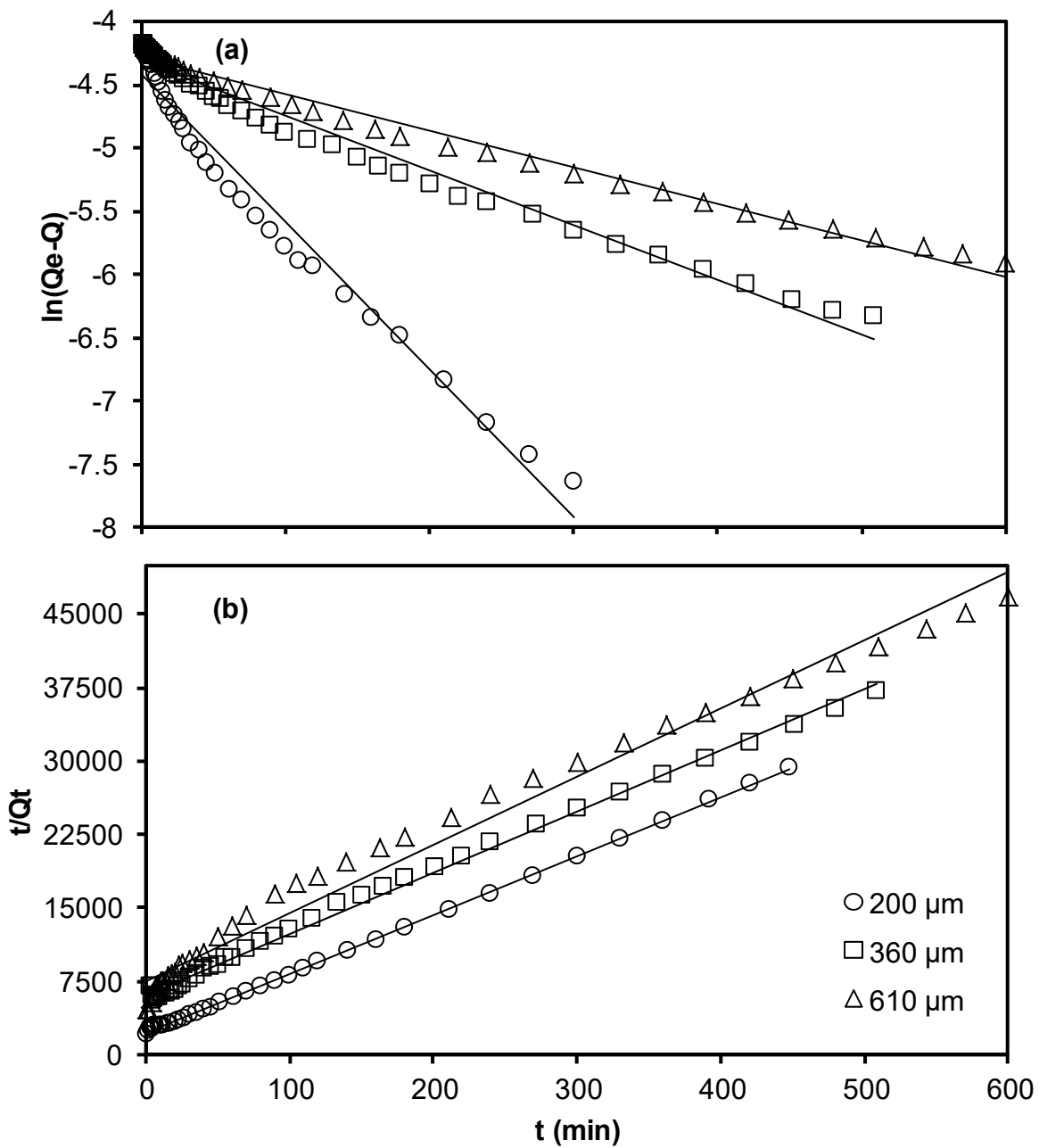
Figure 4.5 Sorption kinetic data plotted for linearized (a) pseudo-first order model, (b) pseudo-second order model for 4-NP sorption in PEBA membrane *(experimental data from Figure 4.2(d))*
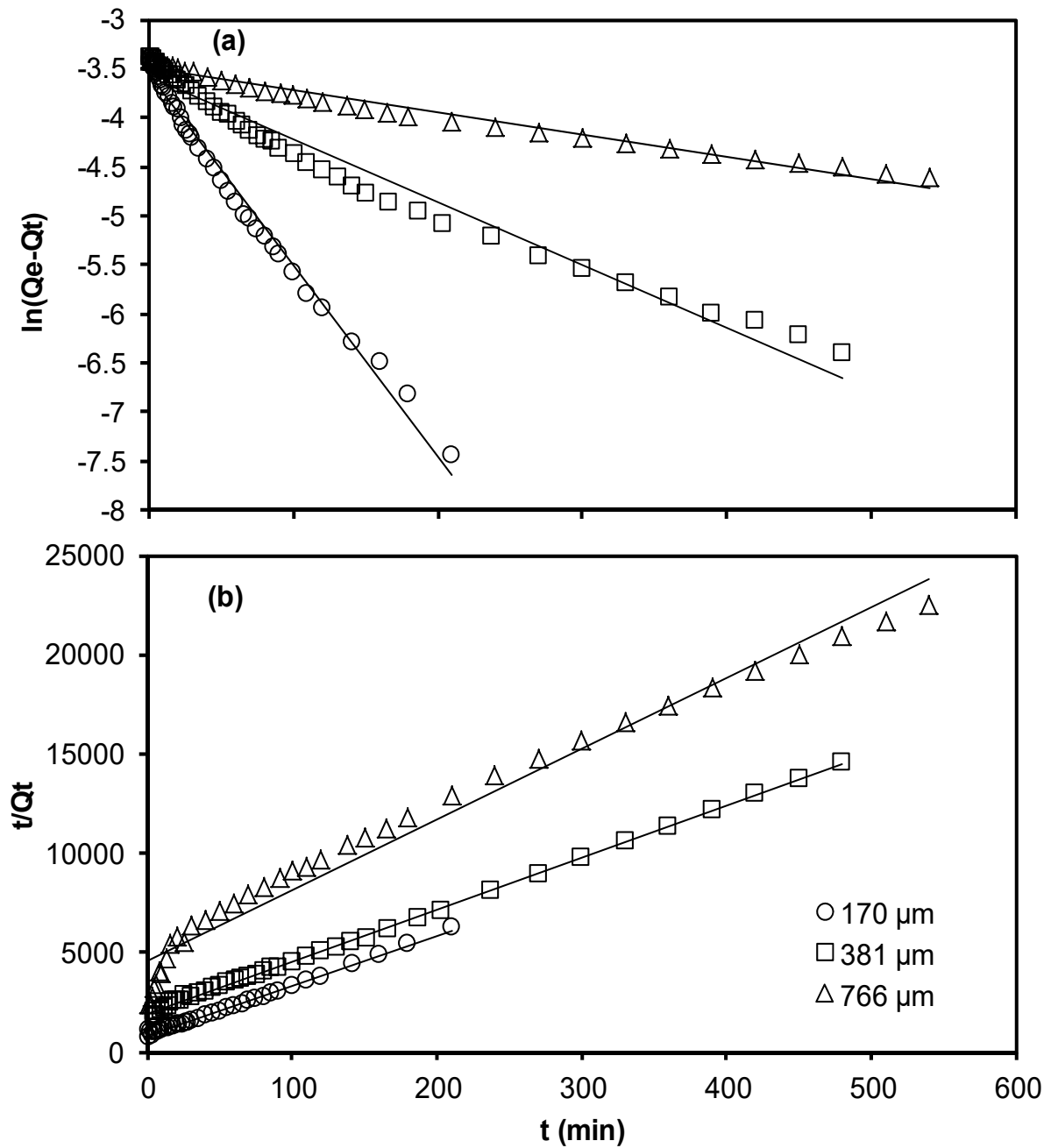
Figure 4.6 Sorption kinetic data plotted for linearized (a) pseudo-first order model, (b) pseudo-second order model for 4-MP sorption in PEBA membrane *(experimental data from Figure 4.2(b))*
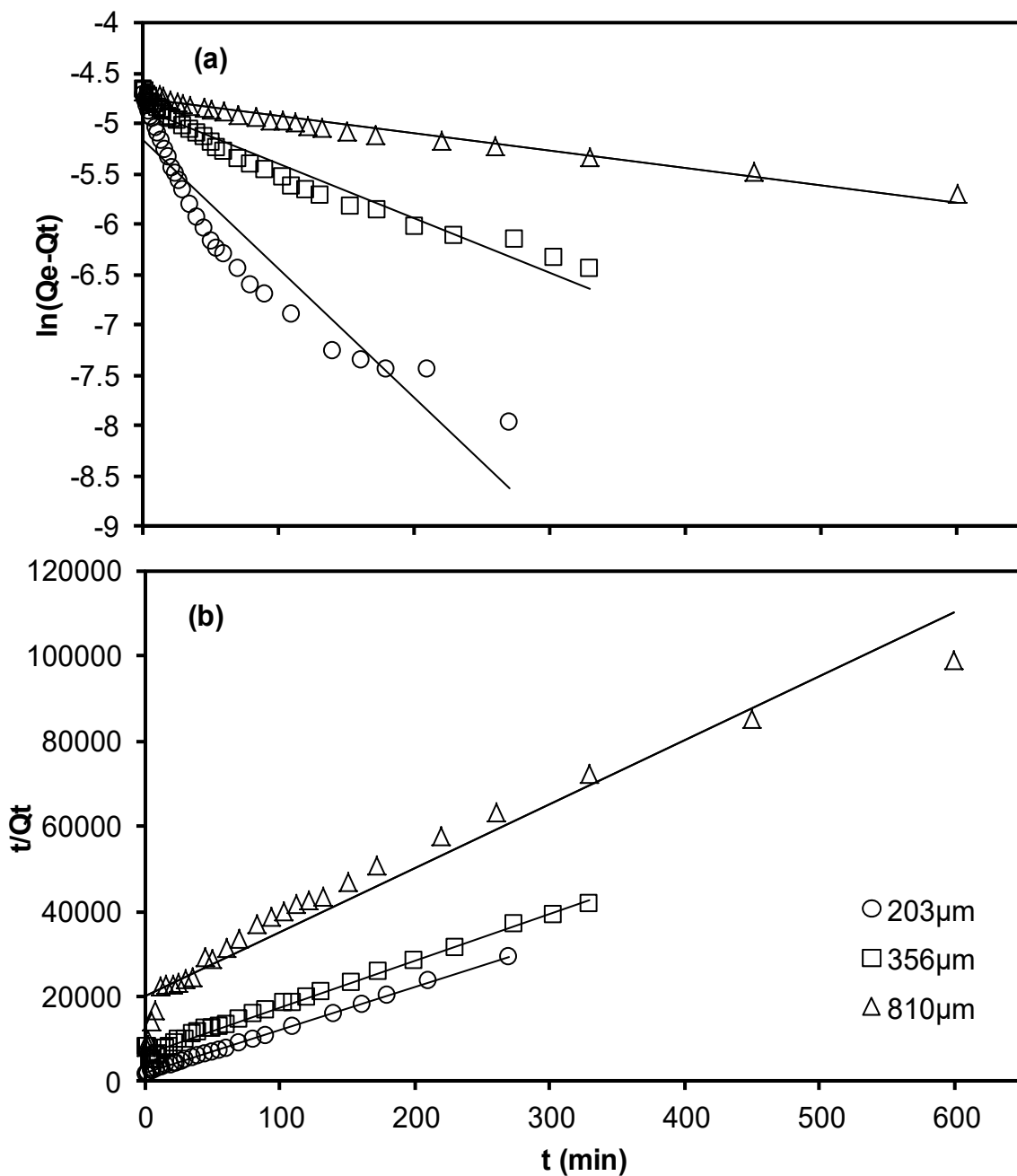
Figure 4.7 Sorption kinetic data plotted for linearized (a) pseudo-first order model, (b) pseudo-second order model for catechol sorption in PEBA membrane *(experimental data from Figure 4.2(e))*

Table 4.1 Kinetic parameters of phenolic compound sorption in PEBA at 298 K

Membrane thickness	Pseudo-first order			Pseudo-second order			Experimental
	k_1 (min^{-1})	Q_e (mmol/g)	R^2	k_2 g/(mmol·min)	Q_e (mmol/g)	R^2	Q_e (mmol/g)
Phenol							
172 μm	0.0208	0.0167	0.960	2.93	0.0281	0.999	0.0272
305 μm	0.0145	0.0197	0.983	1.45	0.0288	0.999	0.0272
610 μm	0.00400	0.0220	0.978	0.542	0.0271	0.993	0.0269
4-CP							
127 μm	0.00990	0.0426	0.936	0.496	0.0627	0.999	0.0593
305 μm	0.00560	0.0502	0.976	0.213	0.0602	0.996	0.0590
707 μm	0.00310	0.0499	0.988	0.127	0.0535	0.987	0.0590
4-NP							
200 μm	0.0117	0.0120	0.977	1.62	0.0166	0.999	0.0153
360 μm	0.00430	0.0134	0.981	0.644	0.0160	0.997	0.0155
610 μm	0.00290	0.0138	0.987	0.640	0.0144	0.984	0.0155
4-MP							
170 μm	0.0194	0.0287	0.977	0.751	0.0397	0.997	0.0340
381 μm	0.00640	0.0282	0.981	0.339	0.0385	0.997	0.0346
766 μm	0.00230	0.0306	0.987	0.274	0.0282	0.973	0.0340
Catechol							
203 μm	0.0129	0.00580	0.889	5.51	0.00990	0.999	0.00950
356 μm	0.00540	0.00780	0.947	1.85	0.00910	0.993	0.00950
810 μm	0.00170	0.00860	0.959	1.14	0.00660	0.939	0.00940

For most of the systems studied, the pseudo-second order model has correlation coefficients slightly higher than the pseudo-first order model, and the Q_e values calculated from the pseudo-second order model are closer to experimental Q_e value than those evaluated from the pseudo-first-order model. This indicates that the experimental data can be approximated adequately by the pseudo-second-order model. However, the Q_e values calculated from the pseudo-second order model deviates from the experimental value for thick membranes. For instance, for the sorption of 4-CP, 4-MP and catechol in membranes with thicknesses of 707, 766, and 810 μm, respectively, the predicted Q_e values are smaller

than the corresponding experimental values determined directly. As shown in Figures 4.3-4.7 there is a clear deviation between the pseudo-second order model and the experimental data during the initial stage of sorption of phenolic compounds in thick membranes.

As shown in Table 4.1, the rate constant k_2 decreased with an increase in the membrane thickness for the sorption of phenolic compounds in PEBA. For a chemical reaction system, it is known that the rate constant depends on temperature only. If the surface reaction is the only rate-controlling step, k_2 values for sorption of the phenolic compounds in PEBA membranes would be independent of the membrane thickness.

However, the k_2 values obtained are not without reservation. Actually, there are some issue about the term Q_e in Eq. (2.27) [198]. Plazinski et al. [198] pointed out that the Q_e values estimated from Eq. (2.29) are not the "actual values" of Q_e, and a good linearity of t/Q_t vs. t plots does not necessarily indicate a good estimation of Q_e. In fact, an unreliable estimation of Q_e values, in spite of good linearity in t/Q_t vs. t plots, has been observed in numerous studies [122]. To our knowledge, no further attempts have been made to examine this issue. In the following section, the term Q_e in Eq. (2.27) will be discussed.

4.3.3 Modification of the pseudo-second-order equation

Table 2 lists a few sorption systems reported in the literature that use the pseudo-second order model to describe the sorption kinetics. The Q_e value obtained from the kinetics model was close to the Q_e value determined experimentally when the initial concentration of the solute was relatively low [199-202] or when the solute concentration change was small during the sorption process [21, 203, 204]. However, a significant deviation of Q_e from the experimental value was observed in sorption systems where the solute concentration in the feed significantly changed during the sorption process [9, 10, 205]. Azizian [195] formulated

the pseudo-second order model from the classical Langmuir model of sorption kinetics and concluded that the sorption kinetics follows the pseudo-second order model at low initial solute concentrations. Liu and Shen [206] simplified the Langmuir kinetics to the pseudo-second order model and they found Langmuir kinetics would be reduced to the pseudo-second order equation only at $k_1/k_2 \ll \theta_e$, and the simplification was C_0 dependent. Rudzinski and Plazinski [207] derived the pseudo-second order equation for heterogeneous solid surface. One of the assumptions they made was that the solute concentration was constant over time. Therefore, Eq. (2.27) is strongly concentration dependent. However, how to take into account of the solute concentration in Eq. (2.27) has never been investigated.

In almost all the studies reported so far, Q_e in Eq. (2.27) was considered as a constant that is related to the solute concentration at equilibrium. However, during the batch sorption experiment, the solute concentration decreases as adsorption proceeds, and it is reasonable to consider Q_e as a function of instantaneous solute concentration. The relationship between Q_e and instantaneous solute concentration C_e' can be represented by the equilibrium isotherm. For sorption systems that obey the Freundlich isotherm, the relationship between Q_e and C_e' can be expressed by:

$$Q_e = K_F C_e'^{1/n} \tag{4.2}$$

The mass balance equation of a batch adsorption process gives:

$$Q = \frac{(C_0 - C_e')V}{M} \tag{4.3}$$

where M represents the mass of PEBA membrane (g), Q is the uptake of phenolic compounds at time t (mmol/g), C_0 is the initial adsorbate concentration (mmol/L) and C_e' is the instantaneous solute concentration (mmol/L).

Eq. (4.3) can be rearranged to

$$C_e{}' = C_0 - \frac{QM}{V}$$

(4.4)

Combining Eq. (4.4) with Eq. (4.2), we obtain

$$Q_e = K_F(C_0 - \frac{QM}{V})^{1/n}$$

(4.5)

Substituting Eq. (4.5) into Eq. (2.27), the pseudo-second order equation can be modified as:

$$\frac{dQ}{dt} = k_2[K_F(C_0 - \frac{QM}{V})^{1/n} - Q]^2$$

(4.6)

where the constant Q_e term in Eq. (2.27) is substituted by a function of Q, which is changing as sorption proceeds. Parameters K_F and $1/n$ were determined from the equilibrium isotherm in Chapter 3.

By fitting Eq. (4.6) to the kinetic data in Figures 4.2(a)-(e), the rate constant k_2 (g·mol⁻¹·min⁻¹) was recalculated by a numerical solution program developed in FORTRAN. The recalculated k_2 were presented in Table 4.3. To check the validity of the modified model, a comparison between the modified-pseudo-second-order model fitting data and experimental data was presented in Figures 4.8(a)-(e).

Figures 4.8(a)-(e) show that the data regenerated from modified pseudo-second model equation appear to be in good agreement with the experimental data, especially for the initial stage of the sorption, which is not well fitted by the unmodified model equation. The modified pseudo- second-order equation gives a reliable estimation of k_2 values based on the corrected understanding of Q_e values in Eq. (2.27). However, the recalculated k_2 values seem to be also affected by the membrane thickness, as shown in Table 4.3.

One important assumption of the pseudo-second order model is that surface reaction controls the overall sorption kinetics, that is, the mass transfer on the liquid/solid interface controls the overall rate of the sorption process [198]. The term "surface reaction" may not necessarily mean chemical reaction; interactions of physical nature (e.g., van der Waals forces) may also play a role. In this study, the interactions between phenolic compounds and the PEBA sorbent may be explained by "electron donor and acceptor" system. The aromatic ring of phenol tends to accept electrons [192], while the PEBA sorbent tends to donate electrons because of lone pairs around N (polyamide segment) and O (polyether segment) in the polymer. The acceptor-donor complexes are formed between the aromatic ring and the PEBA sorbent, and such intermolecular forces may attribute to surface interaction.

Different k_2 values obtained from different membranes are presumably due to diffusion of sorbate molecules in the membrane. As such the sorption process is not solely controlled by the surface reaction but the internal diffusion also plays a role. Thus the diffusion aspect will be evaluated below.

Table 4.2 Pseudo-second order kinetic model of various related systems from the literature

Sorbent	Sorbate	C_0 (mg/L)	C_e (mg/L)	Q_e(exp.) (mg/g)	Q_e(cal.) (mg/g)	Ref.
NAD-701			852	296	296	
XAD-4	4-nitrophenol	100	916	169	169	[21]
Activated carbon			884	232	233	
Activated carbon	Acetic acid	103.9	5.9	98	102	[205]
		190.4	17.4	173	178.6	
		404	64	340	357.1	
		624.5	154.5	470	500	
Activated carbon	Cd(II)	20	2	18*	18.2	[202]
	Ni(II)	20	1.7	18.3*	18.5	
Activated carbon	Congo red	20	6.67	3.333	3.096	[208]
		40	17.6	5.606	5.408	
		60	36.9	5.789	5.821	
		80	55.6	6.107	5.886	
Aeromonas aciae	Cr(VI)	5	2.48	5.05	5.19	[203]
		50	42.58	42.58	40	
Activated carbon	2,4-dichlorophenol	10	0.466	4.767	4.675	[200]
		20	1.040	9.480	9.533	
		30	4.36	12.82	12.72	
		40	6.52	16.74	17.18	
Fly ash	Congo red	25	1.7	2.33	2.33	[209]
		50	2.4	4.76	4.81	
		75	3.3	7.17	7.18	
		100	3.8	9.62	9.62	
Microcystis	Ni(II)	20	14.3	71.5	75.1	[204]
		50	41.2	110	115.9	
		100	87.0	162	166	

Microcystis	Cr(VI)	20	17.7	29.2	29.6	
		50	45.2	59.8	60.8	[204]
		100	90.5	119	120	
Sawdust	Cd(II)	1-10	-	1.95	1.94	[199]
	Pb(II)	1-10	-	1.97	1.96	
Cation exchanger	Cu(II)	25	-	12.24	12.36	
		50	-	24.31	24.57	[210]
		75	-	35.93	36.46	
		100	-	46.10	47.16	
Granular sludge	Malachite green	90	0.552	37.27	37.346	
		120	1.632	49.32	48.736	[211]
		150	1.848	61.73	56.056	
Seed Hulls	Methyl violet	25	0.115	16.59	17.02	
		50	6.98	28.68	29.16	
		100	18.96	54.03	59.88	
		150	52.49	65.01	71.43	[9]
		200	84.4	77.10	85.47	
		250	128	81.09	87.72	
		300	165	90.07	95.24	
Oil palm trunk	Malachite green	25	4.435	13.71	16.49	
		50	12.47	25.02	30.30	
		100	36.55	42.30	55.34	
		150	66.29	55.81	69.46	[10]
		200	98.21	67.86	91.43	
		250	125	83.09	117.72	
		300	153	97.78	129.46	
Perlite	Methylene blue	5	1.27	0.28	0.29	
		10	2.4	0.57	0.59	[201]
		20	7.47	0.94	1.01	

*data estimated from the figure
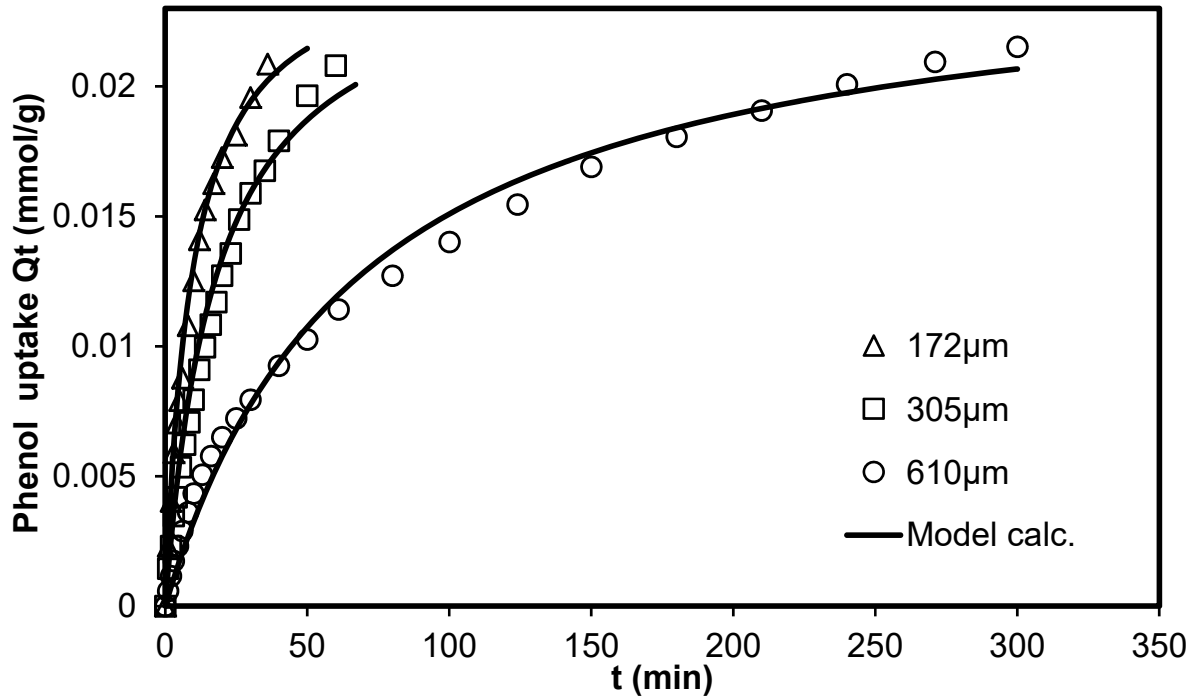
Figure 4.8(a) Comparison of experimental data for the sorption of phenol in PEBA with regenerated data from modified kinetic model equation
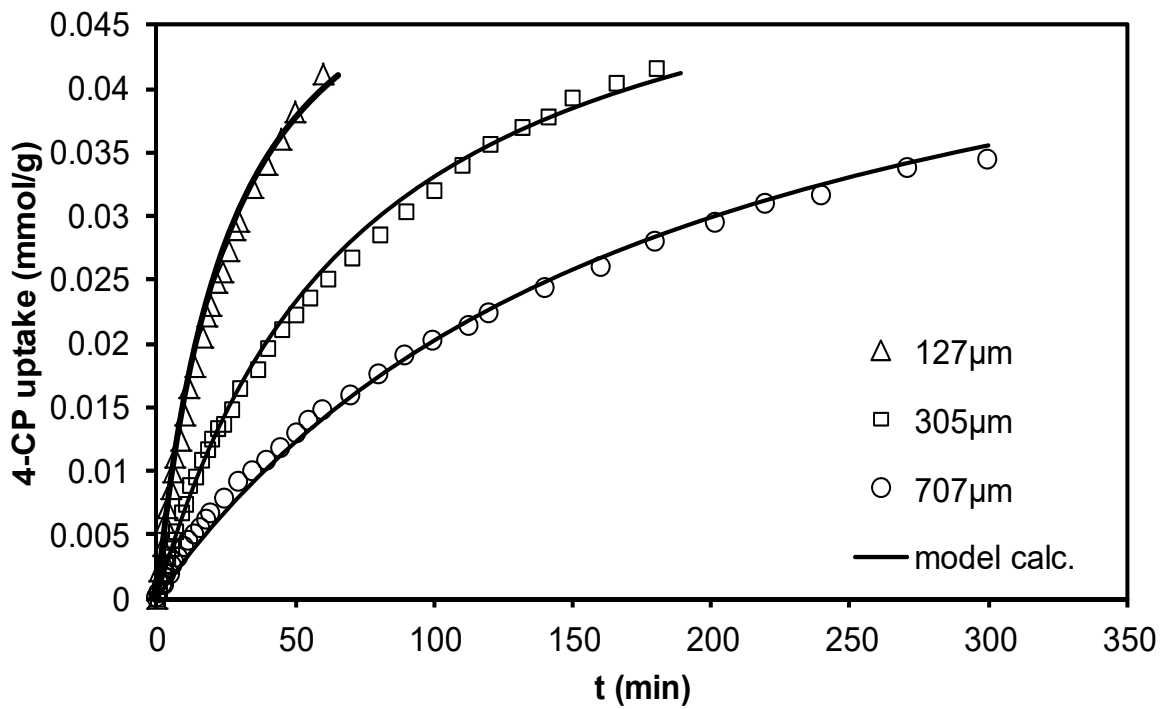
Figure 4.8(b) Comparison of experimental data for the sorption of 4-CP in PEBA with regenerated data from modified kinetic model equation
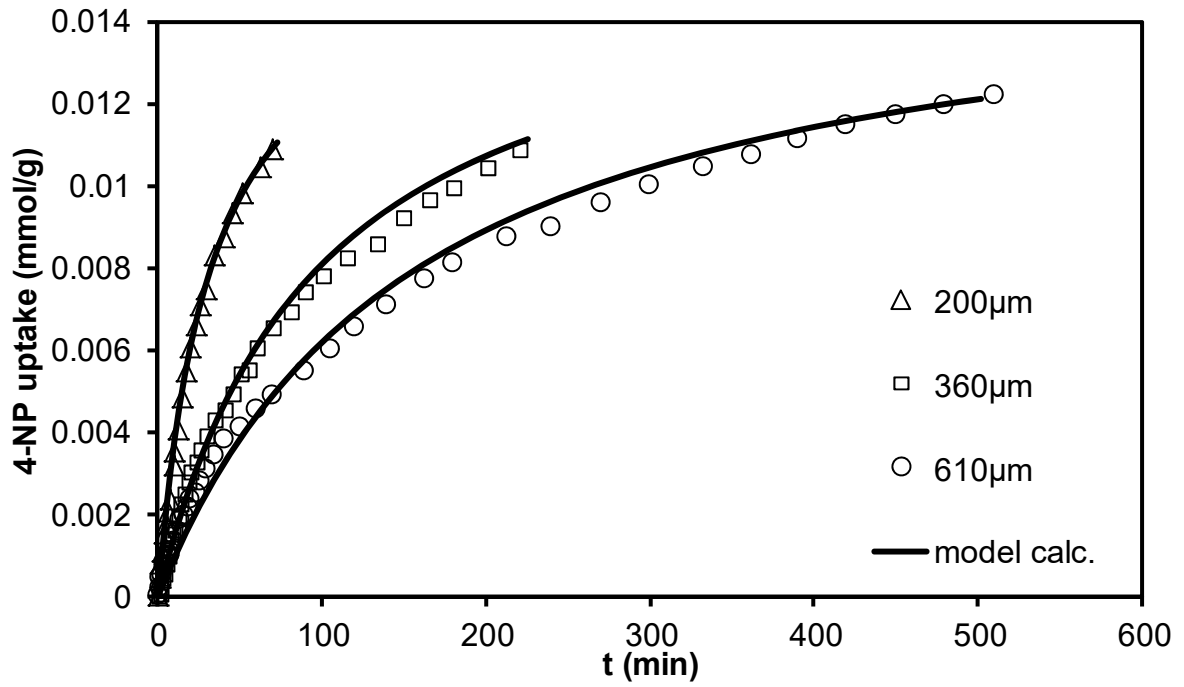
Figure 4.8(c) Comparison of experimental data for the sorption of 4-NP in PEBA with regenerated data from modified kinetic model equation
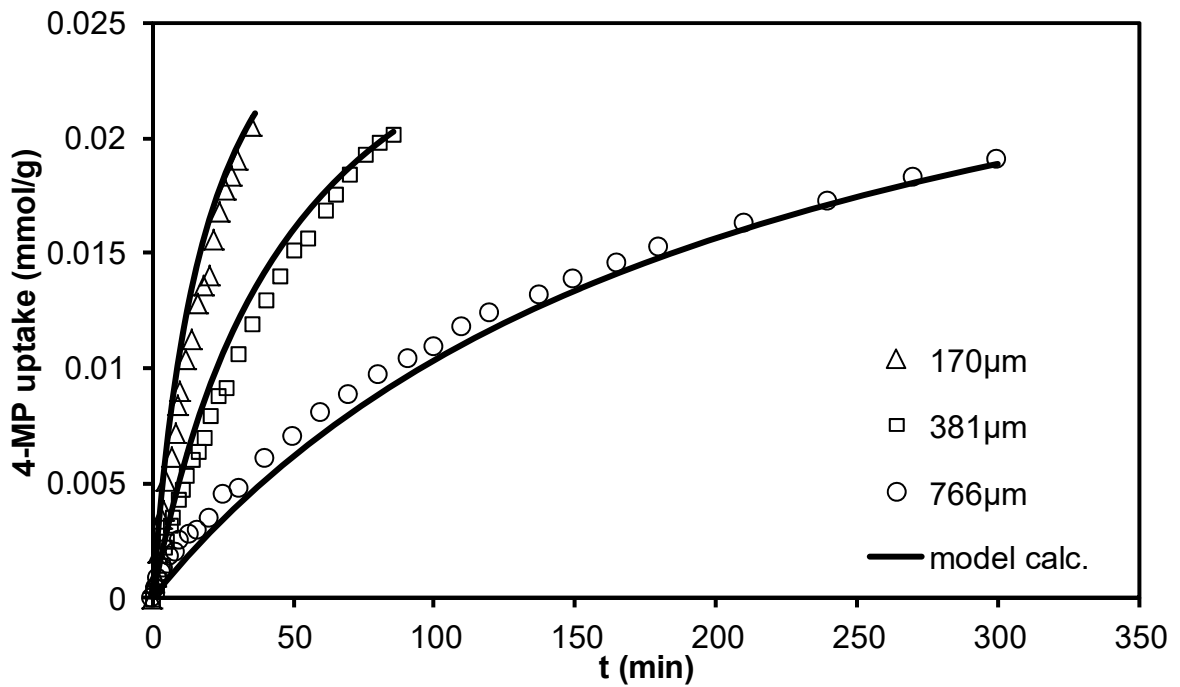
Figure 4.8(d) Comparison of experimental data for the sorption of 4-MP in PEBA with regenerated data from modified kinetic model equation
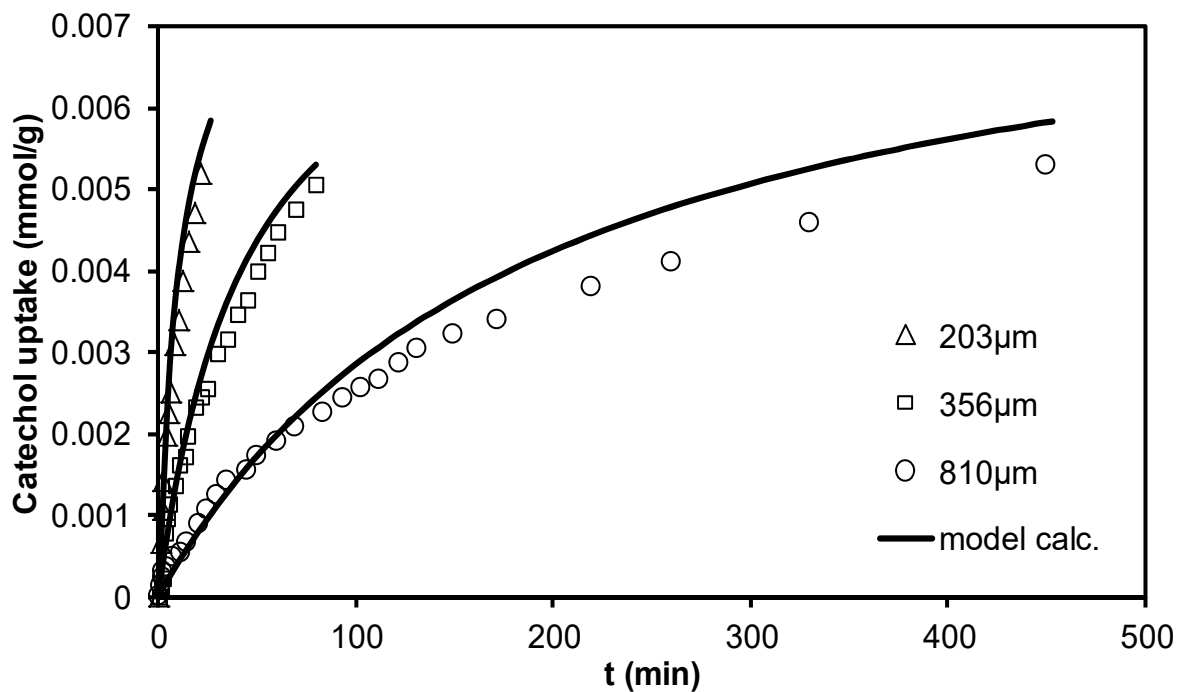
Figure 4.8(e) Comparison of experimental data for the sorption of catechol in PEBA with regenerated data from modified kinetic model

Table 4.3 Recalculated rate constant k_2^* for sorption of phenolic compounds in PEBA

Phenol		4-CP		4-NP		4-MP		Catechol	
Membrane thickness	k_2^* Recal.	Membrane thickness	k_2^* Recal.	Membrane thickness	k_2^* Recal.	Membrane thickness	k_2^* Recal.	Membrane thickness	k_2^* Recal.
172 μm	2.41	127 μm	0.0274	200 μm	0.113	170 μm	0.234	203 μm	2.98
305 μm	1.25	305 μm	0.0103	360 μm	0.0380	381 μm	0.0899	356 μm	0.768
610 μm	0.333	707 μm	0.00390	610 μm	0.0230	766 μm	0.0254	810 μm	0.198

Rate constant k_2^* was recalculated based on Eq. (4.6)

4.3.4 Diffusion model

In order to evaluate the effects of diffusion on the sorption process, the experimental data in Figures 4.2(a)-(e) were further analyzed by the intraparticle diffusion model. If intraparticle diffusion is the rate-limiting step, good linearization of the data should be observed for the initial phase of the sorption. The plots of initial uptake (for uptake ≤ 35%) versus $t^{1/2}$ are given in Figure 4.9 for the adsorption of phenolic compounds in PEBA.

Figure 4.9 shows good linearity for the initial phase of sorption of phenolic compounds in PEBA membrane. The straight line indicates internal diffusion is indeed not negligible. However, if the internal diffusion is the sole rate limiting step, the straight line should pass origin [193]. Clearly this is not the case in this study, which indicates the rate of sorption is controlled by internal diffusion together with other processes.

The parameters of the diffusion model were listed in Table 4.4. Diffusivity D_c is calculated from the plot of fractional uptake versus $t^{1/2}$, as shown in Figures 4.10 (a)-(e). For the initial stage of diffusion $Q_t/Q_e < 0.3$ when boundary layer effect is insignificant, the expression for the uptake curve for membrane can be written as [212]:

$$\frac{Q_t}{Q_e} \approx \frac{4}{l} (\frac{D_c t}{\pi})^{1/2} \tag{4.7}$$

where l refers to the thickness of the membrane (m), Q_t represents the sorption uptake at time t, Q_e is the uptake at equilibrium, Q_t/Q_e refers to the fractional sorption uptake relative to sorption equilibrium. The value of D_c for each sorption process is calculated and presented in Table 4.4.
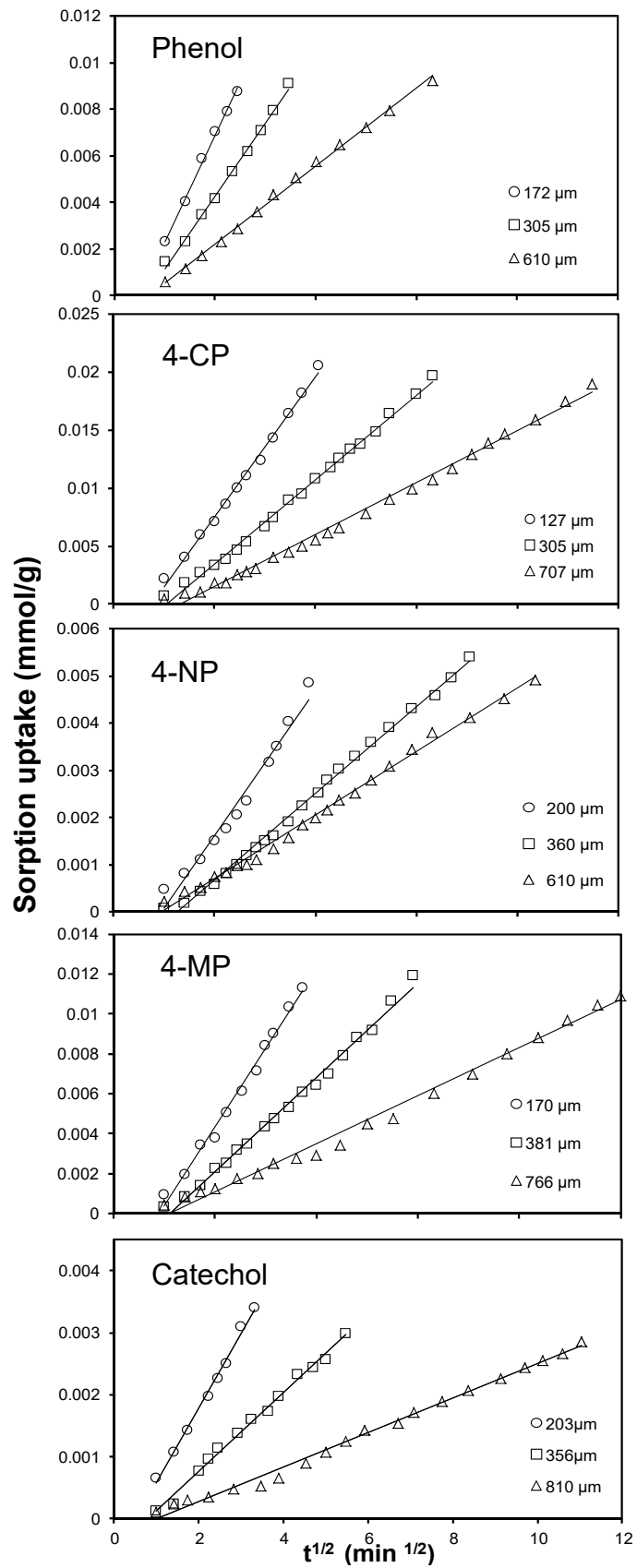
Figure 4.9 Sorption uptakes vs. $t^{1/2}$ for phenolic compounds in PEBA
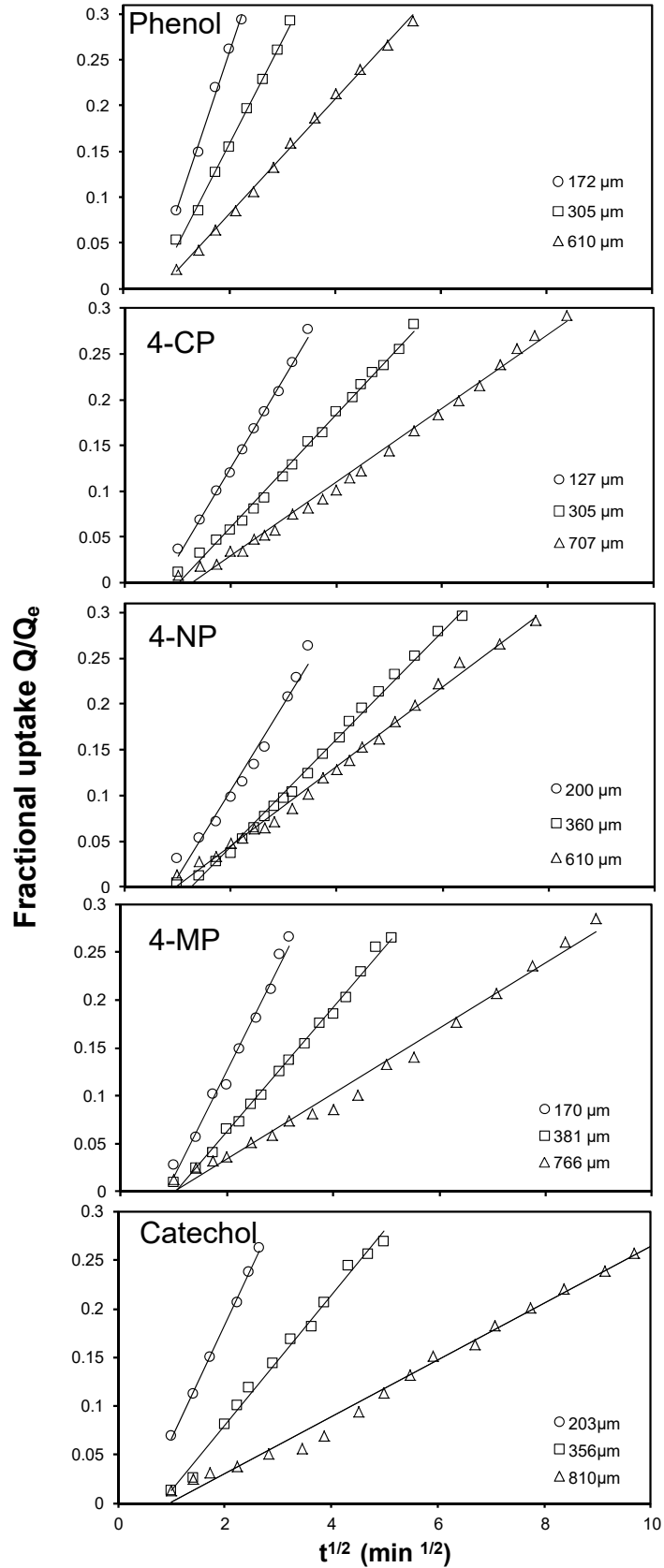
Figure 4.10 Plots of fractional sorption uptake vs. $t^{1/2}$ for phenolic compounds in PEBA

114

Table 4.4 Parameters of intraparticle diffusion model for the sorption of phenolic compounds in
PEBA membranes with different thicknesses

Solute	Membrane thickness (μm)	k_i mmol/(g·min$^{1/2}$)	C mmol/g	R^2	$D_c \times 10^{10}$ m^2/min
Phenol	172	0.0045	-0.0022	0.9952	1.75
	305	0.0031	-0.0019	0.9967	2.31
	610	0.0017	-0.0011	0.9979	2.84
4-CP	127	0.0060	-0.0046	0.9954	0.299
	305	0.0036	-0.0038	0.9960	0.693
	707	0.0022	-0.0030	0.9941	1.59
4-NP	200	0.0015	-0.0015	0.9728	0.704
	360	0.00090	-0.0012	0.9960	0.885
	610	0.00070	-0.00060	0.9952	1.38
4-MP	170	0.0039	-0.0035	0.9909	0.702
	381	0.0024	-0.0026	0.9929	1.19
	766	0.0012	-0.0013	0.9913	1.34
Catechol	203	0.0012	-0.00060	0.9943	1.12
	356	0.00060	-0.00050	0.9936	1.10
	810	0.00030	-0.00030	0.9933	1.10

Values of C were negative in Table 4.4, which is probably due to the boundary layer
effect. For a given pair of two species, diffusion coefficient should be the same. Table 4.4
shows that the diffusion coefficient for catechol sorption is basically the same for membranes
with different thicknesses. It indicates that intra-particle diffusion is the only rate controlling
step in sorption of catechol in PEBA. However, for the sorption of phenol, 4-CP, 4-NP and 4-
MP, the diffusion coefficient is different for membranes with different thicknesses,
presumably due to the effect of surface reaction. Clearly, the experimental data are net effect
of a combination of surface reaction and diffusion rather than diffusion alone.

4.3.5 Activation energy

The sorption kinetics of phenolic compounds in PEBA was carried out at different temperatures. In order to investigate the effect of temperature on the sorption rate, membranes were made with the same weight and same surface area for tests with a given solute. The kinetic data for the sorption of phenolic compounds in PEBA were presented in Figures 4.11 (a)-(e).

The kinetic data in Figures 4.11 (a)-(e) were analyzed by Eq. (4.6) and the values of k_2 for the sorption of phenolic compounds at different temperatures were presented in Table 4.5. The kinetic data were also analyzed by the diffusion model. The plots of fractional uptake versus $t^{1/2}$ for the adsorption of phenolic compounds in PEBA at different temperatures were shown in Figure 4.12. The diffusion coefficients D_c were calculated from the slope of the straight line using Eq. (4.7), and they were shown in Table 4.5.
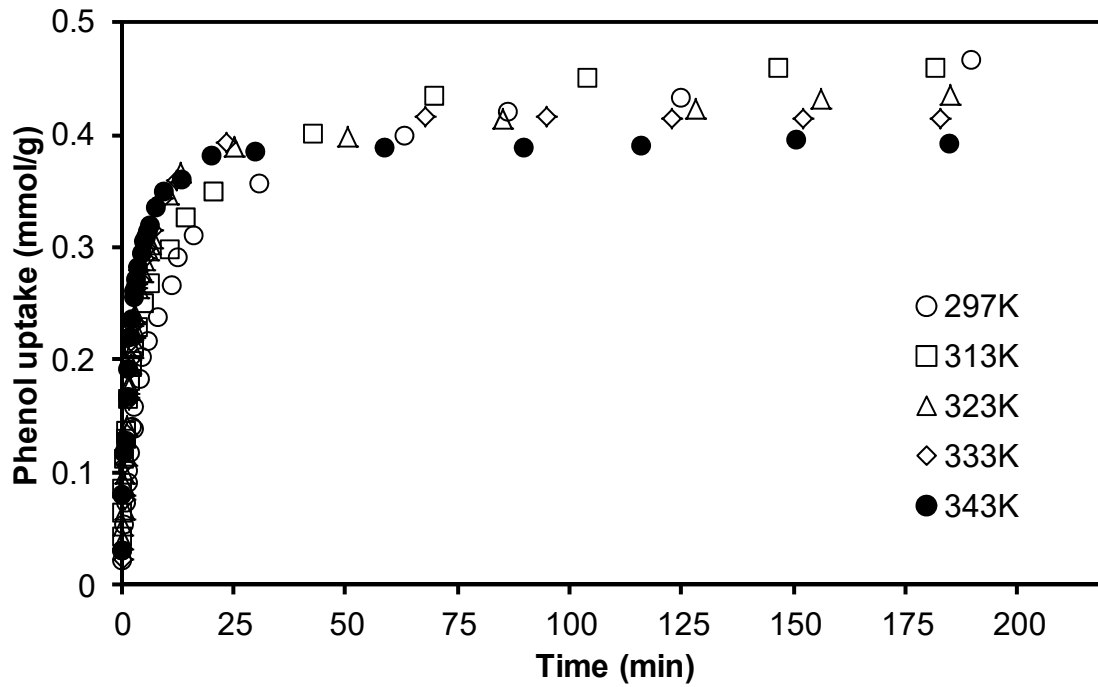
Figure 4.11(a) Sorption of phenol in PEBA at different temperatures *(**membrane thickness 500 μm, initial concentration phenol = 3000 ppm**)*
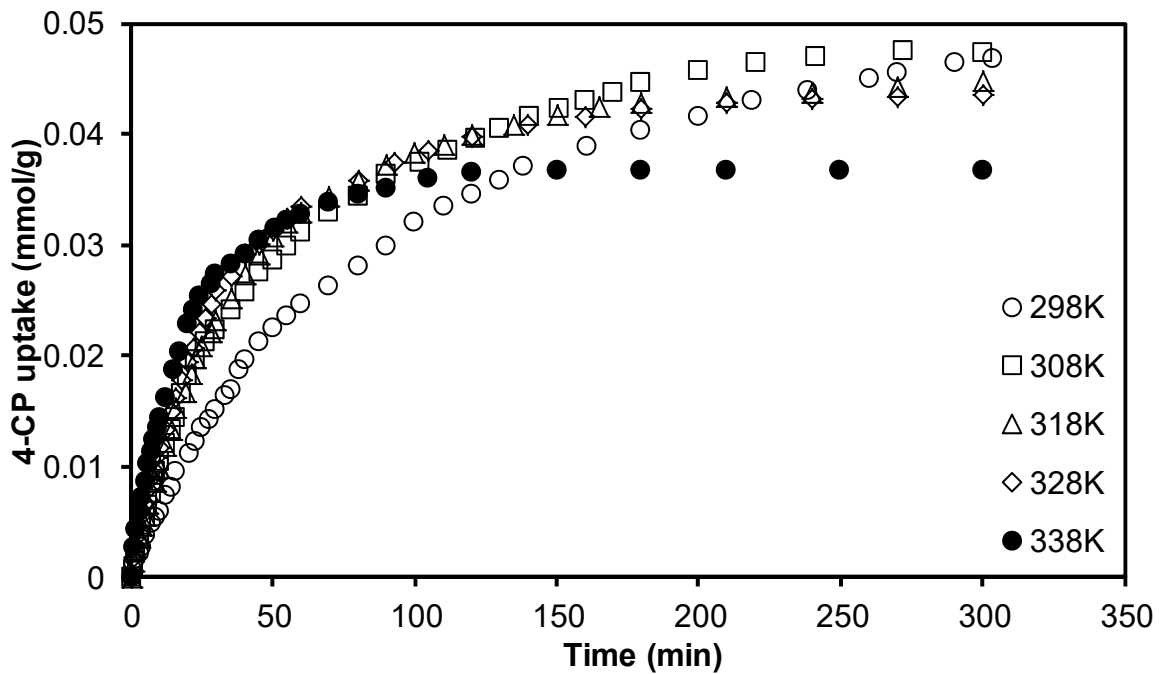
Figure 4.11(b) Sorption of 4-CP in PEBA at different temperatures *(**membrane thickness 380 μm, initial concentration 4-CP = 40 ppm**)*
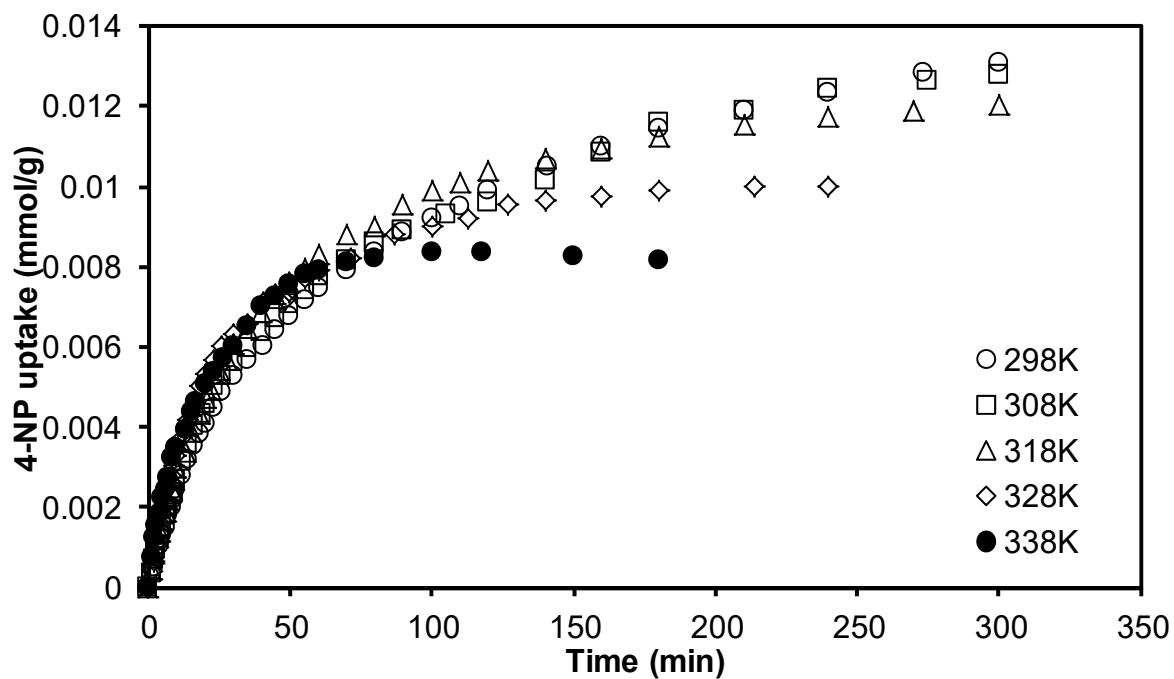
Figure 4.11(c) Sorption of 4-NP in PEBA at different temperatures *(membrane thickness 380 μm, initial concentration 4-NP = 20 ppm)*
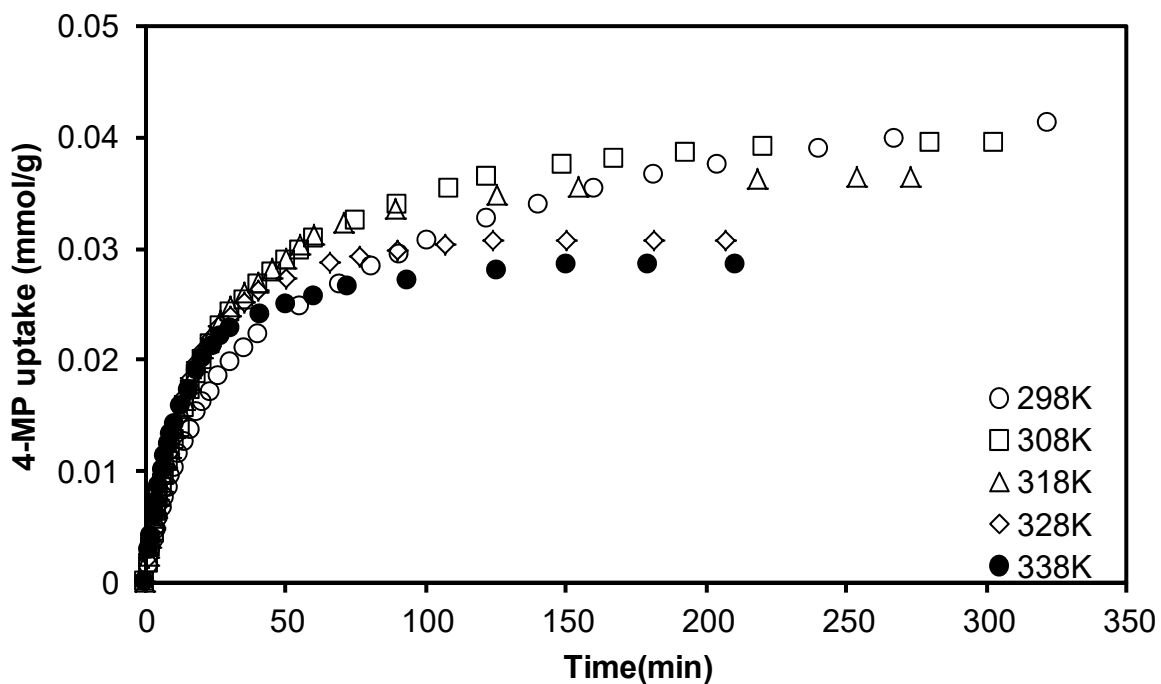
Figure 4.11(d) Sorption of 4-MP in PEBA at different temperatures *(membrane thickness 305 μm, 4-MP initial concentration 4-NP = 50 ppm)*
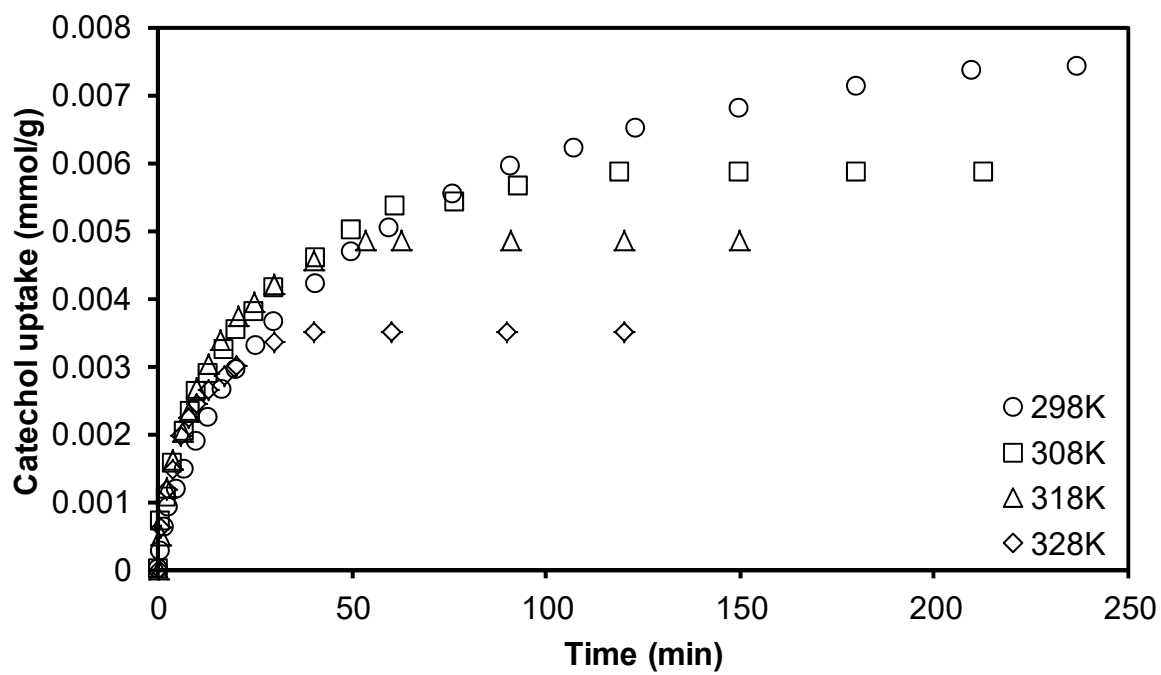
Figure 4.11(e) Sorption of catechol in PEBA at different temperatures *(**membrane thickness 482 μm, initial concentration catechol = 40 ppm**)*
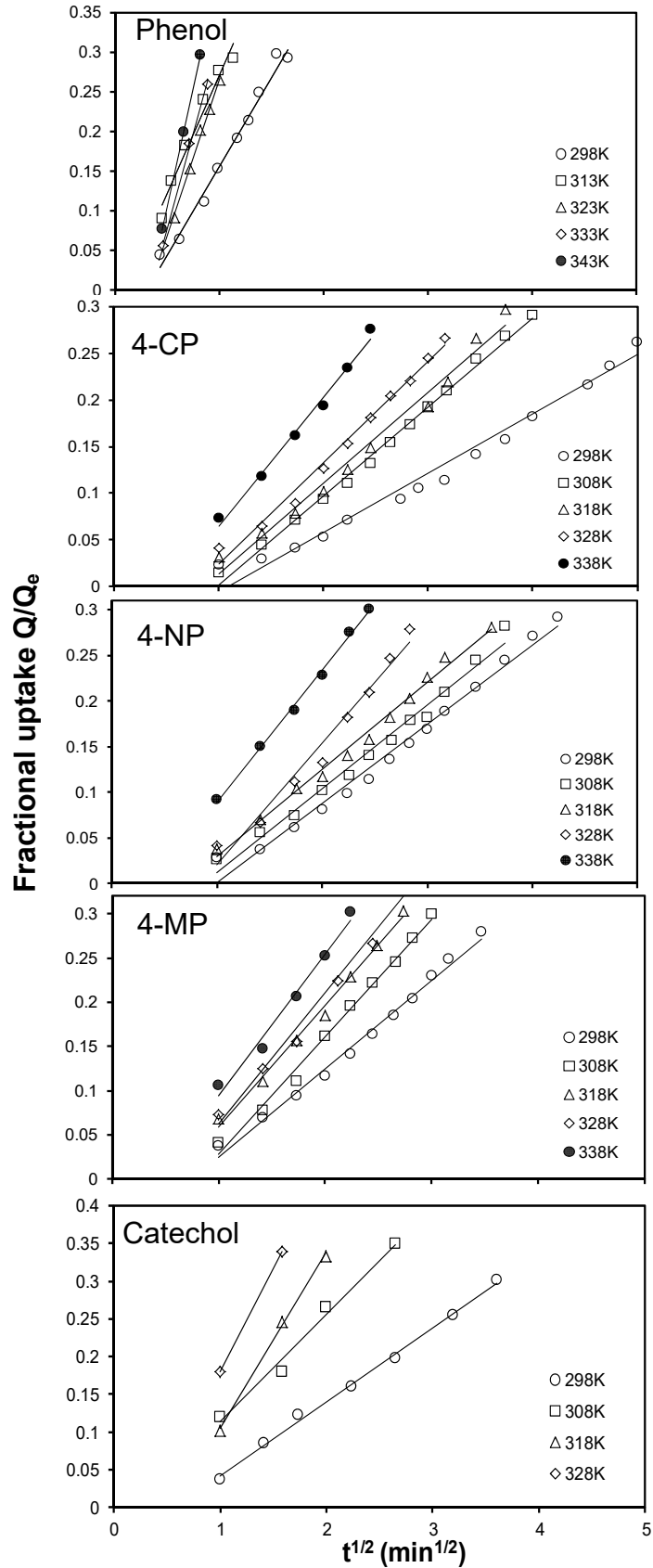
Figure 4.12 Fractional uptake of phenolic compounds in PEBA vs. $t^{1/2}$ at different temperatures

120

Table 4.5 Rate constant k_2 based on surface reaction and diffusion coefficient D_c based on internal diffusion for the sorption of phenolic compounds in PEBA at different temperatures

	k_2	$D_c \times 10^{10}$
	g/(mmol·min)	m²/min
Phenol		
298 K	0.0427	24.7
313 K	0.0809	43.3
323 K	0.165	77.6
333 K	0.220	112
343 K	0.296	176
4-NP		
298 K	0.0967	1.01
308 K	0.211	2.27
318 K	0.826	2.37
328 K	1.68	2.96
338 K	3.09	4.77
4-CP		
298 K	0.0159	1.87
308 K	0.0362	2.09
318 K	0.0831	2.30
328 K	0.169	4.43
338 K	0.441	5.20
4-MP		
298 K	0.340	1.83
308 K	0.625	3.23
318 K	1.18	3.43
328 K	1.63	3.99
338 K	2.49	4.74
Catechol		
298 K	2.55	2.73
308 K	5.42	5.79
318 K	8.00	15.4
328 K	13.6	21.5

The activation energy can be calculated from Arrhenius equation, which can be expressed as:

$$k_2 = A\, e^{-E_a/RT} \qquad (4.9)$$

The plots of k_2 in log scale versus 1/T gives a straight line, as shown in Figure 4.13(a), and the activation energy is calculated from the slope of the straight line. Table 4.6 shows the activation energy so calculated.

If the sorption is considered to be diffusion controlling, the activation energy for diffusion can be determined by

$$D_c = D_0 e^{-E_d/RT} \qquad (4.10)$$

where activation energy for diffusion (E_d) can be calculated from the Arrhenius plots shown in Figure 4.13(b), and the values of the diffusion activation energy are shown in Table 4.6.

Table 4.6 The activation energy for sorption of phenolic compounds in PEBA

	Phenol	4-CP	4-NP	4-MP	Catechol
Activation energy(kJ/mol) calculated from k_2	37.0	68.4	75.6	41.5	44.2
Activation energy(kJ/mol) calculated from D_c	36.5	28.3	23.2	17.9	58.4

The activation energies of diffusion are typically in the range of 12-21 kJ/mol [124]. Activation energy of diffusion for sorption of 4-MP in the PEBA membrane seems to fall into this range. However, the activation energies of diffusion for sorption of phenol, 4-CP, 4-NP and catechol are slightly larger. This confirms that diffusion is in general not the only mechanism of the sorption process.
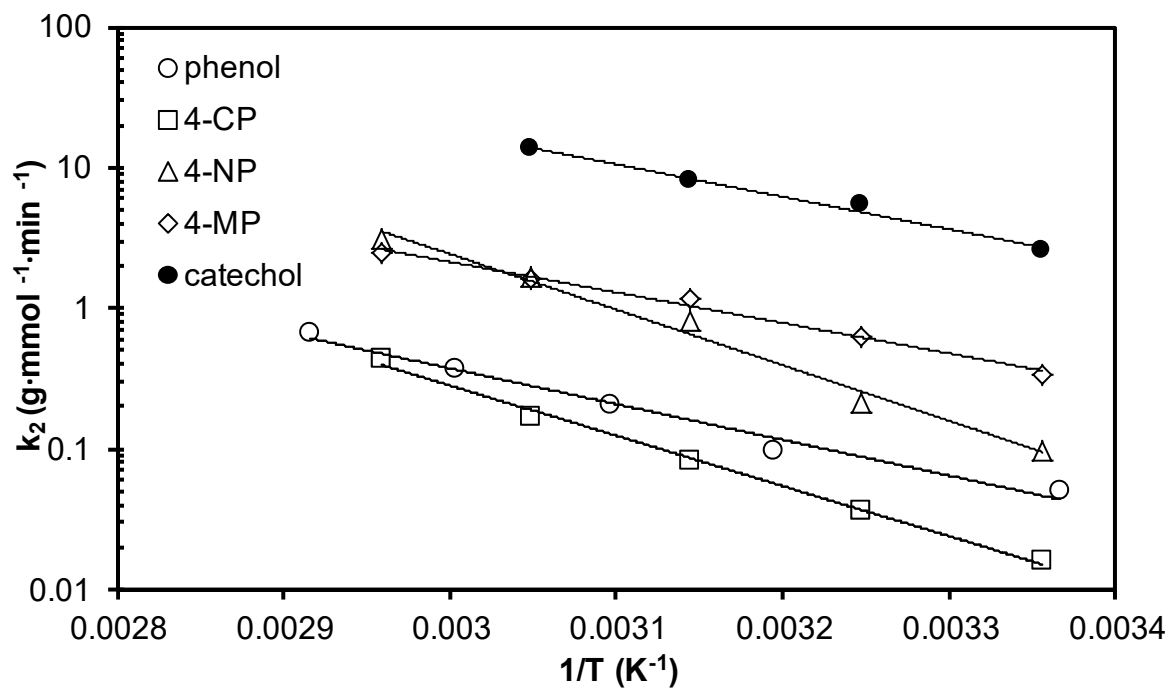
Figure 4.13(a) Plots of k_2 in log scale versus 1/T for sorption of phenolic compounds in PEBA
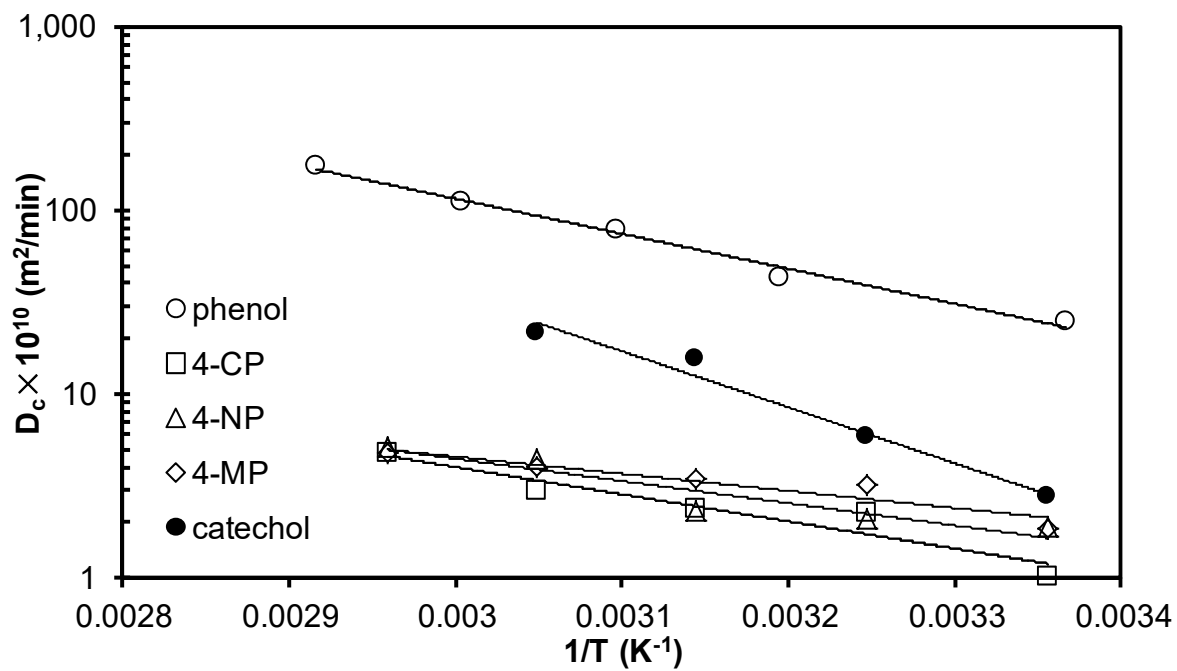
Figure 4.13(b) Plots of D_c in log scale versus 1/T for sorption of phenolic compounds in PEBA

4.4 Conclusions

1. Sorption of phenol, 4-CP, 4-NP, 4-MP and catechol in PEBA membrane took place at the surface of the membrane, followed by the diffusion in the membrane. The sorption uptake was determined by the mass of the PEBA sorbent, not the surface area of the sorbent.

2. The overall sorption rate of phenol, 4-CP, 4-NP, 4-MP and catechol in PEBA was not controlled by surface reaction or internal diffusion alone, and both steps appeared to be important.

3. In general, sorption kinetics of phenol, 4-CP, 4-NP, 4-MP and catechol by PEBA membrane could be described by the modified pseudo-second order reaction model equation, although diffusion inside the membrane was not negligible for thick membranes.

Chapter 5

Sorption of phenolic compounds in PEBA: multi-solute systems

5.1 Introduction

The previous work focused on removing single phenolic compound solute from water. In practical applications, it is more likely to deal with removal of multiple phenolic compounds from aqueous solutions. The sorption of one species may be affected by others in the mixture, possibly affecting not only the sorption capacity but also the sorption rate of each solute component. An early study of Webber and Morris indicated that a solute was influenced adversely by both sorption rate and equilibrium sorption capacity by other solutes present in bi-solute systems [213]. However, there was no consistent relationship between the uptake capacity and sorption rate for other systems. Ho et al. [214] reported a decrease in the equilibrium uptake and an increase in the sorption rate constant for the sorption of nickel ions in the bi-solute system. Thus it is imperative to investigate the interaction between different phenolic compounds in multi-solute systems to determine how the solute-solute interactions affect the sorption capacity and sorption rate.

The effect of competitive sorption on equilibrium capacity of each component in a multi-component system is of particular interest for sorptive process design. At low solute concentrations for which there are abundant surface sorption sites available for sorption, the competitive effect between the solute components is likely not significant. However, at higher solute concentrations in the solution, the surface sites available on the sorbent are

rapidly occupied and different solute molecules start to compete for the sorption sites. For a surface-based adsorptive process, a reduction in the sorption capacity due to competitive sorption effect is anticipated, especially at high solute concentrations. However, insignificant sorption competition has been reported in sorption processes characterized by a partitioning-type mechanism [215, 216]. In addition, not all solute-solute interaction lead to competitive sorption, and cooperative effects between phenolic compounds have been observed in multi-solute systems in some studies, especially at low solute concentrations [131, 133, 217].

In this study, binary solute systems and a quinary solute system of the aqueous phenol solutions were studied to investigate how the interactions among the phenolic compounds affect their sorption in PEBA. In order to quantify these effects, multi-solute sorption isotherm models were applied to analyze the experimental data. Since all the phenolic compounds studied obey the Freundlich isotherm for single solute sorption systems, the multi-solute sorption isotherm data was fitted by the competitive Freundlich model together with the IAST theory model to obtain a better understanding of the sorption mechanism.

Apart from sorption capacity, sorption rate was another important parameter for sorptive process design. Thus, the sorption kinetics of phenolic compounds in binary- and quinary- solute systems was evaluated. Previous studies showed that the pseudo-second order rate model and the diffusion model were adequate to represent the sorption kinetics for the single-solute system. However, these two models have also been used for multi-solute systems [214]. The sorption kinetics for the multi-solute system was analyzed based on the pseudo-second order model and diffusion model.

5.2 Experimental

5.2.1 Multi-solute sorption equilibrium

To determine multi-solute sorption isotherms, batch sorption experiments were performed using the same procedure as described for single-solute sorption (section 3.3.2). For the binary solute systems, feed solutions containing two phenol solutes with the same initial mass concentration were prepared. For the quinary solute system, solutions containing all five phenol solutes were prepared with the same initial mass concentration for each phenolic compound. The prepared solutions (30 mL, 0-10000 mg/L) were placed in a glass bottle and PEBA membranes with predetermined weights were immersed into the feed solutions. The sorption experiments were carried out in the sealed bottles kept at 298 K. After sorption equilibrium of 24 h, the PEBA membrane sample was removed with tweezers. The solution was filtered with a 0.45-μm membrane (Millipore), and the filtrate sample was analyzed using a high performance liquid chromatograph (HPLC, Agilent 1100) equipped with a C-18 column (Agilent Zorbax SB-C18, 4.6 mm ID×250 mm, 5 μm packing). The operating conditions for the HPLC were: the mobile phase, 40% methanol and 60% water; flow rate, 1.0 mL/min; sample volume, 5 μL; column temperature, 22°C; and the detector wavelength, 225 nm.

5.2.2 Multi-solute sorption kinetics

The solute initial concentration was set at 50 ppm for each of the phenol solutes in the sorption kinetics studies. For each run, 2 L of the feed solution placed in a glass container was continuously stirred at room temperature (298 K). The PEBA membrane sorbent (thickness=203 μm, weight =7.658 g) was carefully placed to the solution. As the sorption proceeded, the solute concentrations in the solution were monitored using the HPLC; a 0.5

ml sample of solution was withdrawn at appropriate time intervals for composition analysis. During the entire course of the kinetic study, the total amount of the solution sample withdrawn was approximately 15 mL, which was less than 1% of the initial volume. Therefore, the change in phenol concentration in the feed solution due to sampling is negligible. Since the regeneration experiments of PEBA sorbent in Chapter 6 demonstrated that the phenolic compounds in PEBA could be stripped off with 0.15 mol/L NaOH solution, the PEBA membrane was regenerated with 500 mL of 0.15 mol/L NaOH, followed by thorough washing with deionized water, for reuses. The procedure was repeated for three times to ensure complete regeneration of the PEBA membrane sorbent. Therefore, all the sorption kinetic studies (single-solute, binary-solute and quinary-solute systems) were performed with an identical membrane.

5.3 Results and discussion

5.3.1 Sorption isotherms of multi-solute systems

Figures 5.1(A-J) shows sorption isotherms of phenol, 4-CP, 4-NP, 4-MP and catechol in PEBA, for comparison, sorption isotherms of single-solute systems were also shown in the figures. The sorption of phenol in binary system as shown in Figures 5.1(A), (B), (C) and (D) revealed that the uptake of phenol was inhibited by the presence of 4-CP and 4-NP (Figures 5.1(A), 5.1(B)) whereas the presence of 4-MP and catechol did not affect phenol sorption significantly (Figures 5.1(C), 5.1(D)).

For single-solute sorption systems, the uptakes of phenolic compounds followed the trend: 4-CP>4-NP>4-MP>phenol>catechol. It appeared that the sorption of phenol was inhibited if other solutes present were strongly sorbed. The inhibiting effects of strongly-sorbed substituted phenols on phenol sorption were also observed in some other studies [126,

128

127, 132, 133]. Khan et al. [130] noticed no competitive sorption in a binary solute system of 2-chlorophenol/4-chlorophenol, where no preferential affinity to the sorbent was present. However, competitive sorption may be also related to the molecular size of the sorbate molecules. Webber and Morris [213] reported that the larger solute molecules affected the uptake of small phenol molecules. Kim and Song [143] observed that phenols with a stronger affinity to the sorbent might occupy larger adsorption sites than other solute components that have weaker affinity to the sorbent. In our study, the molecular weights of 4-NP and 4-CP are much larger than that of phenol (Table 3.1). Therefore, the inhibiting effect of 4-NP and 4-CP on phenol sorption may be attributed to the molecular size or affinity aspect, or both, of the binary solute systems.

A comparison of sorption of 4-CP with and without the presence of a second solute in the solution (Figures 5.1(A), (E), (F), and (G)) revealed that the uptake of 4-CP was reduced by the presence of 4-NP, 4-MP and phenol, especially when they were at high concentrations. However, the sorption of 4-CP was not affected by catechol. It was worth noting that no obvious decrease in 4-CP sorption was noticed at low solute concentrations in the solution. The total amount of solutes seemed to play an important role in the competitive sorption. At a lower solute concentration, the sorption sites are readily available; whereas when the solute concentration is sufficiently high, active sites available for sorption becomes are limited and competitive sorption becomes significant. A similar trend was reported by Cho et al. [218], who found that sorption competition between solutes occurred at high solute concentrations, and no significant competitive effect was observed at low solute concentrations during solid phase micro-extraction process of multi-component solutes. In some studies [127, 131],

although competitive sorption was observed at higher solute concentrations, enhanced solute sorption was also observed at low solute concentrations.

As shown in Figures 5.1(A), (E), (H) and (I), a significant decrease in the sorption capacity of 4-NP was observed in binary solute systems except for the 4-NP/phenol binary solute system. The molecular mass of 4-NP is the largest, among the phenolic compounds studied here, and phenol is the smallest. The presence of small solute molecules did not appear to affect the sorption of large solute significantly. Similar results on the effects of solute molecular size on competitive sorption were reported by Weber and Morris [213].

The sorption behaviour of 4-MP in binary solute systems was different from other phenolic solutes studied, as shown in Figures 5.1(C), (F), (H), and (J). The sorption of 4-MP was substantially suppressed by the presence of 4-CP, whose affinity to PEBA was the strongest among all the phenols studied here. This trend was expected in view of the different affinities of phenol solute to the sorbent. However, the sorption of 4-MP was hardly affected by the presence of 4-NP and phenol in binary solute systems. For a surfaced-based sorption process, competitive sorption was expected because solutes will compete for the limited binding sites at the surface when multiple solutes are involved. However, if the sorption process is a partitioning process, the competitive surface sorption will no longer be important [215-217].

Figure 5.1(J) shows that the sorption of 4-MP was slightly enhanced by the presence of catechol in the binary solute systems. The result suggested that there was no competition between the two phenolic compounds, but their interactions favoured the sorption of both components. Mutual enhancement of sorption of different solutes in multi-solute systems was observed at low solute concentrations in other studies [131, 133]. Sheng et al. [217] studied

the sorption of trichloroethylene on organoclays with and without the presence of carbon tetrachloride, nitrobenzene and ethyl ether. It was found the uptake of trichloroethylene was increased in the presence of carbon tetrachloride and nitrobenzene while decreased in the presence of ethyl ether. The enhanced sorption of trichloroethylene was ascribed to the increased solvency of trichloroethylene in the solid phase due to the presence of other organic compounds. In our study, it is likely that the interactions between catechol and 4-MP favoured the sorption of 4-MP in PEBA.

Figures 5.1(D), (G), (I), and (J) show that the sorption of catechol was slightly decreased by the presence of 4-NP and 4-CP, and not affected by the presence of phenol and 4-MP. It seemed that the inhibiting effect of other phenol solutes on the sorption of catechol was not obvious.

Figure 5.2 shows the competitive sorption of quinary solute systems. The sorption capacity of individual solute decreased for all five phenolic compounds studied in the quinary solute system. Due to the increased amount of solutes in the solution, stronger competitive effects among the different phenolic compounds were anticipated in the quinary solute systems than that in binary solute systems. A study of Huh et al. [127] showed that the uptake of phenol in ternary solute systems decreased more than that in binary solute systems. Kim et al. [143] also reported the percent decreases in sorption uptakes of 2-chlorophenol, 4-nitrophenol and 3-cyanophenol were greater in the ternary solute systems than those in binary solute systems.

In the following, the experimental data will be quantified with multi-component isotherm models to measure the effects of interactions among the solutes in the solution on the sorption of individual solute in PEBA sorbent.
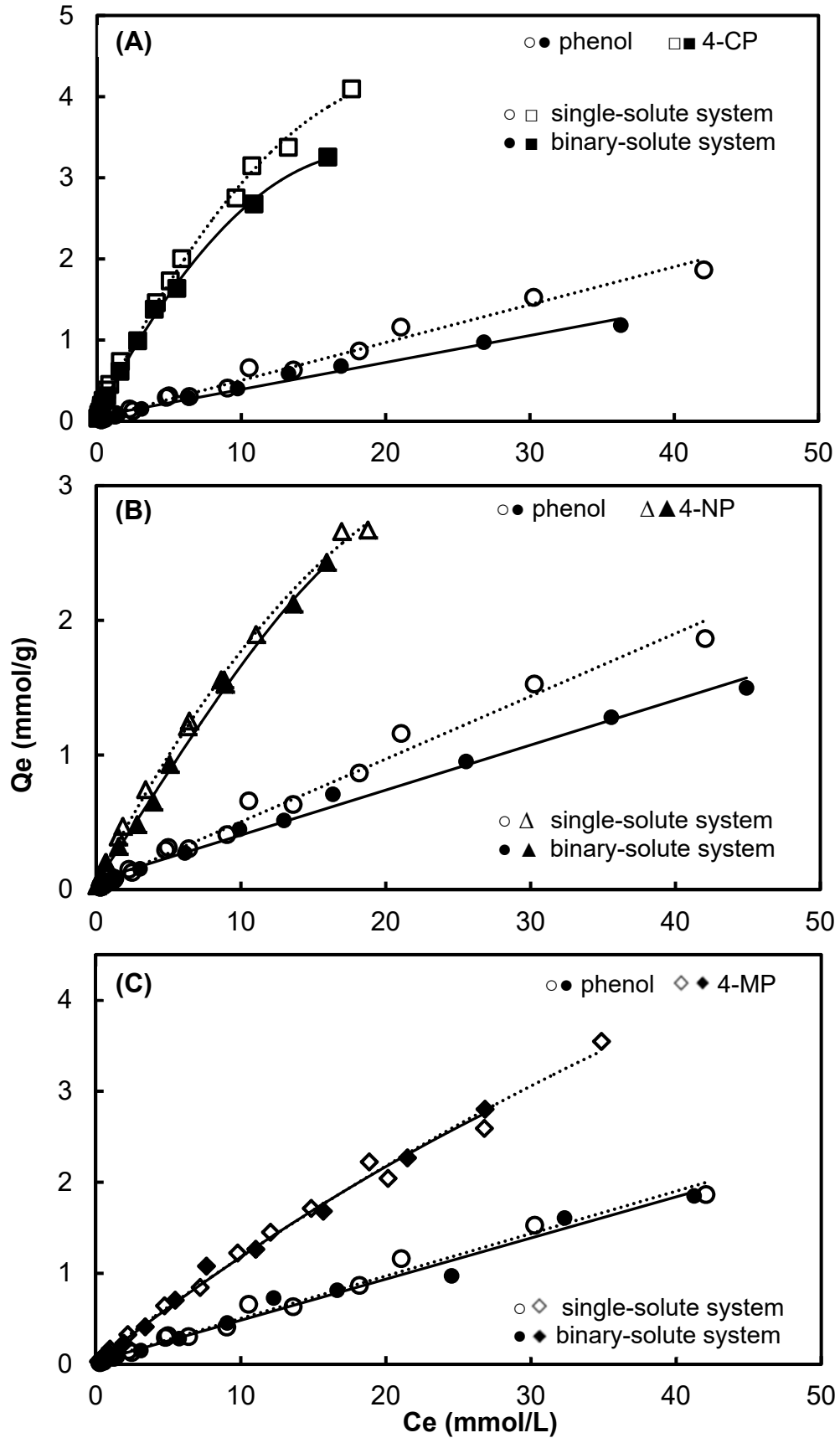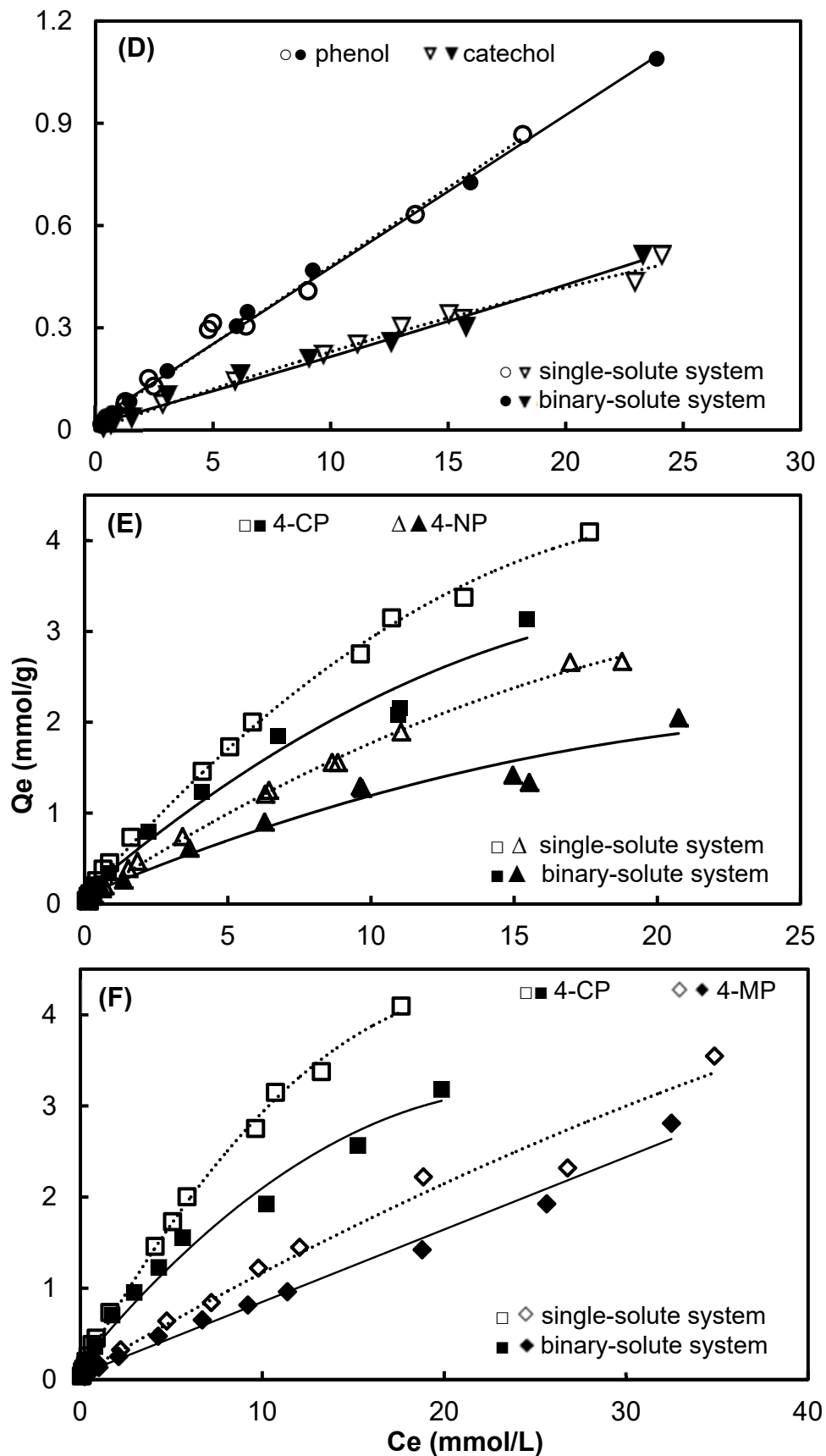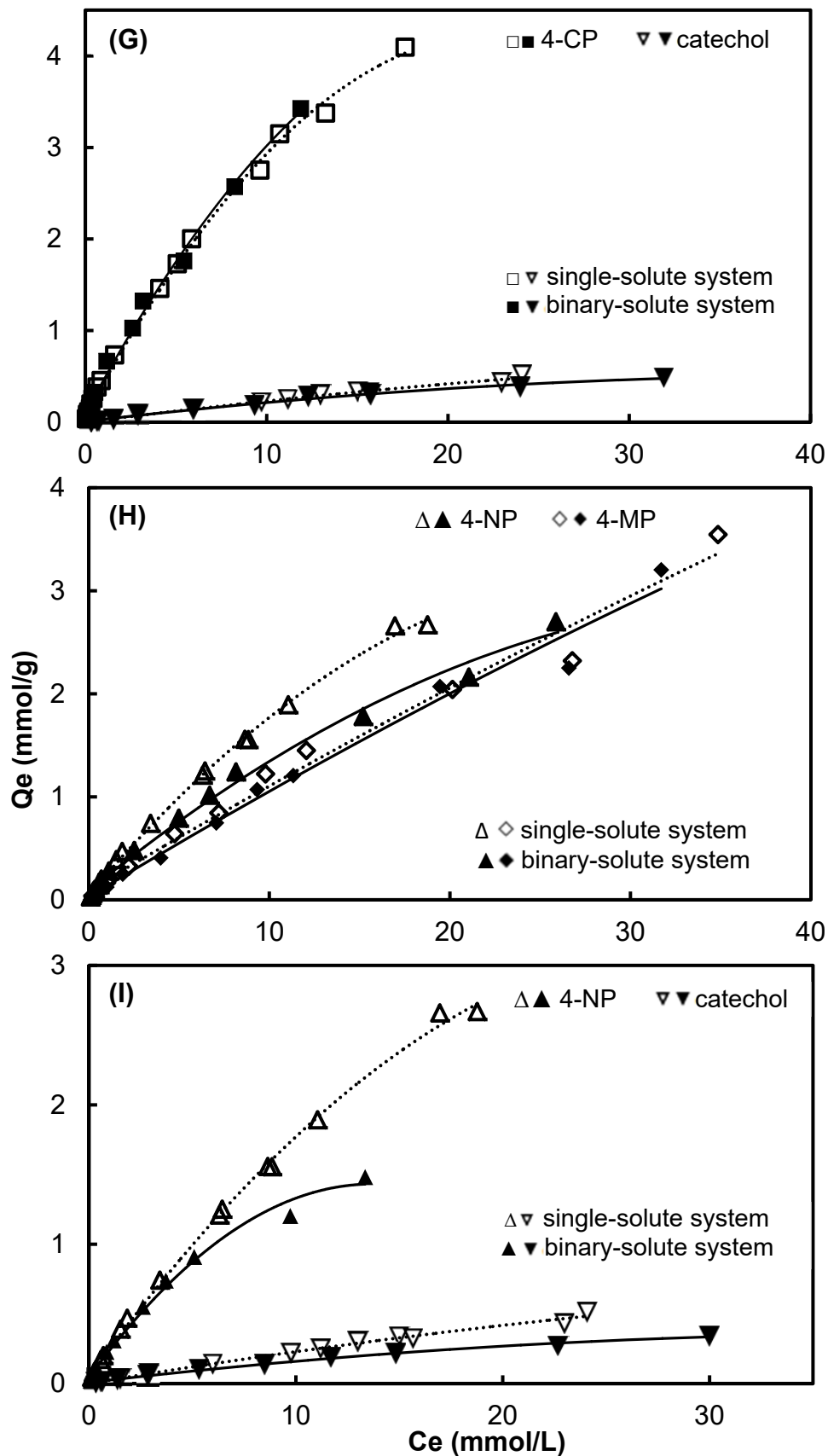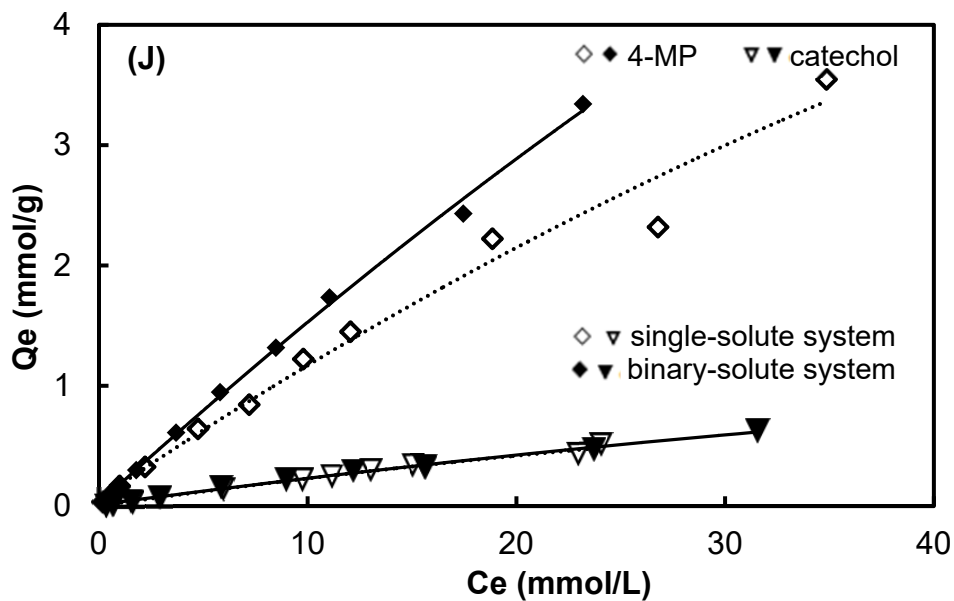
Figure 5.1 Sorption of phenolic compounds by PEBA in the single- and binary-solute systems. Dotted lines represent isotherms in the single-solute systems and solid lines indicate isotherms in the binary-solute systems.
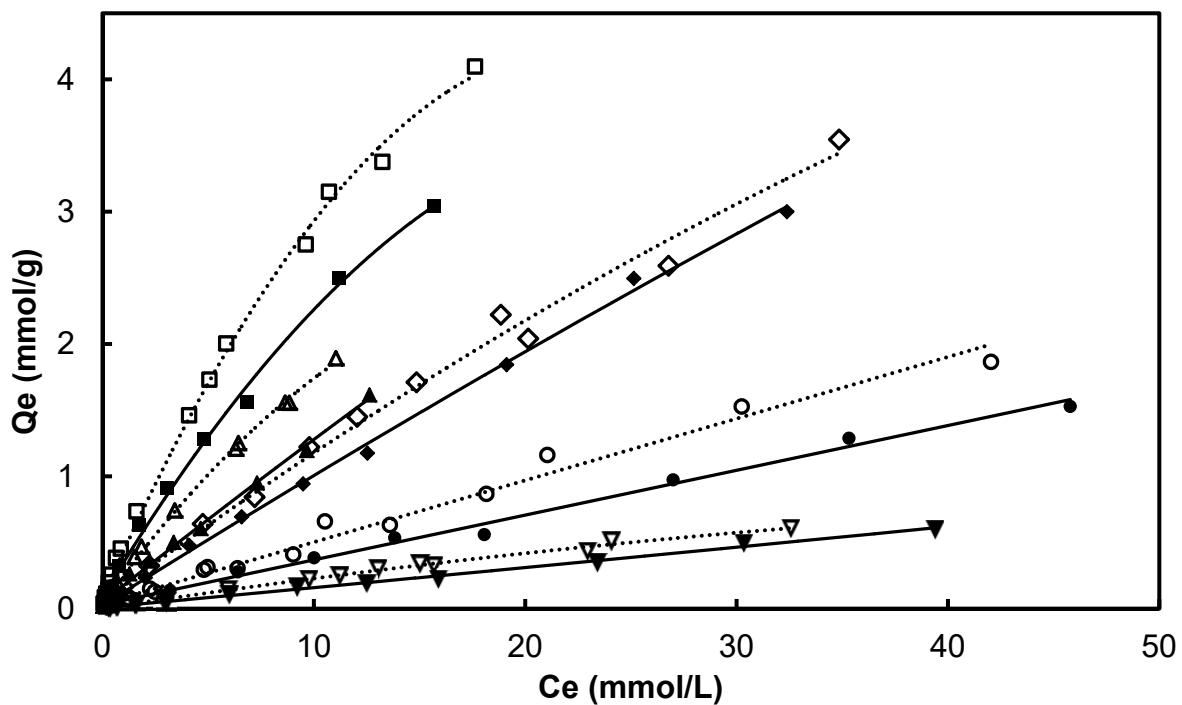
Figure 5.2 Sorption of phenol ($\circ$ $\bullet$), 4-CP ($\square$ $\blacksquare$), 4-NP ($\triangle$ $\blacktriangle$), 4-MP ($\lozenge$ $\blacklozenge$), and catechol ($\triangledown$ $\blacktriangledown$) by PEBA in the single- and quinary-solute systems. Dotted lines represent isotherms in the single-solute systems and solid lines indicate isotherms in the quinary-solute system.

135

5.3.2 Multi-component isotherm modelling

Previous studies showed that the sorption of all the five phenol solutes in PEBA obey the Freundlich-type isotherm. Thus the competitive Freundlich model, which assumes that the Freundlich isotherm applies to all single solute systems, was applied to analyze the multi-component sorption data. For the binary solute systems, experimental data was analyzed by Eqs. (2.36) and (2.37) with the non-linear curve fitting of the Origin software, parameters K_F and 1/n for each phenolic compound were considered to be the same as those for single solute systems, which were available in Table 3.3. The sum of squared errors (SSE) of the fitting was given in Table 5.1, which was calculated by

$$\text{SSE} = \sum_{i=1}^{n}(Q_{e,cal}-Q_{e,exp})_i^{2} \tag{5.1}$$

In addition, the IAST model was also employed for fitting of the experimental data. The model calculation based on the IAST model can be conducted by solving a series of equations simultaneously, as shown in Figure 5.3. SSE values for fitting the IAST equations to the binary solute sorption data were presented in Table 5.1.

obtain C_1, C_2, $Q_{1(exp)}$, $Q_{2(exp)}$ from experimental data	estimate $Q_{1(cal)}$ & $Q_{2(cal)}$ using Eq. (2.44)
calculate z_1 and z_2 by using Eq. (2.41)	estimate $Q_{T(cal)}$ by using Eq. (2.43)
estimate $C_1{}^0$ by using Eq. (2.42)	calculate $Q_2{}^0$ by using Eq. (2.50)
estimate $Q_1{}^0$ by using Eq. (2.48)	estimate φ by using Eq. (2.49)
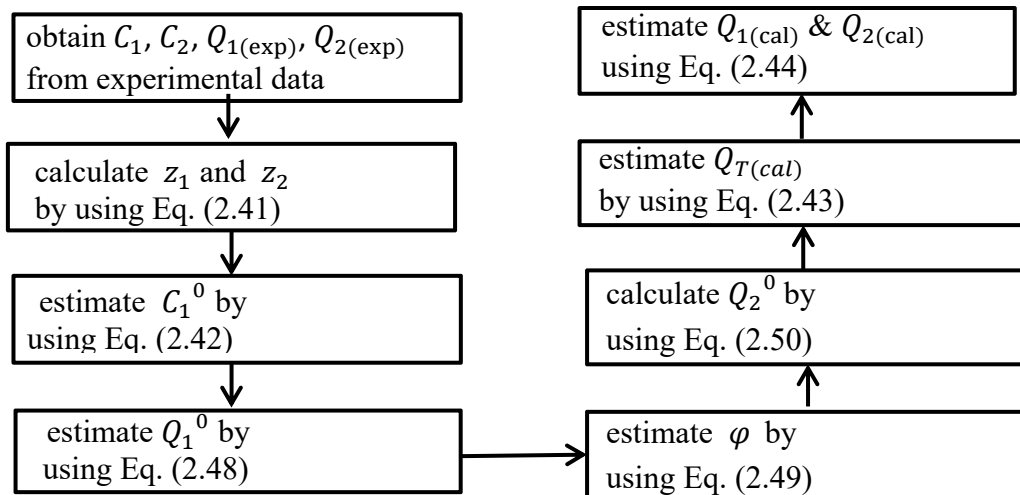
Figure 5.3 Model calculation process based on the IAST model
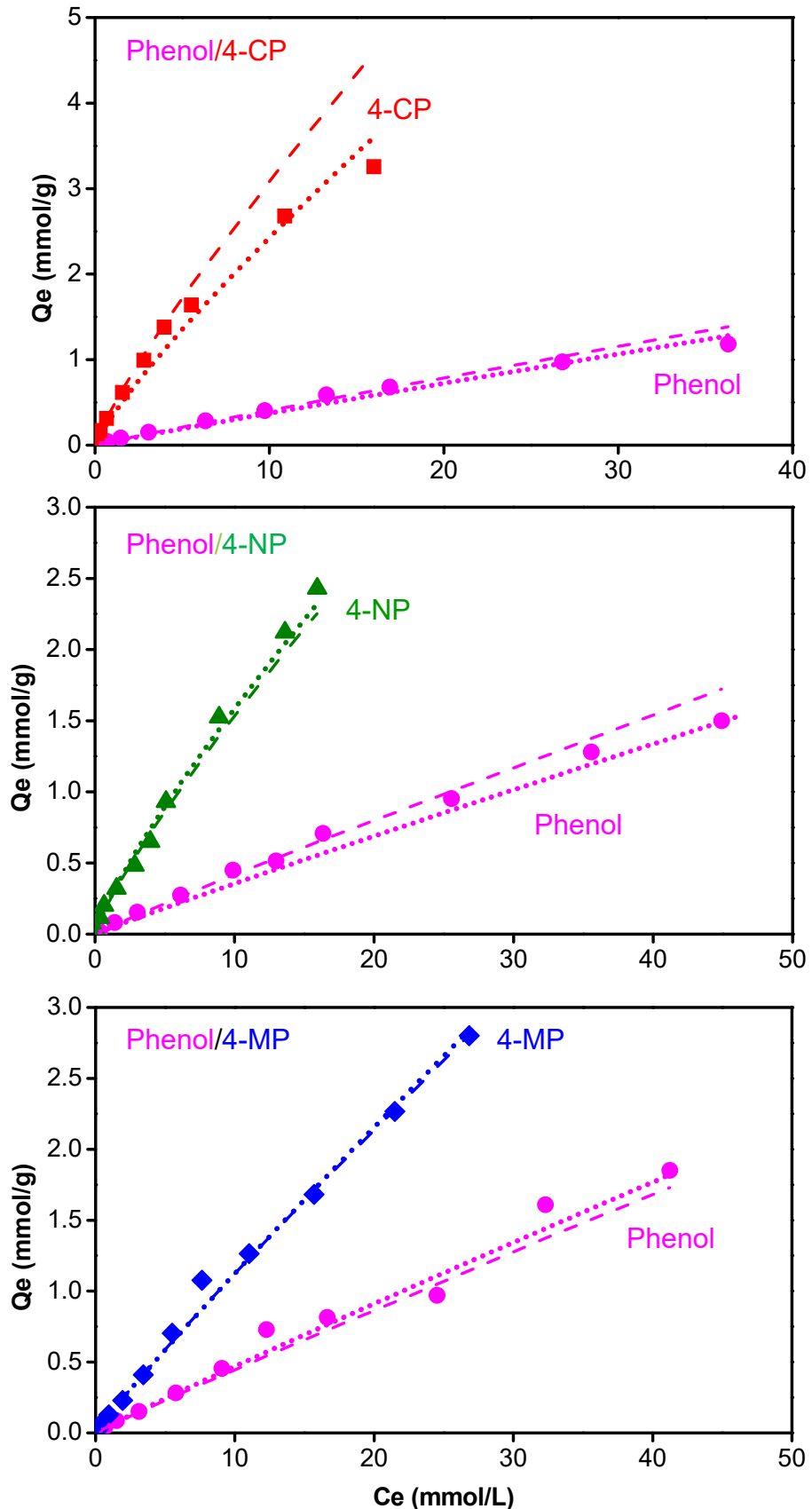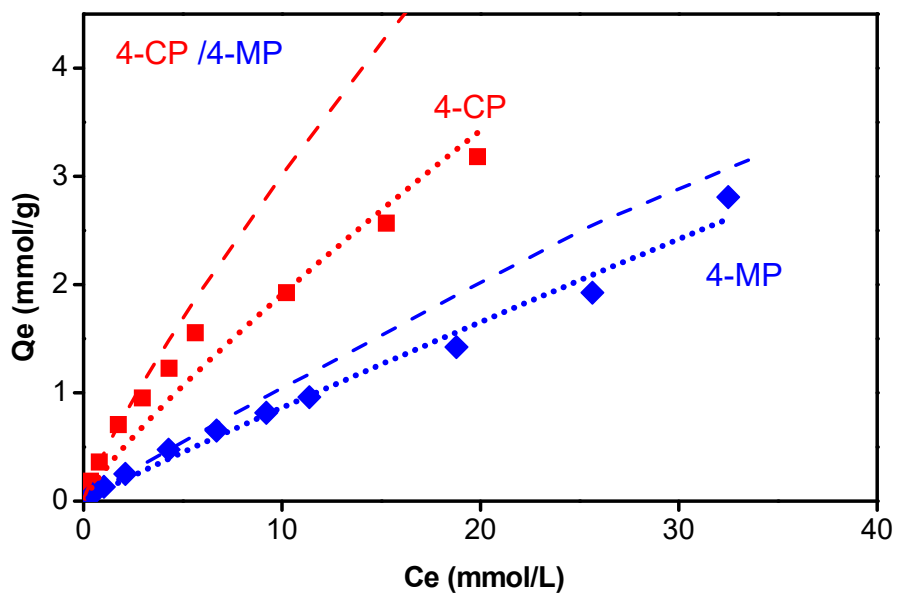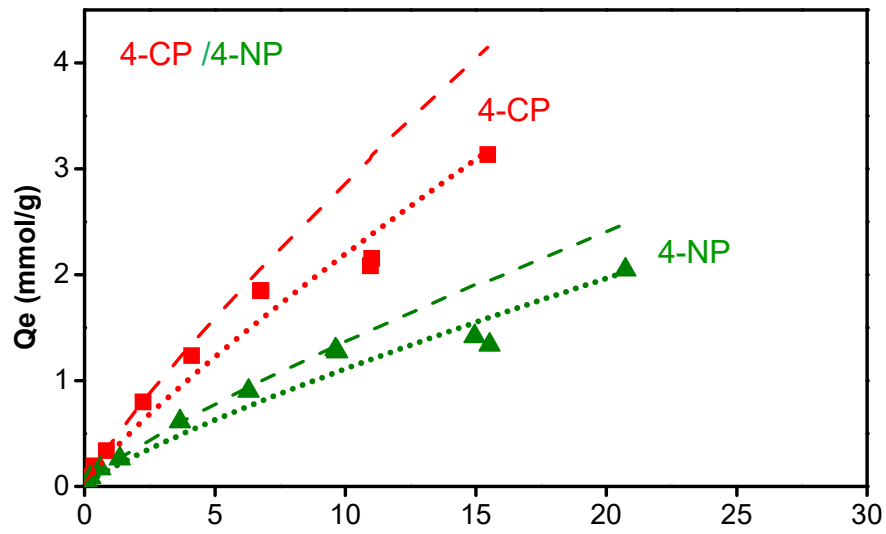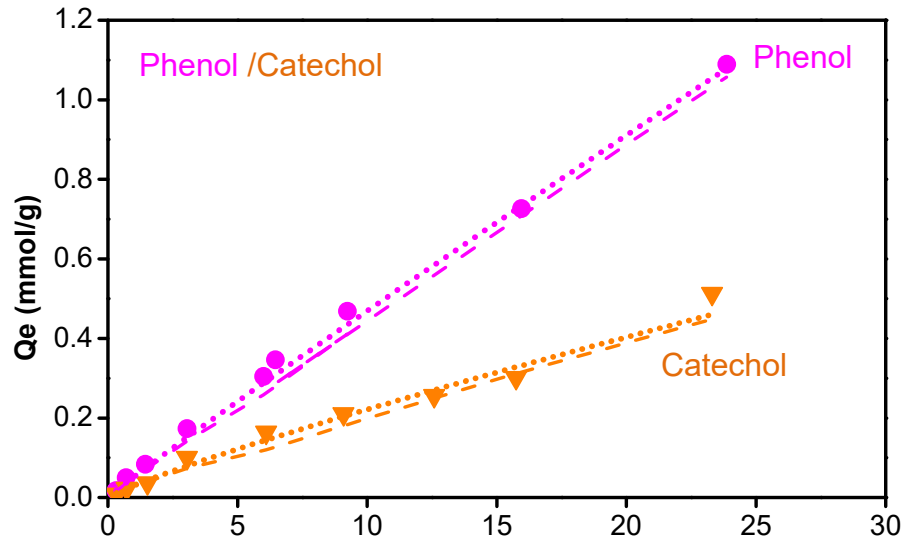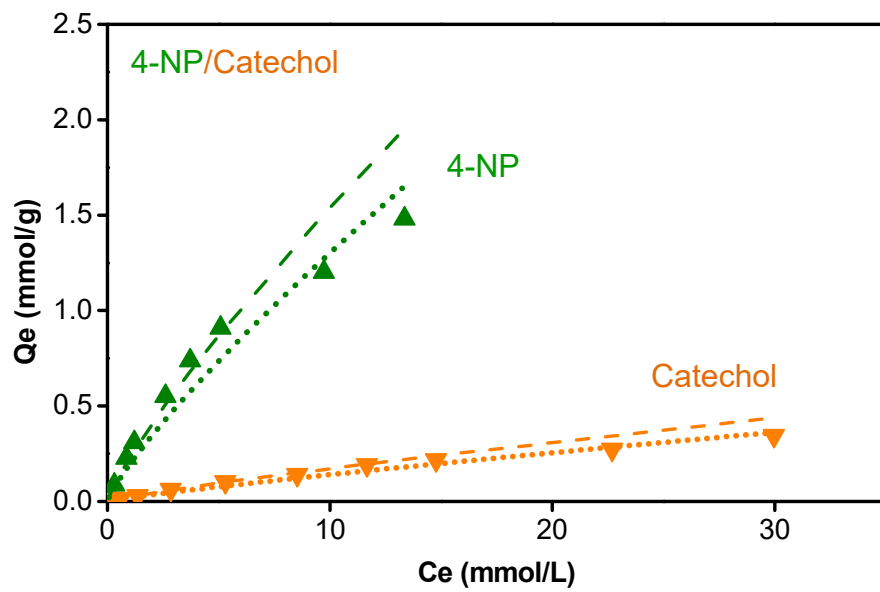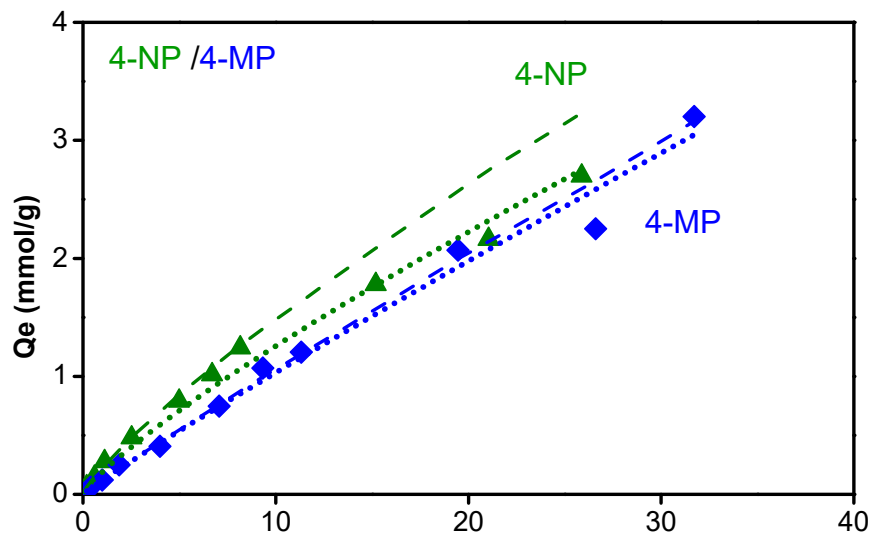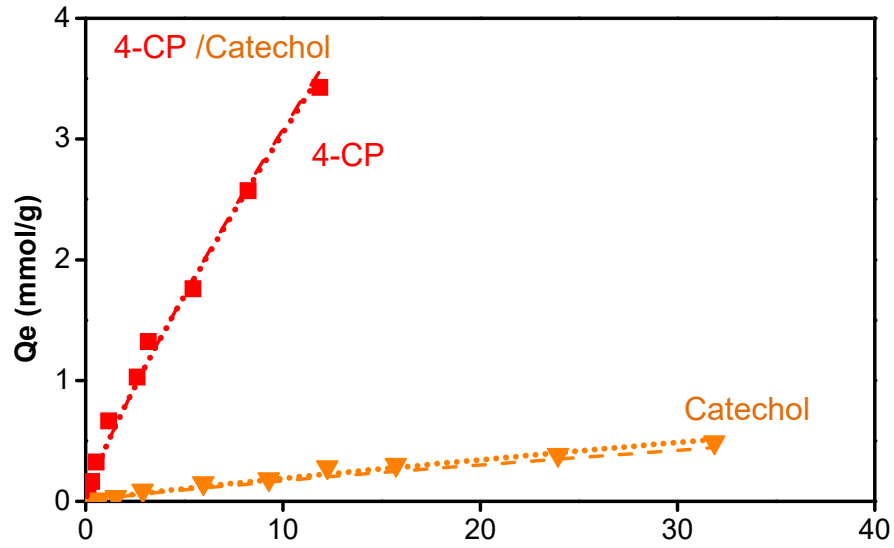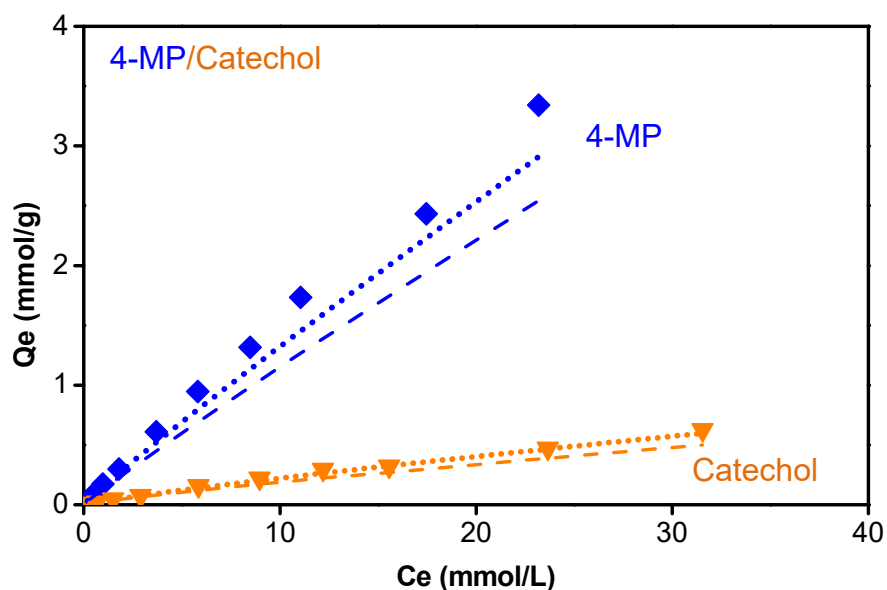
Figure 5.4 Comparison of experimental data and model calculations based on the IAST model and the competitive Freundlich model for sorption of phenolic compounds by PEBA in binary solute systems. (……) predicted by the competitive Freundlich model, (− − −) predicted by the IAST model.

A comparison of experimental data and the model calculations based on the competitive Freundlich model (dot line) and the IAST model (dash line) were presented in Figure 5.4. It was observed that the competitive Freundlich model can be fitted to the experimental data better than the IAST model for binary solute systems, especially for sorption of 4-CP and 4-NP. Table 5.1 shows that the SSE values for the model predictions based on the competitive Freundlich model is less than those based on the IAST model for most of the binary solute systems studied.

For low uptake solutes such as phenol and catechol, the IAST model provided a good fit to the experimental data. However, for strongly sorbed solutes such as 4-CP and 4-NP, the model predictions based on the IAST model deviated significantly from the experimental data at high solute concentrations. The deviation was mainly due to the non-ideal behaviour of the solid phase at high solute concentrations in the solid phase. Among the phenolic

compounds studied, 4-CP and 4-NP had a larger sorption capacity in the PEBA sorbent, and because of the high sorbate loading, the sorbate mixture is anticipated to behave nonideally in the sorbent phase. Rade and Prausnitz [219] found that compared with weakly adsorbed acetone-propionitrile system, the sorption of 4-MP and 4-CP, which had a higher sorption uptake, showed a more significant deviation from the IAST model predictions especially at higher concentration ratios. In another study of the sorption of 4-CP on XAD-16 in the presence of phenol, the IAST model was found to over predict the equilibrium uptake of 4-CP in binary solute solutions at high concentrations [129].

Figure 5.4 shows the model predictions based on the competitive Freundlich model were in good agreement with the experimental data for all the binary solute systems studied. The model parameter a_{ij}, which characterizes the inhibitive effect of component j on component i [138], is presented in Table 5.2 for all the binary solute systems. In order to visualize the competitive effect of other phenolic compounds on a specific component, the radar charts were employed to represent competition coefficient values of competing solutes on the target solute. Figure 5.5 shows the competition coefficients of all the studied phenols on phenol (A), 4-CP (B), 4-NP (C), 4-MP (D), and catechol (E) in binary solutes systems.

Table 5.1 SSE values for model calculations based on the IAST model and competitive Freundlich model in binary solute and quinary solute systems

Sorption system	Solute	SSE (The IAST model)	SSE (The competitive Freundlich model)
Phenol/4-CP	Phenol	0.048	0.025
	4-CP	2.2	0.36
Phenol/4-NP	Phenol	0.066	0.078
	4-NP	0.078	0.16
Phenol/4-MP	Phenol	0.21	0.076
	4-MP	0.095	0.052
Phenol/Catechol	Phenol	0.012	0.0037
	Catechol	0.0079	0.0046
4-CP/4-NP	4-CP	4.2	0.39
	4-NP	1.2	0.20
4-CP/4-MP	4-CP	9.2	0.55
	4-MP	1.5	0.11
4-CP/Catechol	4-CP	0.084	0.081
	Catechol	0.016	0.0050
4-NP/4-MP	4-NP	0.73	0.10
	4-MP	0.18	0.17
4-NP/Catechol	4-NP	0.32	0.14
	Catechol	0.015	0.0017
4-MP/Catechol	4-MP	1.3	0.35
	Catechol	0.034	0.0025
Phenol/4-CP/4-NP/4-MP/Catechol	Phenol	0.80	0.018
	4-CP	7.3	0.79
	4-NP	0.13	0.61
	4-MP	1.0	0.49
	Catechol	0.0093	0.11

Table 5.2 Competition coefficients for phenolic compounds in binary solute systems based on the competitive Freundlich model

	Phenol (1)	4-CP (2)	4-NP (3)	4-MP (4)	Catechol (5)
a_{1i}	1.00	487	683	0.214	0
a_{2i}	1.82	1.00	6.46	9.20	0.0838
a_{3i}	0	8.60	1.00	2.19	0.899
a_{4i}	0.825	284	10.2	1.00	-0.616
a_{5i}	0.00790	6.11	63.3	0	1.00

a_{ji}: the competition coefficient for sorption of solute j in the presence of solute i, and $a_{ii}=1$.

According to Eq. (2.36) and (2.37), if the sorption of component i is not affected by the presence of the component j in the binary solute system, then a_{ij} would be close to zero; if the sorption of component i was reduced greatly in the presence of j, then a_{ij} would be larger than zero. The larger a_{ij} is, the greater competitive effect of component j on i; if cooperative sorption of component i occurs in the presence of j, then a_{ij} should be less than zero.

Figure 5.5(A) indicated that the a_{ij} values for phenol sorption in the presence of 4-NP and 4-CP were much larger than that of 4-MP and catechol. The high a_{ij} values in the phenol/4-CP and phenol/4-NP systems were in accordance with the general trend (i.e., the sorption of weakly sorbed phenols was inhibited by the presence of more strongly sorbed phenols). Similar trend was found in a study of competitive sorption of phenols on modified hexaniobate, where large a_{ij} values were observed in the phenol/2,4-dichlorophenol and 2-chlorophenol/2,4-dichlorophenol systems for which the solute-sorbent affinity was different for different solutes. Small a_{ij} values were observed in phenol/2-chlorophenol system where the solute affinity to the sorbent were of the same magnitude [133].

The sorption of 4-CP was affected by 4-NP and 4-MP whose affinity to PEBA were significant, as shown in Figure 5.5(B). However, PEBA was able to selectively sorb 4-CP in spite of the presence of phenol and catechol, whose affinities to the sorbent were much lower. Similarly, 4-CP has the highest a_{ij} value on 4-NP, as shown in Figure 5.5(C).

A negative a_{ij} value (-0.616) was obtained for the 4-MP/catechol system, as shown in Table 5.2. The sorption of 4-MP was slightly enhanced in the presence of catechol. A possible reason is that the interaction between 4-MP and catechol favours the sorption of 4-MP. Figure 5.5(d) shows that the competition coefficient was the highest for the 4-CP/4-MP system, indicating that the presence of strongly sorbed solute 4-CP would significantly decrease the uptake of 4-MP.

For the competitive sorption of catechol, the highest competition coefficient was observed in the 4-NP/catechol system (Figure 5.5(E)). This competitive behaviour is different from other systems. Since 4-CP had a greater affinity to PEBA than 4-NP, the competition coefficient of 4-CP on catechol was expected to be higher than that of 4-NP on catechol. Note that the competitive behaviour is not determined by the affinity to the sorbent alone, and the molecular size of the solute may also play a role [213]. Although 4-NP has a smaller affinity to the sorbent than 4-CP, 4-NP has a larger molecular size. Once large 4-NP molecules occupy the sorption sites, it will be difficult for the smaller catechol molecules to find available sorption sites in the sorbent.
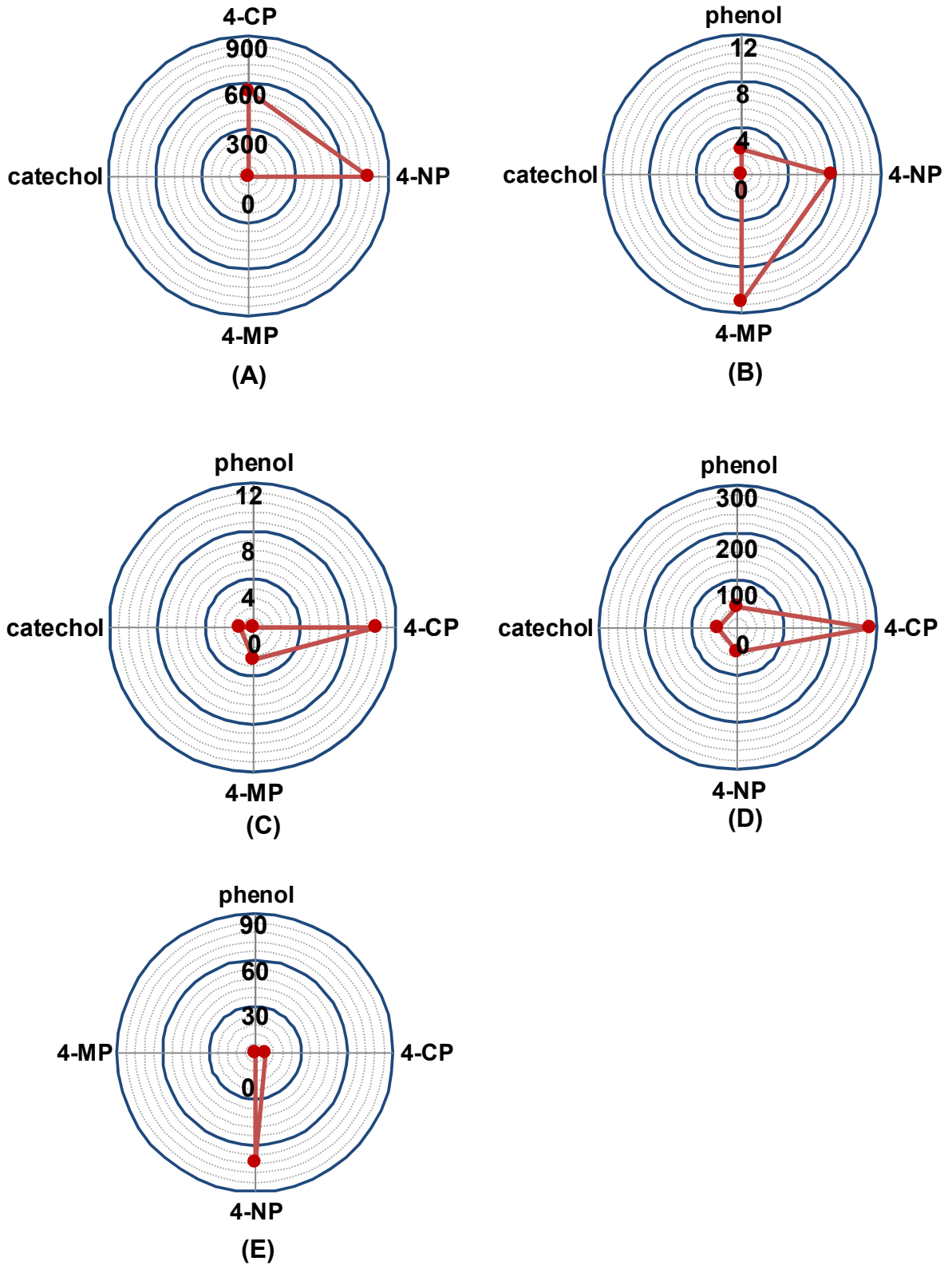
Figure 5.5 Competition coefficients (a_{ij}) of other solutes on the sorption of phenol (A), 4-CP (B), 4-NP (C), 4-MP (D), and catechol (E) for binary-solute systems based on the competitive Freundlich model
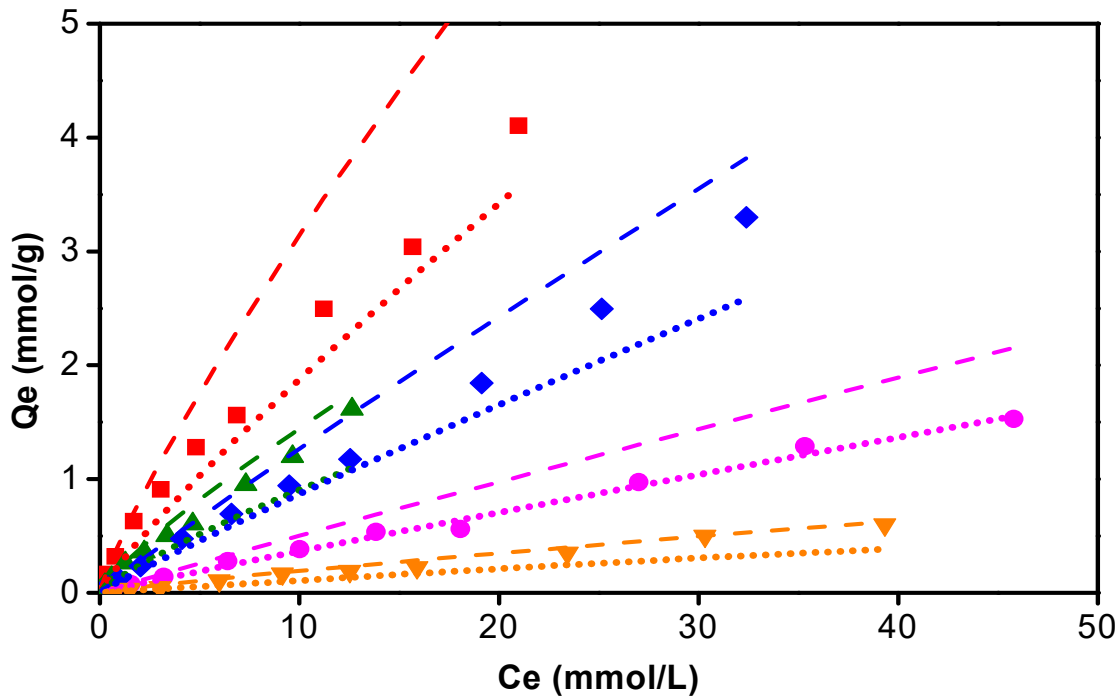
Figure 5.6 Comparison of experimental data and multi-component isotherm model calculation data for quinary systems. Experimental data phenol (●), 4-CP (■), 4-NP (▲), 4-MP (♦) and catechol (▼). (……) calculated by the competitive Freundlich model, (– – –) calculated by the IAST model.

For the quinary system, the multi-component isotherm data was analyzed by both the IAST model and the competitive Freundlich model. With the IAST model, the calculation method was similar to that used in binary systems, which was presented in Figure 5.2. With the competitive Freundlich model, Eqs. (2.38)-(2.40) were used, where the competitive coefficients were considered to be the same as those from binary solute systems. The SSE values for the prediction of quinary solute systems based on the two models were also presented in Table 5.1.

A comparison between experimental data and model calculations using the competitive Freundlich model (dot line) and the IAST model (dash line) were presented in Figure 5.6. Although the competitive Freundlich model showed a good agreement with the

experimental data in binary solute systems, significant deviations between model calculations and experimental data were observed in the quinary solute systems, especially for the sorption of 4-NP, 4-MP and catechol. The reason was that competition coefficients determined from the binary solute systems were used in the quinary solute systems in Eqs. (2.59)-(2.61). It is possible that the competition coefficients for a pair of solutes will be affected by the presence of the other additional solute components in the mixture. Therefore, in order to more accurately look into the competition behaviour in the quinary solute systems, competitive sorption behaviours in ternary and quaternary solute systems should also be investigated.

Figure 5.6 shows that the predicted data based on the IAST model deviated from experimental data significantly, especially at high concentrations. This is due to the non-ideality of the sorbed phase for a quinary solute system, where the total uptake of solutes was much larger than that for binary solute systems. Interactions among the sorbed-species increased with increasing sorption loadings [219], and therefore, an activity coefficient may be considered in the sorbed phase to correct for the non-ideality of the sorbed phase in the model.

5.3.3 Sorption kinetics of multi-solute systems

The interactions among different solutes in a mixture affect not only the uptake capacity, but also the sorption rate of each component. Figure 5.7 shows sorption uptake of phenolic compounds in PEBA sorbent for binary solute systems as sorption proceeded with time. Figures 5.7(A), (B), (C) and (D) show that although the equilibrium uptake of phenol decreased in the presence of the second solute component, the sorption rate of phenol in PEBA seemed to be enhanced. For the sorption of 4-CP, Figures 5.7(A), (E), (F), and (G)

show that the sorption rate of 4-CP was slightly enhanced by the presence of phenol, and its sorption rate was not significantly affected by the presence of 4-NP, 4-MP and catechol. Figures 5.7(B), (E), (H), and (I) that the sorption rate of 4-NP in binary solute systems was not affected by the presence of the other phenol solute. The sorption rate of 4-MP was enhanced by the presence of phenol, and the presence of the other phenolic solutes did not affect the sorption rate of 4-MP. The sorption rate of catechol was enhanced by the presence of phenol, 4-CP and 4-NP, and the opposite was true when 4-MP was present, indicating the inhibiting effect of 4-MP on catechol sorption rate. Sorption kinetics of solutes in the quinary solute system was shown in Figure 5.8. In order to quantify the sorption rate, kinetic models will be applied to fit the experimental data in the following section.
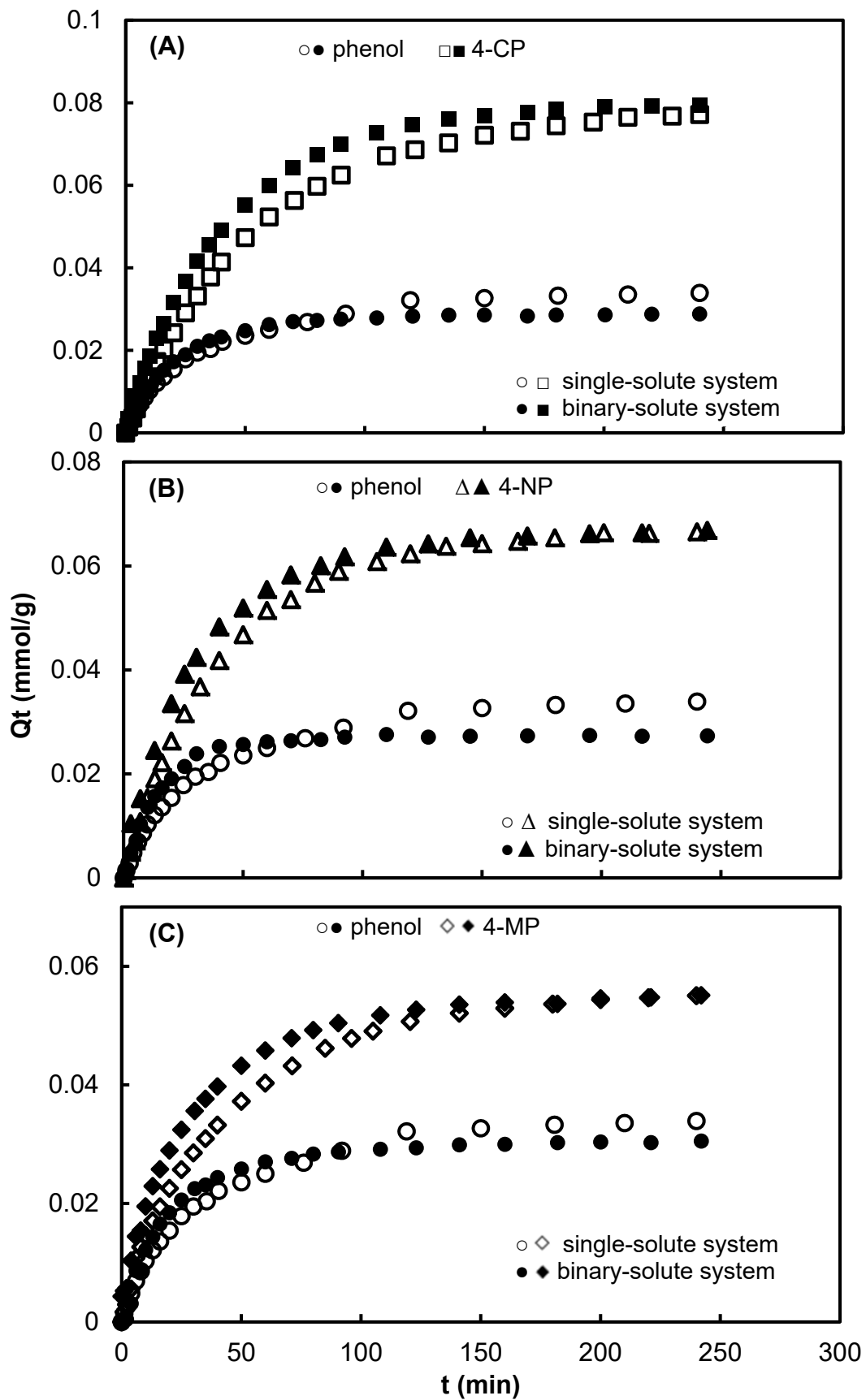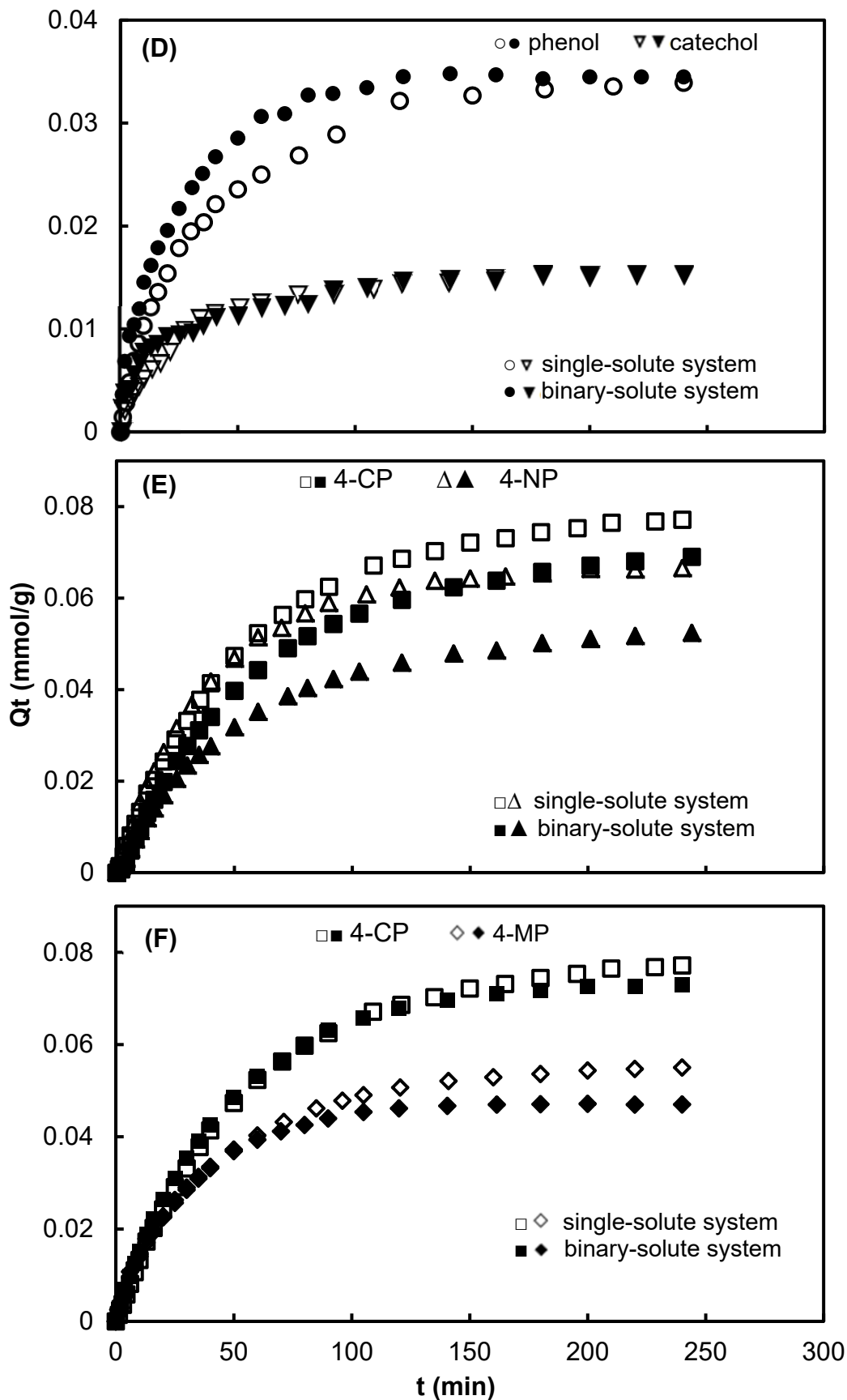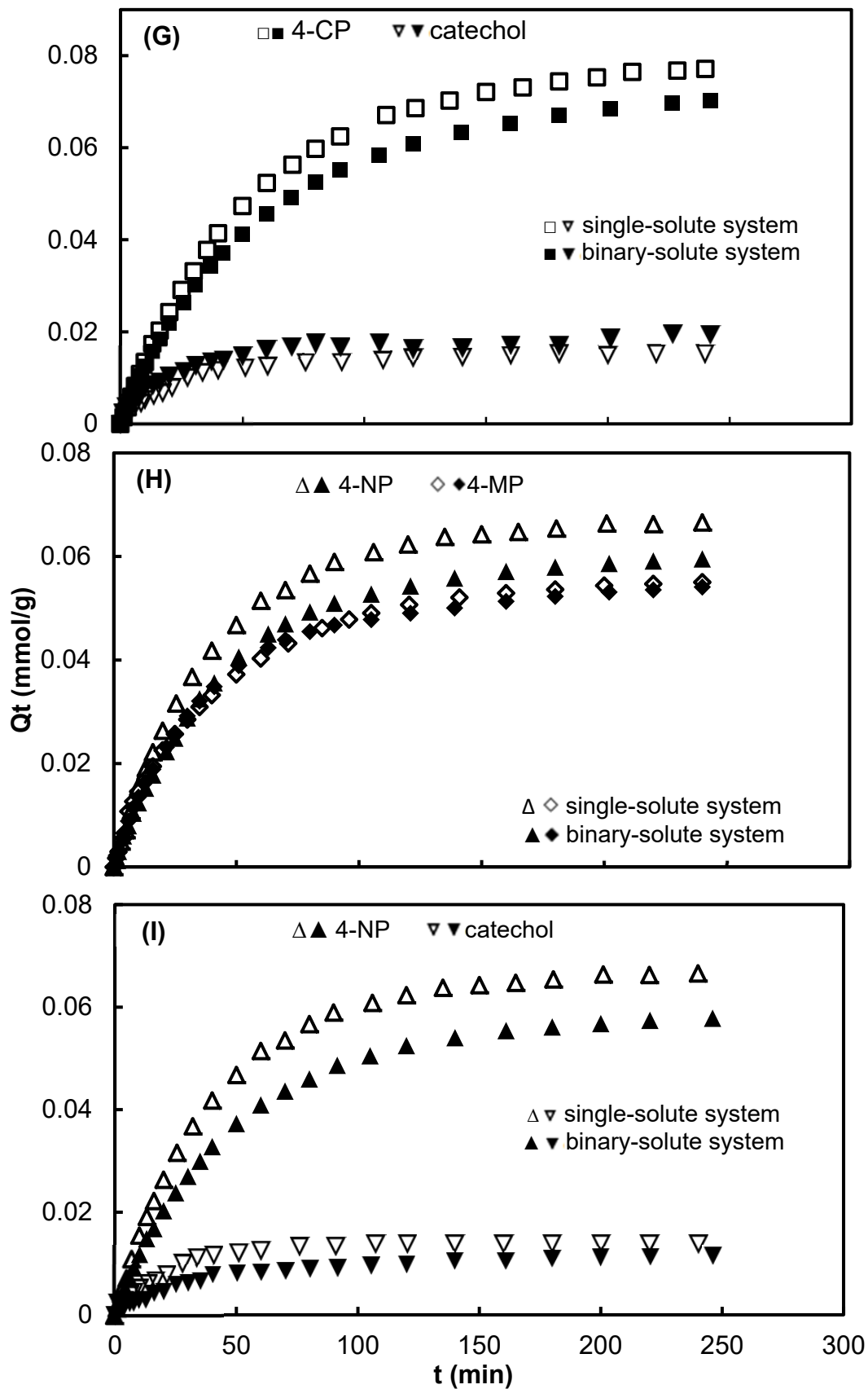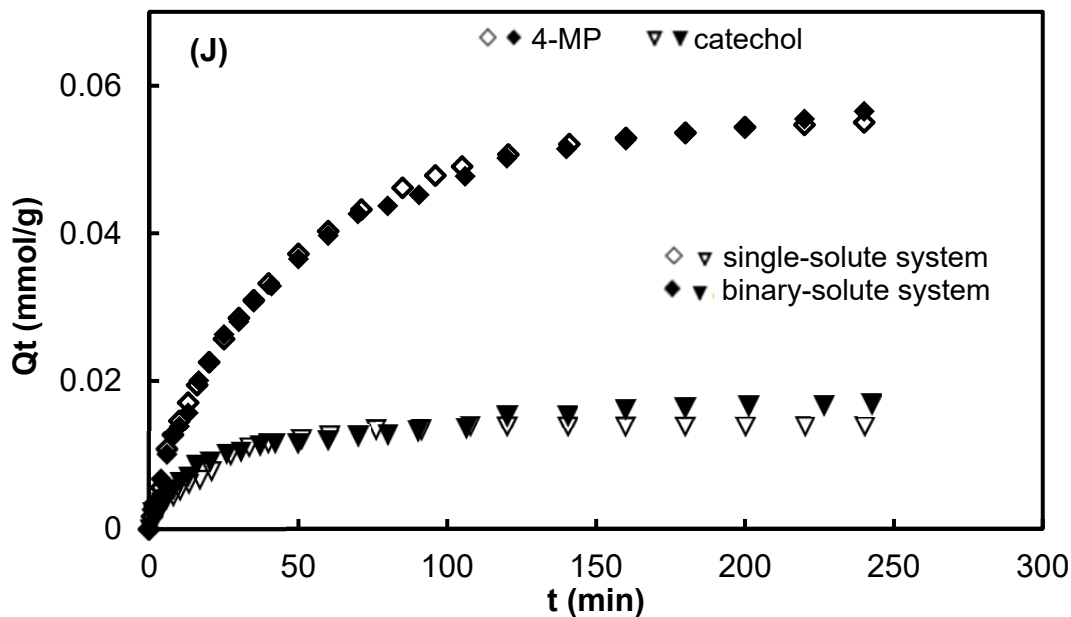
Figure 5.7 Sorption kinetics of competitive sorption of phenolic compounds by PEBA in single- and binary- solute systems
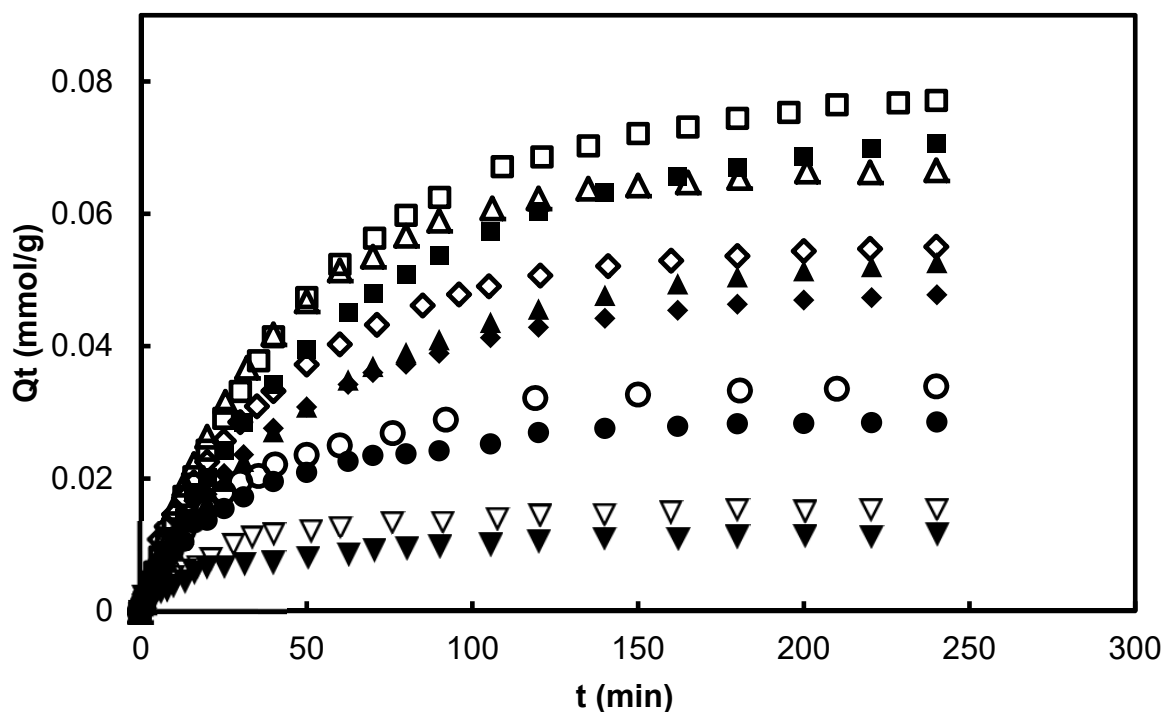
Figure 5.8 Sorption kinetics of phenol (○●), 4-CP (□■), 4-NP (△▲), 4-MP (◊♦), and catechol (▽▼) by PEBA in the quinary solute system. The open symbols represent the data in single-solute systems whereas solid symbols represent the data in the quinary-solute system.

5.3.4 Kinetic model fitting for multi-solute sorption

In order to quantify the sorption kinetics of phenolic compounds in PEBA in multi-solute systems, the pseudo-second order model and the diffusion model were employed to analyze the kinetic data.

5.3.4.1 The pseudo-second order model for multi-solute systems

The pseudo-second order equation was denoted by Eq. (4.6). Parameters K_F and 1/n were obtained from the multi-component isotherm data presented in Figures 5.1(A-J) and Figure 5.2. Sorption rate constant k_2 (g·mmol^{-1}·min^{-1}) for multi-solute sorption were obtained in the same way as described in section 4.3.3 and they were presented in Table 5.3. The data fitting results were presented in the Appendix. For easy comparison of sorption rate constant between single-solute and multi-solute systems, the normalized sorption rate constant (k_2 of a solute component in multi-solute system divided by the k_2 of the solute component in single solute system) were presented in radar charts 5.9(A)-(E).

Table 5.3 shows that for the sorption of phenolic compounds in single-solute system, the sorption rate constant k_2 decreased in the order catechol>phenol>4-MP>4-NP>4-CP. However, the sorption uptake capacity decreased in the order 4-CP>4-NP>4-MP>phenol>catechol. It seemed there was an adverse relationship between the equilibrium uptake capacity of a phenolic compound and its sorption rate constant when the feed solution had only one phenolic solute. This is consistent with the results from a study of competitive sorption of metal ions, where a high sorption rate constant k_2 was correlated with a low equilibrium sorption uptake Q_e [11].

Figure 5.9(A) indicates that there is no significant difference between sorption rate constant of phenol in the quinary solute system and that in single-solute systems, whereas the sorption rate constant was greatly enhanced in all the binary solute systems. The initial concentrations of the two solutes in binary solute system were relatively low (50 ppm for each solute) in this study, and competition of the sorption sites was not significant at low solute concentrations. Thus, there was no significant depressing effect on the sorption rate. In addition, the interactions between phenol and other solute components appeared to have enhanced the sorption rate of phenol, resulting in an increased phenol sorption rate in binary solute systems. Ho et al. [214] studied heavy metal sorption and found that the nickel sorption rate was increased despite of the decreased Q_e values in the cooper/nickel bi-solute system. This result was attributed to the size of nickel ions and the chemical nature of the binding species. However, in quinary solute systems, the initial concentrations for each solute were set the same (50 ppm), but the total solute concentration of the feed solution was substantially higher than the feed solution of binary-solute systems. Therefore, the competitive effect of other components on phenol sorption was more pronounced in quinary-solute systems than that in binary solute systems, which resulted in a sorption rate of phenol in quinary solute system lower than that in binary-solute systems.

Figure 5.9(B) showed that the sorption rates of 4-CP in binary systems followed the same trend as those of phenol. The increased sorption rate of 4-CP by the second solute in binary solute systems was considered to be due to the absence of competitive behaviour at low solute concentrations, together with the interactions between 4-CP and other phenols which favoured the sorption rate of 4-CP. The sorption rate of 4-CP in the quinary solute

154

system is slightly higher (9.7%) than that in the single-solute system. This is probably because 4-CP has the highest affinity to the PEBA sorbent among all the phenols.

The kinetics of 4-NP sorption in the single-solute and multi-solute system was shown in Figure 5.9(C). Sorption rate of 4-NP was enhanced in the presence of 4-CP, 4-MP and catechol but was not greatly affected by the presence of phenol in binary solute systems. In the quinary solute system, however, the sorption rate constant of 4-NP increased by 81.8% compared with that in the single-solute system. The significantly increased sorption rate of 4-NP in the quinary solute system may be related to the large molecular size of 4-NP. 4-NP is the largest molecule among all the phenolic compounds studied here, and once the large sized 4-CP molecules were bonded to the sorbents, the sorbed 4-CP molecules would block the accessibility of other phenolic solutes to the sorbent. Therefore, the large molecule size of a sorbate is expected to be advantageous in competitive sorption with other solutes in multi-solute systems.

Figure 5.9(D) indicates that the sorption rate of 4-MP was enhanced by the presence of phenol, 4-CP, and 4-NP but suppressed by the presence of catechol in binary solute systems. The reduced sorption rates of 4-MP in the 4-MP/catechol system may be caused by the much higher uptake rate of catechol (k_2=6.6 g·mmol^{-1}·min^{-1}) than 4-MP (k_2=0.38 g·mmol^{-1}·min^{-1}) in their respective single solute systems. The sorption rate of 4-MP in the quinary solute system was almost the same as that in the single-solute system, following the same trend as that of phenol.

For the sorption kinetics of catechol, Figure 5.9(E) shows that the sorption rate of catechol was greatly enhanced by phenol and 4-CP, while 4-NP had a retarding effect on the sorption rate of catechol in the binary solute systems. The reduction in the sorption rate of

catechol in the 4-NP/catechol system may result from the large molecular size of 4-NP. Figure 5.9(E) also indicates a significant reduction in catechol sorption rate (24.2%) in the quinary solute system as compared to the case of single catechol solute in the feed solution. Catechol has the least affinity to the sorbent among all the phenolic compounds studied, and the molecular size of catechol is relatively small. Thus the competition from the other solutes in the solution would retard both the rate of sorption and equilibrium capacity of catechol in the quinary solute system.

Table 5.3 Sorption rate constant k_2 (g·mmol^{-1}·min^{-1}) of phenolic compounds by PEBA in single and multi-solute systems based on the modified pseudo-second order model

Solute	Solute systems	k_2
Phenol	Single-solute	1.9
	Phenol/4-CP	2.5
	Phenol/4-NP	4.7
	Phenol/4-MP	3.5
	Phenol/Catechol	4.1
	Quinary-solute	1.8
4-CP	Single-solute	0.031
	4-CP/phenol	0.083
	4-CP/4-NP	0.054
	4-CP/4-MP	0.080
	4-CP/catechol	0.043
	Quinary-solute	0.034
4-NP	Single-solute	0.11
	4-NP/phenol	0.10
	4-NP/4-CP	0.16
	4-NP/4-MP	0.24
	4-NP/catechol	0.23
	Quinary-solute	0.20
4-MP	Single-solute	0.38
	4-MP/phenol	1.0
	4-MP/4-CP	0.60
	4-MP/4-NP	0.91
	4-MP/catechol	0.26
	Quinary-solute	0.39
Catechol	Single-solute	6.6
	Catechol/phenol	17
	Catechol/4-CP	25
	Catechol/4-NP	4.5
	Catechol/4-MP	6.9
	Quinary-solute	5.0
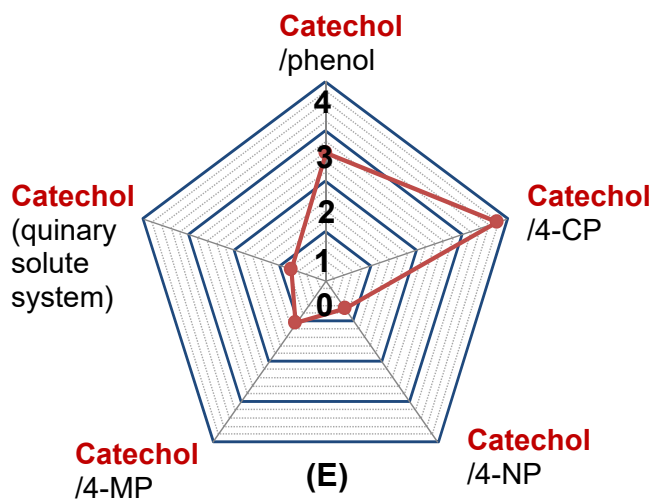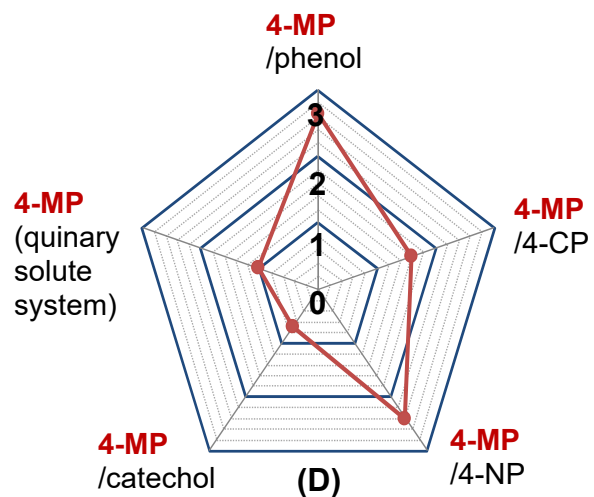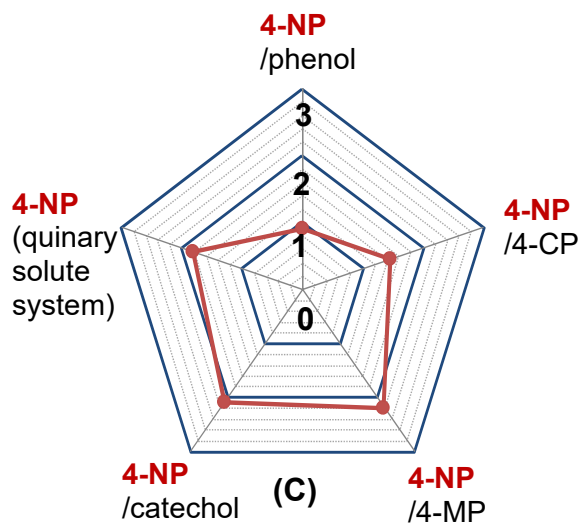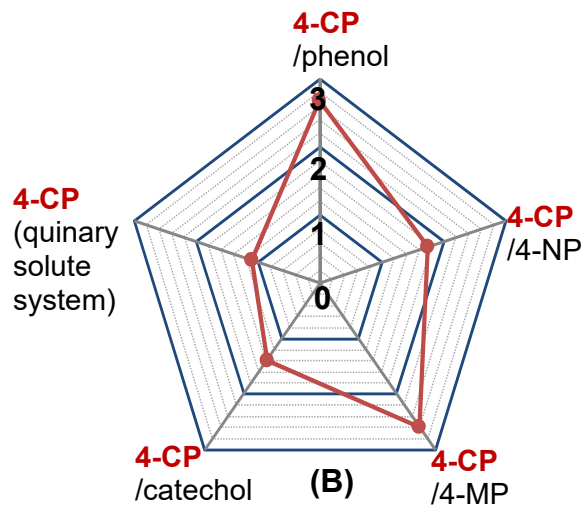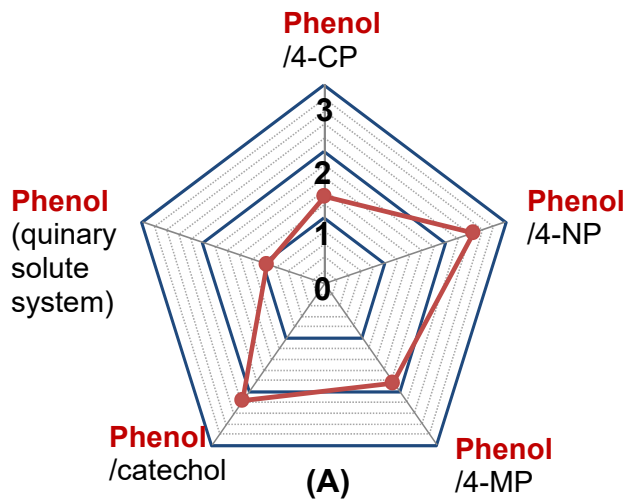
Figure 5.9 Normalized sorption rate constant (k_2) of phenol (A), 4-CP (B), 4-NP (C), 4-MP (D), and catechol (E) for multi-solute systems based on the pseudo-second order model

5.3.4.2 The diffusion model for multi-solute systems

Eq. (4.7) was fitted to the sorption kinetic data in Figures 5.7(A-J) and 5.8, and coefficients D_C (m^2/min) of phenolic compounds in single and multi-solute systems were obtained in the same way as that described in section 4.3.4, and they were presented in Table 7.4. Similar radar charts were used to show the normalized diffusivities (D_c of a solute in multi-solute systems divided by the D_C in the single-solute system), as shown in Figures 5.10(A-E).

Figure 5.10(A) shows that compared with diffusivity of phenol in the single-solute system, the diffusivity of phenol was greatly enhanced by the presence of 4-MP in the solution, and no significant change in phenol diffusivity was observed when catechol was present or when all the five solutes were present in the solution. It seemed that the interaction between phenol and 4-MP favoured the diffusion of phenol. Figures 5.10(B), (D) and (E) showed that the competitive effects of a second phenol on the diffusivities of 4-CP, 4-MP and catechol in multi-solute systems were not significant. This result suggested that the interaction between different phenolic compounds did not greatly affect the diffusion process of the 4-CP, 4-MP and catechol in binary-solute and quinary-solute systems.

The diffusivity of 4-NP followed a quite different trend, as shown in Figure 5.10(C). The diffusivity of 4-NP was enhanced by the presence of phenol, but reduced in the phenol/4-CP, phenol/4-MP and phenol/catechol systems, respectively. The reduced diffusivity of 4-NP in other systems can be ascribed to the competitive effect. Presumably the competitive effect of a second solute will slow down the diffusion process of the large sized 4-NP molecules. In a competitive sorption kinetics study of heavy metal ions on peat, Ho et

al. [214] also found the competitive effect may cause a decrease in the diffusion rate, although it was unclear what was really happened.

In the quinary solute system, the diffusivity of 4-NP was decreased by 34.8% compared with that in single-solute system. On the other hand, the diffusivity of phenol was enhanced slightly by 9.2% in the quinary system, presumably due to its smallest molecular size among the phenolic compounds studied.

Table 5.4 Diffusivity D_c (m^2/min) of phenolic compounds in single-solute and multi-solute systems based on the diffusion model

Solute	Solute systems	$D_c \times 10^{10}$
Phenol	Single-solute	1.3
	Phenol/4-CP	2.0
	Phenol/4-NP	3.2
	Phenol/4-MP	4.1
	Phenol/Catechol	1.2
	Quinary-solute	1.4
4-CP	Single-solute	0.62
	4-CP/phenol	0.72
	4-CP/4-NP	0.70
	4-CP/4-MP	0.76
	4-CP/catechol	0.51
	Quinary-solute	0.52
4-NP	Single-solute	0.92
	4-NP/phenol	1.2
	4-NP/4-CP	0.67
	4-NP/4-MP	0.73
	4-NP/catechol	0.65
	Quinary-solute	0.60
4-MP	Single-solute	1.0
	4-MP/phenol	1.2
	4-MP/4-CP	1.3
	4-MP/4-NP	0.99
	4-MP/catechol	0.90
	Quinary-solute	0.89
Catechol	Single-solute	1.0
	Catechol/phenol	1.4
	Catechol/4-CP	1.3
	Catechol/4-NP	1.0
	Catechol/4-MP	1.3
	Quinary-solute	0.9
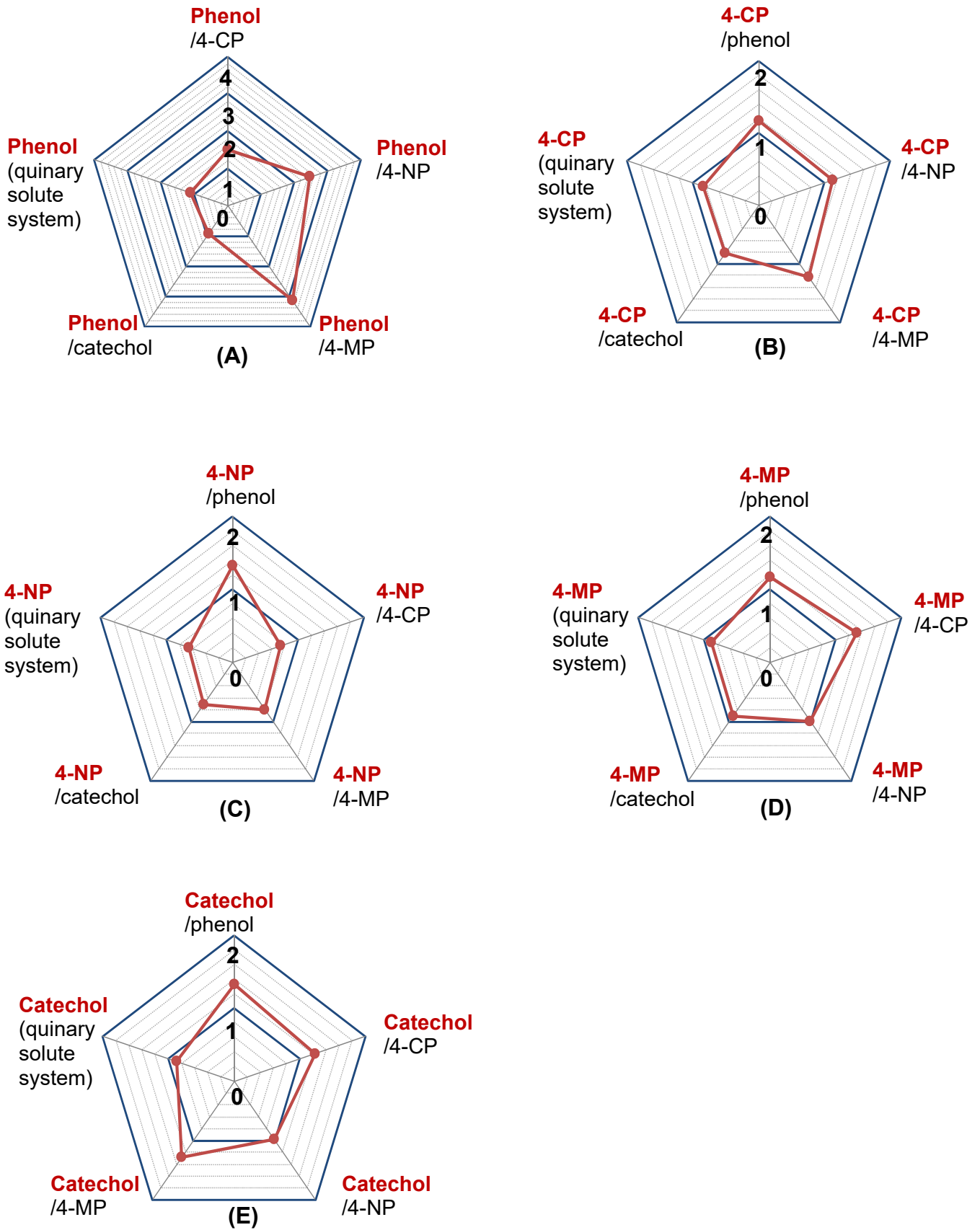
Figure 5.10 Normalized diffusivity (D_c) of phenol (A), 4-CP (B), 4-NP (C), 4-MP (D), and catechol (E) for multi-component systems based on the diffusion model.

5.4 Conclusions

1. The sorption uptake of one solute in the PEBA sorbent may be enhanced, decreased or remain the same when a second solute was added to the feed solution. More specifically, the uptake of 4-MP was slightly enhanced by the presence of catechol; no significant sorption competition was observed for the phenol/4-MP, phenol/catechol, and 4-CP/catechol binary solute systems; mutual depressions were found in other binary solute systems.

2. More significant sorption competition was observed in the quinary solute system than in binary solute systems.

3. The sorption isotherm of a solute in binary solute systems was better represented by the competitive Freundlich model than the IAST model.

4. The pseudo-second order model and the diffusion model were used to describe the sorption kinetics for binary solute and quinary solute systems. Sorption rate constant k_2 and the diffusivity D_c of a solute were affected by the molecular size of the sorbate and its affinity to the sorbent in multi-solute systems.

Chapter 6

Regeneration of PEBA sorbent exhausted by phenolic compounds

6.1 Introduction

After exhaustion of sorption capacity, the sorbents must be replaced with fresh ones or regenerated. For low-cost sorbents such as industrial or agricultural wastes, the sorbents can simply be replaced rather than being regenerated, but the exhausted sorbents need further treatment (e.g., incineration or landfill) for final deposition, which has considerable environmental significance. The regeneration is generally more cost effective than replacement for sorbents with a high production cost, and in this case the performance of the regenerated sorbents will affect the economic feasibility of the sorption process.

A main disadvantage of commercial activated carbon is the high regeneration cost. It has been estimated that the cost of carbon regeneration is around 75% of the operating and maintenance costs [16]. As a thermoplastic elastomer with good mechanical strength, PEBA 2533 is expected to have better regeneration properties. Therefore, it is desirable to investigate the regeneration of the PEBA sorbent.

In this study, both thermal and chemical regeneration of the spent PEBA sorbent were performed. The regeneration tests were conducted in batch sorption using PEBA membranes, the sorption isotherms of phenolic compounds sorbed in pristine PEBA membranes and regenerated PEBA membranes were compared to evaluate the effectiveness of the regeneration process.

A major disadvantage of thermal regeneration is that it needs ex-situ operation in a continuous sorption process. That is, the exhausted sorbent needs to be transported to a heating unit to conduct regeneration and then transported back to the sorption unit [23]. Chemical regeneration can be completed in situ. That is, chemical eluents and wash water are loaded to the exhausted column without repacking. Thus it minimizes the down time for the sorption process. The widely used chemicals for regeneration of sorbent saturated with phenolic compounds include acetone [15, 16], methanol [15-18], ethanol [16, 17, 19, 20], and sodium hydroxide [15, 16, 18, 21, 22]. Therefore, ethanol, methanol, and sodium hydroxide were used as regenerants in this study. The concentration of NaOH solution was selected as 0.15 mol/L according to an earlier study [22].

For the conventional thermal regeneration, phenolic compounds are desorbed from exhausted sorbents at high temperatures (>500°C) [23, 24, 145, 146]. However, the high operating temperature will not only increase the operating cost but also change the morphology of PEBA since its melting point is 134°C. Thus thermal regeneration at high operating temperature is not favourable in our study. As a result, a vacuum-assisted thermal regeneration technique was proposed in our study. It is expected that under vacuum, the sublimation/boiling point will be lowered and a cold trap can be used to condense the sorbed sorbate to form a highly concentrated solution, which is of particular interest from an application point of view. Although thermal regeneration is widely used for regenerating sorbents exhausted by phenolic compounds, very few studies are available on the comparison of thermal regeneration for different phenolic compounds on the same sorbent material. Thermal regeneration and vacuum-assisted thermal regeneration were performed for PEBA loaded with phenol, 4-CP, 4-NP, 4-MP and catechol in this study.

6.2 Experimental

Batch sorption of phenol, 4-CP, 4-NP, 4-MP and catechol in PEBA was performed with the same procedure as described in section 3.3.2. In order to cut the time of the experiment, the initial concentration range was reduced to 50-500 ppm for all the phenolic compounds studied. In conducting the equilibrium sorption experiments, the sorbent were allowed to contact the solution for at least 24 h at room temperature (298 K) to ensure sorption equilibrium was reached. After each regeneration process, the sorption isotherm was determined again to see whether the uptake capacity changed after regeneration.

For chemical regeneration of the sorbent, methanol and ethanol, both reagent grades, were purchased from Sigma-Aldrich and Commercial Alcohols Inc. Canada, respectively. Sodium hydroxide was purchased from Caledon Laboratories, Canada. The phenol-saturated PEBA membrane was treated by 20 mL of the chemicals of interest for 2 hours at room temperature. Then the membrane was washed with large quantity of deionized water to remove any residual regenerants. The surface of the wet membrane was wiped with Kimwipers, and left dry at room temperature. The regenerated membranes were immersed into phenol solutions at the same initial concentrations as used in the first sorption cycle, and the sorption isotherm for the second cycle was obtained. This process was repeated for 4 or 5 times to investigate the effects of sorbent regeneration on the sorption capacity of the regenerated PEBA sorbent.

For thermal regeneration, the phenol-saturated PEBA membrane was placed in an oven at 90°C for 2 h for phenol and 4-MP, at 120°C for 4-CP and catechol and at 130°C for 4-NP. The thermally regenerated membranes were reused in the same way as described. For the vacuum-assisted thermal regeneration, the experimental set up is shown in Figure 6.1.

Phenol-saturated PEBA membranes were placed into a flask which was kept in a water bath at 80°C for 2 h. The vacuum with an absolute pressure of 5 k Pa was applied to assist in evaporation of phenols, and the phenol vapours were condensed and collected with a cold trap immersed in liquid nitrogen.
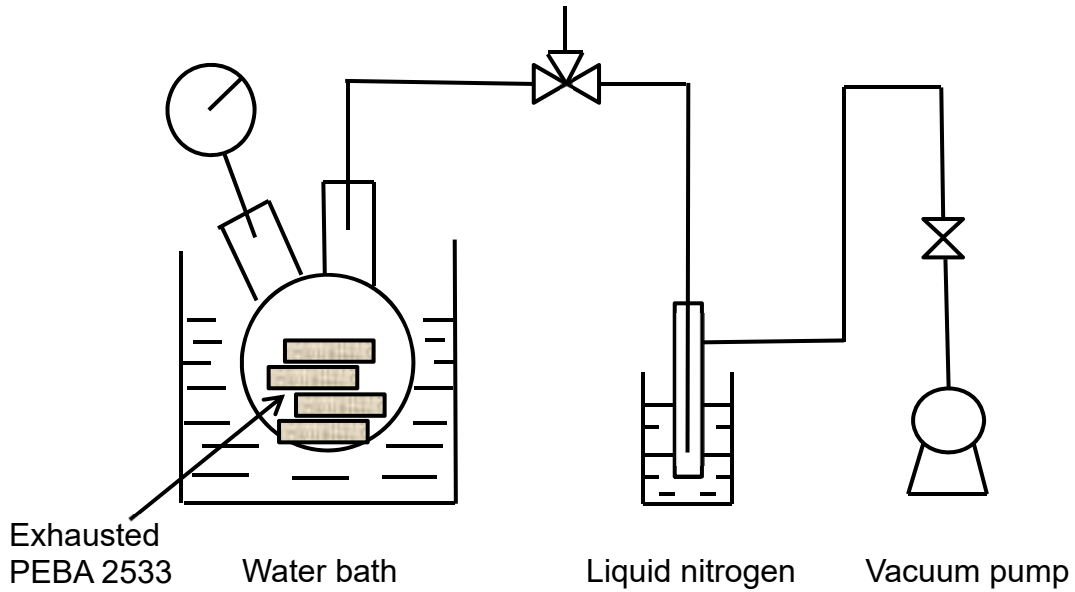
Figure 6.1 Schematic diagrams for vacuum-assisted thermal regeneration

6.3 Results and discussion

6.3.1 Chemical regeneration of PEBA sorbent

6.3.1.1 Regeneration of PEBA sorbent with NaOH

The isotherms of phenol sorption in pristine and NaOH-regenerated PEBA are shown in Figures 6.2(a)-(e). The superposition of the sorption isotherms indicates that there was no significant loss in the phenol sorption capacity after the sorbent was regenerated with NaOH for at least four regeneration cycles.

In order to quantify the regeneration performance, the sorption isotherms obtained for each cycle was fitted with the Freundlich model. Freundlich parameters K_F and $1/n$ were obtained from the data fitting, and the equilibrium sorption uptake Q_e at a given equilibrium solute concentration C_e can thus be evaluated. In the interest of comparing sorption capacity of the sorbent after regeneration cycles, Q_e was calculated at C_e=100 mg/L as a reference. The relative sorption uptake, defined as Q_e of regenerated PEBA divided by Q_e of the pristine PEBA at C_e=100 mg/L, was used for easy comparison. This is shown in Figure 6.3 for phenol sorption. It is shown that after regeneration, there is little change in the sorption capacity, suggesting satisfactory regeneration performance.

It was shown that the phenol-loaded PEBA sorbent can be regenerated using NaOH as regenerant for all the phenolic compounds studied. Similar results have been reported for other sorbents [15, 18, 21, 22, 150]. The main mechanism of sorbent regeneration with NaOH has been ascribed to the formation of soluble salt (i.e., sodium phenate), which facilitates the desorption of phenolic compounds from the sorbent surface [18, 22]. The pKa values listed in Table 3.1 indicate that all the phenols studied have acidic characteristics and can react with NaOH to form soluble salts. A study by Leng and Pinto [18] suggested that the

regeneration efficiency was dependent on NaOH concentration. There will be large amount of OH$^-$ on the sorbent at high NaOH concentrations, and this will hinder the desorption process. Therefore, NaOH concentration should be selected at a certain range to ensure the best regeneration efficiency. In our study, the NaOH concentration was selected as 0.15 mol/L according to an earlier study conducted by Özkaya [22]. Results indicate that 0.15 mol/L NaOH was effective for PEBA exhausted by phenolic compounds studied here.

Figure 6.2(a) Sorption isotherms of phenol in PEBA at 298 K after sorbent regeneration with NaOH

Figure 6.2(b) Sorption isotherms of 4-CP in PEBA at 298 K after sorbent regeneration with NaOH

Figure 6.2(c) Sorption isotherms of 4-NP in PEBA at 298 K after sorbent regeneration with NaOH

Figure 6.2(d) Sorption isotherms of 4-MP in PEBA at 298 K after sorbent regeneration with NaOH

Figure 6.2(e) Sorption isotherms of catechol in PEBA at 298 K after sorbent regeneration with NaOH

Figure 6.3 Relative sorption uptake of phenolic compounds in PEBA at C_e=100 mg/L after sorbent regeneration with NaOH

6.3.1.2 Regeneration of PEBA sorbent with ethanol

The sorption isotherms of phenolic compounds in pristine and ethanol-regenerated PEBA are presented in Figures 6.4(a)-(e). Figure 6.5 shows relative sorption uptake of phenolic compounds in PEBA at C_e=100 mg/L after sorbent regeneration with ethanol. It was shown that the regeneration of PEBA saturated with phenolic compounds by using ethanol as a regenerant also worked well, but it was not as effective as using NaOH as the regenerant. No significant capacity loss was observed after regeneration with ethanol for at least four regeneration cycles. The regeneration mechanism of ethanol was believed to be due to the larger solubility of phenolic compounds in ethanol than that in PEBA sorbent. As a result, the sorbed phenolic compounds would be stripped off by ethanol. Another role of the solvent is to weaken the interaction between the sorbate and sorbent [220].

It was observed from Figure 6.5 that the regeneration efficiency for catechol loaded PEBA sorbent was slightly lower than other phenols. This is probably due to the presence of the electron-donating group –OH. It has been reported that aromatic compounds with strong electron-donating substituent groups such as –OH were more difficult to remove from the spent activated carbon [220]. The hydroxyl group of ethanol can act as an electron donor, and the aromatic ring of phenol can act as an electron receptor. The electron donating substituent such as –OH will increase the electron density of the aromatic ring and weaken the attraction between ethanol and the phenolic compounds.
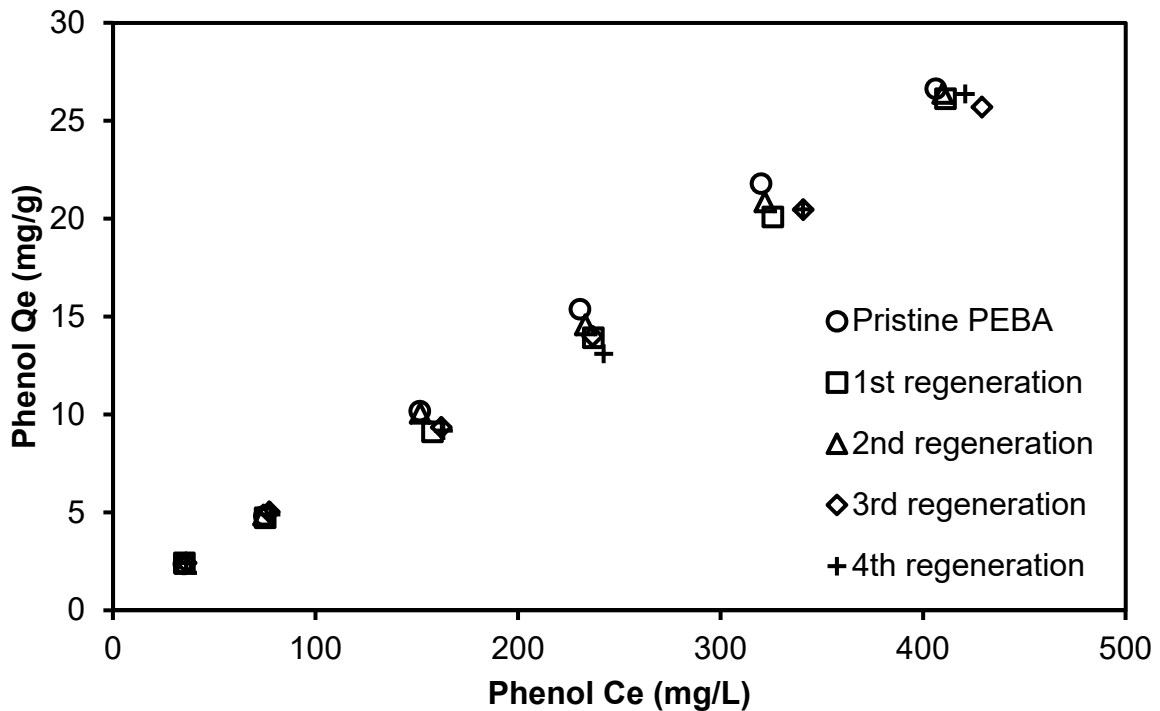
Figure 6.4(a) Sorption isotherms of phenol in PEBA at 298 K after sorbent regeneration with ethanol
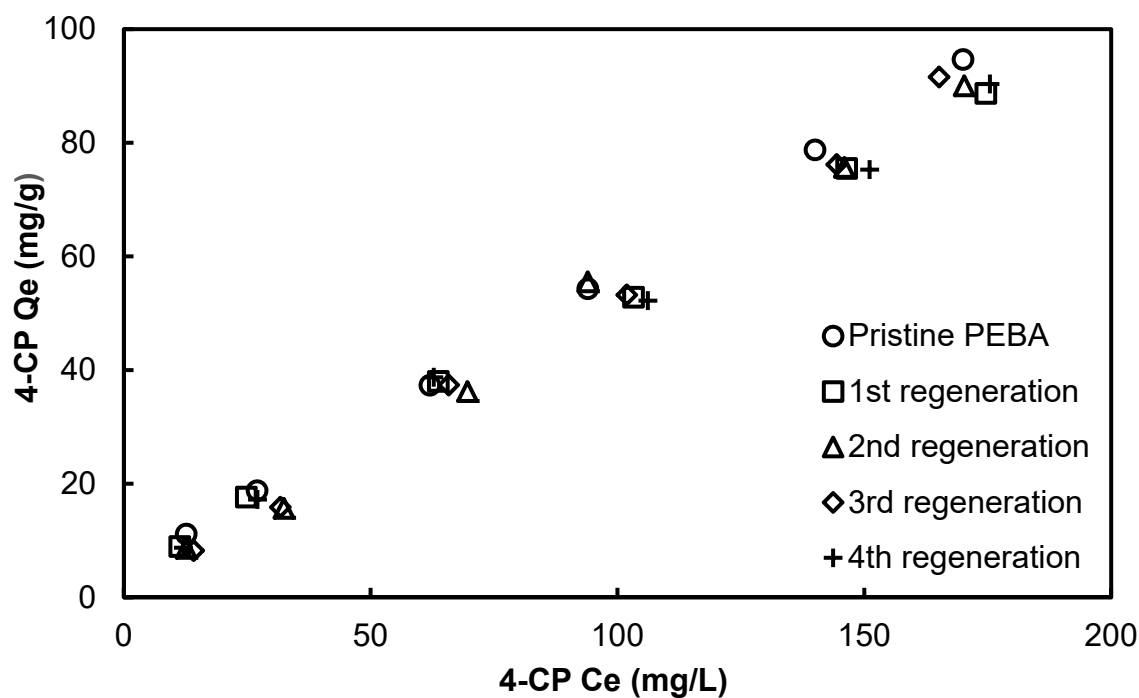
Figure 6.4(b) Sorption isotherms of 4-CP in PEBA at 298 K after sorbent regeneration with ethanol
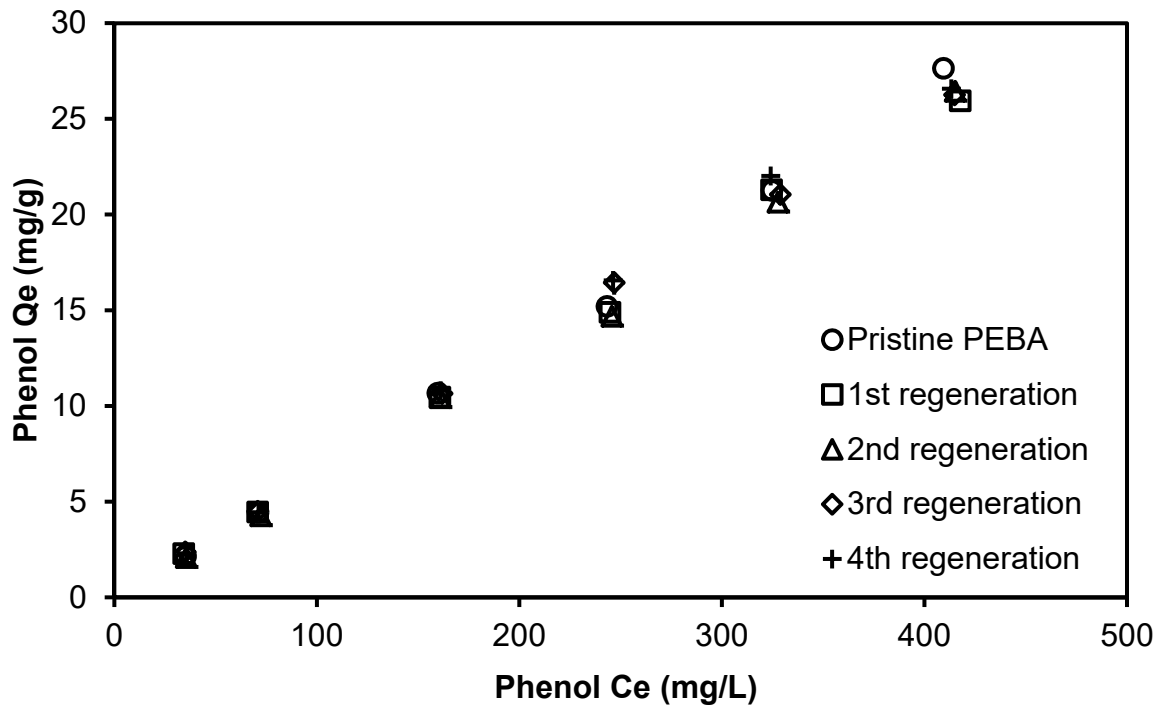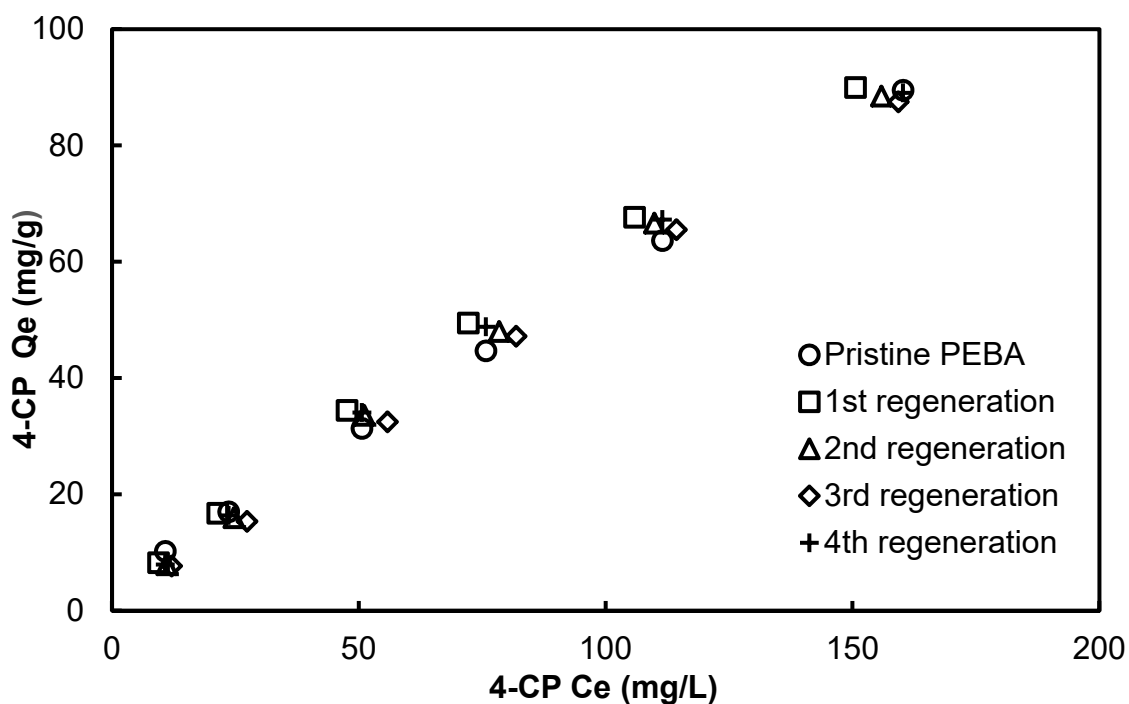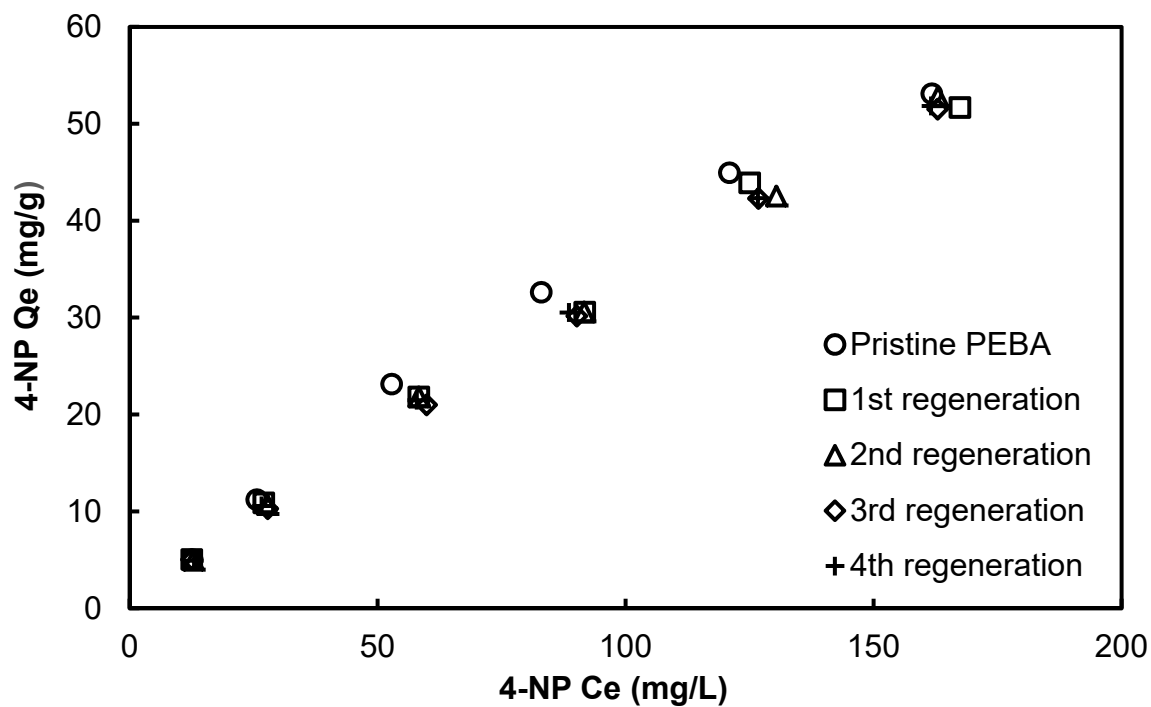

Figure 6.4(c) Sorption isotherms of 4-NP in PEBA at 298 K after sorbent regeneration with ethanol
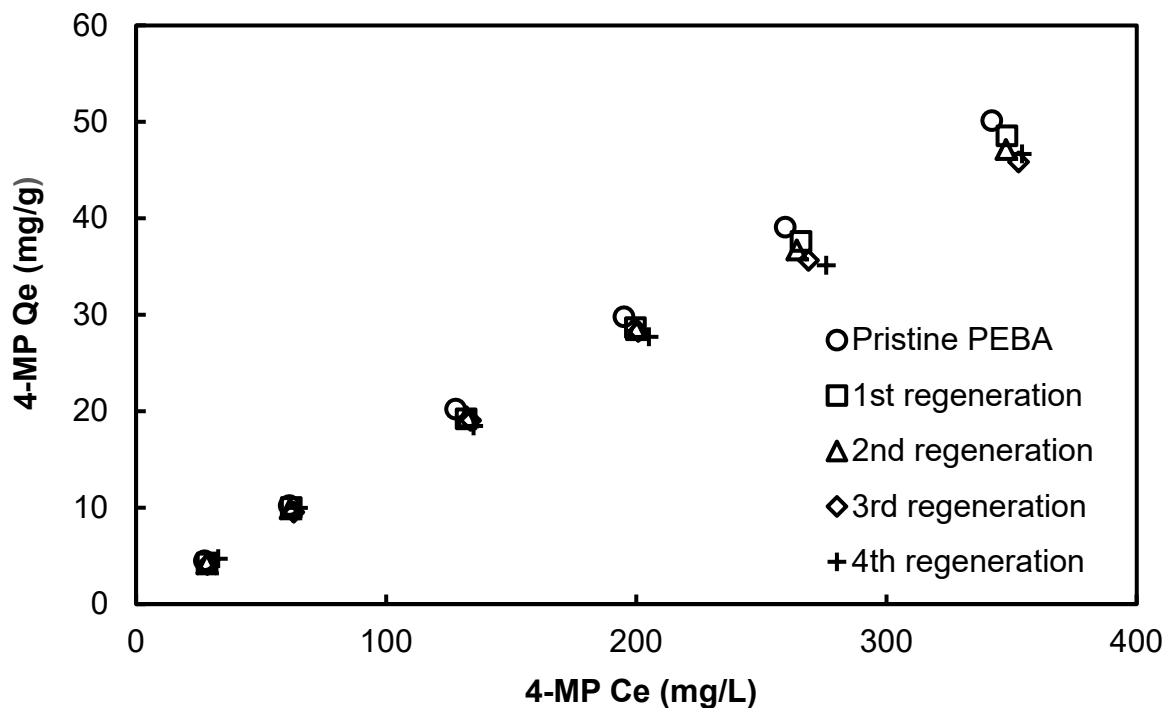
Figure 6.4(d) Sorption isotherms of 4-MP in PEBA at 298 K after sorbent regeneration with ethanol
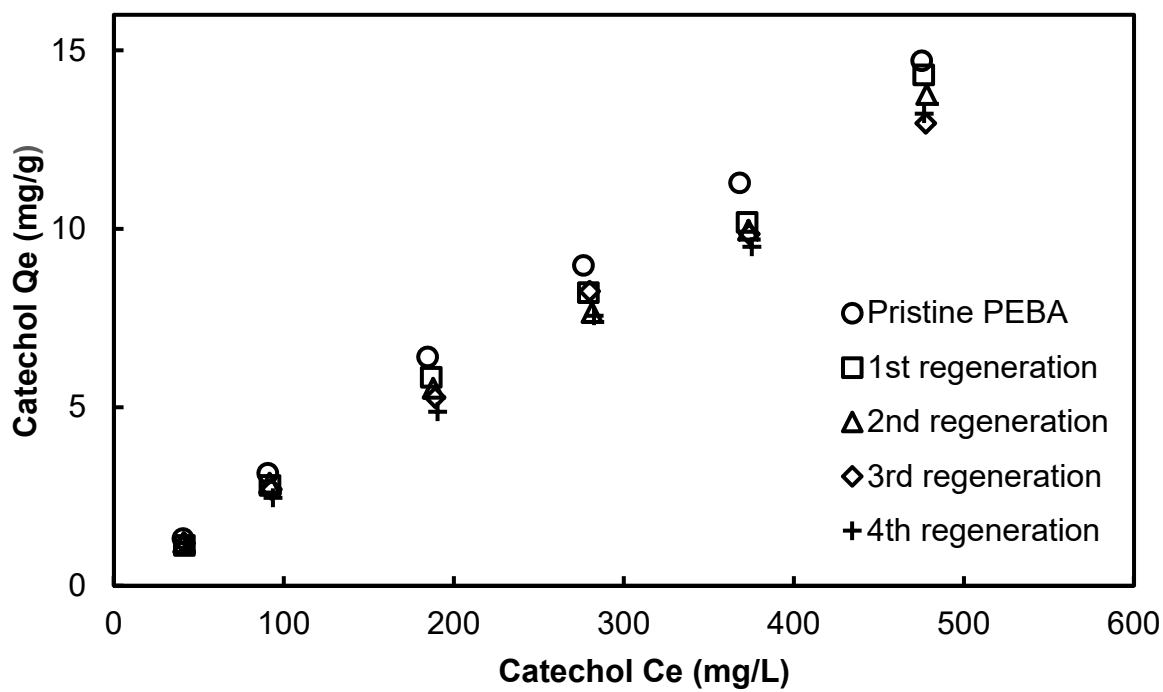
Figure 6.4(e) Sorption isotherms of catechol in PEBA at 298 K after sorbent regeneration with ethanol
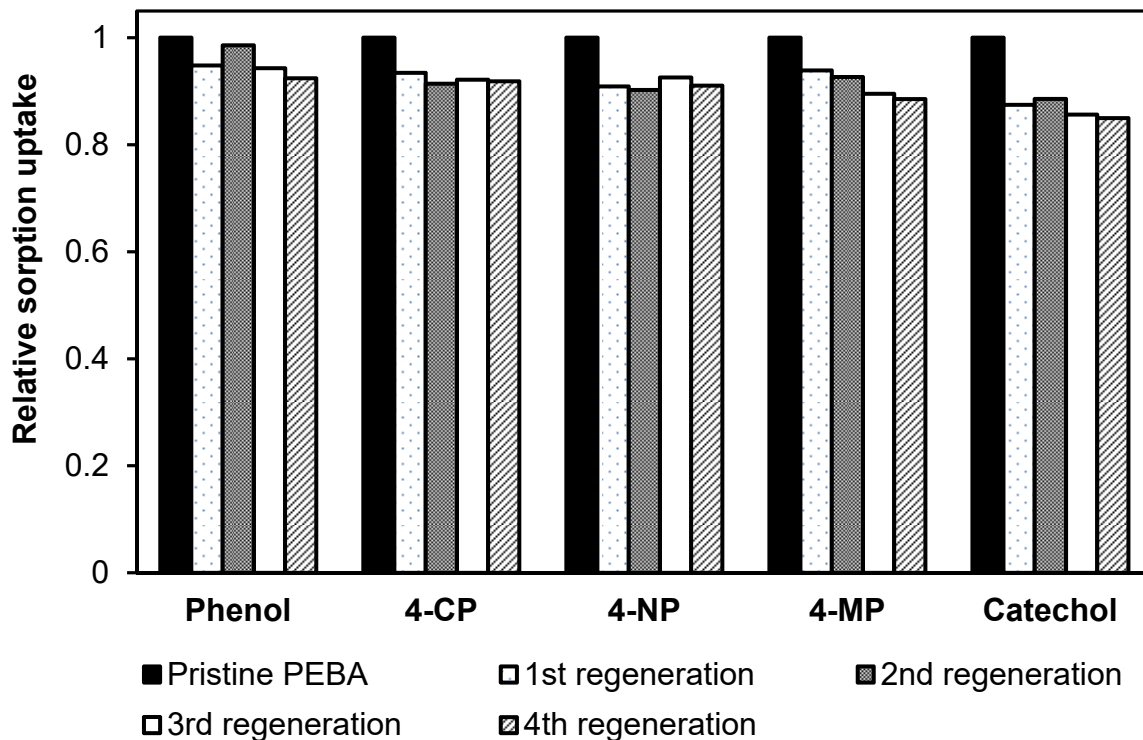
Figure 6.5 Relative sorption uptake of phenolic compounds in PEBA at C_e=100 mg/L after sorbent regeneration with ethanol

6.3.1.3 Regeneration with methanol

The sorption isotherms of phenolic compounds in pristine and regenerated PEBA using methanol as regenerant were presented in Figures 6.6(a)-(e). Figure 6.7 shows the sorption uptake in regenerated PEBA at C_e=100 ppm relative to sorption uptake in pristine PEBA at the same solute concentration. Similar to the results of PEBA regeneration with ethanol, a slight sorption capacity loss was observed for the regenerated PEBA. Effective regeneration of phenol-saturated sorbents has been reported in other studies [16, 129]. Leng and Pinto [18] used water, methanol and micellar solution to determine the importance of the solubility effect in chemical regeneration of spent activated carbon. It was found that the good regeneration efficiency of activated carbon with methanol is due to the high solubility of phenol in methanol. According to a study of Banat et al. [92], phenol molecules have a

dipole moment of 1.6 D and methanol has a dipole moment of 1.7 D. Thus methanol exhibits

an interaction with phenol resulting from the hydrogen bonding between the two. Methanol

was also used as extractant for phenols because of its high phenol solubility [18, 92].

Methanol is cheaper than ethanol, thus the excellent regeneration performance and

low cost make methanol an attractive eluting reagent for regeneration of phenol-saturated
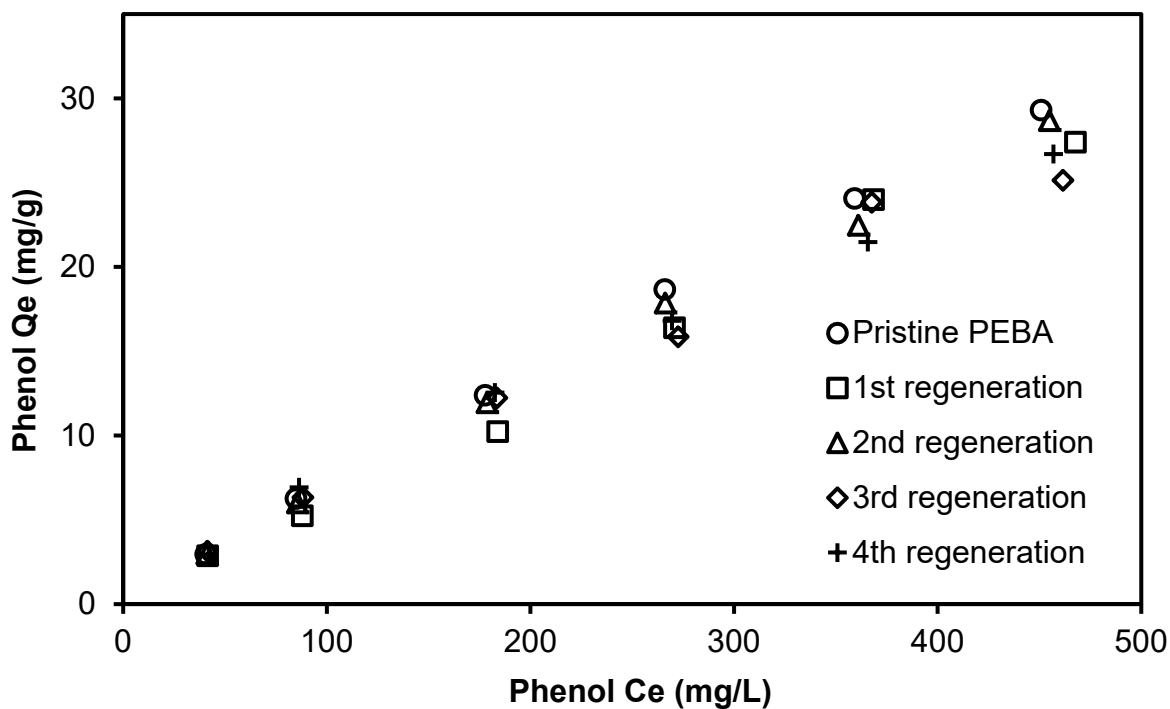
PEBA sorbent.

Figure 6.6(a) Sorption isotherms of phenol in PEBA at 298 K after sorbent regeneration with methanol

Figure 6.6(b) Sorption isotherms of 4-CP in PEBA at 298 K after sorbent regeneration with methanol
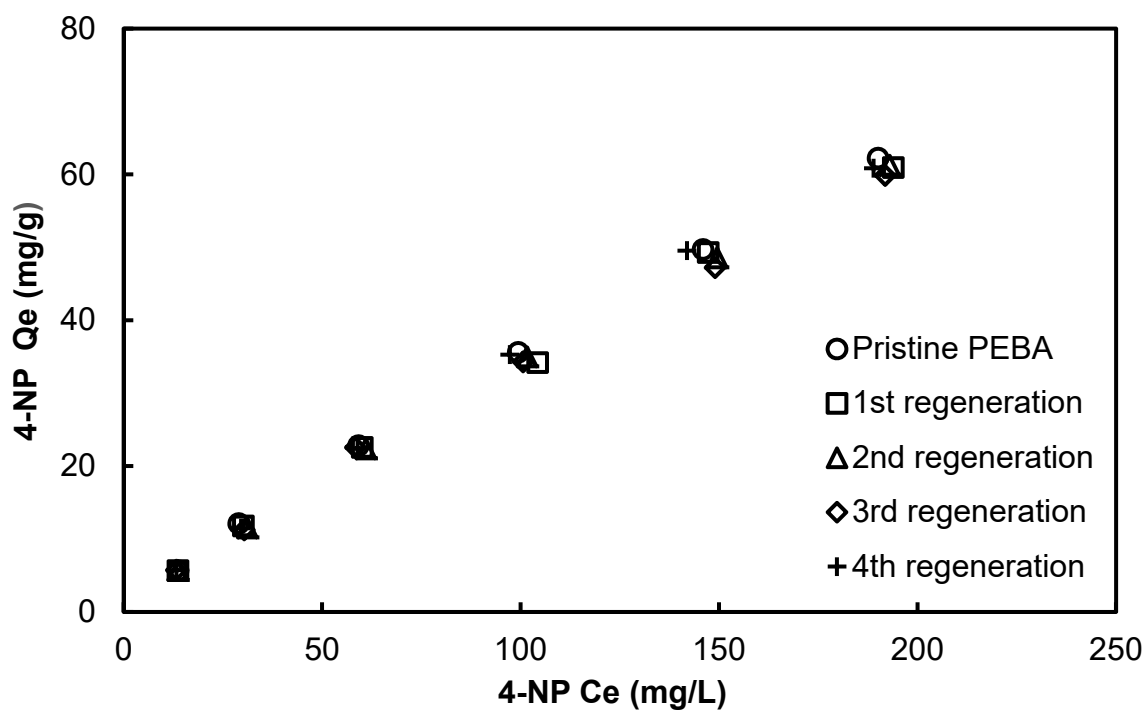

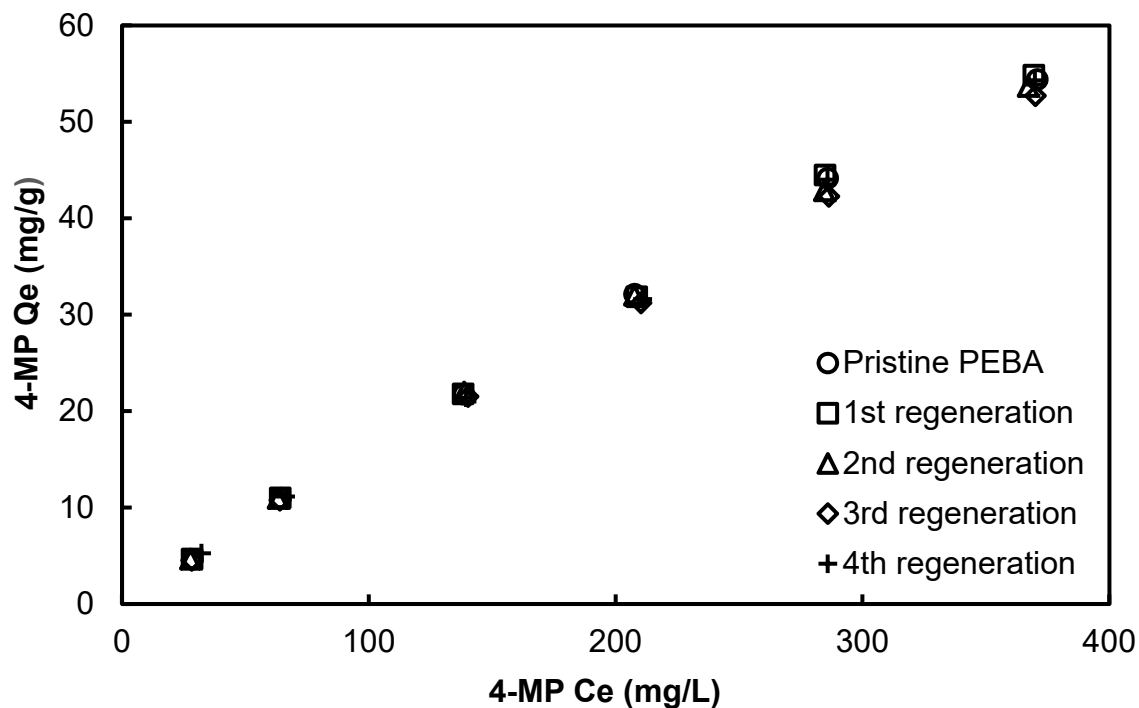Figure 6.6(c) Sorption isotherms of 4-NP in PEBA at 298 K after sorbent regeneration with methanol

178

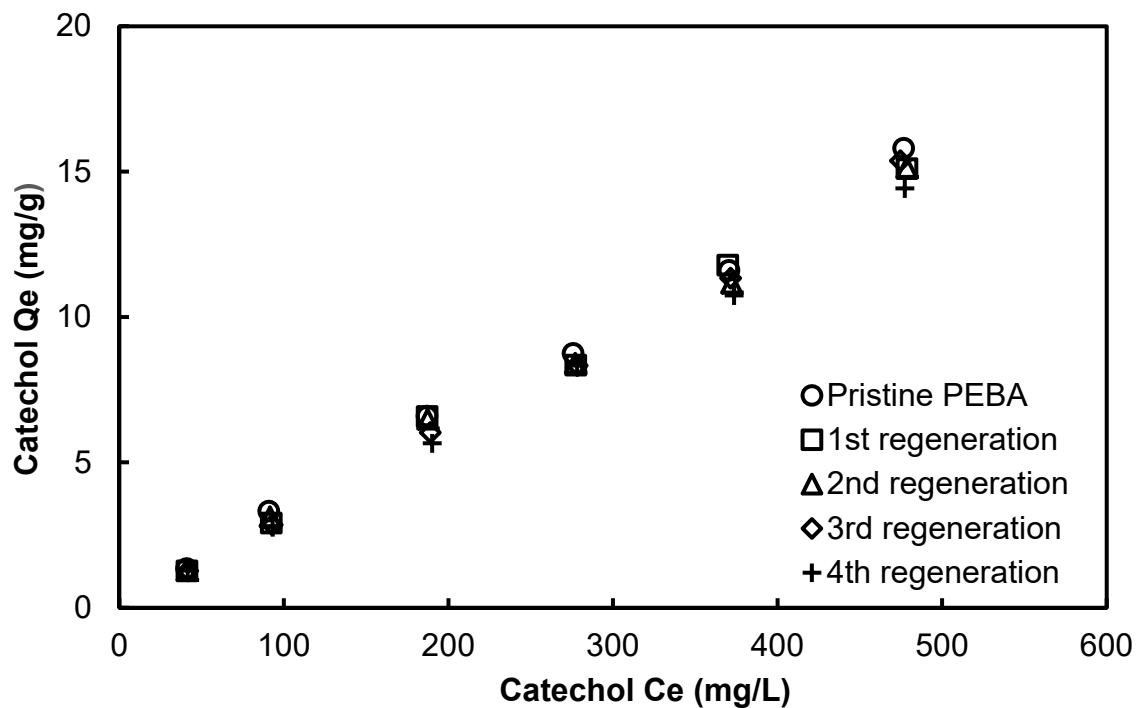Figure 6.6(d) Sorption isotherms of 4-MP in PEBA at 298 K after sorbent regeneration with methanol

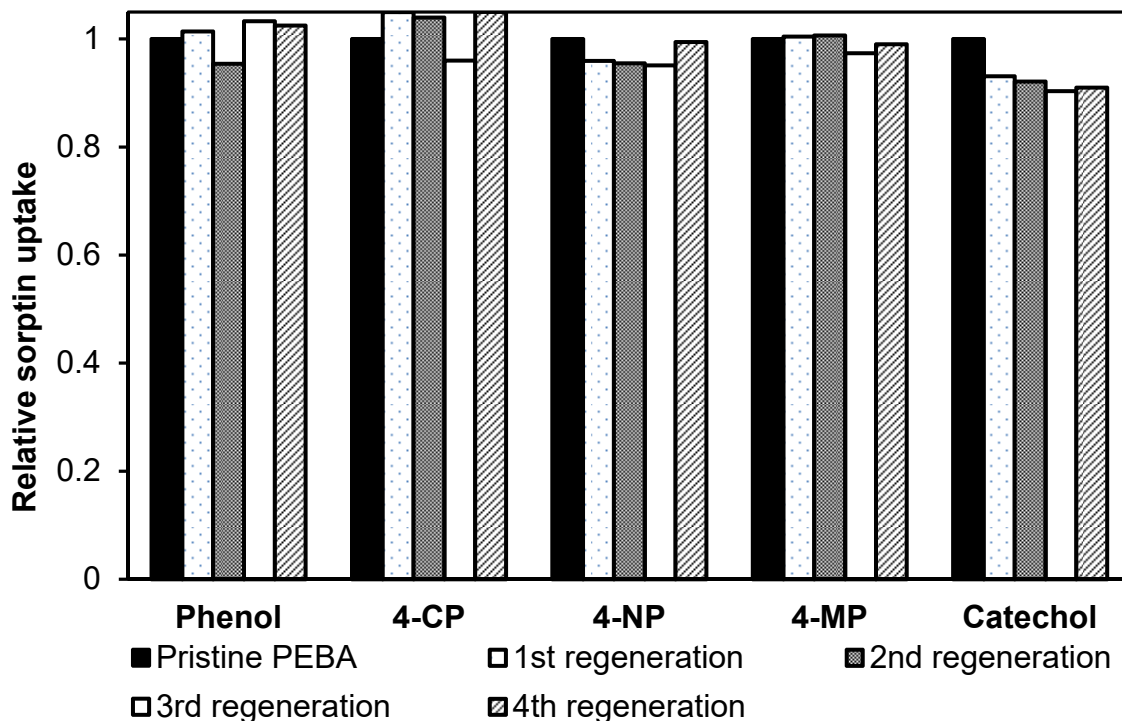Figure 6.6(e) Sorption isotherms of catechol in PEBA at 298 K after sorbent regeneration with methanol
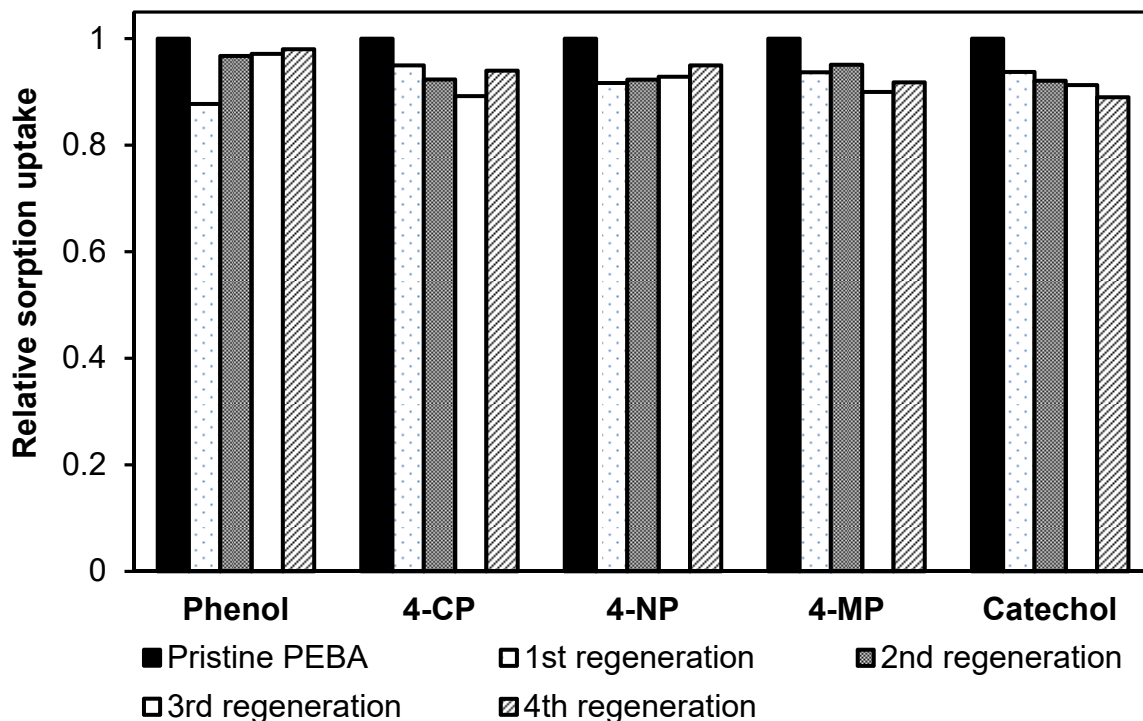
Figure 6.7 Relative sorption uptake of phenolic compounds in PEBA at C_e=100 mg/L after sorbent regeneration with methanol

6.3.2 Thermal regeneration of PEBA sorbent

Figures 6.8(a)-(e) show sorption isotherms of phenolic compounds in pristine and thermally-regenerated PEBA. Figure 6.9 shows the relative sorption uptake at C_e=100 mg/L for each phenolic compound studied as compared to the sorption uptake of pristine PEBA sorbent. It was observed from Figures 6.8(a)-(e) that the sorption isotherm of the fresh membrane was almost identical to that of the regenerated membrane for phenol, 4-CP and 4-MP. Figure 6.9 also shows that there is no significant sorption capacity loss after regeneration. Thus heating the spent sorbent at 90°C for 2 h is effective for complete regeneration of PEBA saturated by phenol and 4-MP, and heating at 120°C for 2 h is effective for regenerating PEBA loaded with 4-CP. This is of particular interest because for commercial activated carbon, the regeneration temperature is usually 600-850°C [23, 24,

146]. A study by Alvarez et al. [25] showed that at least 50% of the overall mass of phenol sorbed in granular activated carbon was not removed by thermal regeneration even at a temperature as high as 1100 K. Torrents et al. [144] noticed that the temperature for thermal regeneration is usually close to 1000°C, and they consider the regeneration at temperature range 110-400°C to be a low-temperature thermal desorption process. The high temperature required for effective regeneration can cause several problems: increased energy cost, excess burnout of the carbon and thus increased attrition rate [144], possible damage of the surface pore structure of carbon and thus reduced sorption capacity [145]. The much lower regeneration temperature (<120°C) required for PEBA loaded with phenol, 4-CP and 4-MP indicated that thermal regeneration is effective for regeneration of PEBA sorbent.

However, for the regeneration of catechol-saturated PEBA, a significant capacity loss was observed in Figure 6.8(e). Figure 6.9 showed that the sorption capacity of the regenerated PEBA decreased by around 30% as compared to that of fresh PEBA at C_e=100 pm. For the regeneration of 4-NP-saturated PEBA, a sorption capacity loss of about 70% was observed for the regenerated PEBA even at a higher regeneration temperature (130°C). The melting point of PEBA 2533 is 135°C. Thus thermal regeneration is in general not very effective for regenerating PEBA sorbent containing sorbates catechol or 4-NP.

The different thermal regeneration efficiencies observed for these phenolic compounds may be explained from their physical properties. The melting point, boiling point and vapour pressure for each phenolic compound are shown in Table 6.1. The performance of thermal regeneration seems to be related to the melting point and boiling point of the phenolic compounds. Phenols with higher boiling point and melting point such as 4-NP and catechol are more difficult to remove from PEBA by thermal regeneration. The melting

process seemed to be vital for the thermal regeneration because phenols with a low melting point (<50°C) have satisfactory thermal regeneration performance while phenols with higher melting points (>100°C) have a significant capacity loss in thermal regeneration. This is not surprising in consideration that thermal regeneration for removal of the sorbate from the sorbent involves melting of phenols followed by evaporation.

Another plausible explanation is that the presence of the different substitute groups may also affect the activation energy and affect the temperature required for desorption. According to Torrents et al. [144], the activation energy of sorption of toluene, chlorobenzene and nitrobenzene on activated carbon were 17.6, 26.0 and 35.6 kJ/mol, respectively. They found the activation energy for sorption followed the substituent order OH> NO_2>Cl>CH_3.

Table 6.1 Physical properties of the phenolic compounds studied

|	Phenol	4-CP	4-NP	4-MP	Catechol
Boiling point (°C)	181.7	220	279	201.8	245.5
Melting point (°C)	40.5	43	113	35.5	105
Vapour pressure (Pa) at 20°C	53	13	0.0032	14	4
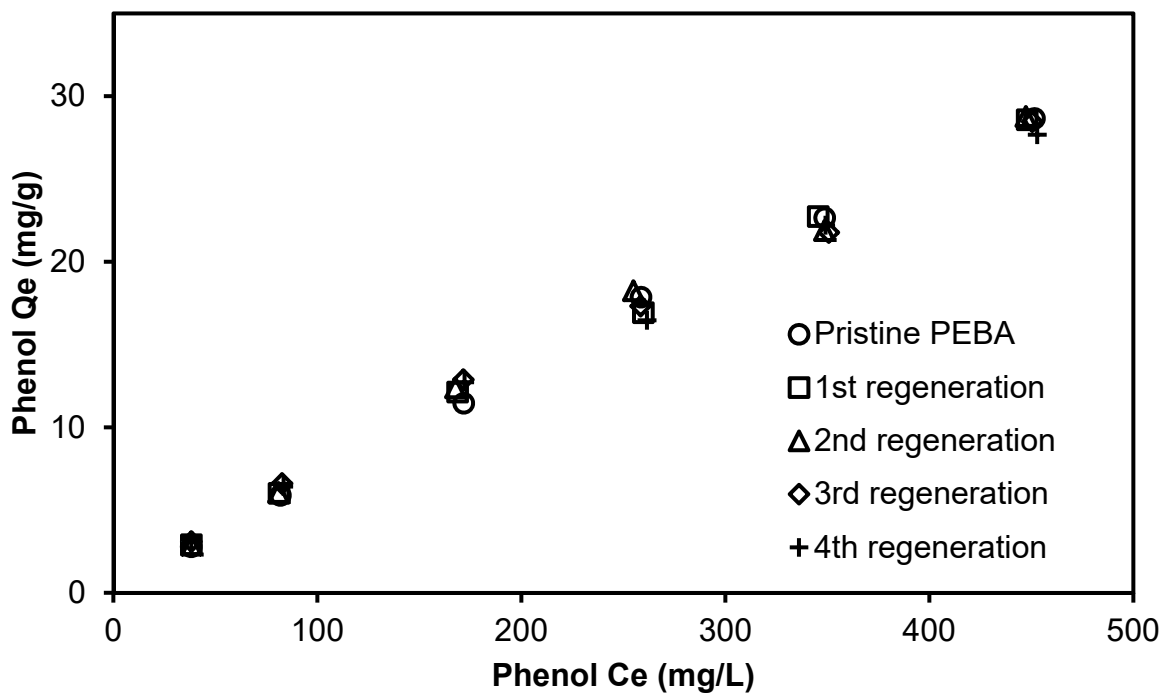
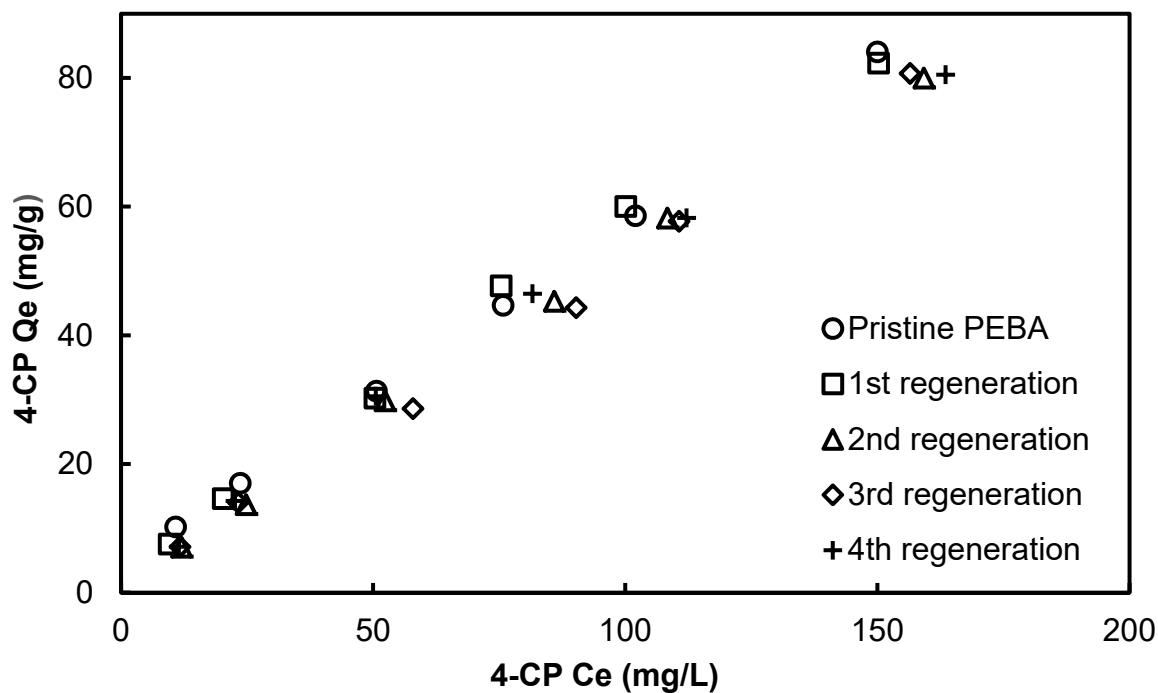Figure 6.8(a) Sorption isotherms of phenol in PEBA at 298 K after thermal regeneration of the sorbent
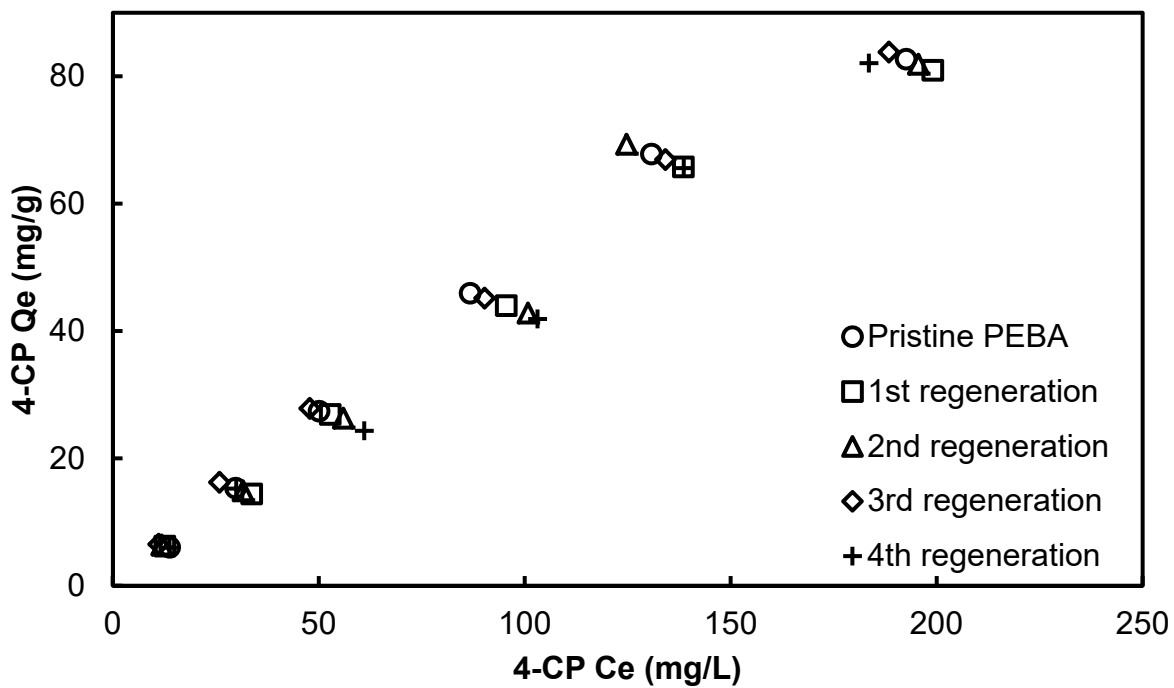
Figure 6.8(b) Sorption isotherms of 4-CP in PEBA at 298 K after thermal regeneration of the sorbent
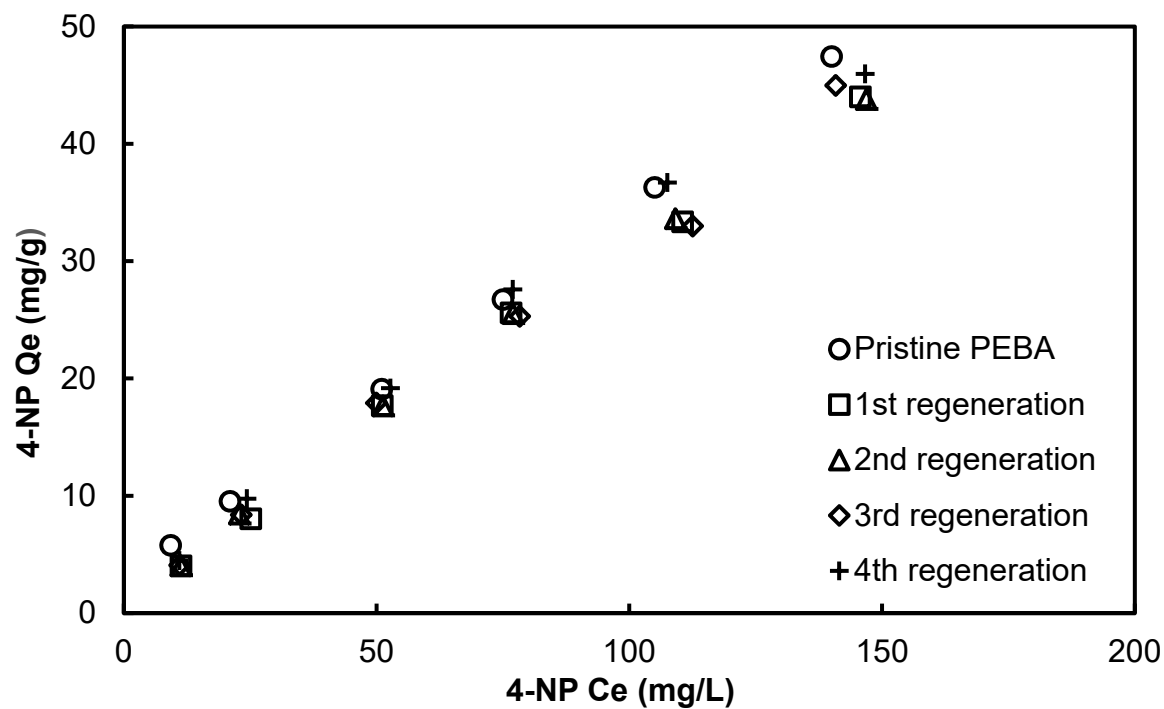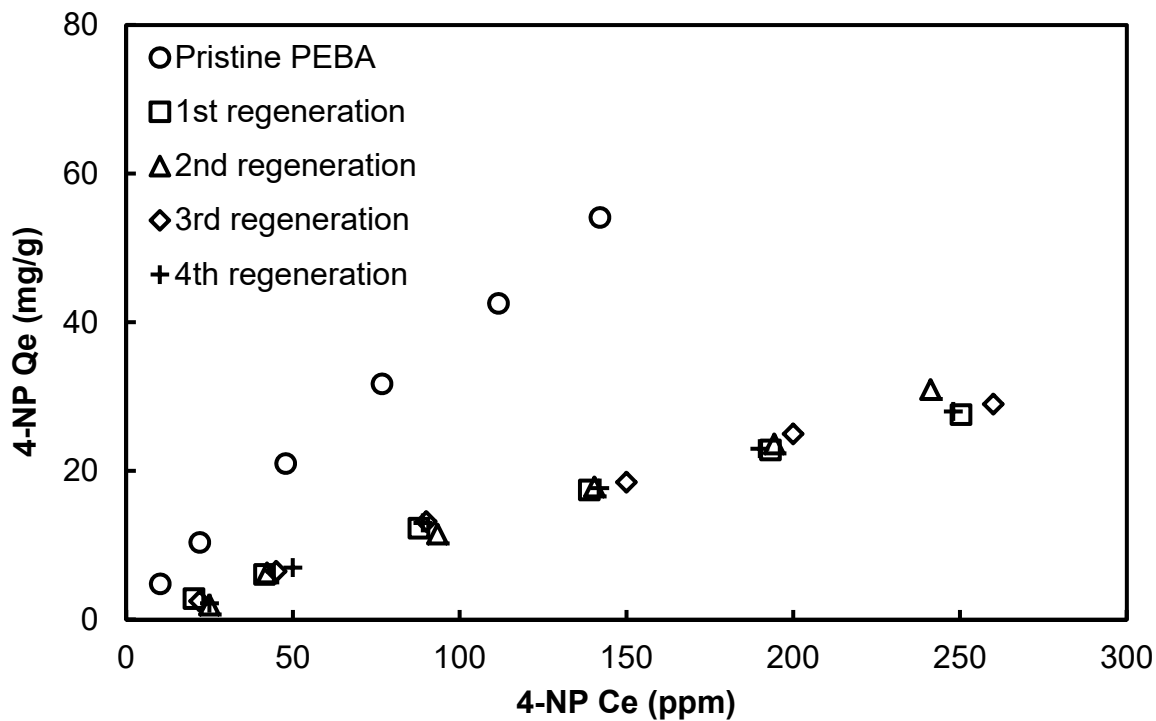
Figure 6.8(c) Sorption isotherms of 4-NP in PEBA at 298 K after thermal regeneration of the sorbent
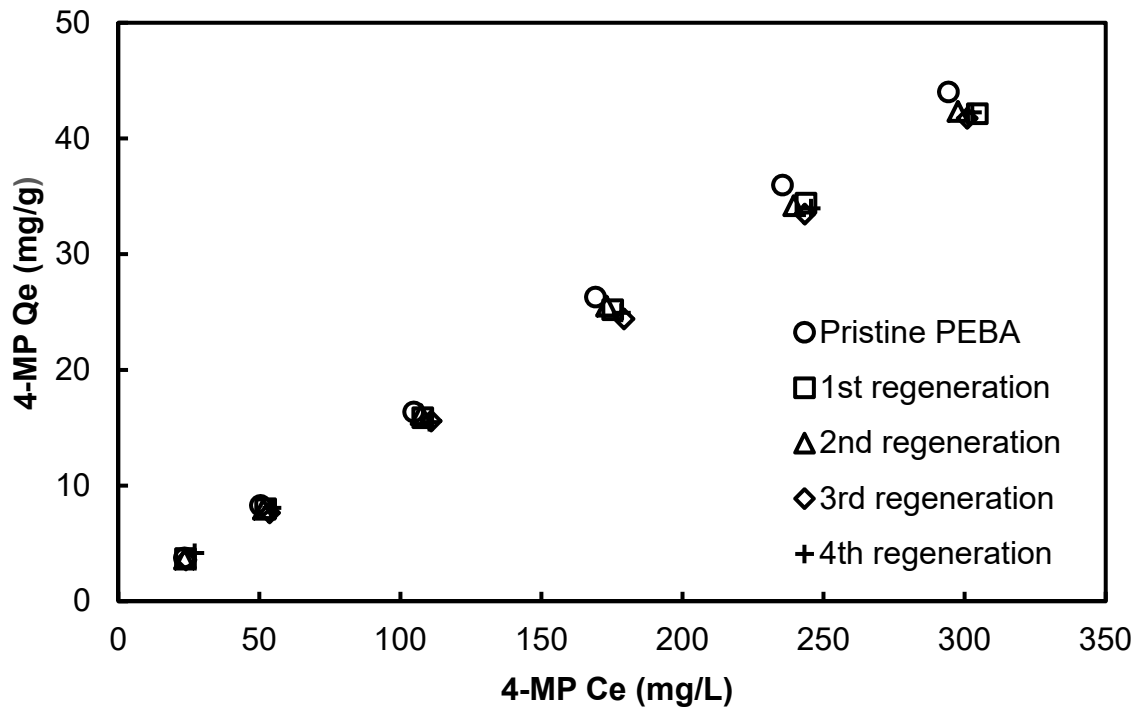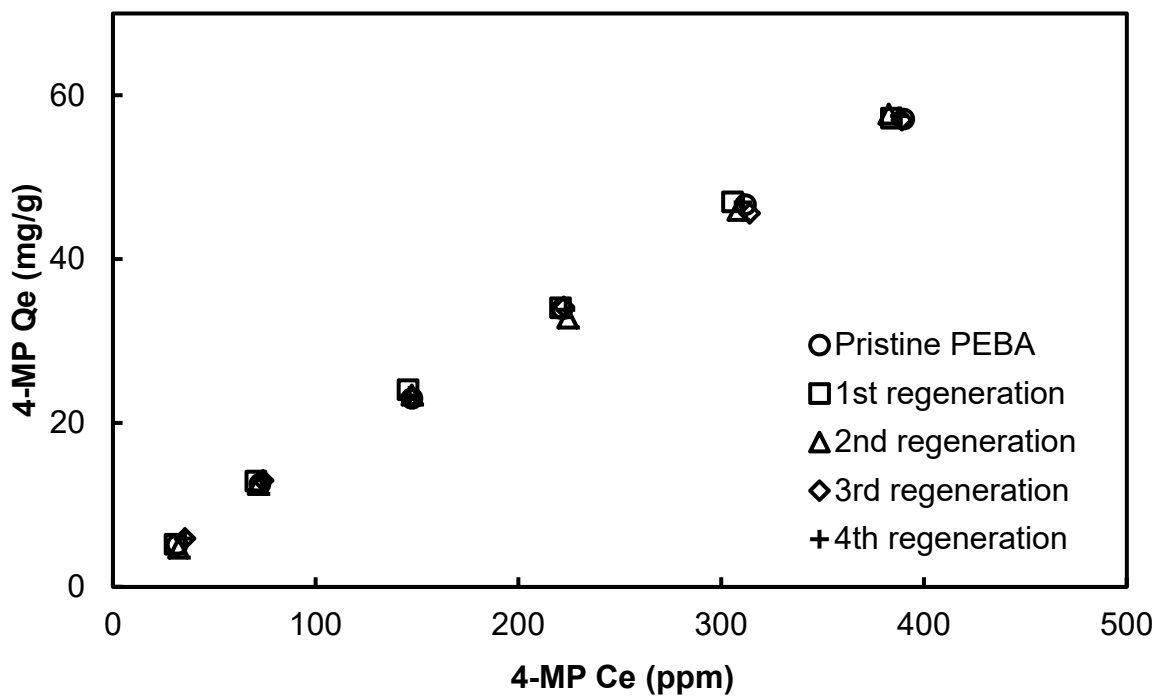

Figure 6.8(d) Sorption isotherms of 4-MP in PEBA at 298 K after thermal regeneration of the sorbent
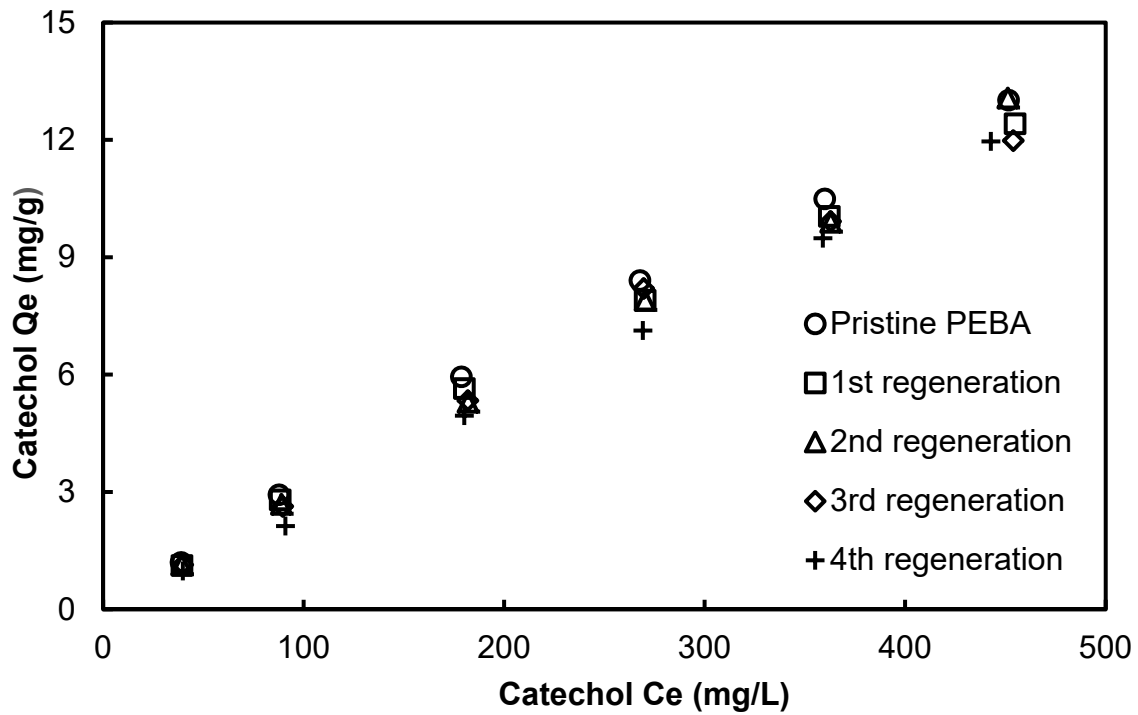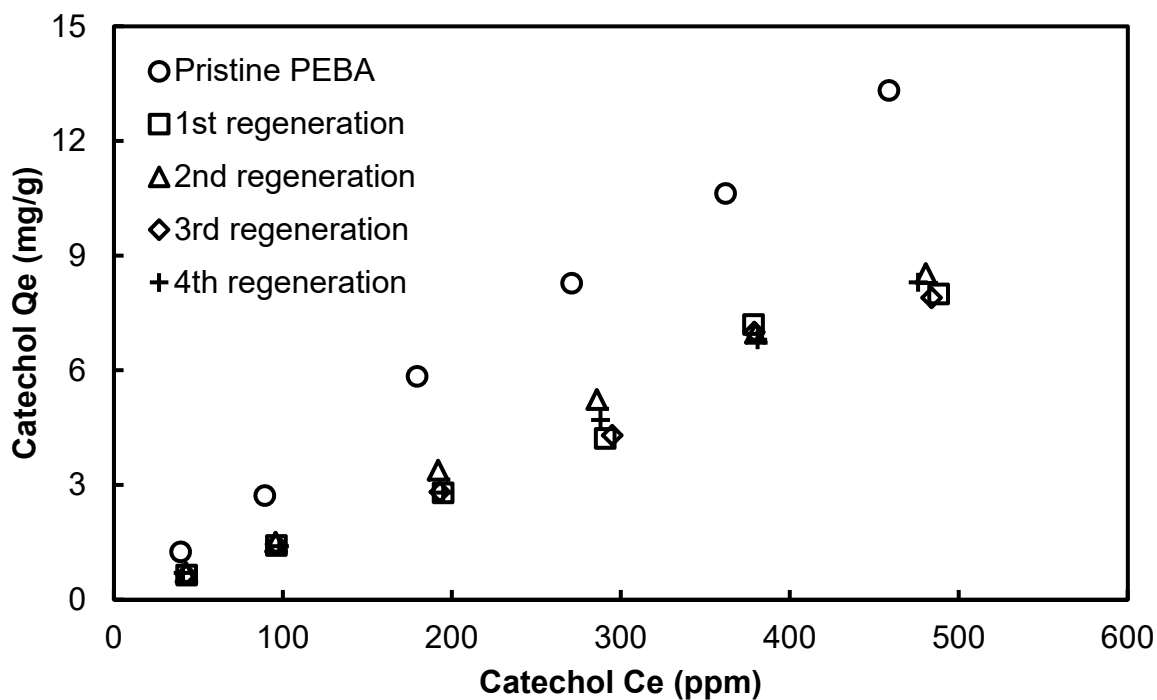
Figure 6.8(e) Sorption isotherms of catechol in PEBA at 298 K after thermal regeneration of the sorbent
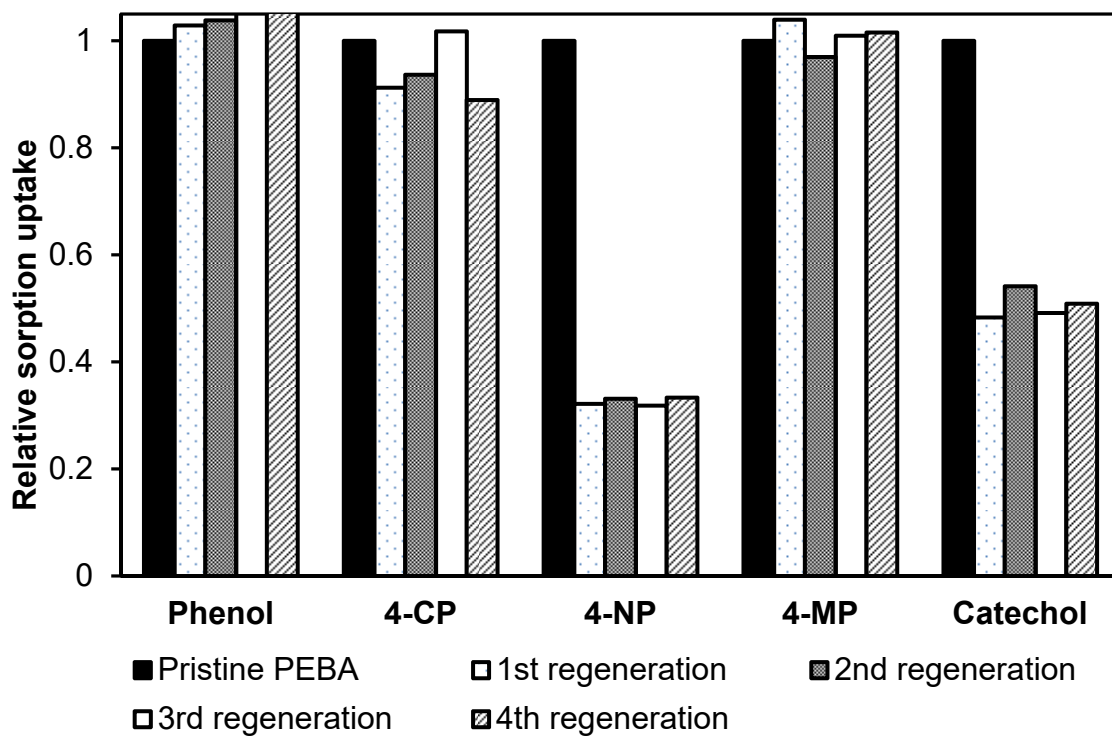
Figure 6.9 Relative sorption uptake of phenolic compounds in PEBA at C_e=100 mg/L after thermal regeneration of the sorbent

6.3.3 Vacuum-assisted thermal regeneration of the PEBA sorbent

The vacuum assisted thermal regeneration of PEBA sorbent was carried out at 80°C for 3 h. A considerable amount of vapour was collected for phenol, 4-CP and 4-MP from the spent PEBA sorbent, whereas little was desorbed for 4-NP and catechol. In addition, even when the temperature was increased to 95°C for 7 h, still little 4-NP and catechol were collected. Thus the vacuum-assisted thermal regeneration at these conditions may not work for 4-NP- and catechol- saturated PEBA sorbent are shown in Figure 6.10(a), (b) and (c), respectively. In order to quantify the desorption efficiency, the ratio of the amount of phenol collected in the cold trap (mg) to the amount of phenol sorbed in the sorption step (mg) was used to characterize the desorption efficiency. The results are shown in Figure 6.11.

It was observed from Figure 6.10(c) and 6.11 that the vacuum-assistant thermal desorption was very effective for 4-MP saturated PEBA at the given experimental conditions (temperature 80°C, duration 3 h). A highly concentrated 4-MP solution ($\approx$70,000 mg/L) was collected in the cold trap for each regeneration cycle, and a desorption efficiency higher than 95% was achieved with the vacuum-assisted thermal regeneration. The vacuum-assistant thermal desorption was also effective for phenol saturated PEBA, at a desorption efficiency higher than 90%; a highly concentrated phenol solution ($\approx$20,000 mg/L) was obtained in the cold trap. This novel regeneration method is advantageous in phenol recovery because a small volume of highly concentrated phenol solutions was obtained, which means no further treatment of wastewater is needed. The low temperature and high recovery rate make this method very attractive for industrial application because of its significant technical and environmental advantages.

For 4-CP spent PEBA, a noticeable loss in sorption capacity was observed in Figure 6.10(b), Figure 6.11 shows that the desorption efficiency of 4-CP saturated PEBA was only around 70%, though a highly concentrated 4-CP solution ($\approx$120,000 mg/L) was obtained in the cold trap. It was observed from Figure 6.10(b) that the sorption isotherms of regenerated PEBA deviated from that of fresh PEBA sorbent more significantly at a lower solute concentration. This is probably due to the incomplete desorption of 4-CP from PEBA. If there is considerable amount of 4-CP remaining in the sorbent, when the regenerated PEBA sorbent was immersed into solutions at a low 4-CP concentration, the observed sorption capacity of 4-CP in regenerated PEBA will be small, as shown in Figure 6.10(b). However, with proper optimization of experimental conditions (i.e., longer desorption time, higher desorption temperature and higher vacuum) more complete desorption of 4-CP from PEBA is expected.
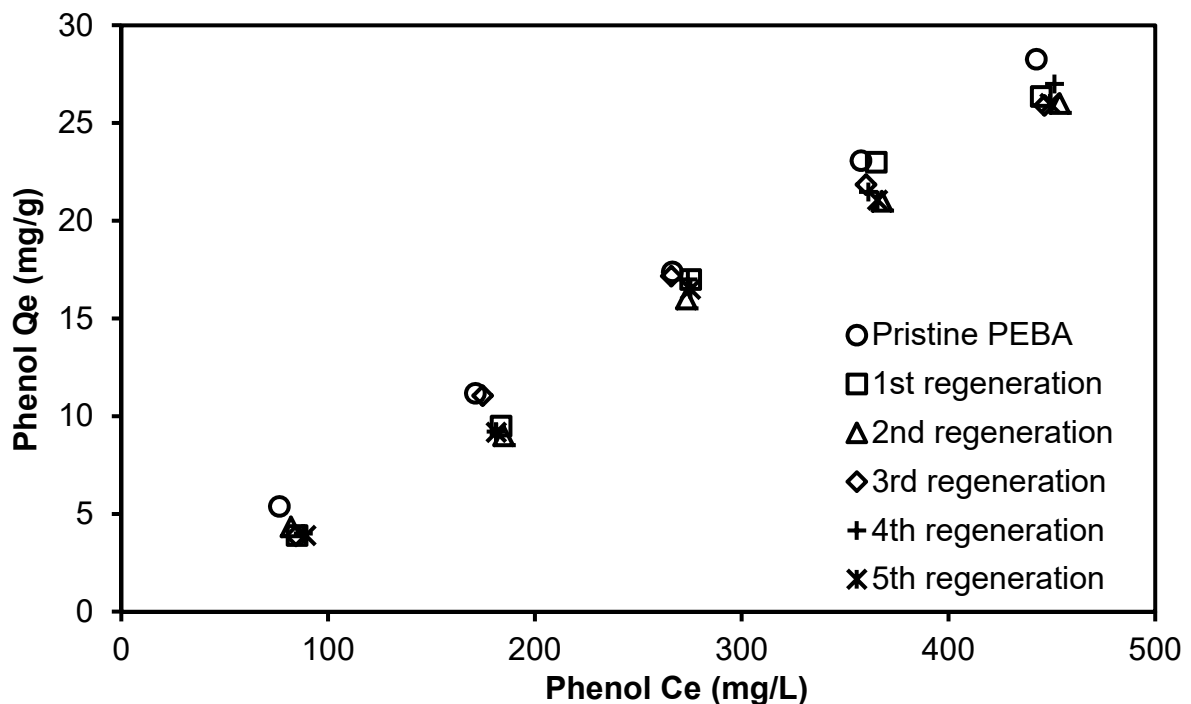
Figure 6.10(a) Sorption isotherms of phenol in PEBA at 298 K after vacuum-assisted thermal regeneration of the sorbent
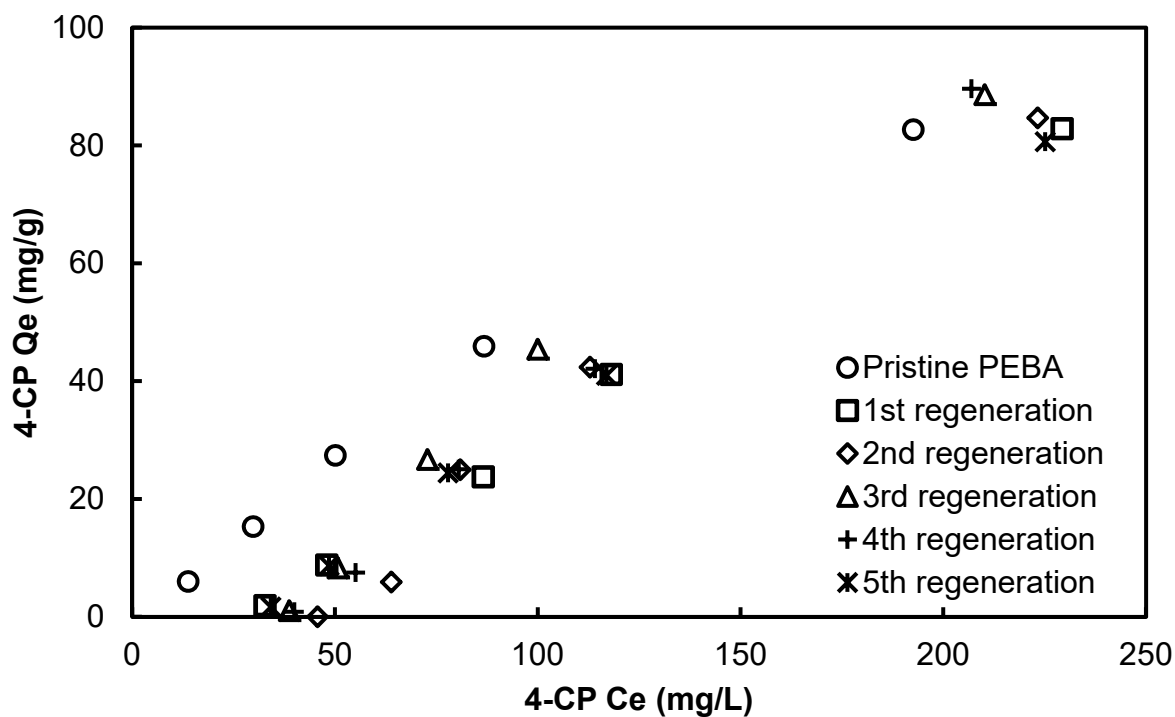
Figure 6.10(b) Sorption isotherms of 4-CP in PEBA at 298 K after vacuum-assisted thermal regeneration of the sorbent
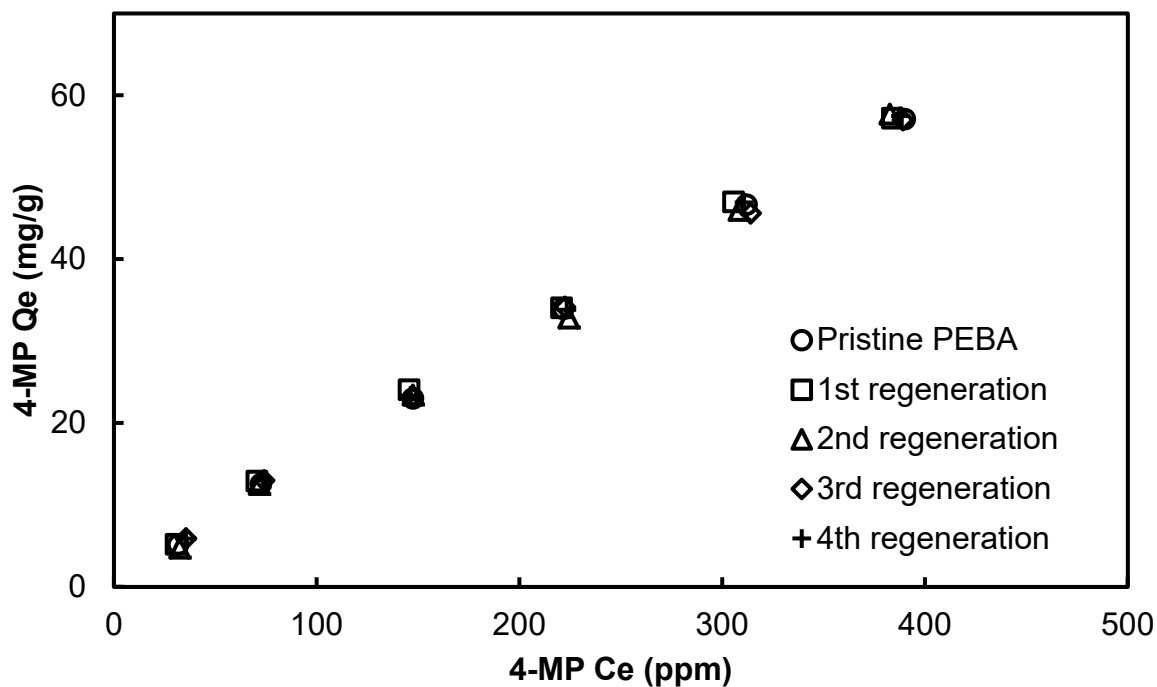
Figure 6.10(c) Sorption isotherms of 4-MP in PEBA at 298 K after vacuum-assisted thermal regeneration of the sorbent
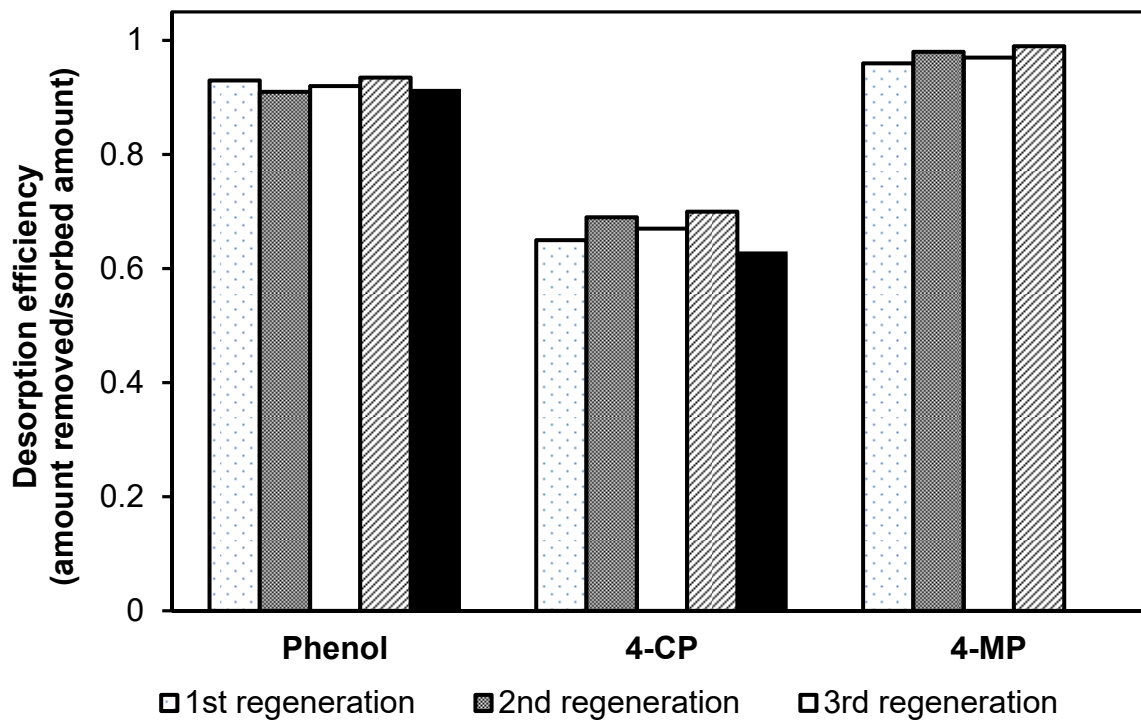
Figure 6.11 Desorption efficiency of phenolic compounds from PEBA after vacuum-assisted thermal regeneration of the sorbent

6.4 Conclusions

1. Ethanol, methanol and 0.15 mol/L NaOH solutions were all effective for regeneration of PEBA sorbent exhausted with phenol, 4-CP, 4-NP, 4-MP and catechol. No significant loss in the sorption capacity of phenolic compounds in regenerated PEBA was observed.

2. Thermal regeneration at 90°C for 2 h was shown to be effective for regenerating PEBA saturated with phenol and 4-MP. The low temperature required for the thermal regeneration was of particular interest from an application point of view.

3. The vacuum-assisted thermal regeneration at 80°C for 3 h at 5 kPa absolute pressure was effective for regenerating PEBA exhausted by phenol and 4-MP, and this novel method could recover the desorbed phenol and 4-MP as a highly concentrated solution, which had significant environmental and economic advantages.

4. PEBA exhausted with the phenolic compounds had excellent regeneration performance and could be reused without significant loss in the sorption capacity.

Chapter 7

Column study: sorption of phenolic compounds by PEBA in continuous flow systems

7.1 Introduction

The research findings from batch study showed that PEBA 2533 was an effective sorbent to capture phenol, 4-CP, 4-NP, 4-MP and catechol from aqueous solutions. However, batch operation is limited to treat small volumes of wastewater. In comparison, packed bed operation, where sorbents are packed in a column and contacted by a continuous flow of the fluid phase, is preferred in industrial designs. In addition, unlike batch studies where the contact time can be long enough to achieve equilibrium, the residence time in a packed column is generally controlled until a breakthrough is reached before attainment of equilibrium. Many studies [15, 221, 222] have reported that there are discrepancies between sorption capacities in packed columns and those obtained from batch measurements. Thus it is necessary to conduct column studies to provide valuable information for the column design suitable for sorptive separation of phenolic compounds from aqueous solutions.

In order to maximize the performance of column sorption, the mass transfer resistance in the PEBA sorbent needs to be reduced. The previous results showed that the diffusive mass transfer resistance in the sorbent was not negligible. Compared with flat membranes used in batch studies, sorbents in the form of fine fibres can increase the specific external surface area for the fluid-solid contact, and thus increase the sorption rate. In addition, fine fibres are easily immobilized as a bundle, which provides effective contact

between the solid phase and liquid phase. More importantly, the void space among the fibres can provide passageways for the fluid flow with a low pressure drop, which is desirable in the column sorption system [223]. However, the passageways among the fibres may cause channelling effect, thus there is a trade-off between pressure drop and channelling effect. PEBA fibres were prepared for the column sorption studies. To our best knowledge, this is the first attempt to immobilize PEBA fibres in a packed column.

The sorption performance of packed bed columns can be described by the breakthrough curves (i.e., the ratio of effluent concentration to feed concentration versus time). In a packed bed sorption process, as the feed water containing the solute continually flows into the column in an up flow mode, the bottom part of the column will first become saturated, and then the mass transfer zone where dynamic sorption occurs will migrate towards the top of the column. When the concentration front reaches the outlet of the column, the solute will come out in the effluent. The point at which the effluent concentration reaches its maximum allowable value is referred to as breakthrough [224]. At this point, the column is considered to be used up and subjected to regeneration. In our study, the breakthrough point will be defined as $C/C_0 =0.08$. The shape of the breakthrough curve will be affected by the characteristics of the sorbent-sorbate system as well as operating conditions (e.g., inlet concentration, flow rate, bed depth and sorbent size, etc.).

Experimental determination of breakthrough curve is usually time-consuming, and mathematical models are often used to predict the breakthrough curves under different operating conditions. In this study, packed-bed sorption of phenol, 4-CP, 4-NP, 4-MP and catechol in PEBA fibres were performed at different inlet solute concentrations, flow rates,

192

and fibre diameters. Experimental data were analyzed using three widely used mathematical models (that is, the BDST model, Clark model, and Yoon-Nelson model).

It is worth noting that successful mathematical simulation of experimental data is not sufficient to validate the application of the model. This is especially true when more than one mathematical model can be fitted to the experimental data. Thus there is a need for techniques which can assist in revealing mechanisms responsible for the dynamic sorption. In our study, flow-interruption tests, proposed by Helfferich [225], was used to investigate the rate-limiting step of the dynamic sorption process. In the interruption test, the inlet flow was stopped for a period of time and then resumed. If there is no significant enhancement in the uptake of the sorbate after the flow interruption, then the film diffusion is likely the rate-limiting step. If the uptake of sorbate significantly increases, then the internal diffusion is likely the rate limiting step [224]. In addition, the column sorption capacity determined from the flow-interruption tests was compared with the sorption capacity obtained in batch studies.

As shown in Chapter 6, chemical regeneration of PEBA sorbent with NaOH solution was effective. Thus, NaOH was used for column regeneration, and six continuous sorption-regeneration cycles of the column runs were performed to test the regeneration performance of PEBA sorbent in the packed-bed system.

7.2 Experimental

7.2.1 Preparation of PEBA fibres

The experimental setup for fibre preparation is illustrated in Figure 7.1. The PEBA solution at 15 wt.%, which was prepared in the same procedure as described in Section 3.3.1, was placed inside a stainless steel tank which was connected to a fine needle spinneret. The polymer solution was kept at 80°C using a water bath to maintain its fluidity. N_2 gas (at 50

kPa) was used to force the solution to pass through the spinneret, followed by immersion in a water tank to induce solvent-nonsolvent exchange. When fully solidified, the fine fibres were taken up by a motor driven spinning device. The diameter of fibres can be controlled by the extrusion rate and take-up speed. Fibres were rinsed with deionized water to remove residual solvents completely, and dried at room temperature.
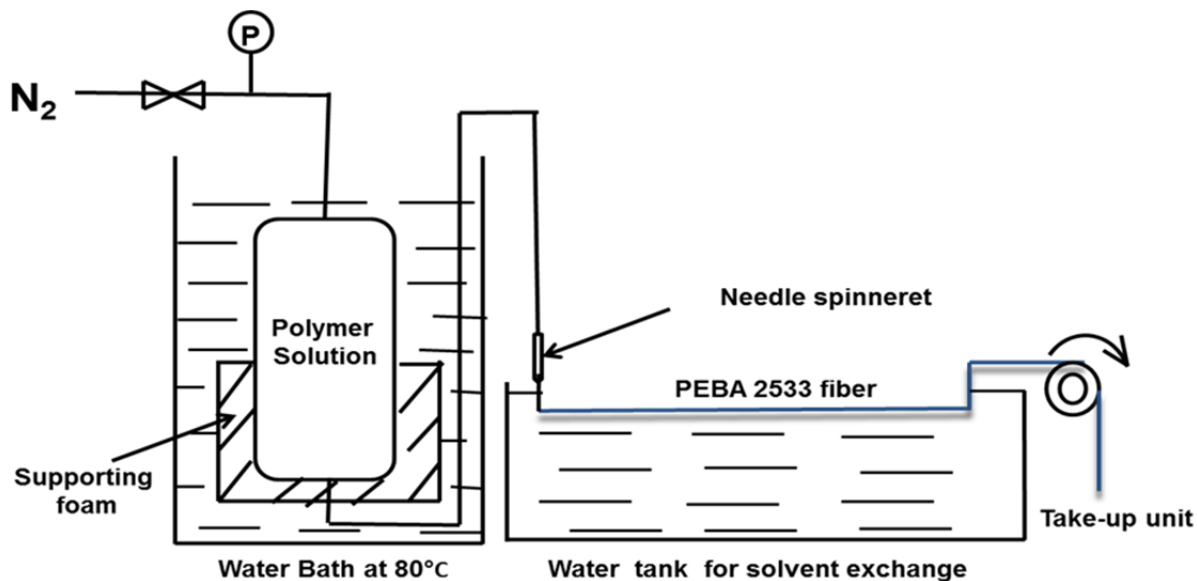
Figure 7.1 Schematic diagram of experimental setup for fibre preparation

7.2.2 Column sorption experiments

The schematic diagram of the column sorption experiment is shown in Figure 7.2. The column study was performed in a glass column with an inner diameter of 1.1 cm and a length of 30 cm. 8-9 g PEBA fibres were packed within the column yielding a bed height of 25±1 cm and a packing density of 330-380 g/L. A thin layer of glass wool was placed at both ends of the column. To ensure uniform contact between the fluid and the sorbent and to avoid the short-cut passageway for fluid flow, the column sorption was conducted with an up-flow mode using a Masterflex peristaltic pump (Cole-Parmer Instrument Co.). The feed solution of phenolic compounds at a known concentration (ranged 30-200 ppm) was loaded to the

column using the peristaltic pump at room temperature (298 K). The column was preconditioned with deionized water for two hours, and time (t) was recorded once the influent entered the column to contact the fibres. The flow rate (1-18 mL/min) was controlled using the peristaltic pump, and the effluent flow rate was determined gravimetrically to double check the feed flow rate. Samples were taken from the effluent at timed intervals and analyzed for phenol concentration using UV-Vis Spectrophotometer.

Flow interruption tests were conducted so that the feed flow was stopped for a given period of time (12 h on weekdays and 60 or 36 h on weekends) and then resumed, and the effects of flow interruption on the breakthrough curve were examined. The flow-interruption test was terminated when the effluent concentration was close to the inlet concentration.
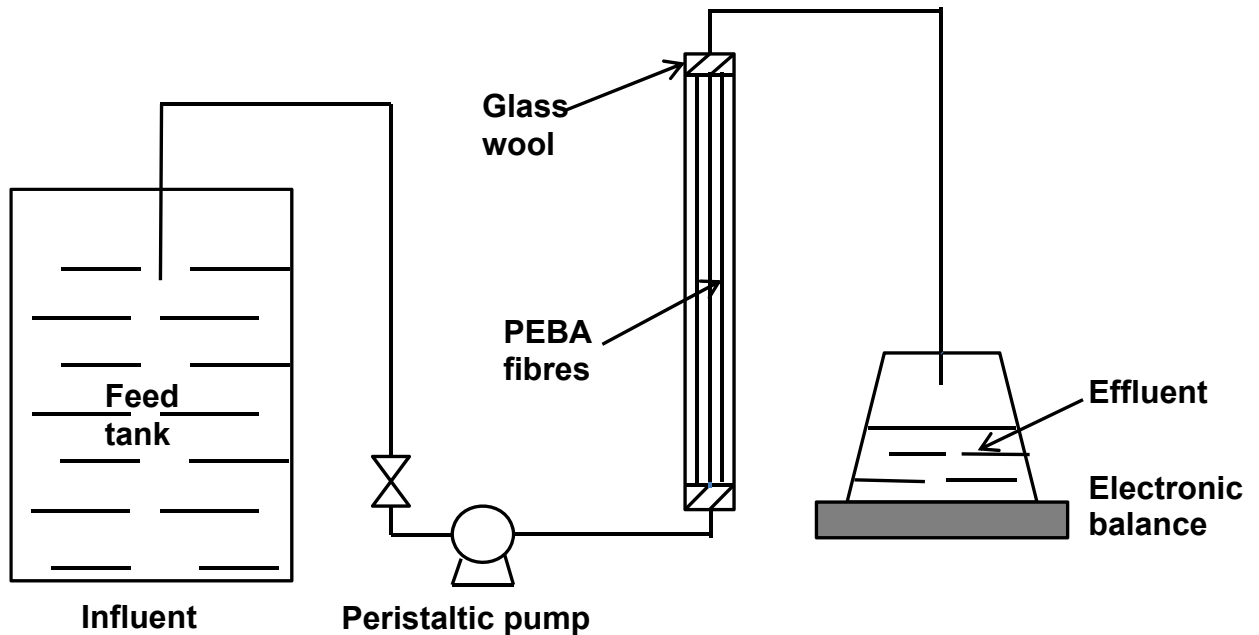
Figure 7.2 Schematic diagram of experimental setup for column sorption

7.2.3 Column regeneration

The reusability of the sorption column was evaluated by using a 0.15 mol/L NaOH solution as the regenerant. The breakthrough curve was obtained at a certain inlet solute concentration, flow rate and with a known fibre size using the same procedure as described previously. After a certain time period of continuous feed flow or when the column become saturated with the sorbate, the column sorption experiment was stopped, and 0.15 mol/L NaOH was admitted to the column at a flow rate of 4 mL/min for 2.5 h, followed by flowing of deionized water at the same flow rate for 75 min to remove the residual NaOH. This corresponded to approximately 600 g of 0.15 mol/L NaOH solution and 300 g of deionized water passing through the column in each regeneration step. Excessive amount of NaOH solution and wash water were used to achieve complete regeneration of the column. A preliminary study showed that 600 g of NaOH solution was enough for complete desorption of phenols and that 300 g of deionized water was enough for effective rinse. Once the column regeneration was done, the feed phenol solution was charged again into the column at the same inlet concentration and flow rate for the second sorption cycle, and new breakthrough curve was recorded. The above sorption-regeneration procedure was repeated, and six sorption-regeneration cycles were performed to evaluate the reusability of the packed column.

7.3 Results and discussion

7.3.1 The effect of inlet concentration on sorption breakthrough

Figures 7.3(a)-(e) showed the breakthrough curves for the sorption of phenol, 4-CP, 4-NP, 4-MP and catechol in PEBA at different inlet concentrations.

For the sorption of 4-CP, 4-NP and 4-MP, it is obvious that the higher the inlet solute concentration is, the earlier the breakthrough will occur. Take the sorption of 4-NP for example, if we take C/C_0=0.08 as the breakthrough point, then the breakthrough time for 4-NP at inlet concentrations 50, 100 and 150 ppm was found to be 116, 91 and 75 min, respectively. This can be attributed to the rapid exhaust of sorption sites at higher concentrations. Because of finite amount of the sorption sites available, an increase in the inlet concentration will result in a faster saturation of the bed.

For the sorption of phenol and catechol, however, the effect of inlet concentration on the breakthrough curve is not very obvious within the studied concentration range (50-150 ppm). The breakthrough curves at different inlet concentrations are close one another as shown in Figures 7.3(a) and (e). A possible explanation is that the sorption capacity of phenol and catechol in PEBA are smaller than those of the other three phenols, which means only a small portion of sorption sites are occupied for phenol and catechol at equilibrium. Thus the saturation of the sorption bed does not become substantially faster at higher inlet concentrations. However, it should be noted that if the inlet concentration is high enough, the breakthrough time may be shortened considerably.
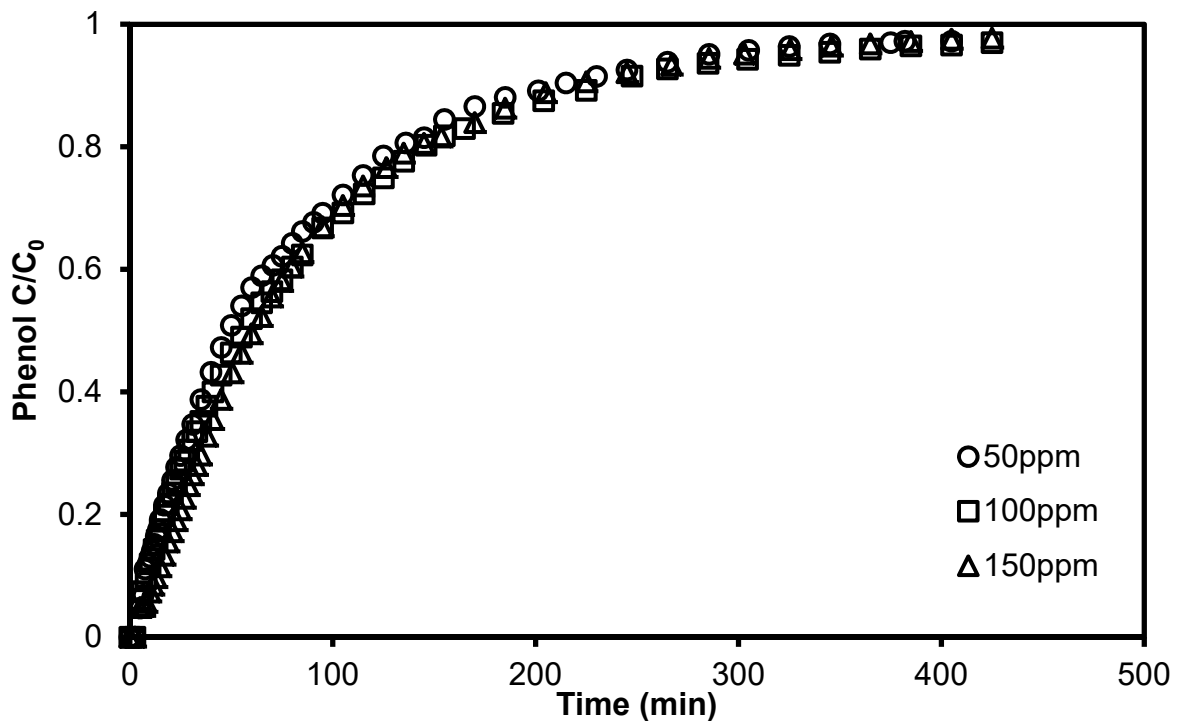
Figure 7.3(a) The effect of inlet concentration on phenol sorption in PEBA column *(**Flow rate=7±0.3 mL/min, fibre diameter=229 μm**)*
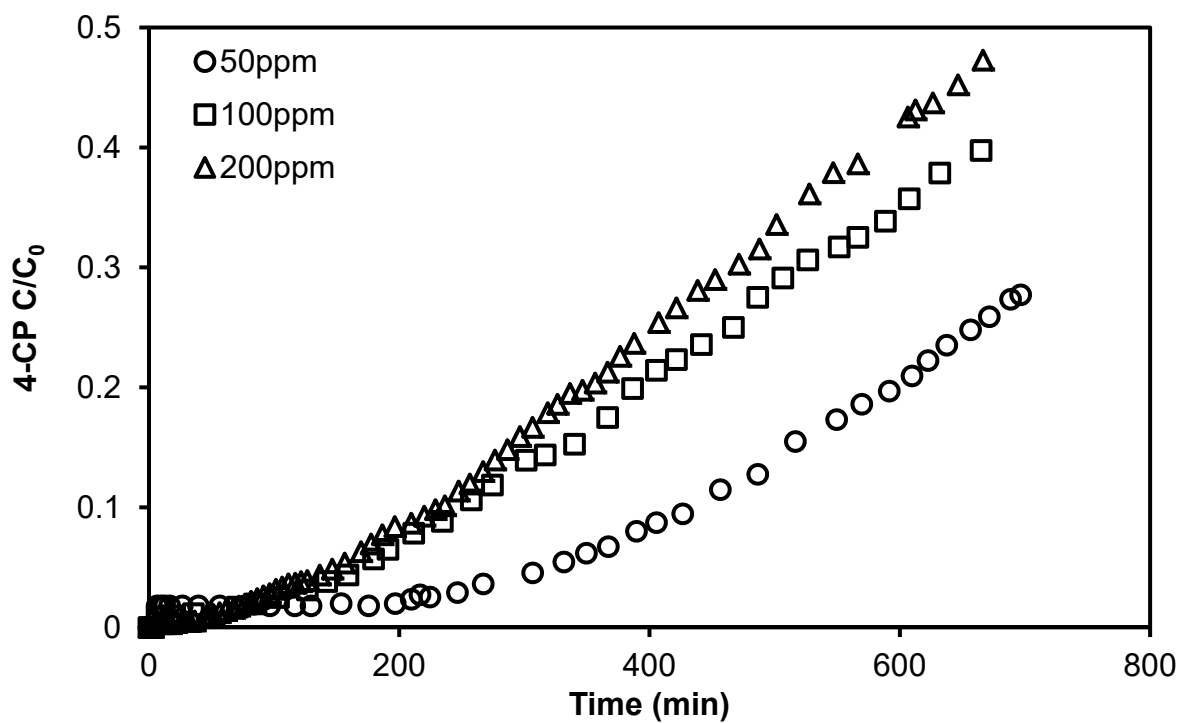
Figure 7.3(b) The effect of inlet concentration on 4-CP sorption in PEBA column *(**Flow rate=5.5±0.3 mL/min, fibre diameter=102 μm**)*

198
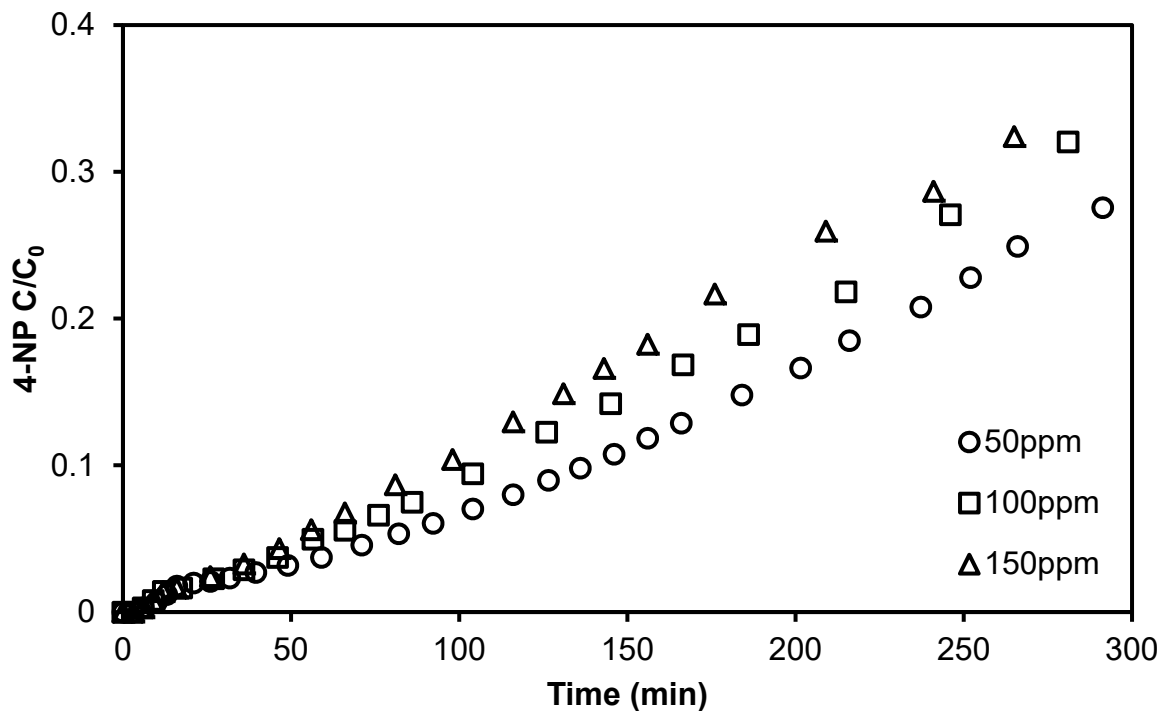
Figure 7.3(c) The effect of inlet concentration on 4-NP sorption in PEBA column*(Flow rate=5.0±0.3 mL/min, fibre diameter=102 μm)*
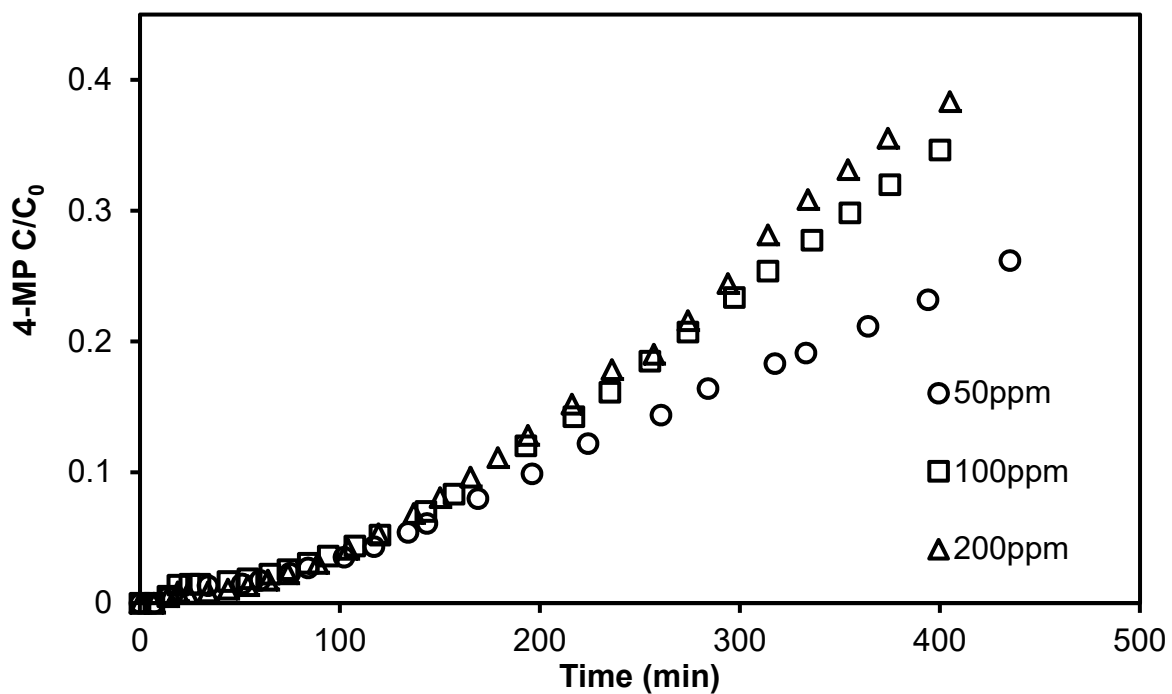
Figure 7.3(d) The effect of inlet concentration on 4-MP sorption in PEBA column *(Flow rate=2.5±0.3 mL/min, fibre diameter=90 μm)*
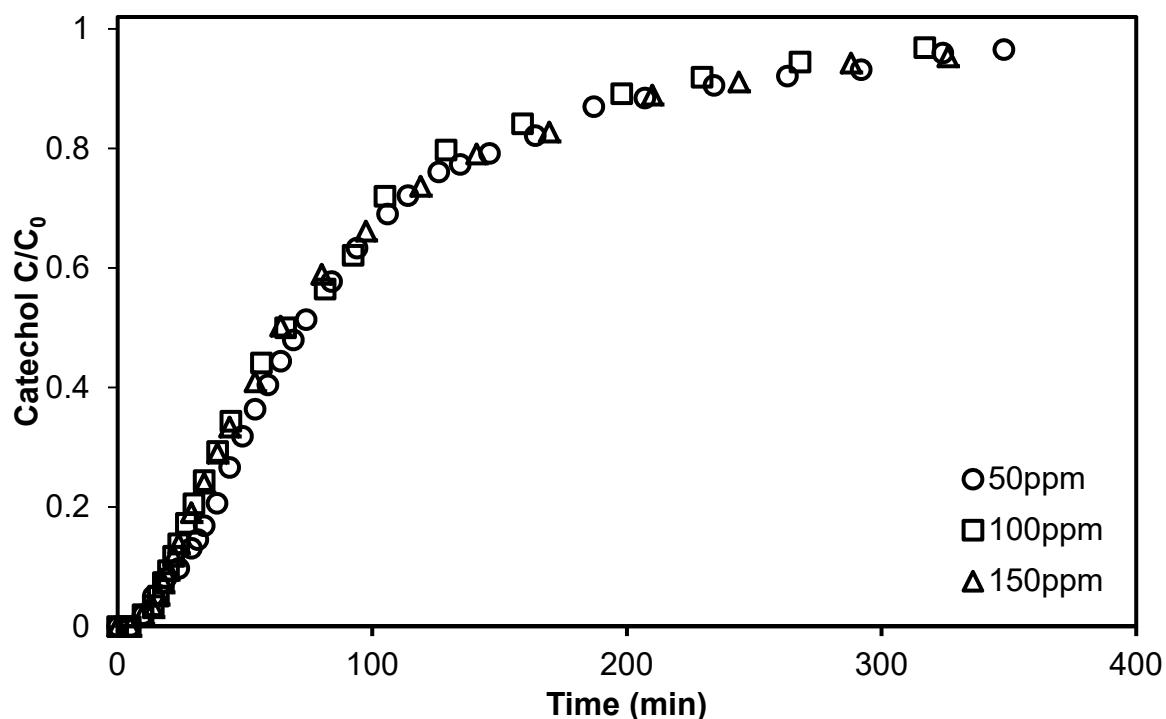
Figure 7.3(e) The effect of inlet concentration on catechol sorption in PEBA column*(Flow rate=2.5±0.3 mL/min, fibre diameter=90 μm)*

7.3.2 The effect of flow rate on sorption breakthrough

The breakthrough curves for dynamic sorption of phenolic compounds at different flow rates are shown in Figures 7.4(a)-(e). It is shown that the shape of breakthrough curve was sensitive to the flow rate, and much sharper breakthrough curves were obtained at higher flow rates. It is also shown that the total sorbed solute quantity, which may be represented by the integration area above the breakthrough curve, also decreased with increasing flow rates for the sorption of phenol and catechol.

The above mentioned behaviour can be explained on the basis of mass transfer fundamentals. At a higher flow rate, the front of the mass transfer zone will reach the exit of the sorption column earlier, thereby giving an earlier breakthrough time. The sensitivity of the column sorption to the liquid flow rate is probably due to the fact that the liquid residence

time within the column is critical for the dynamic sorption process. If the sorption process is limited by the external mass transfer, a higher flow rate is favoured because the liquid film resistance will be decreased at higher flow rates. If the process is controlled by the internal mass transfer, then a lower flow rate is favoured because a lower flow rate allows a longer liquid residence time in the column [168]. It may thus be concluded that in our study an increase in the flow rate resulted in an insufficient contact time between the liquid phase and the solid phase, which caused incomplete utilization of sorption sites at the end and hence a decreased phenol sorption capacity.
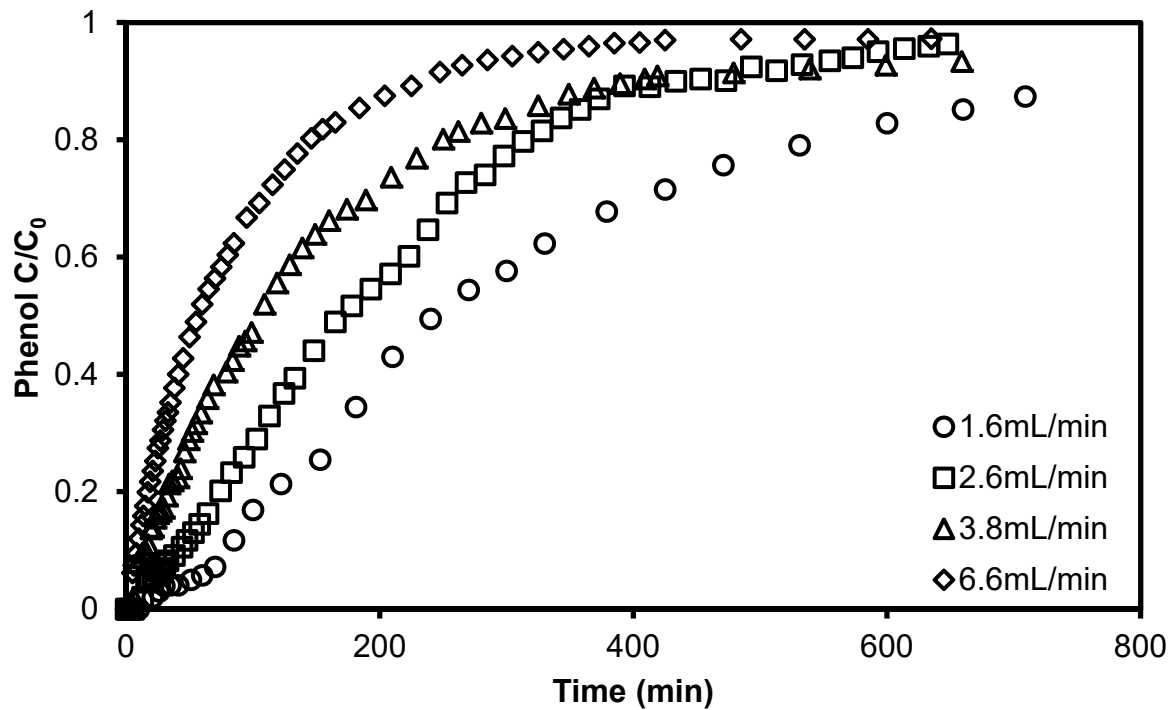
Figure 7.4(a) The effect of flow rate on phenol sorption in PEBA column (*Initial phenol concentration=100 ppm, fibre diameter=190 μm*)
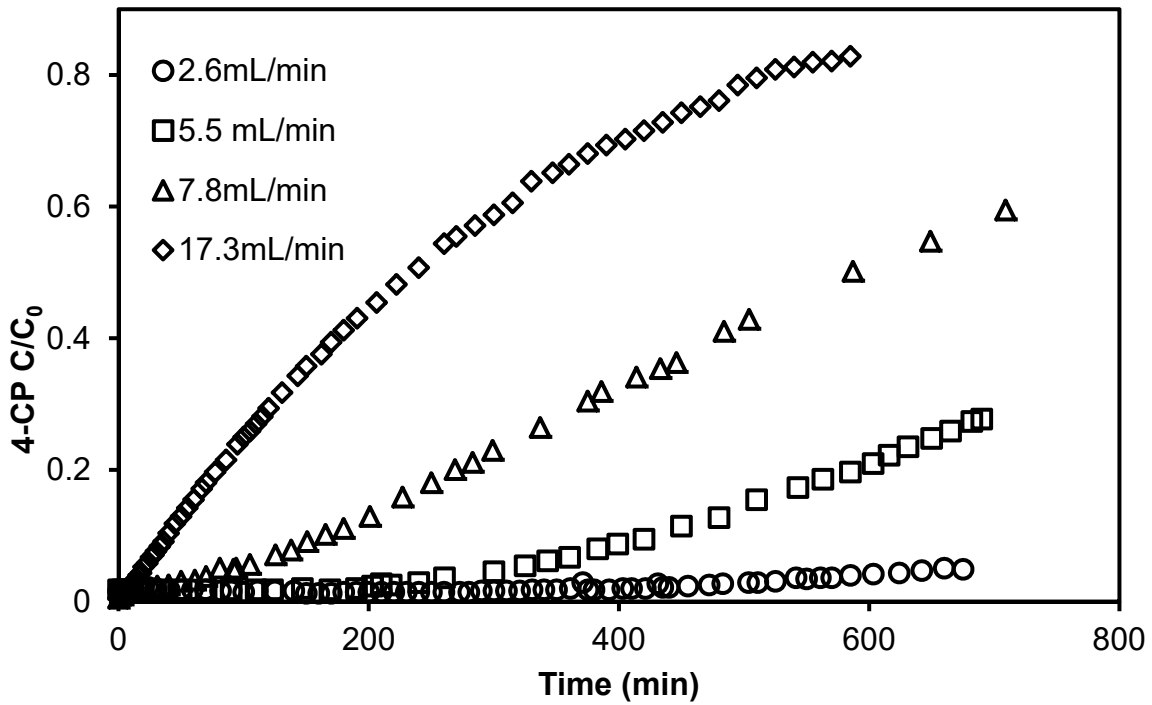
Figure 7.4(b) The effect of flow rate on 4-CP sorption in PEBA column (*Initial 4-CP concentration=50 ppm, fibre diameter=102 μm*)
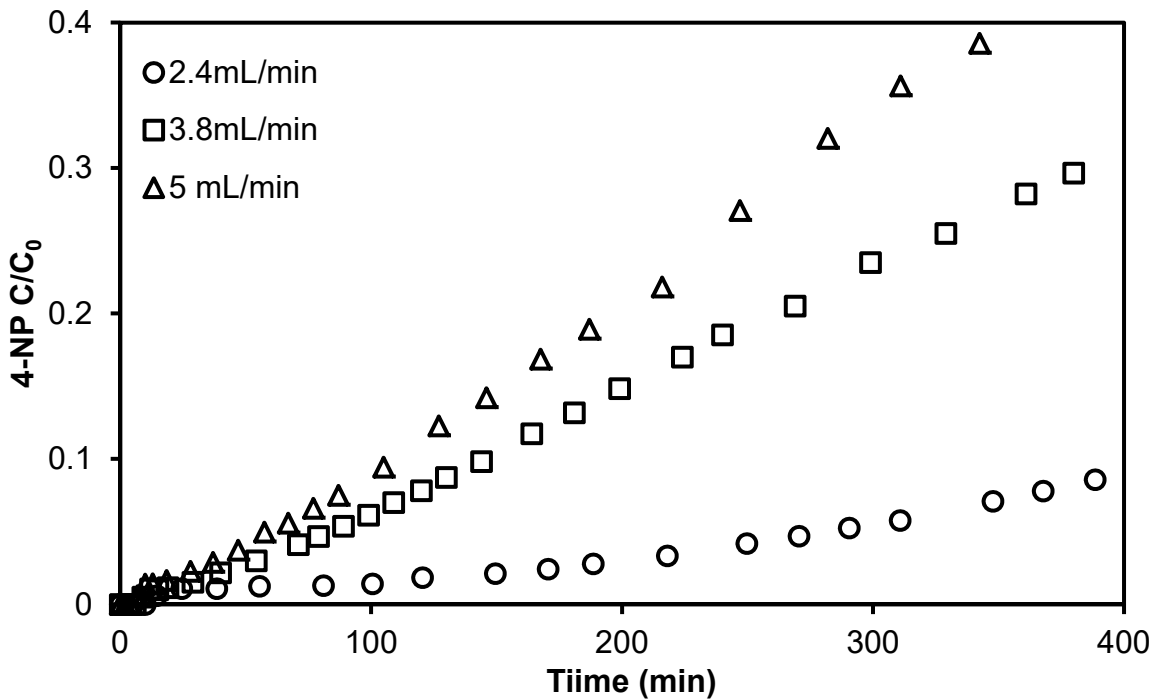
Figure 7.4(c) The effect of flow rate on 4-NP sorption in PEBA column (*Initial 4-NP concentration=100 ppm, fibre diameter=102 μm*)
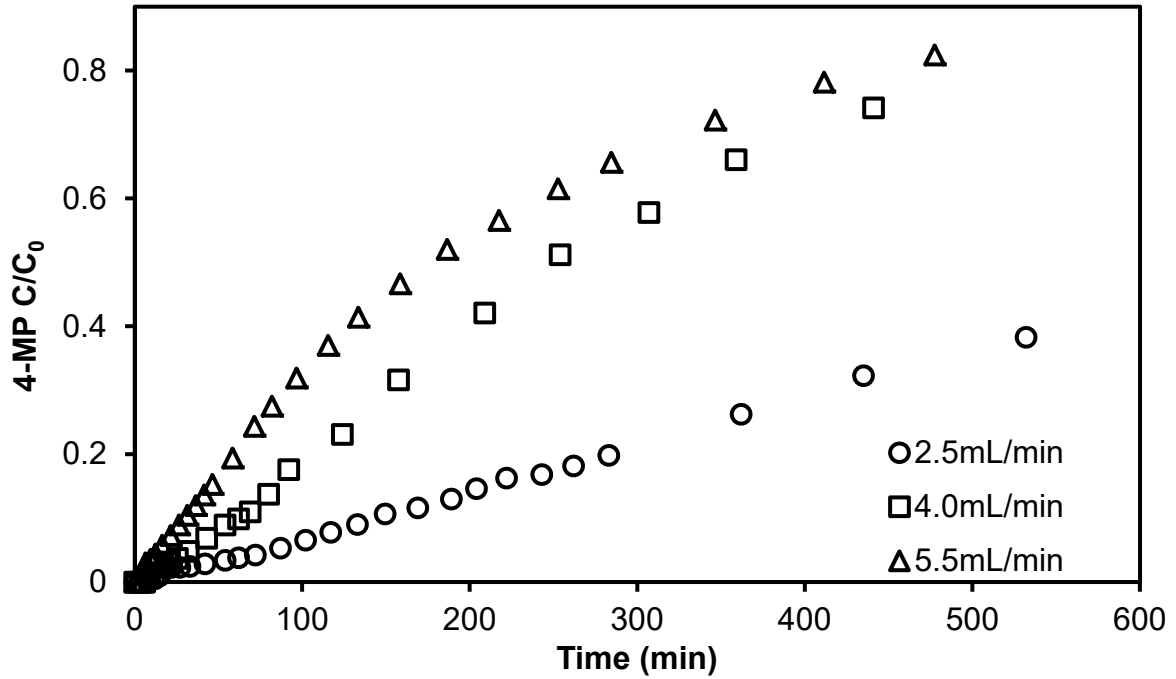
Figure 7.4(d) The effect of flow rate on 4-MP sorption in PEBA column (*Initial 4-MP concentration=50 ppm, fibre diameter=102 μm*)
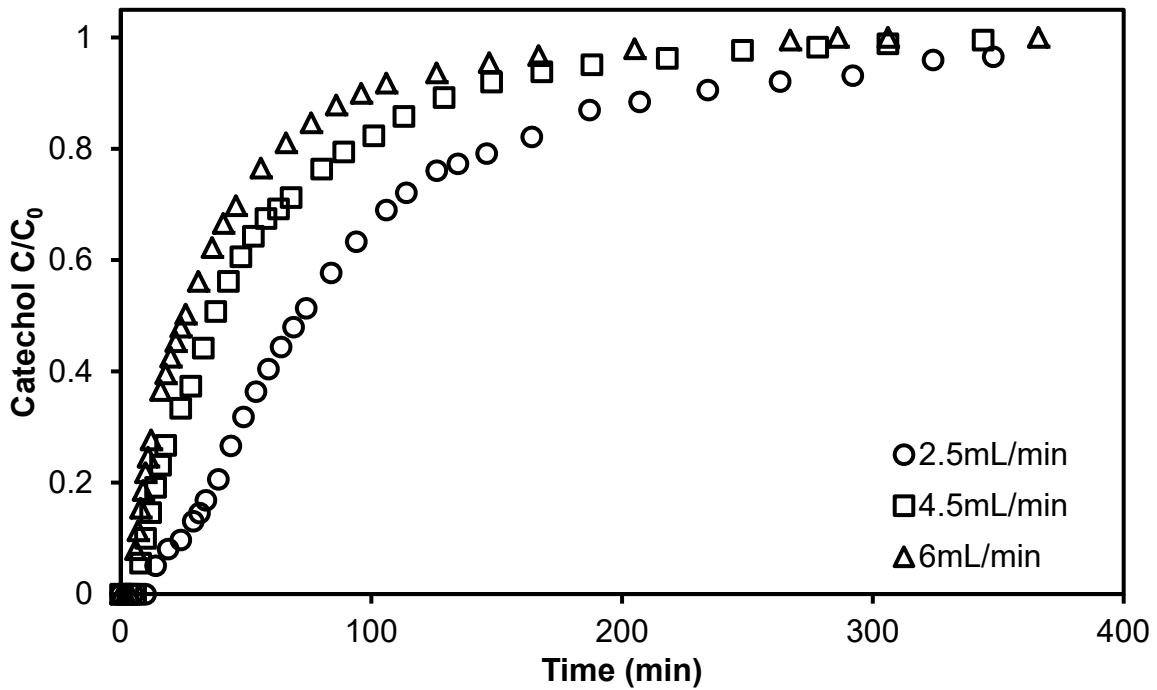
Figure 7.4(e) The effect of flow rate on catechol sorption in PEBA column (*Initial catechol concentration=50 ppm, fibre diameter= 127 μm*)

7.3.3 The effect of fibre diameter on sorption breakthrough

Figures 7.5(a)-(e) show the effect of fibre diameter on sorption breakthrough of phenolic compounds. The breakthrough is considerably affected by the fibre size. Sharper breakthrough curves, decreased breakthrough time and decreased column sorption capacity were obtained for phenol sorption with larger fibres. This is because an increase in the fibre diameter increased the internal resistance to mass transfer and thus decreased the mass transfer rate of the sorbate. The decreased mass transfer rate increased the length of mass transfer zone in the packed column and decreased the time prior to sorption breakthrough.

Similar to the effect of flow rate, insufficient liquid phase residence time may also be a plausible explanation. With larger fibre size, the internal diffusion process became more dominant, and thus at a given flow rate, a larger fibre size would result in insufficient liquid residence time in the column and incomplete sorption site utilization at the end. Fibres with a small diameter are preferred from the standpoint of mass transfer rate. However, in practical applications, a tight packing of small fibres will increase the pressure drop of liquid flow in the column at a given flow rate, which is not desirable for effective column sorption [223]. However, a loose packing of large fibres will cause channelling effect, since the void space among large fibers were larger than those among fine fibers at a given packing density. Thus a proper fibre size should be selected to give a sufficiently long breakthrough time for the solute and a relatively small pressure drop of the fluid.
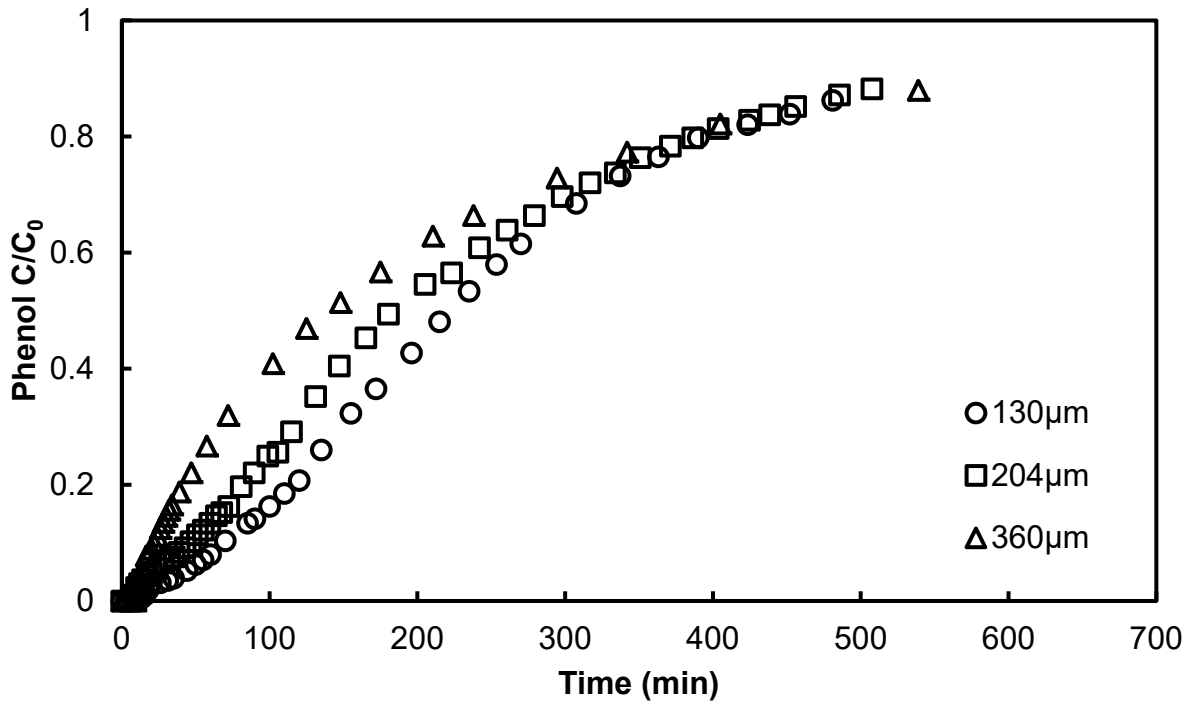
Figure 7.5(a) The effect of fibre diameter on phenol sorption in PEBA column (*Initial phenol concentration=100 ppm, flow rate=2.5±0.3 mL/min*)
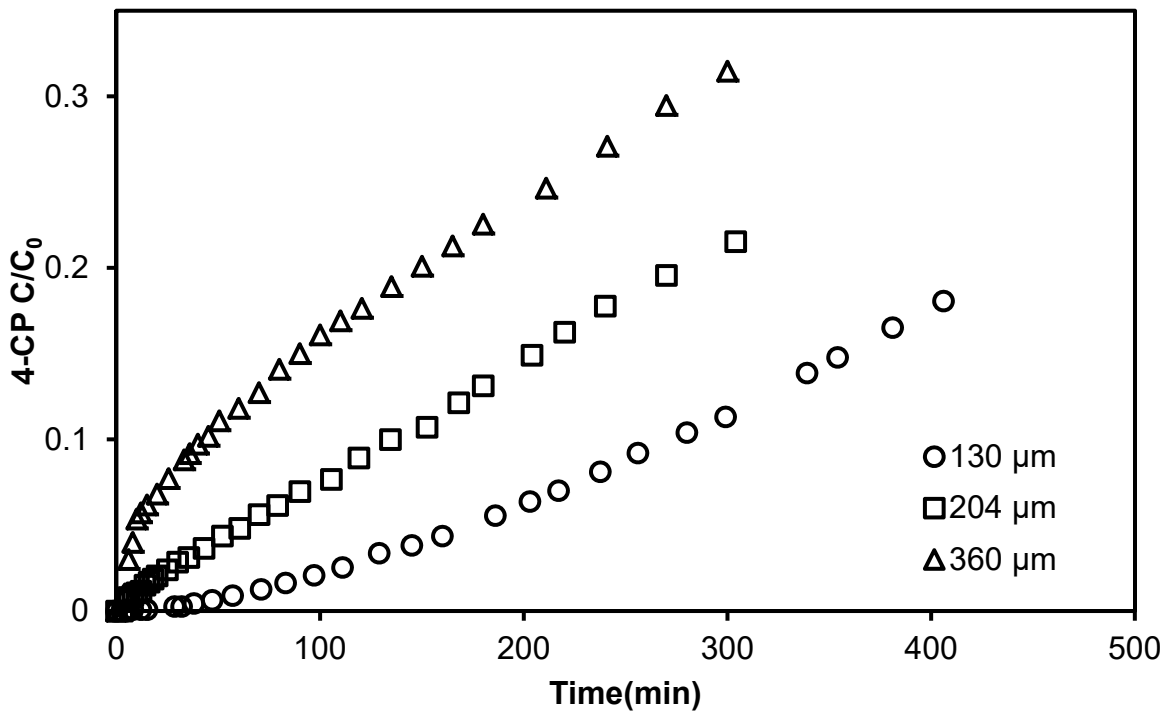
Figure 7.5(b) The effect of fibre diameter on 4-CP sorption in PEBA column (*Initial 4-CP concentration=100 ppm, flow rate=5.5±0.3 mL/min*)
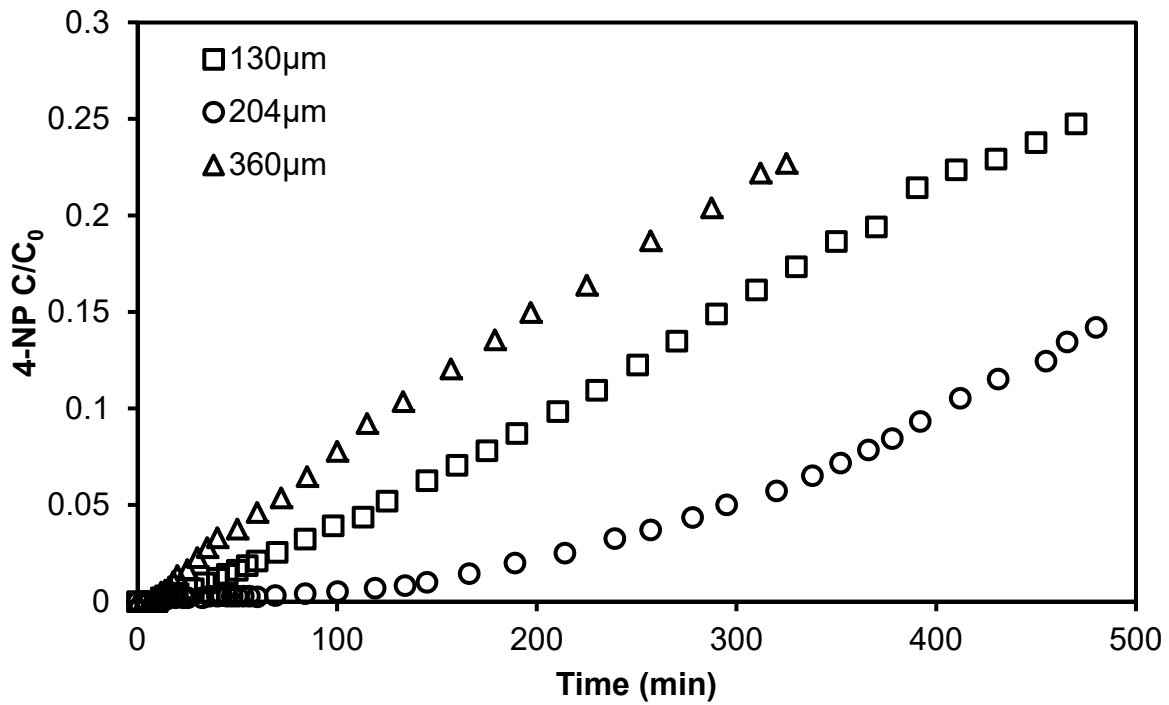
Figure7.5(c) The effect of fibre diameter on 4-NP sorption in PEBA column *(**Initial 4-NP concentration=60 ppm, flow rate=2.5±0.3 mL/min**)*
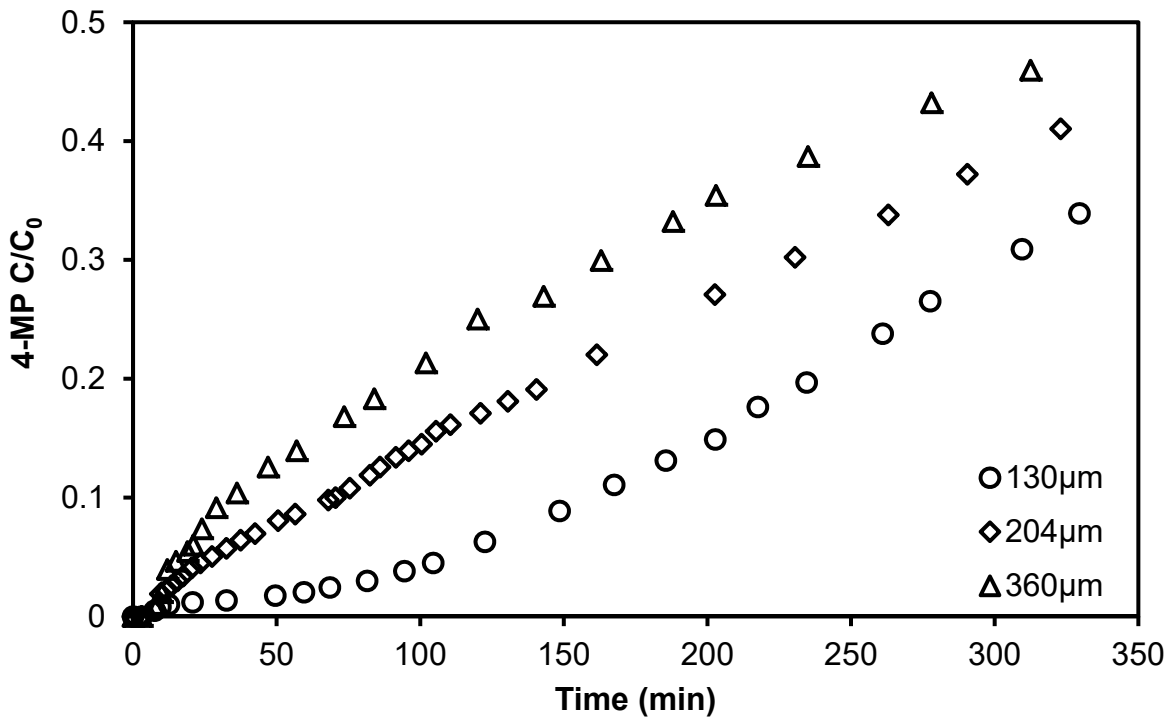
Figure 7.5(d) The effect of fibre diameter on 4-MP sorption in PEBA column *(**Initial 4-MP concentration=50 ppm, flow rate=3.0±0.3 mL/min**)*
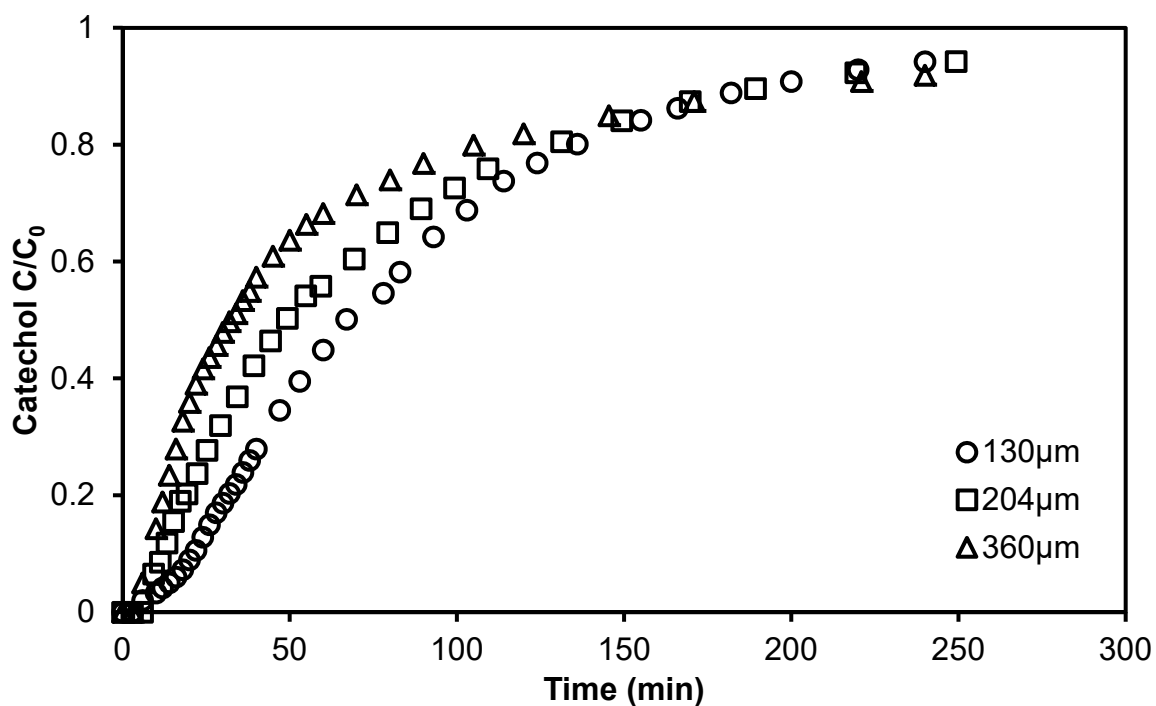
Figure 7.5(e) The effect of fibre diameter on catechol sorption in PEBA column (*Initial catechol concentration=50 ppm, flow rate=2.5±0.3 mL/min*)

7.3.4 Modelling of sorption data in PEBA columns

Most mathematical models developed to predict breakthrough curves are derived by solving a series of equations with specified initial conditions and boundary conditions. They generally include (1) macroscopic mass conservation equation (i.e., Eq. (2.53)); (2) equations of sorption kinetics; and (3) equilibrium isotherms. The selection of packed bed sorption model should be based on characteristics of the sorption system as well as the assumptions of the model. A brief summary of the five most widely used column models in the literature are presented in Table 7.1. The BDST, Wolborska and Thomas models have similar mathematical forms. The Wolborska model becomes the BDST model if $\ln(\frac{C_0}{C} - 1) \cong ln\frac{C_0}{C}$ and β_a equals $k_{BD}N_0$. The BDST model and the Thomas model are equivalent, since $k_{BD} = k_{Th}$, the linear flow rate u (cm/min) is proportional to volumetric flow rate F (mL/min), and the mass of sorbent m is proportional to the bed height Z at a given packing density, the column sorption capacity Q_0 (mg/g) should be proportional to bed capacity N_0 (mg/L). Therefore, it was decided to use only one of the three similar models in this study, and the BDST model was selected. In addition, the Clark model (which is based on Freundlich isotherm) and the empirical Yoon-Nelson model were also used to analyze the experimental data.

Table 7.1 Comparison of widely used column sorption models

Model	Equation	Assumptions	Limitations
BDST	$\ln(\frac{C_0}{C} - 1) = \frac{k_{BD}N_0Z}{u} - k_{BD}C_0 t$	The rate of reaction is proportional to residual adsorption capacity of the sorbent and to the solute concentration	1. Ignores internal diffusion resistance and film diffusion resistance. 2. Only applicable to low concentration range
Wolborska	$\ln\frac{C_0}{C} = \frac{\beta_a}{u}Z - \frac{\beta_a C_0 t}{N_0}$	1. The low-concentration region is characterized by constant kinetic coefficients; 2. The process rate is controlled by the external mass transfer (i.e., film diffusion and axial diffusion)	Only applicable to low concentration region
Thomas	$\ln\left(\frac{C_0}{C} - 1\right) = \frac{k_{Th}Q_0 m}{F} - k_{Th}C_0 t$	1. Langmuir sorption isotherm 2. Second-order reversible reaction kinetics 3. Diffusion is not a rate-determining factor	Only applicable to early stages where the external and the internal diffusion resistance are negligible
Clark	$C = \left(\frac{C_0^{n-1}}{1 + Ae^{-rt}}\right)^{(\frac{1}{n-1})}$	1. Freundlich sorption isotherm 2. Expression of sorption rate: $u\frac{dc}{dz} = k_T(C - C_e)$	Ignores the accumulation of sorbate concentration
Yoon-Nelson	$\ln\frac{C}{C_0 - C} = k_{YN}t - \tau k_{YN}$	The rate of decrease in the probability of adsorption for each molecule is proportional to the probability for adsorption and breakthrough.	The simple form is less valuable for predicting process variables

7.3.4.1 The BDST model

The BDST model equation has the form of:

$$\ln(\frac{C_0}{C} - 1) = \frac{k_{BD}N_0Z}{u} - k_{BD}C_0t \tag{7.1}$$

where k_{BD} is the sorption rate constant (L·mg^{-1}·min^{-1}), N_0 (mg/L) is the bed capacity (i.e., amount of solute (mg) sorbed per volume (L) of packed bed), Z (cm) is the bed depth (i.e., the length of the packed PEBA fibres), u (cm/min) is the linear flow rate (i.e., the volumetric flow rate divided by the cross sectional area of the column) and C_0 is the initial solute concentration (mg/L). The plots of $\ln(\frac{C_0}{C} - 1)$ vs. time should give a straight line if the BDST model applies. In this study, the low concentration region is defined as $C/C_0 < 0.15$ according to the study of Aksu and Gönen [165]. Figures 7.6(a)-(c) show the plots of $\ln(\frac{C_0}{C} - 1)$ vs. t for the sorption of phenolic compounds in PEBA columns at $C/C_0 < 0.15$. The model parameters along with correlation coefficients were listed in Tables 7.2(a), (b) and (c). The parameters were then used to calculate the breakthrough curve using Origin software. The simulated breakthrough curves based on the BDST model was compared with experimental data, as shown in Figures 7.7(a), (b) and (c). It is shown that the BDST model is valid for the initial part of the sorption breakthrough (i.e., $C/C_0 < 0.15$) while large discrepancies were found between the experimental data and model calculations above this level ($C/C_0 > 0.15$) for phenolic compounds sorption in the packed column.

The data in Table 7.2(a) show that the sorption capacity of the packed bed increased with an increase in the inlet concentration for all the phenolic compounds studied here. This is because a higher concentration will provide a higher driving force for the sorption and thus a higher sorption capacity, which is in agreement with the equilibrium sorption data. It is also

observed from Table 7.2(a) that the value of k_{BD}, which characterizes the rate of solute transferring from the fluid phase to the solid phase, decreased with an increase in the inlet concentration. This is because the consumption rate of the available sorption site is higher at higher inlet solute concentrations, and thus the mass transfer rate decreased and resulted in decreased breakthrough time as it is indicated in Figures 7.3(a)-(e). For the effect of flow rate, the data in Table 7.2(b) show that rate constant was influenced by the flow rate significantly. k_{BD} increased with an increase in the flow rate. It seems that the sorption kinetics was affected by the external mass transfer at the initial stage of the sorption, increasing the flow rate reduced the external mass transfer resistance in the boundary layer surrounding the sorbent fibres. The data in Table 6.2(c) show that the sorption capacity of the packed bed (N_0) decreased with an increase in the fibre diameter. At a given flow rate, as fibre diameter increased, the internal diffusion was more significant, and liquid residence time in the packed column decreased, resulting in a lower sorption capacity.
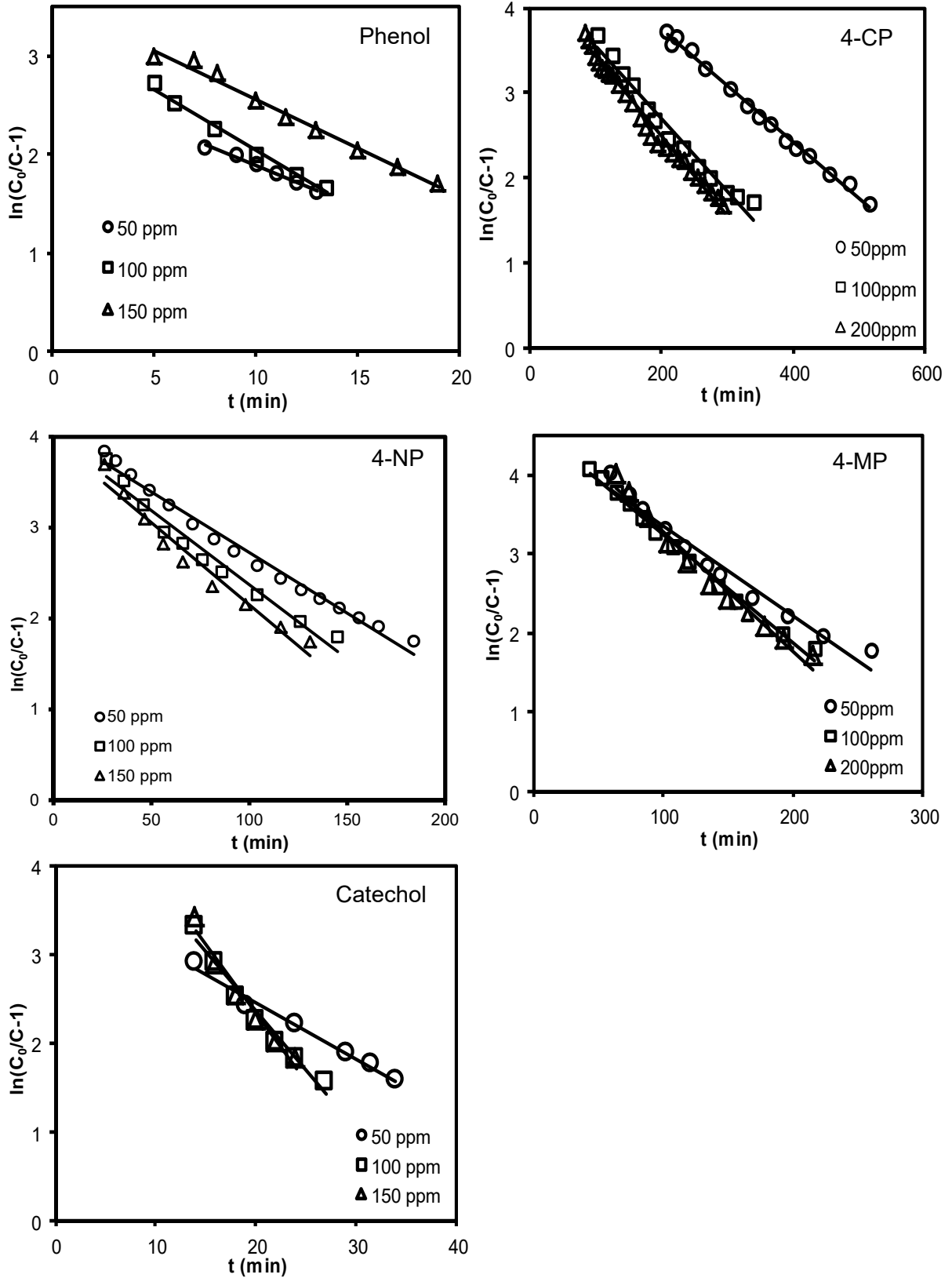
Figure 7.6(a) Plots of $\ln(\frac{C_0}{C} - 1)$ vs. t for sorption of phenolic compounds in PEBA columns at different initial solute concentrations based on the BDST model
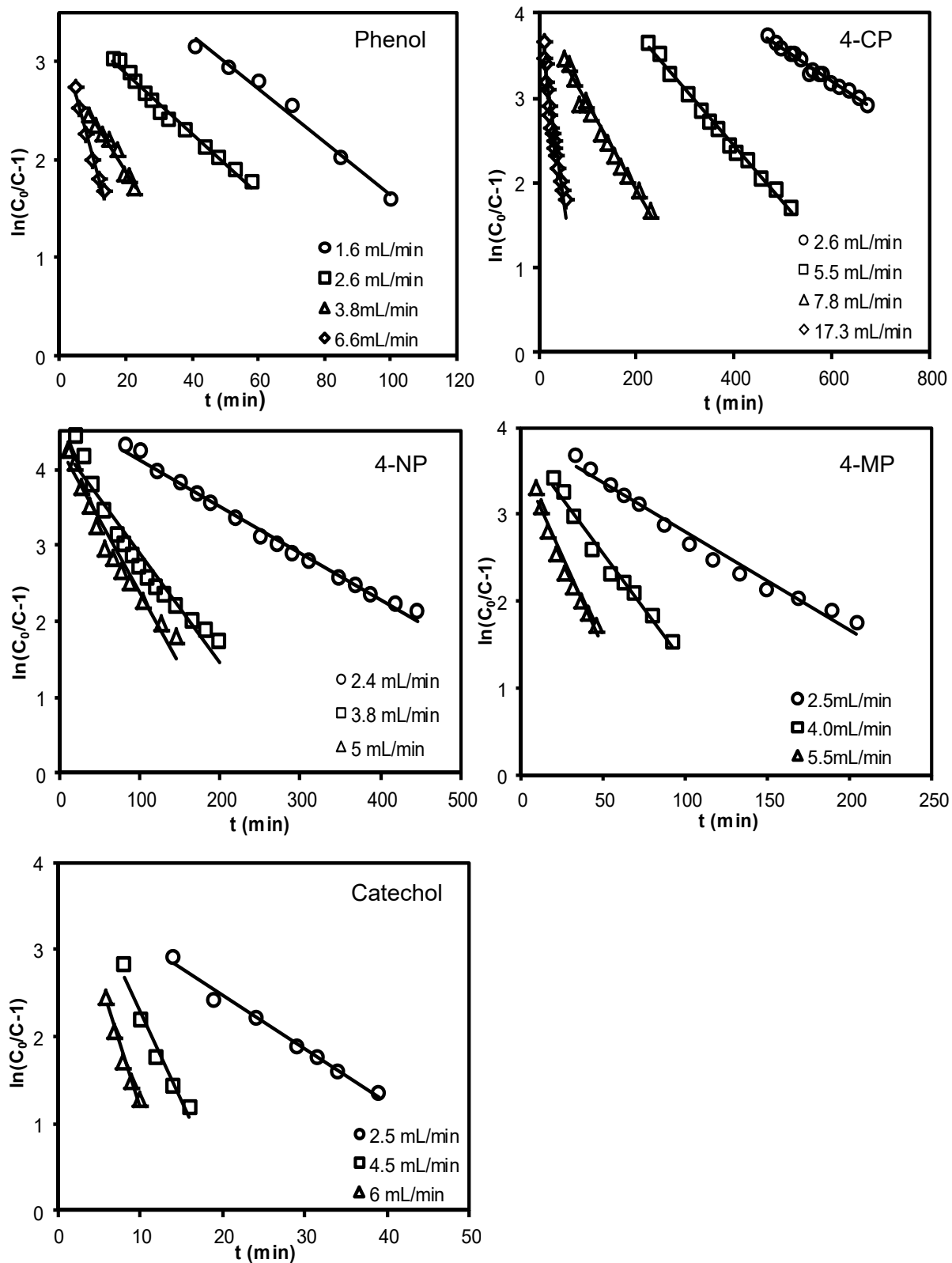
Figure 7.6(b) Plots of $\ln(\frac{C_0}{C} - 1)$ vs. t for sorption of phenolic compounds in PEBA columns at different flow rates based on the BDST model
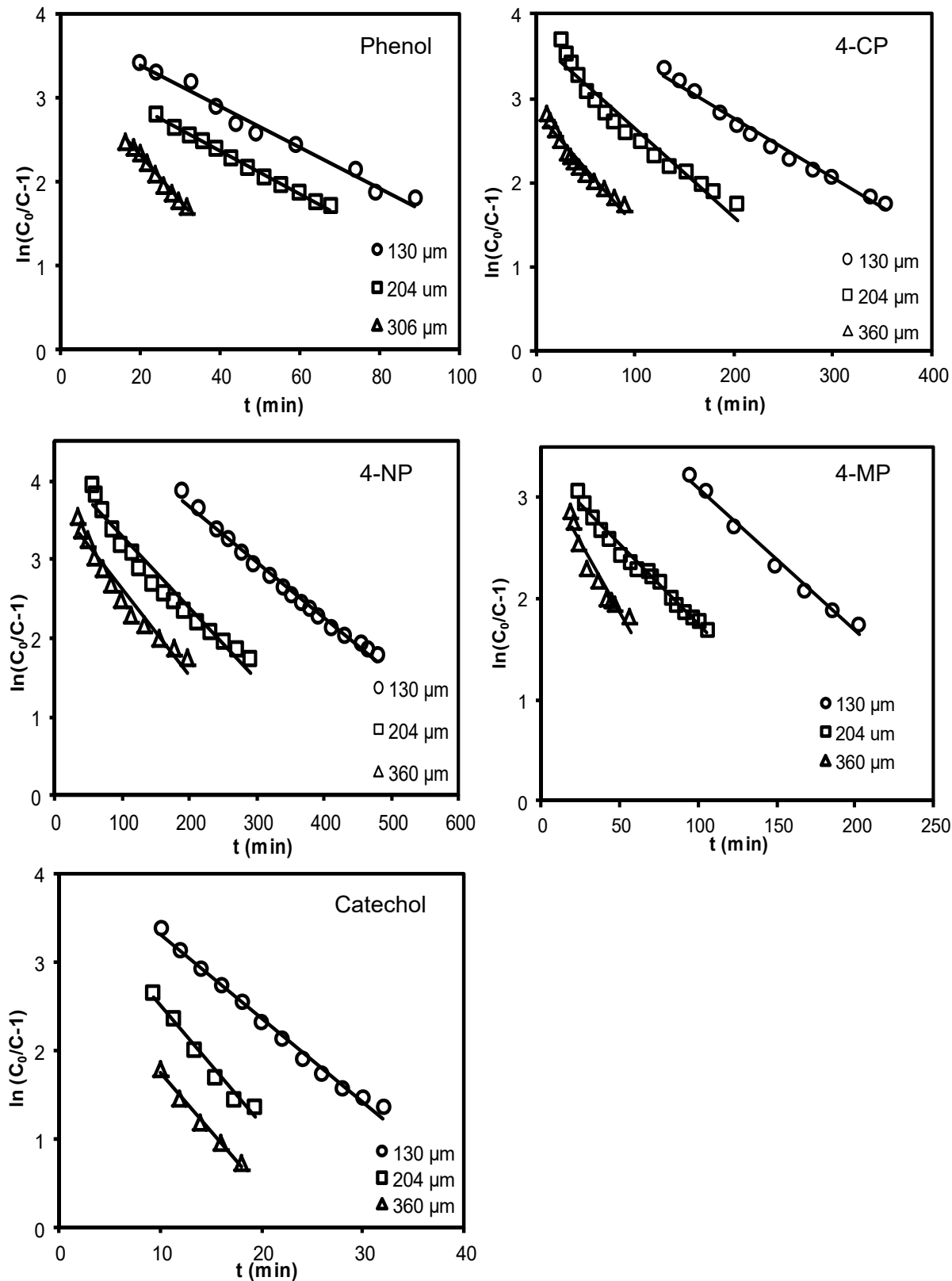
Figure 7.6(c) Plots of $\ln(\frac{C_0}{C} - 1)$ vs. t for sorption of phenolic compounds in PEBA columns at different fibre diameters based on the BDST model

Figure 7.7(a) Comparison of experimental data and model predictions based on the BDST model for sorption of phenolic compounds in PEBA columns at different inlet concentrations

Figure 7.7(b) Comparison of experimental data and model predictions based on the BDST model for sorption of phenolic compounds in PEBA columns at different flow rates

Figure 7.7(c) Comparison of experimental data and model predications based on the BDST model for sorption of phenolic compounds in PEBA columns at different fibre diameters

7.3.4.2 The Clark model

The Clark model is expressed by:

$$C = \left(\frac{C_0^{n-1}}{1 + Ae^{-rt}} \right)^{\left(\frac{1}{n-1} \right)}$$ (7.2)

where n is a Freundlich parameter determined by the batch experiment, C_0 is the inlet solute concentration (mg/L), A is a model parameter relative to the film diffusivity , r is the model parameter relative to the sorption rate.

A close examination of Eq. (7.2) reveals that The Clark equation is applicable neither to the initial stage when no solute escaped in the effluent (C/C_0=0) nor the final stage when the column is exhausted (C/C_0=1). Thus this equation can only represent breakthrough behaviour for a certain C/C_0 range ($0 < C/C_0 < 1$). Srivastava et al. [164] applied the Clark equation at C/C_0 ratios of over 0.08, and they found that the Clark model could well describe the sorption behaviour. Aksu and Gonen [165] also reported that the Clark model could not apply to experimental data at C/C_0 <0.08 in their study. Therefore, in our study, the experimental data at the range of $0.08 < C/C_0 < 0.99$ were fitted to the Clark model. A comparison of the experimental and breakthrough curves predicted by the Clark model for phenolic compounds at different conditions are shown in Figures 7.8(a), (b) and (c). The predicted curves were obtained from Eq. (7.2) by nonlinear curve fit using Origin software.

It appears in Figure 7.8(a) that the Clark model worked well to represent the experimental data. Figure 7.8(b) shows that the Clark model works better at lower flow rates, for the sorption of 4-CP and 4-MP. However, model predictions deviated significantly from experimental data for the sorption of 4-CP and 4-MP when the fibre diameter was considerably large. The Clark model is based on the assumption that the external mass

transfer is the rate limiting step. This is, however, not the case when the internal diffusion is the rate determining step, especially at high flow rates and large fibres. Thus the assumption of the Clark model did not hold and poor simulations were observed in these cases.

The model parameters and correlation coefficient of the regression at different conditions were listed in Table 7.2(a), (b) and (c). No obvious correlation between the Clark model parameters and the inlet feed concentration were observed. Similar results were also reported by Srivastava et al. [164] for phenol removal by Bagasse. Table 7.2(a) shows values of r and A at different inlet concentrations are very similar, which is probably due to the narrow concentration range selected in our study. Table 7.2(b) shows that with an increase in the flow rate, the value of r increased, while the value A decreased. The correlations between r and the flow rate were in agreement with results of some other studies [164, 165]. An explanation is that parameter r is related to the mass transfer rate. High flow rates would increase the migration rate of the mass transfer zone within the packed column and lead to sharp breakthrough curves and large r values.
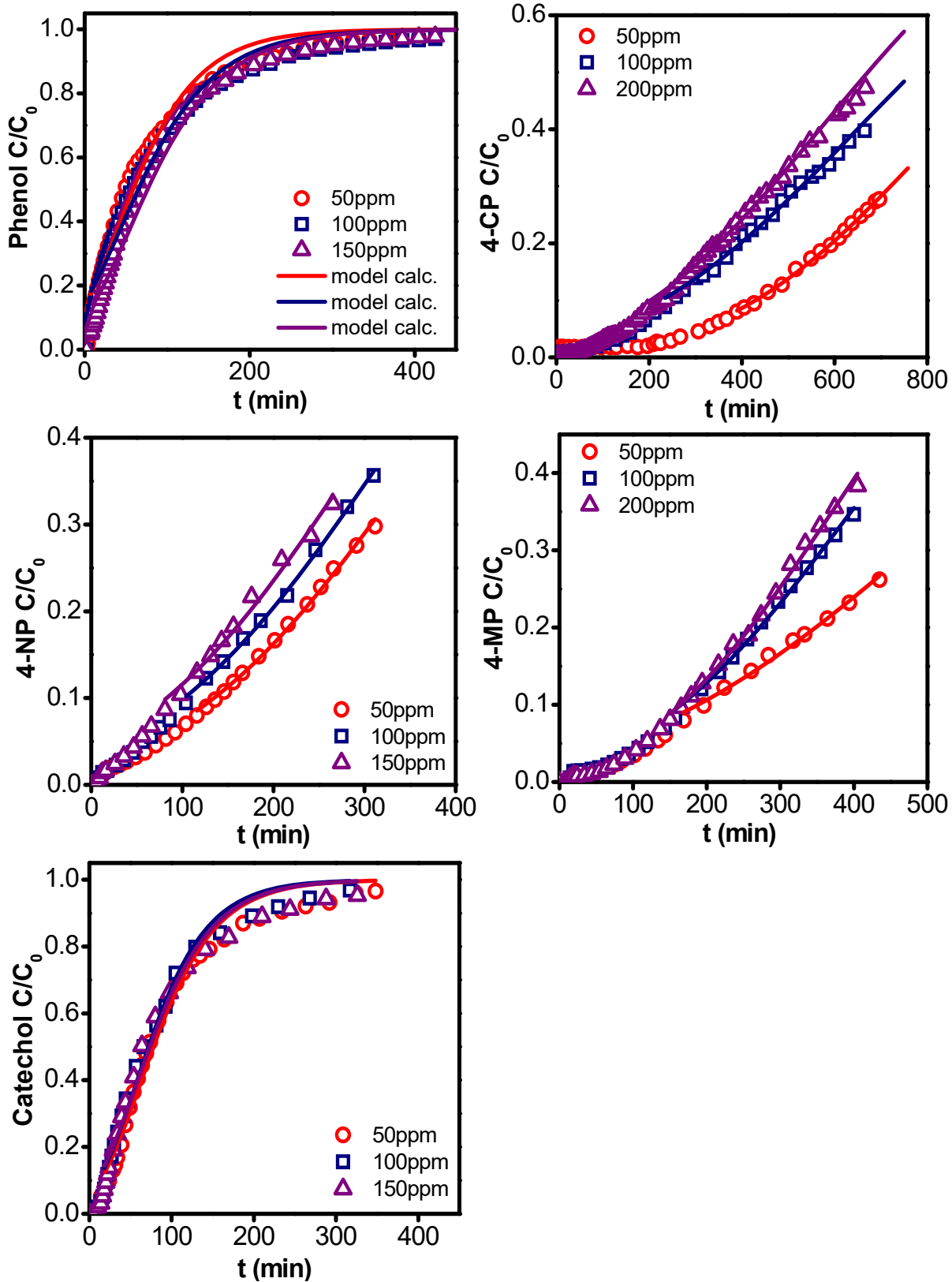
Figure 7.8(a) Comparison of experimental data and predictions based on the Clark model for sorption of phenolic compounds in PEBA columns at different inlet concentrations
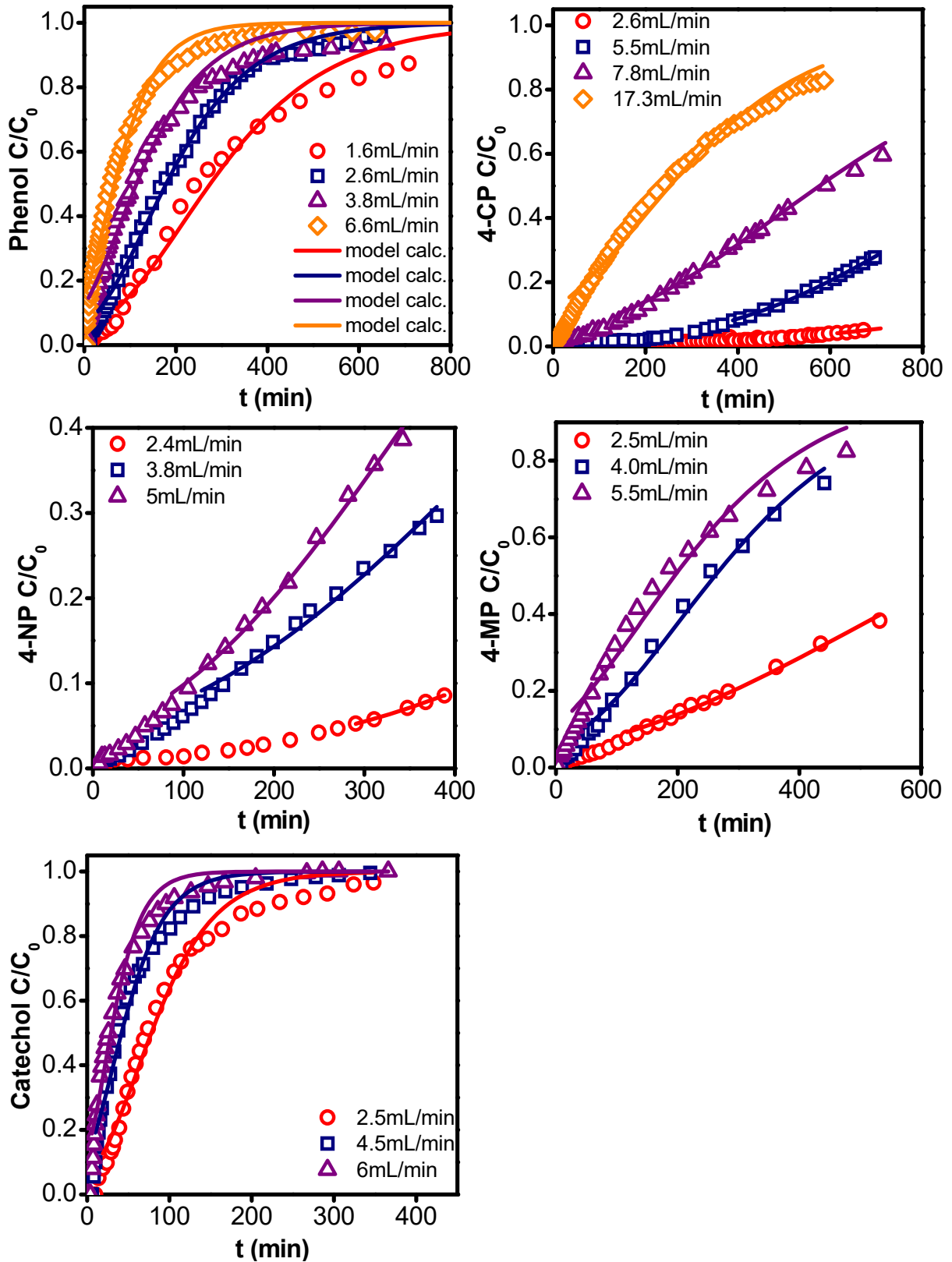
Figure 7.8(b) Comparison of experimental data and predications based on the Clark model for sorption of phenolic compounds in PEBA columns at different flow rates
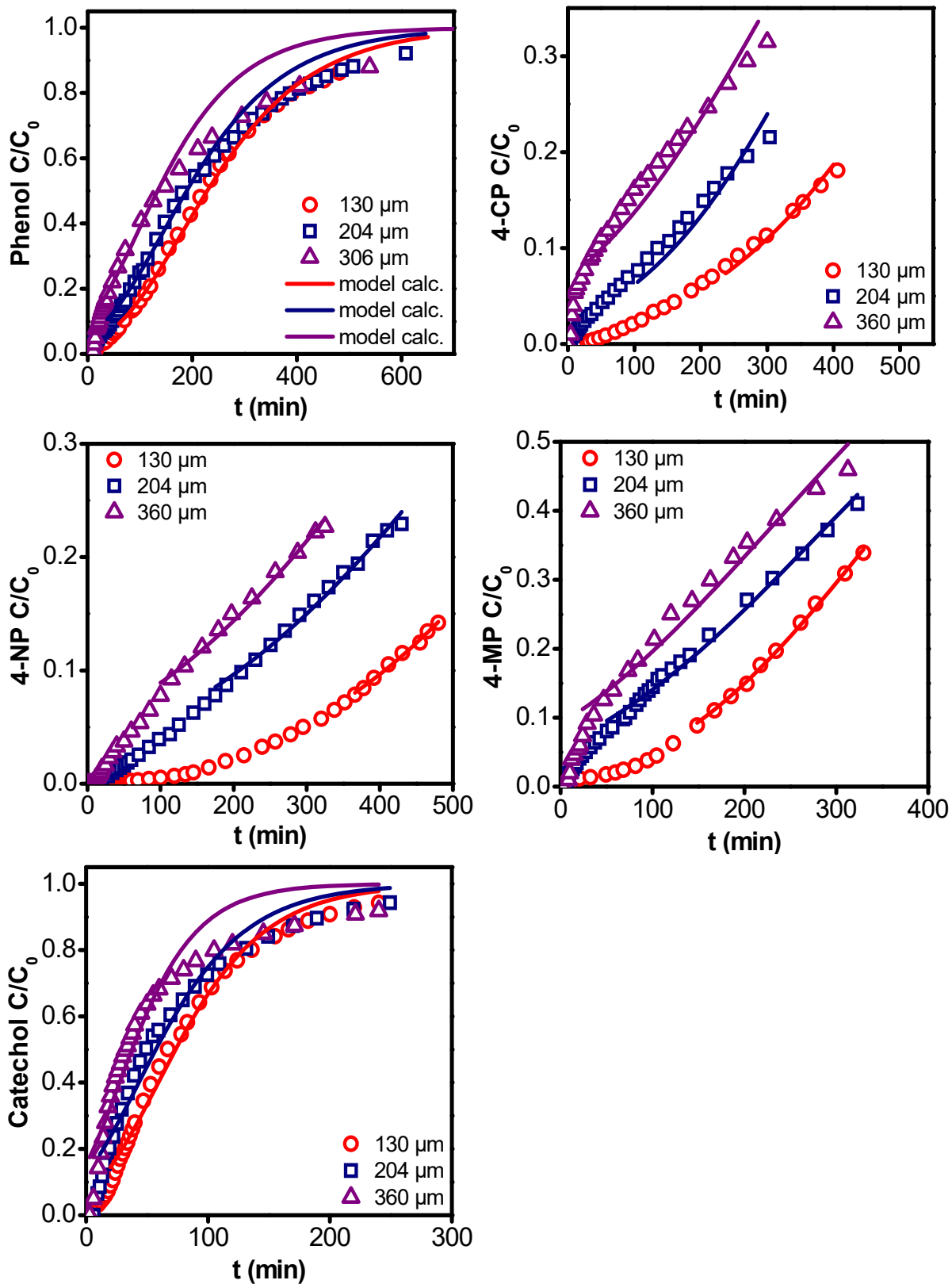
Figure 7.8(c) Comparison of experimental data and predications based on the Clark model for sorption of phenolic compounds in PEBA columns at different fibre sizes

7.3.4.3 The Yoon-Nelson model

The empirical Yoon-Nelson model is expressed as:

$$ln\frac{C}{C_0 - C} = k_{YN}t - \tau k_{YN} \qquad (7.3)$$

where k_{YN} is the rate constant (min^{-1}), τ (min) is the time required to obtain 50% breakthrough (i.e., $C_b/C_0 = 50\%$). Rearranging the above equation:

$$\frac{C}{C_0} = 1/[1 + \exp(-k_{YN}t + k_{YN}\tau)] \qquad (7.4)$$

In our study, experimental data over the region of $0.08 < C/C_0 < 0.99$ were fitted to Eq. (7.4) using the Origin software, based on an earlier study by Aksu and Gönen [165]. The model parameters k_{YN} and τ along with correlation coefficients at different conditions were listed in Table 7.2(a), (b) and (c). Table 7.2(a) shows that for the sorption of 4-CP, 4-NP and 4-MP, the 50% breakthrough time decreased with an increase in the inlet solute concentration. For the sorption of phenol and catechol, the τ values did not change substantially in the studied concentration range. Table 7.2(b) and (c) show that the parameter τ decreased with an increase in the flow rate and fibre size for all the phenolic compounds investigated here. A higher flow rate led to faster migration of the mass transfer zone and thus decreased the 50% breakthrough time. As far as the effect of fibre diameter is concerned, the mass transfer rate with larger fibres decreased due to the internal diffusion resistance, resulting in a decrease in the 50% breakthrough time.

A comparison of the experimental data and the model predictions based on the Yoon-Nelson model was shown in Figure 7.9(a), (b) and (c). The experimental data is close to those predicted by the Yoon-Nelson model in the applied concentration region. However, by comparing Figure 7.8 with Figure 7.9, it was found that the deviation between the

experimental data and model predictions is larger than that predicted by the Clark model. Thus, it appears that the Clark model is more suitable to represent the sorption breakthrough of phenolic compounds in the packed columns studied here.
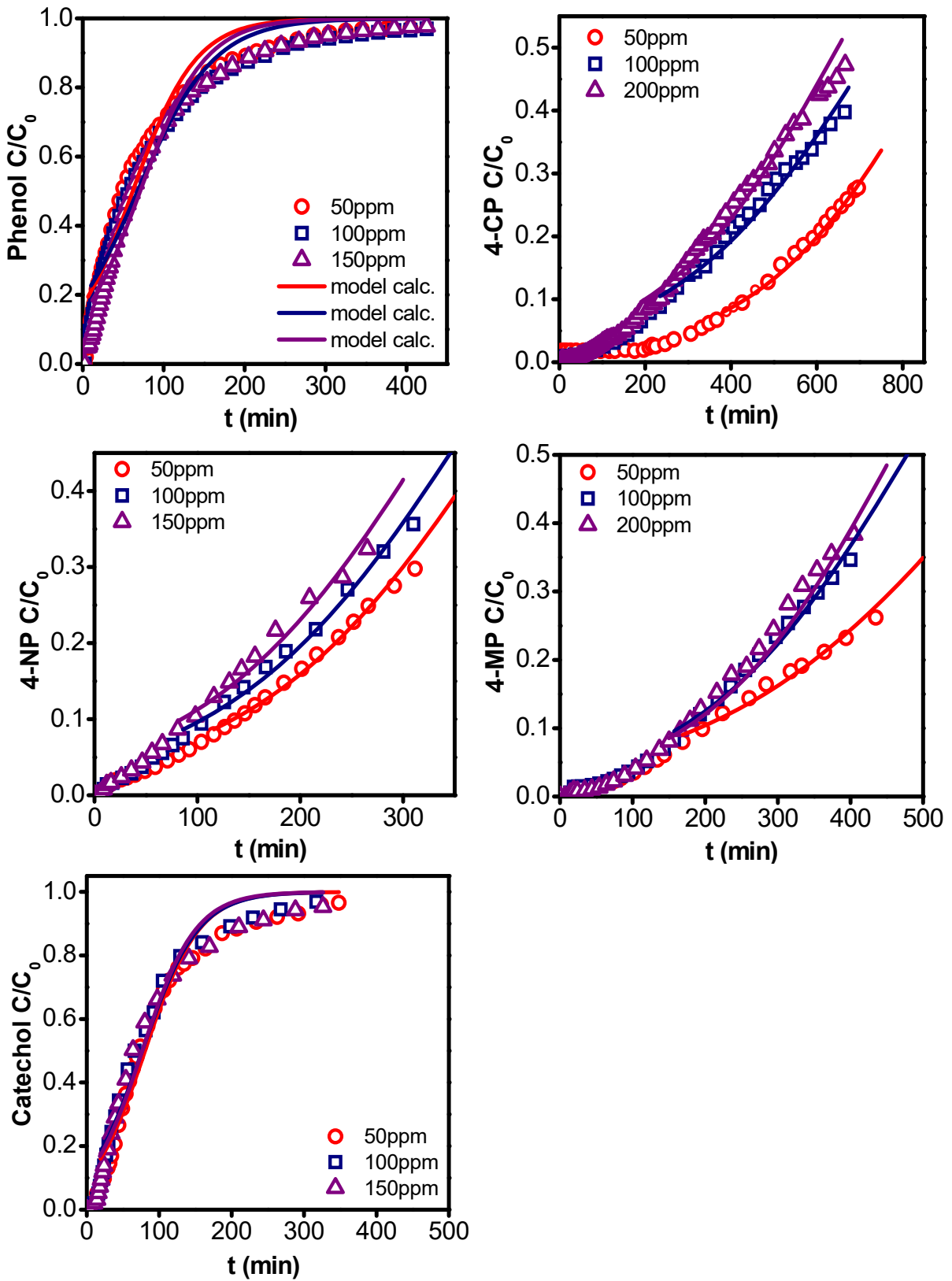
Figure 7.9(a) Comparison of experimental data and predications based on the Yoon-Nelson model for sorption of phenolic compounds in PEBA columns at different inlet concentrations
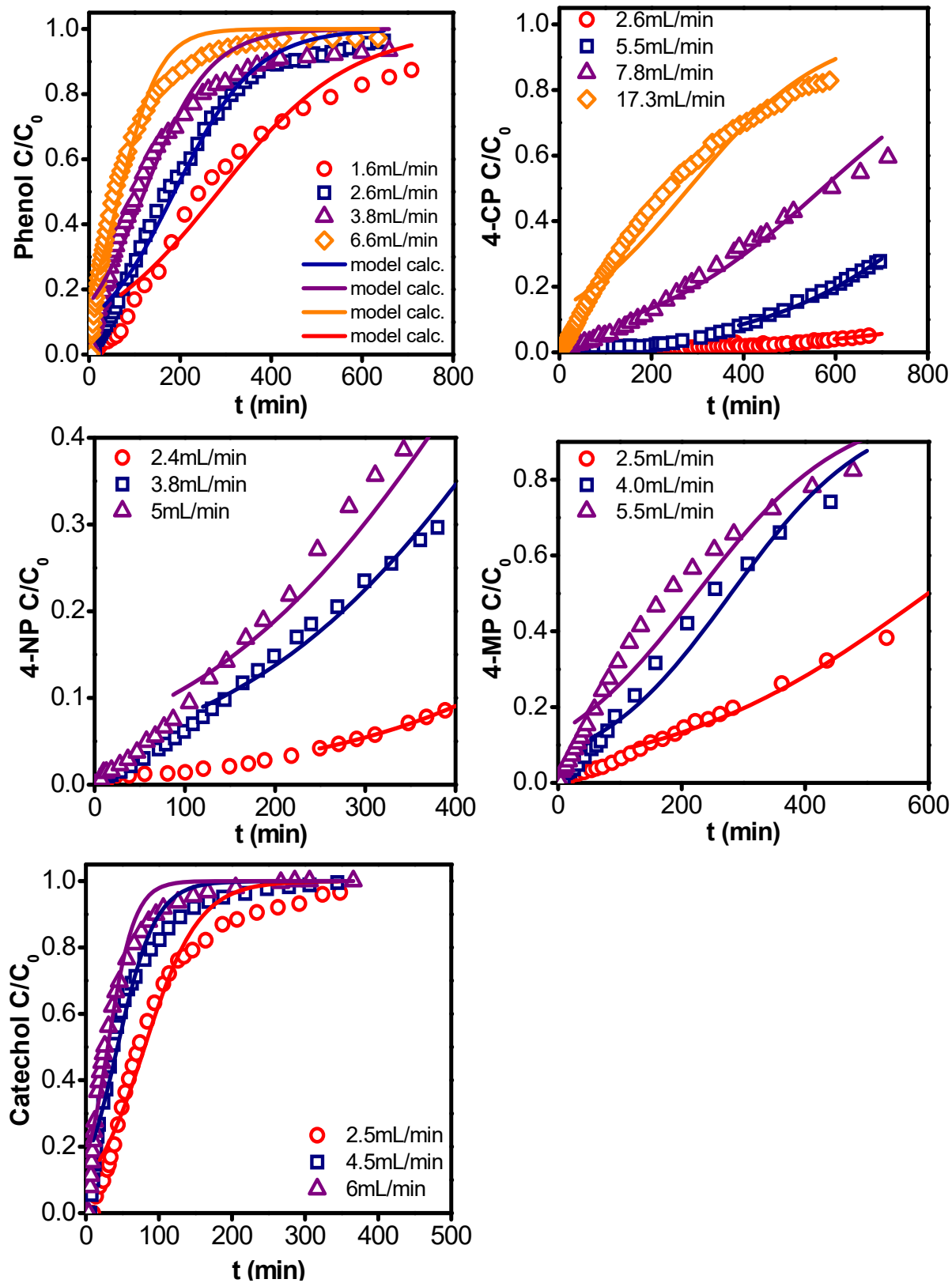
Figure 7.9(b) Comparison of experimental data and predications based on the Yoon-Nelson model for sorption of phenolic compounds in PEBA columns at different flow rates

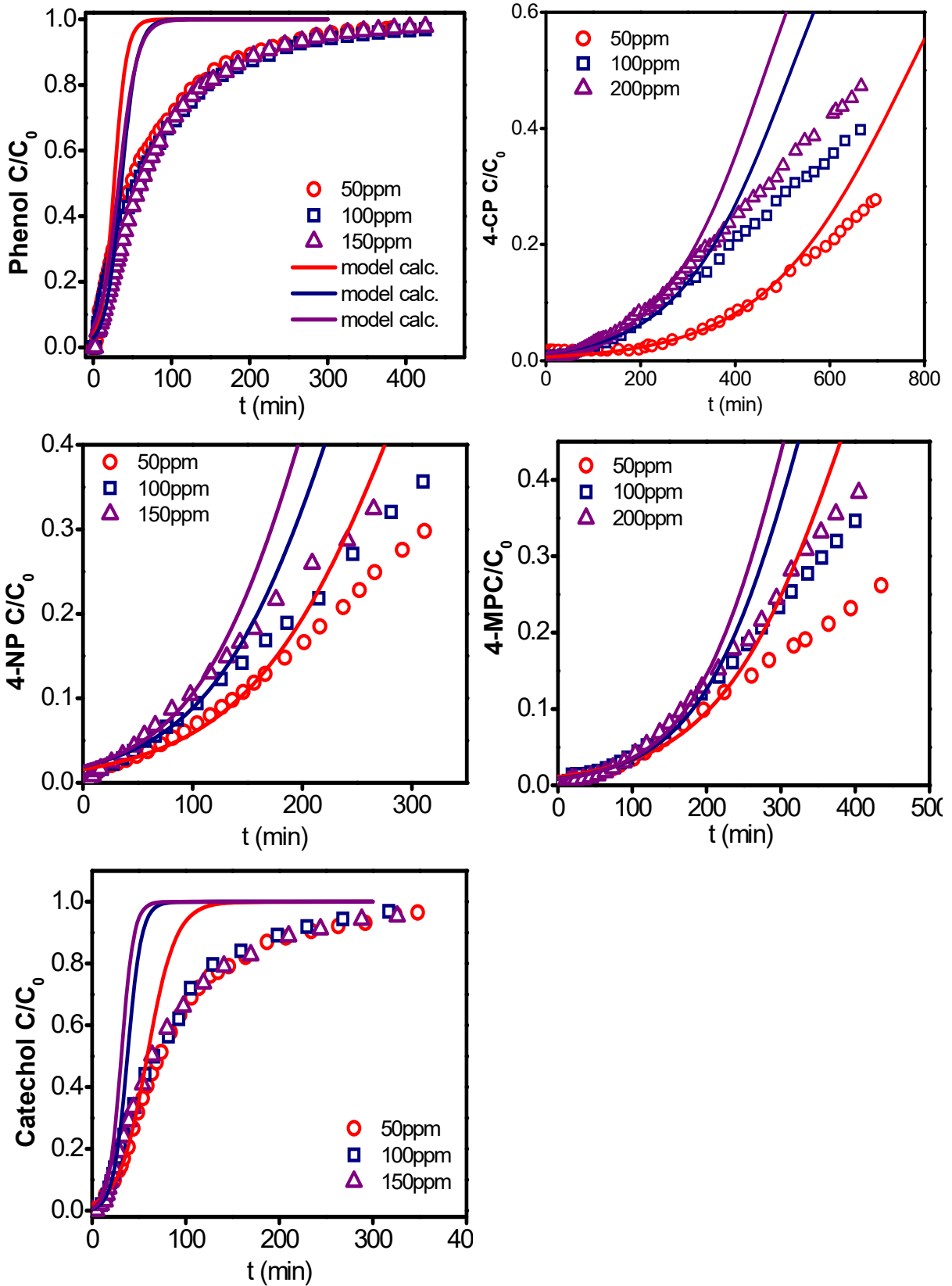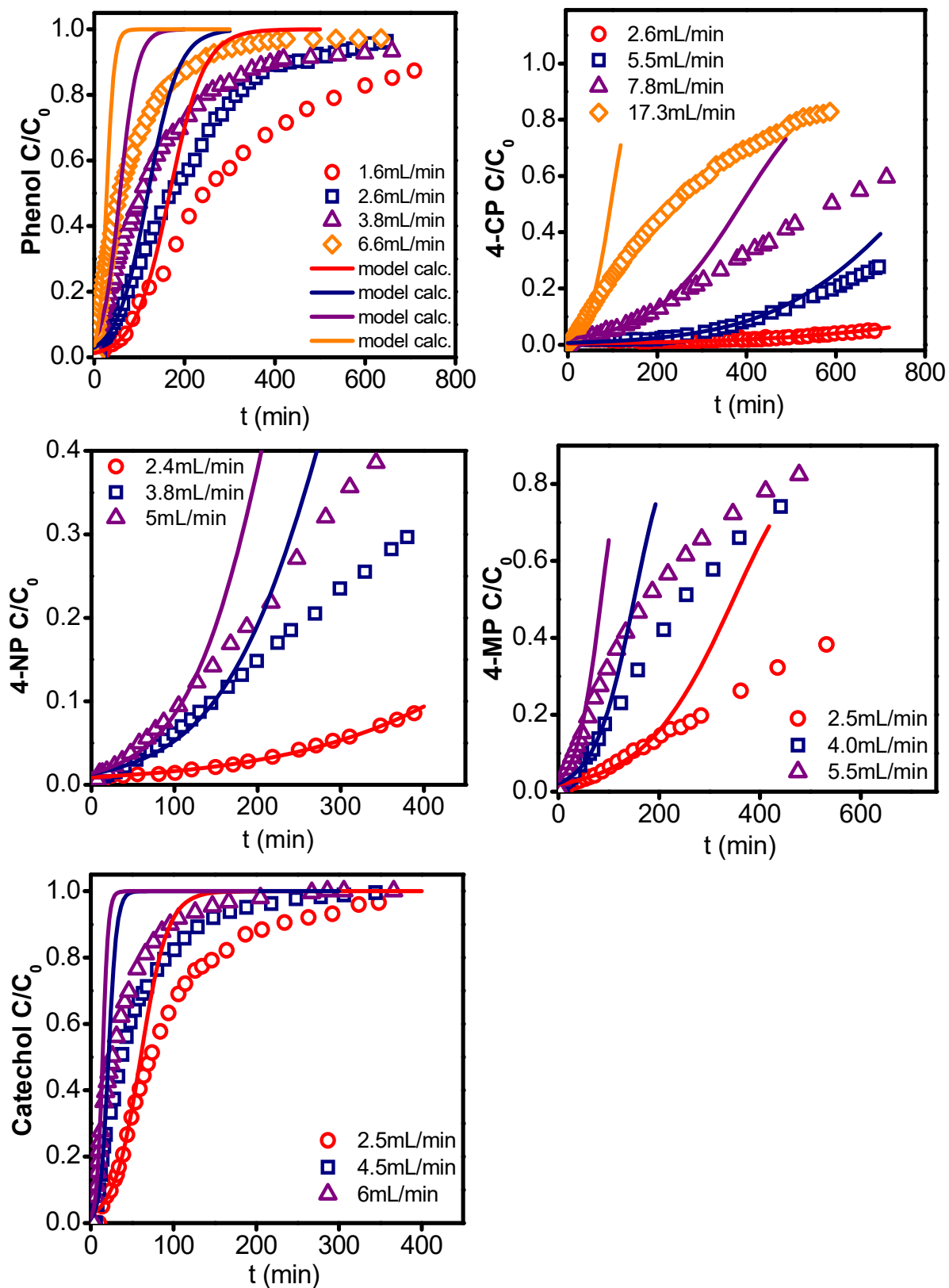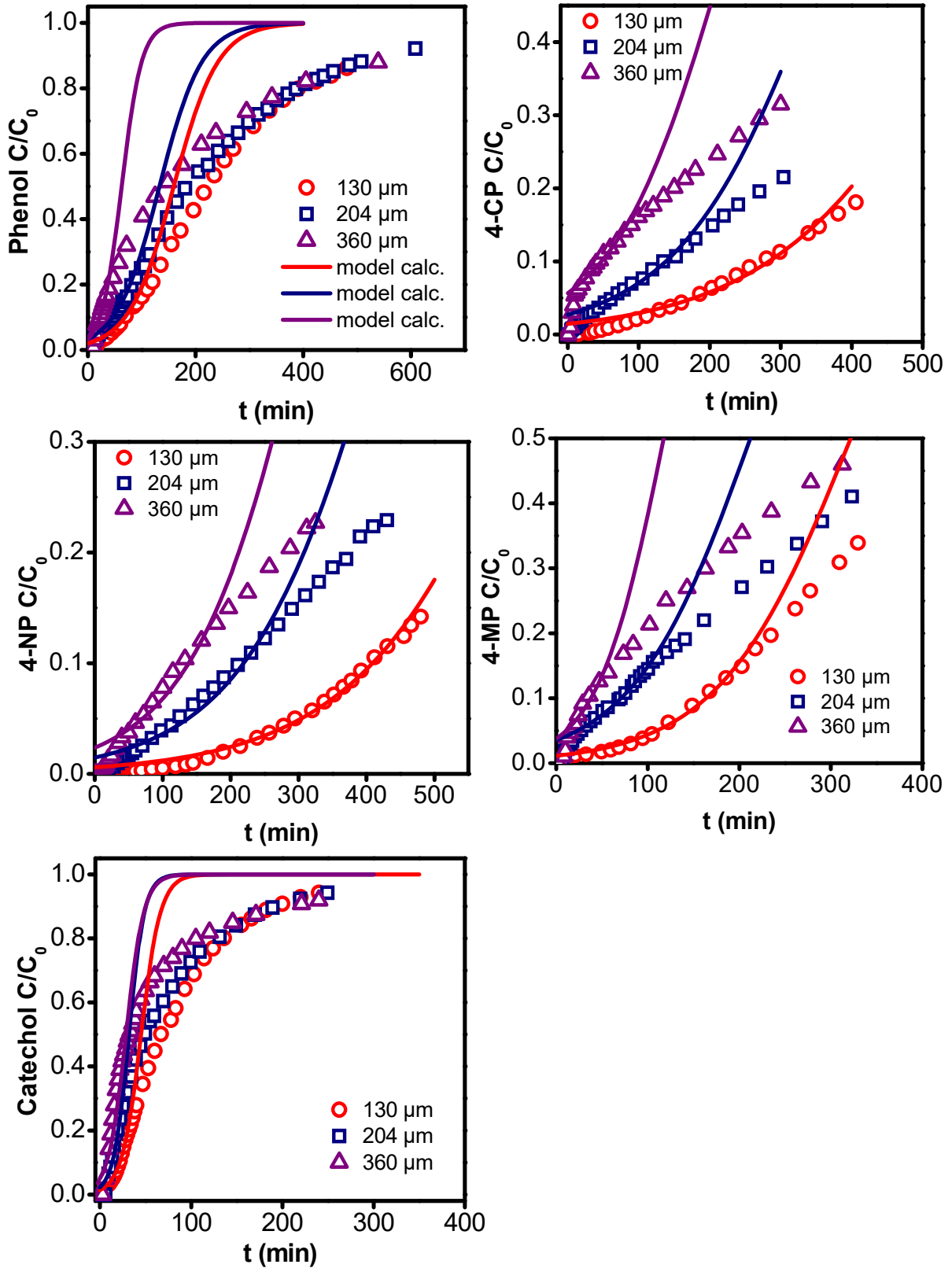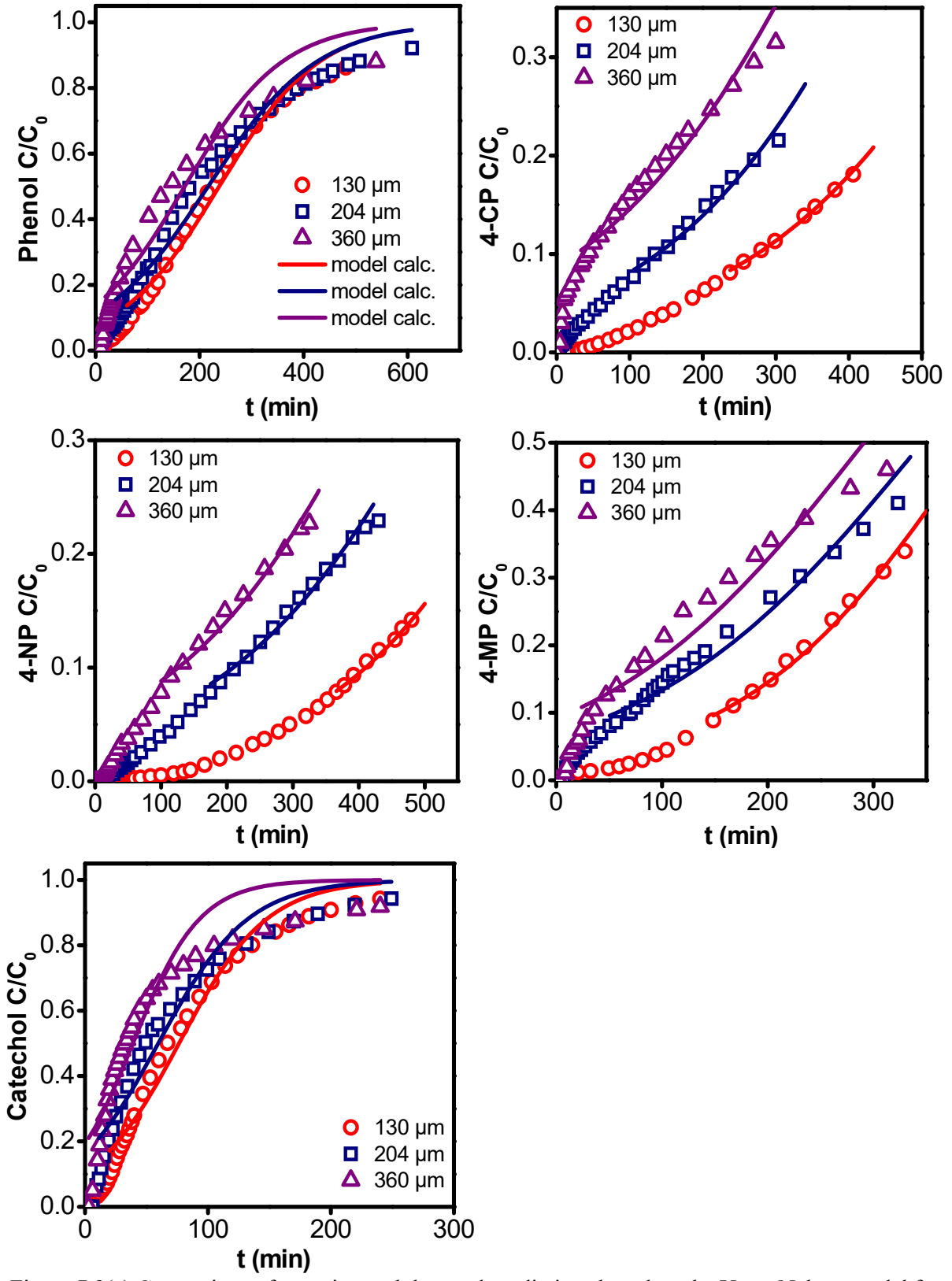Figure 7.9(c) Comparison of experimental data and predictions based on the Yoon-Nelson model for sorption of phenolic compounds in PEBA columns at different fibre diameters

Table 7.2(a) Model parameters for sorption of phenolic compounds in packed PEBA columns at different inlet concentrations

	C ppm	F mL/min	D μm	$K_{BD} \times 10^3$ L/(mg.min)	N_0 mg/L	R^2	r min^{-1}	A	R^2	τ min	k_{YN} min^{-1}	R^2
				BDST model			**Clark model**			**Yoon-Nelson model**		
Phenol	50			4.2	1.9E+02	0.99	0.019	0.094	0.98	62	0.026	0.96
	100	7.0	229	2.5	3.3E+03	0.99	0.016	0.091	0.98	68	0.021	0.97
	150			1.4	6.2E+02	0.99	0.018	0.11	0.99	71	0.025	0.97
4-CP	50			0.13	9.1E+03	0.99	0.0026	1.7	0.99	8.9E+02	0.0048	0.99
	100	5.5	102	0.085	1.3E+04	0.97	0.0025	0.95	0.99	7.3E+02	0.0043	0.98
	200			0.047	2.3E+04	0.99	0.0029	0.98	0.99	6.5E+02	0.0049	0.98
4-NP	50			0.18	3.9E+03	0.99	0.0042	1.1	0.99	4.0E+02	0.0082	0.99
	100	5.0	102	0.16	5.3E+03	0.97	0.0047	1.1	0.98	3.7E+02	0.0083	0.98
	150			0.12	6.7E+03	0.96	0.0038	0.81	0.98	3.4E+02	0.0086	0.97
4-MP	50			0.22	2.0E+03	0.97	0.0024	0.25	0.99	6.2E+02	0.0051	0.97
	100	2.5	90	0.14	3.5E+03	0.99	0.0036	0.29	0.99	4.8E+02	0.0070	0.96
	200			0.075	6.8E+03	0.98	0.0040	0.31	0.99	4.6E+02	0.0077	0.96
Catechol	50			1.3	2.1E+02	0.99	0.020	0.56	0.98	80	0.027	0.96
	100	2.5	90	1.3	4.0E+02	0.97	0.020	0.52	0.98	76	0.026	0.96
	150			1.0	5.7E+02	0.97	0.023	0.61	0.97	76	0.027	0.96

Table 7.2(b) Model parameters for sorption of phenolic compounds in packed PEBA columns at different flow rates

	C	F	D	BDST model			Clark model			Yoon-Nelson model		
				$k_{BD} \times 10^3$	N_0	R^2	r	A	R^2	τ	k_{YN}	R^2
	ppm	mL/min	µm	L/(mg.min)	mg/L		min^{-1}			min	min^{-1}	
Phenol	100	1.6	190	0.52	5.7E+02	0.99	0.0058	0.16	0.98	2.9E+02	0.0069	0.95
		2.6		0.59	7.3E+02	0.99	0.0082	0.14	0.99	1.9E+02	0.011	0.99
		3.8		1.0	4.6E+02	0.97	0.010	0.099	0.98	1.2E+02	0.014	0.96
		6.6		2.4	3.9E+02	0.99	0.016	0.091	0.98	68	0.022	0.97
4-CP	50	2.6	102	0.076	8.8E+03	0.98	0.0010	2.1	0.96	1.5E+03	0.0034	0.97
		5.5		0.13	9.1E+03	0.99	0.0026	1.7	0.99	8.9E+02	0.0048	0.99
		7.8		0.20	6.6E+03	0.99	0.0031	0.83	0.99	5.7E+02	0.005	0.97
		17.3		0.81	3.6E+03	0.95	0.0051	0.51	0.99	2.8E+02	0.0067	0.94
4-NP	100	2.4	102	0.061	7.0E+03	0.99	0.0021	1.6	0.99	8.2E+02	0.0055	0.99
		3.8		0.15	4.3E+03	0.95	0.0029	0.94	0.99	5.1E+02	0.006	0.97
		5.5		0.19	4.6E+03	0.96	0.0040	0.93	0.99	4.4E+02	0.0062	0.95
4-MP	50	2.5	102	0.23	1.6E+03	0.98	0.0025	0.23	0.99	6.0E+02	0.0047	0.97
		4.0		0.51	1.1E+03	0.98	0.0059	0.22	0.99	2.8E+02	0.0089	0.96
		5.5		0.84	8.8E+02	0.97	0.0065	0.16	0.97	2.2E+02	0.0084	0.91
Catechol	50	2.5	127	1.2	2.3E+02	0.99	0.020	0.56	0.98	80	0.027	0.96
		4.5		4.0	1.8E+02	0.97	0.030	0.40	0.98	43	0.038	0.97
		6		5.8	1.6E+03	0.98	0.040	0.36	0.98	30	0.055	0.97

Table 7.2(c) Model parameters for sorption of phenolic compounds in packed PEBA columns at different fibre sizes

	C ppm	F mL/min	D μm	$K_{BD} \times 10^3$ L/(mg.min)	N_0 mg/L	R^2	r min^{-1}	A	R^2	τ min	k_{YN} min^{-1}	R^2
				BDST model			Clark model			Yoon-Nelson model		
Phenol	100	2.5	130	0.46	9.7E+02	0.98	0.0074	0.17	0.99	2.4E+02	0.010	0.98
			204	0.48	7.8E+02	0.99	0.0069	0.13	0.99	2.2E+02	0.0095	0.97
			360	1.0	3.9E+02	0.99	0.0074	0.11	0.97	1.7E+02	0.011	0.94
4-CP	100	5.5	130	0.071	1.2E+04	0.99	0.0033	1.2	0.96	6.8E+02	0.0054	0.99
			204	0.10	8.2E+03	0.95	0.0033	0.87	0.99	5.0E+02	0.006	0.98
			360	0.13	4.9E+03	0.96	0.0036	0.66	0.99	4.1E+02	0.0058	0.95
4-NP	60	2.5	130	0.11	5.0E+03	0.99	0.0030	2.2	0.99	8.0E+02	0.0057	0.99
			204	0.15	3.2E+03	0.96	0.0026	1.1	0.99	6.5E+02	0.005	0.98
			360	0.18	2.3E+03	0.96	0.0034	1.0	0.99	5.4E+02	0.0053	0.98
4-MP	50	3.0	130	0.27	2.0E+03	0.99	0.0046	0.34	0.99	4.0E+02	0.0091	0.99
			204	0.31	1.3E+03	0.99	0.0039	0.20	0.99	3.5E+02	0.0076	0.96
			360	0.54	7.0E+03	0.92	0.0040	0.17	0.97	2.9E+02	0.0079	0.94
Catechol	50	2.5	130	1.9	2.2E+02	0.99	0.021	0.54	0.99	76	0.028	0.97
			204	2.7	1.4E+02	0.97	0.022	0.39	0.97	60	0.027	0.95
			360	2.7	1.1E+02	0.99	0.024	0.28	0.92	39	0.037	0.90

7.3.5 Flow-interruption test

The results of flow-interruption tests for sorption of phenol, 4-CP, 4-NP, 4-MP and catechol in PEBA were shown in Figures 7.10(a)-(e). For the sorption of phenol, 4-MP and catechol, there is a significant dip in the breakthrough curve. This proves that the sorption of phenol, 4-MP and catechol in PEBA 2533 is a rate-limited rather than an instantaneous process. When the flow was stopped, sorption continued to proceed in the fibre, resulting in a decreased solute concentration in the liquid phase. Therefore, when the flow was resumed, the concentration of the effluent was lower than the effluent concentration prior to the flow interruption. Garcia-Mendieta et al. [226] also performed the flow-interruption test on sorption of phenol and 4-CP on activated carbon packed in a column, and a similar drop in the effluent concentration was observed. They concluded that mass diffusion within the activated carbon was the rate-determining step of the system. Similar results were reported by Solache-Rios et al. [227] in column sorption of phenol and 4-chlorophenol on a Mexican tuff.

For the sorption of 4-CP, six flow-interruptions were conducted at different stages of the sorption process. As shown in Figure 7.10(b), no significant concentration decrease due to flow interruption was observed during the first three interruptions, and the concentration drop was observed for the last three interruptions. Similar trends were observed in Figure 7.10(c) for the sorption of 4-NP: the effluent concentration of 4-NP even went up after the first interruption, but a concentration decrease was obtained for the second and third interruption test.

Besides the diffusion within the fibre, longitudinal diffusion along the column also affects the effluent concentration exiting the column after the interruption. When the flow

interruption test was conducted in the early range of the sorption where effluent concentration was low (e.g., the first three interruptions of 4-CP), the longitudinal diffusion of phenols along the column was significant. During the flow interruption period, molecular diffusion would redistribute phenols from the bottom of the column toward the top of the column, and thus increased the concentration of effluent exiting the packed column after the flow interruption. In this case, even sorption of phenols continued in the fibre bed during this period, the decrease in the solute concentration due to continued sorption were compensated by an increase in the solute concentration resulting from the longitudinal diffusion. Thus the magnitude of concentration drop obtained at low effluent concentration was not easily discerned from the experimental data. However, flow interruption at a higher effluent concentration would result in a lower concentration gradient along the column and weaken the effect of longitudinal diffusion. In this case, the effect of longitudinal diffusion along the column could not counter balance the continued sorption in the fibre during the interruption period, and a significant concentration drop was observed after the feed flow resumed.

Zogorski et al. [228] performed flow interruption test for column sorption of 2,4-dichlorophenol on granular activated carbon, and a marked increase in 2,4-dicholorophenol removal was observed for interruption tests conducted at a higher concentration, but there was no significant change in the breakthrough curve for interruption test conducted at a lower concentration, which was in agreement with the results of our study. Brusseau et al. [229] studied solute redistribution resulting from the longitudinal diffusion and it was shown that the effluent concentration could increase by 17% due to the longitudinal diffusion.
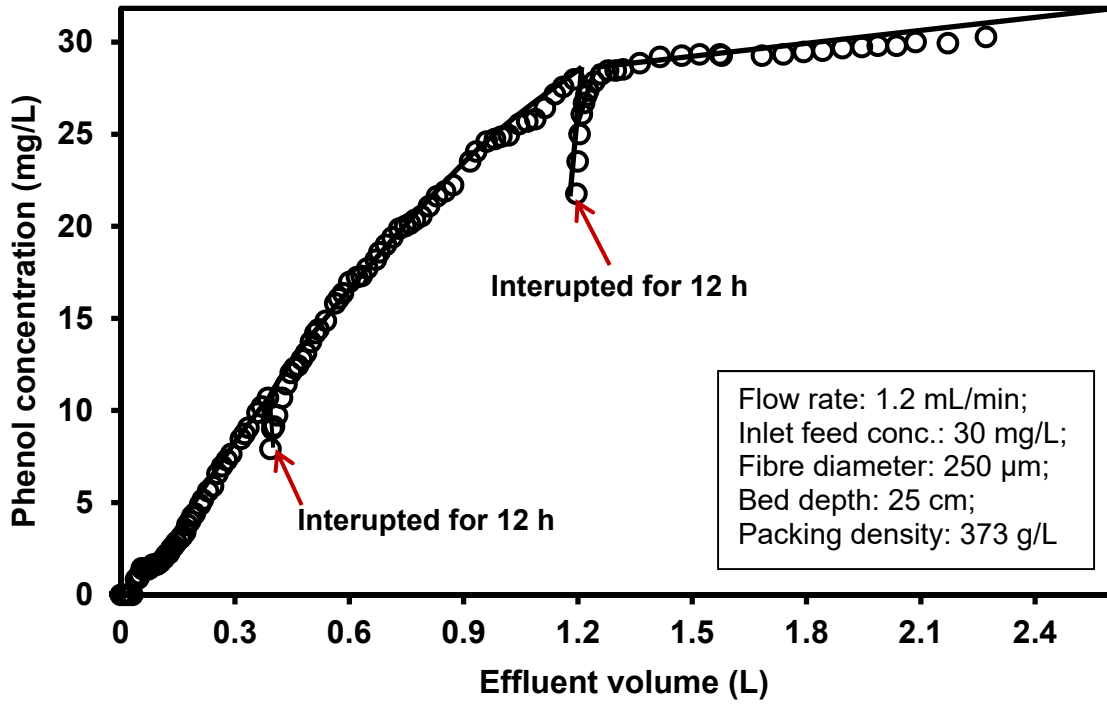
Figure 7.10(a) Flow-interruption tests of phenol sorption in the packed PEBA bed
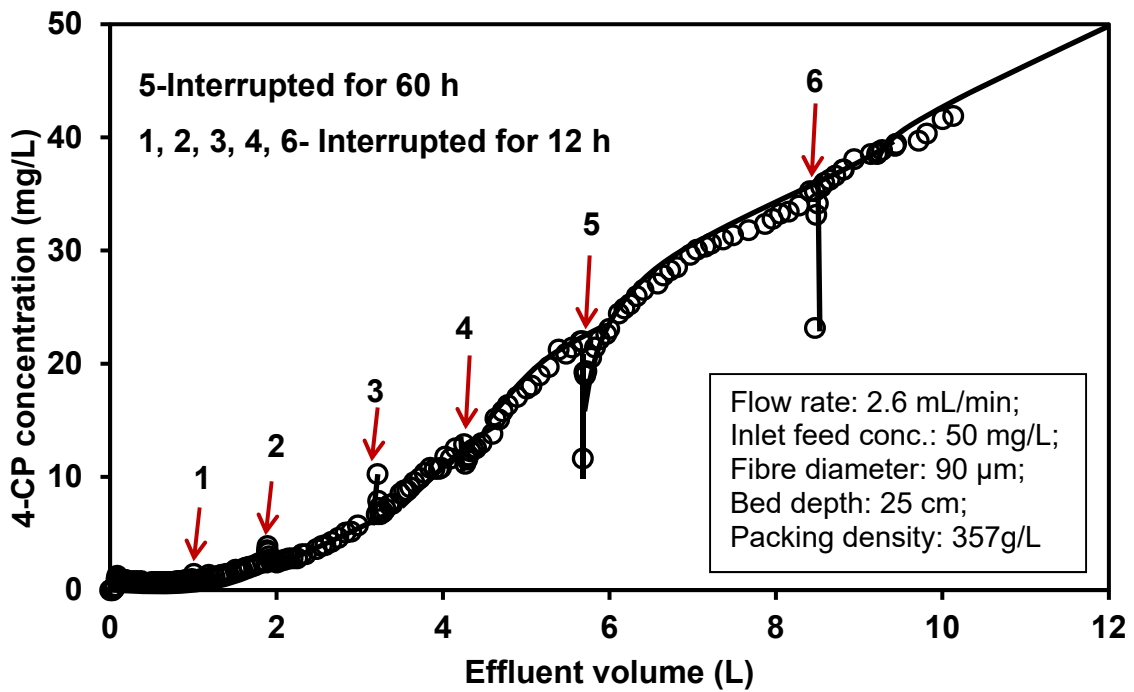
Figure 7.10(b) Flow-interruption tests of 4-CP sorption in the packed PEBA bed
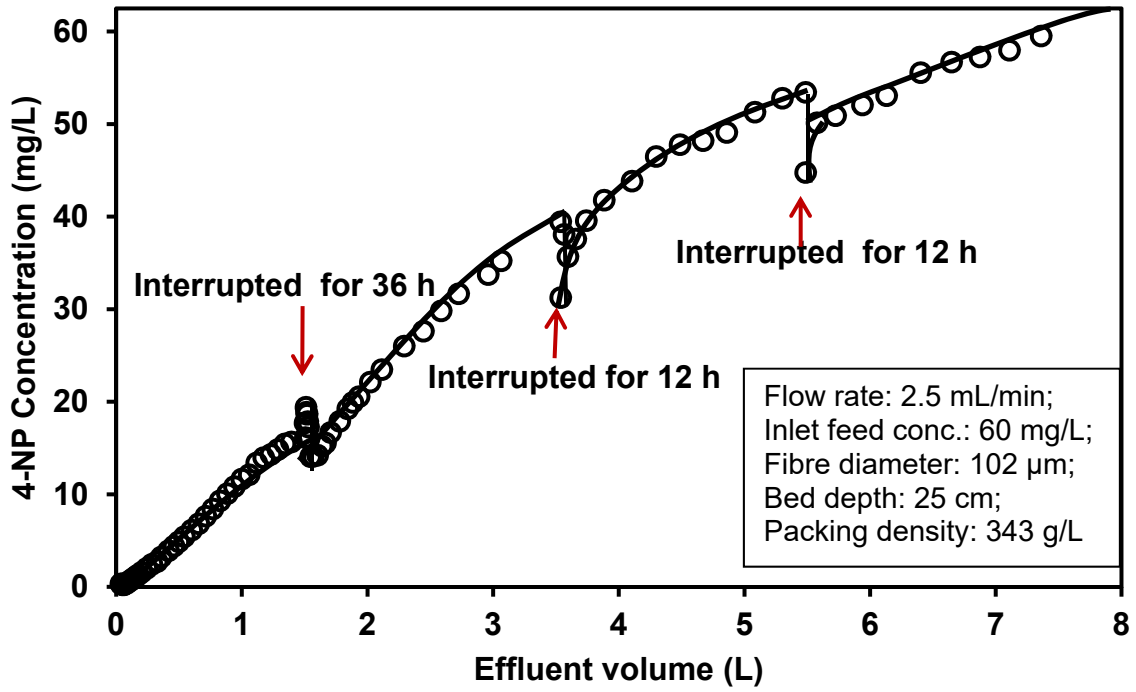
Figure 7.10(c) Flow-interruption tests of 4-NP sorption in the packed PEBA bed
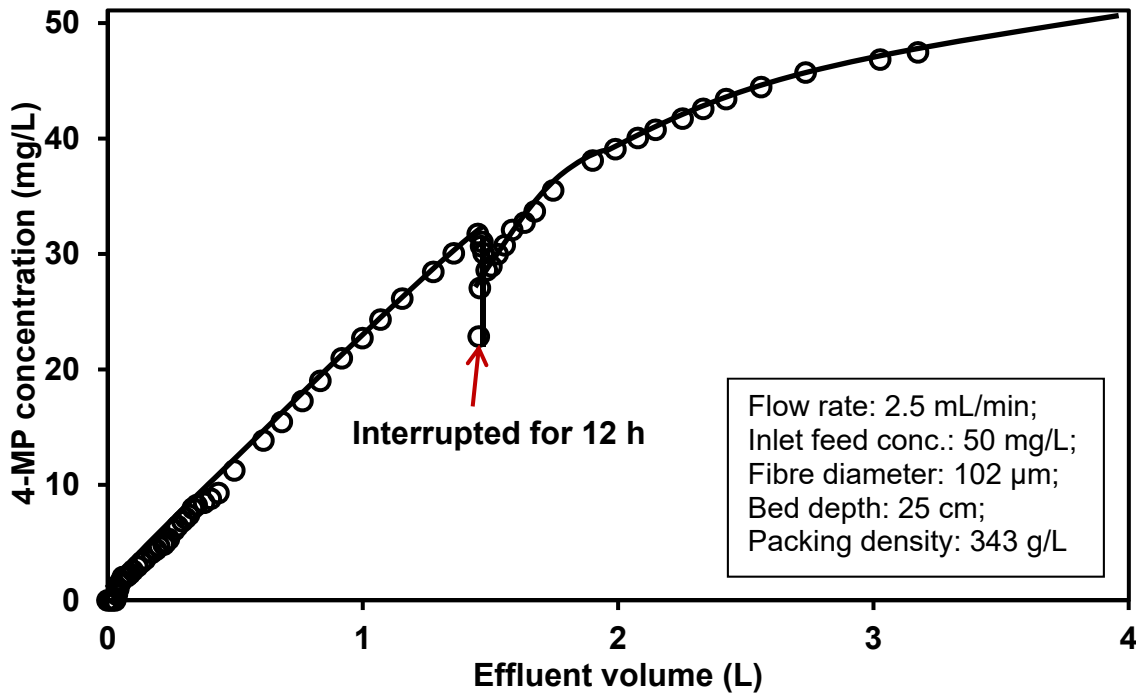
Figure 7.10(d) Flow-interruption tests of 4-MP sorption in the packed PEBA bed
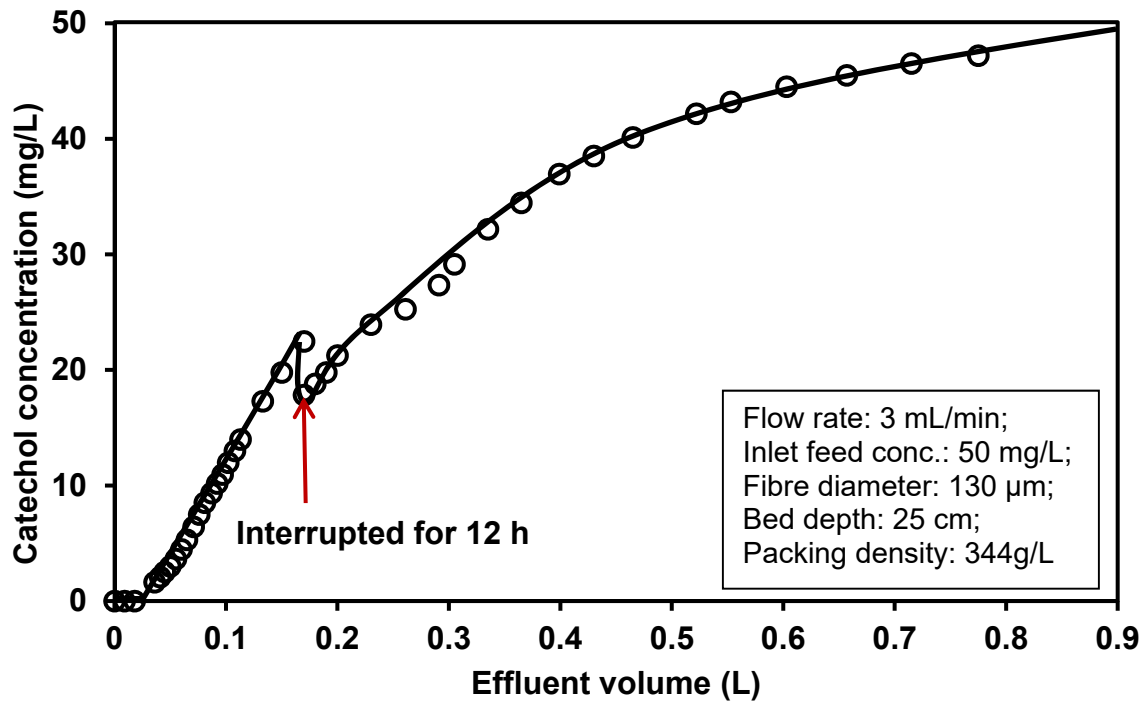
Figure 7.10(e) Flow-interruption test of sorption of catechol in the packed PEBA bed

Since sorption processes in Figures 7.10(a)-(e) were not terminated until the effluent concentration was close to the inlet feed concentration, the equilibrium sorption capacity of phenolic compounds in the packed PEBA column can be calculated by:

$$Q_e = \frac{\int_{V=0}^{V=V_{total}}(C_0 - C)dV}{M} \tag{7.5}$$

where C_0 is the inlet phenol concentration (mmol/L), C is the outlet solute concentration (mmol/L), V is the volume of the effluent (L), V_{total} is the total volume of the effluent at the end of the experiment (L), M is the mass of PEBA fibres packed in the column (g), q_{eq} is the equilibrium sorption capacity of phenolic compounds in the packed PEBA column. The integration terms in Eq. (7.5) can be determined by a gravimetrical method. For example, 7.10(a) was divided into the area above the breakthrough curve (shaded area A) and the area under the breakthrough curve (shaded area B). Area A and B were carefully cut off along the

235

breakthrough curve on a paper as shown in Figure 7.11, and then the ratio of these two shaded areas were determined gravimetrically. Then the integration term was calculated:

$$\int_{V=0}^{V=V_{total}} (C_0 - C)dV = \frac{m_1 C_0 V_{total}}{m_1 + m_2} \tag{7.6}$$

where m_1 is the mass of area A on the paper (g), m_2 is the mass of area B on the paper (g).
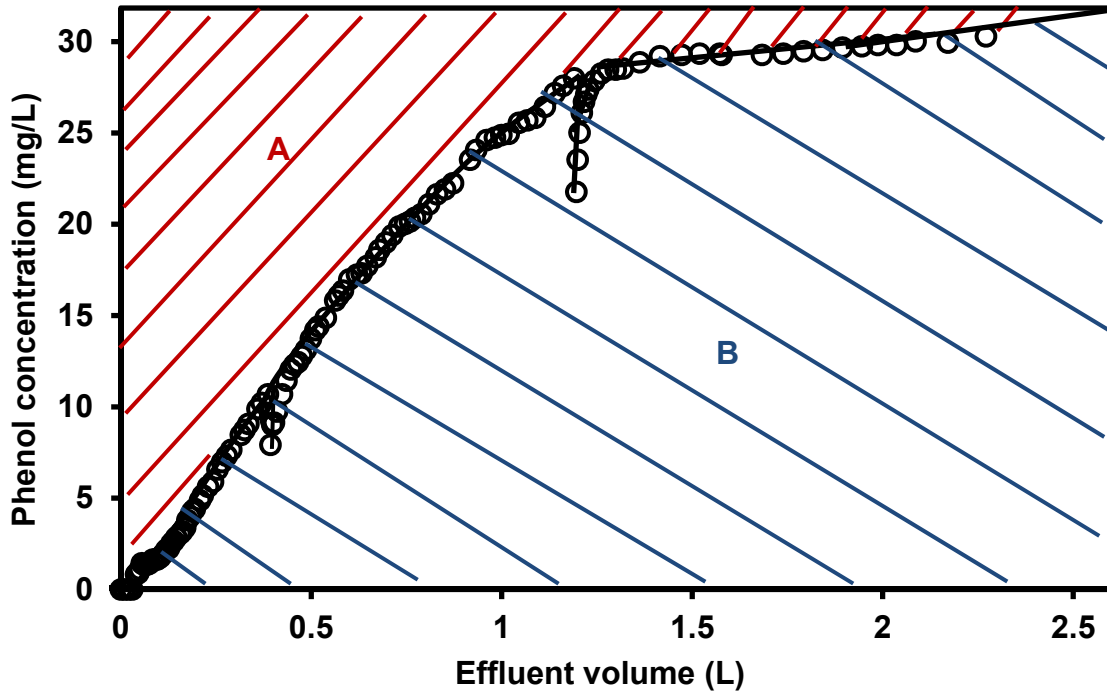
Figure 7.11 Sorption of phenol in the packed PEBA column

The mass of area A in Figure 7.11 on the paper was 0.192 g, the mass of area B on the paper is 0.55 g, the inlet phenol concentration was 31.84 mg/L, the effluent volume was 2.6 L, the molecular mass of phenol is 94.11 g/mol and the mass of PEBA fibres packed in the column was 8.852 g. Therefore, the sorption capacity of phenol in the packed PEBA column was obtained:

$$q_{eq} = \frac{0.192\ g}{0.55\ g + 0.192\ g} \times \frac{31.84\ mg/L \times 2.6\ L}{94.11\ g/mol \times 8.852\ g} = 0.0257\ mmol/g$$

Sorption capacities of other phenolic compounds in the packed PEBA column were calculated in the same way, and they were presented in Table 7.3. For comparison purposes, sorption capacities of phenolic compounds in PEBA (Q_e) at a given equilibrium concentration (i.e., the inlet solute concentration C_0) were calculated from the sorption isotherms obtained in batch operations, and they were also presented in Table 7.3. It is shown that the sorption capacities of phenolic compounds in the packed PEBA column were similar to the sorption capacities of phenolic compounds in PEBA obtained from batch operations.

Table 7.3 Sorption capacity of phenolic compounds in PEBA in packed bed and batch operations

	Phenol	4-CP	4-NP	4-MP	Catechol
q_{eq} (mmol/g) in PEBA calculated from packed bed operations	0.0257	0.288	0.171	0.0773	0.0156
Q_e (mmol/g) in PEBA obtained from batch operations	0.0211	0.254	0.170	0.0770	0.0153

7.3.6 Column regeneration with NaOH

Six continuous sorption-regeneration cycles of an identical packed column were performed to test the regeneration property of PEBA 2533 saturated by phenolic compounds. Breakthrough curves for sorption of phenolic compounds in pristine and regenerated PEBA packed columns are presented in Figure 7.12(a)-(e). It was observed that the breakthrough curve of sorption of phenolic compounds in pristine packed PEBA column was almost identical to that in regenerated PEBA column, indicating that a complete column regeneration of PEBA was achieved by the above mentioned regeneration procedure, (i.e., 600 g 0.15 mol/L NaOH solution followed by 300 g deionized water). The results suggest that PEBA 2533 can be regenerated for repeated use with negligible capacity loss, and this was significant for practical application of the packed-bed sorption system.

One issue to consider with continuous sorption-regeneration operation cycles is the swelling properties of the PEBA sorbent, which will affect the pressure drop of liquid flow in the packed-bed column. PEBA 2533 has been reported to have a water absorption of 1.2 wt.% at 23°C and 24 h in water, a study of Mandal and Bhattacharya [230] also revealed that the sorption of pure water by PEBA 2533 is negligibly small (0.01%) at 60°C. The sorption uptake of water by PEBA 2533 was found to be around 3% at a phenol concentration of 5 w.t%. in an aqueous solution [5]. Therefore, the swelling of the PEBA sorbent during the continuous sorption-regeneration process is insignificant.
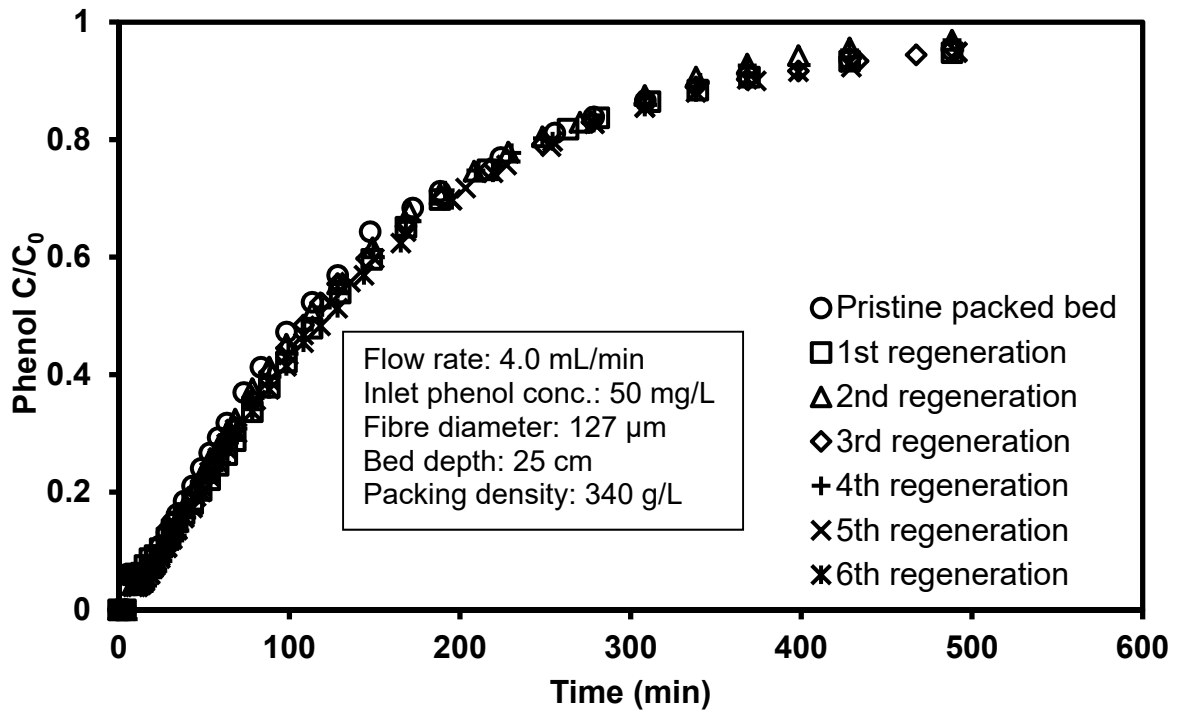
Figure 7.12(a) Sorption of phenol in packed PEBA columns after regeneration with NaOH
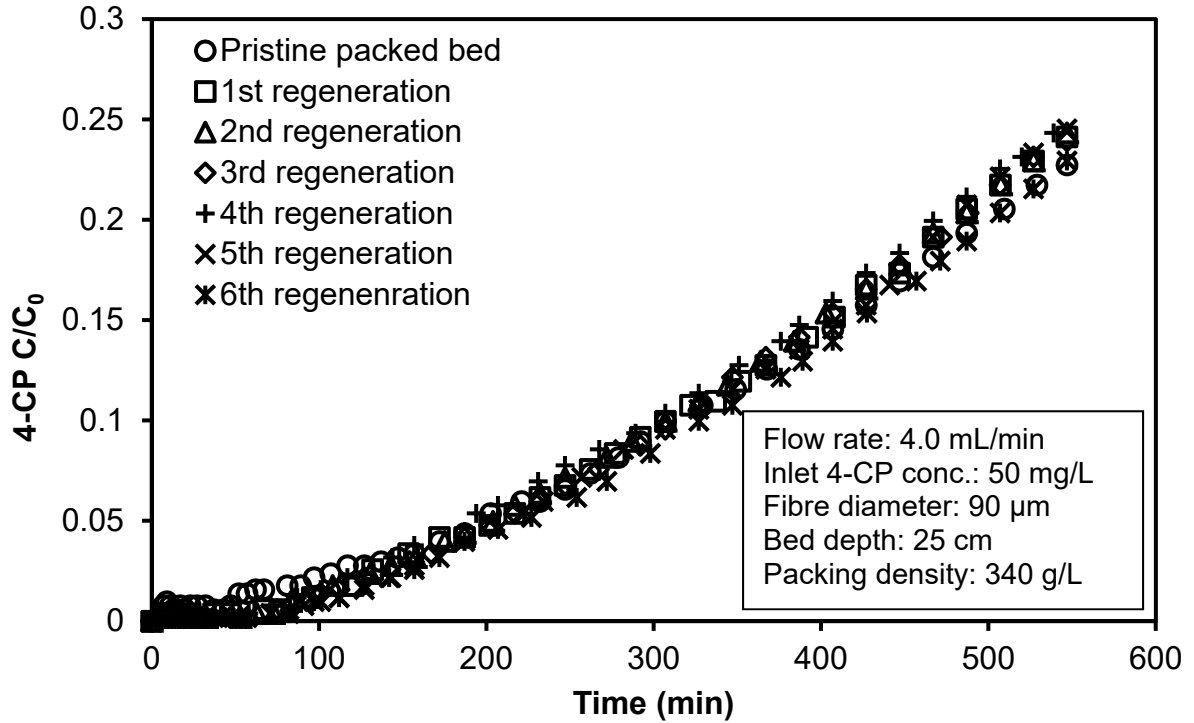
Figure 7.12(b) Sorption of 4-CP in packed PEBA columns after regeneration with NaOH
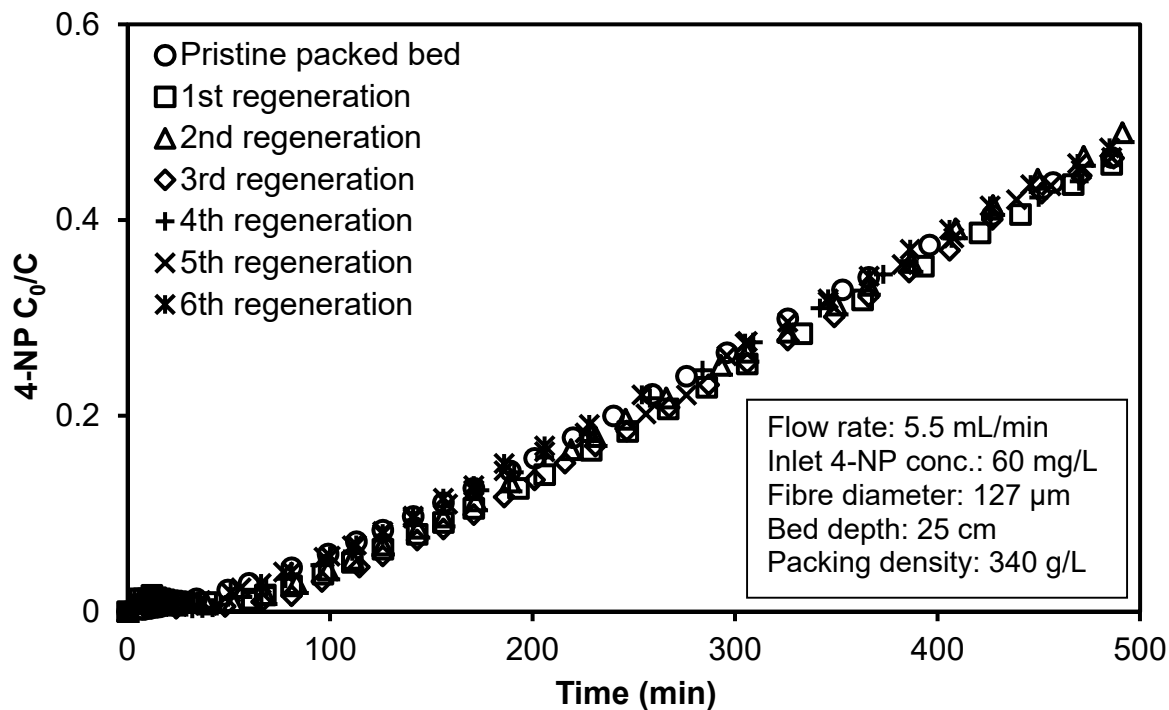
Figure 7.12(c) Sorption of 4-NP in packed PEBA columns after regeneration with NaOH
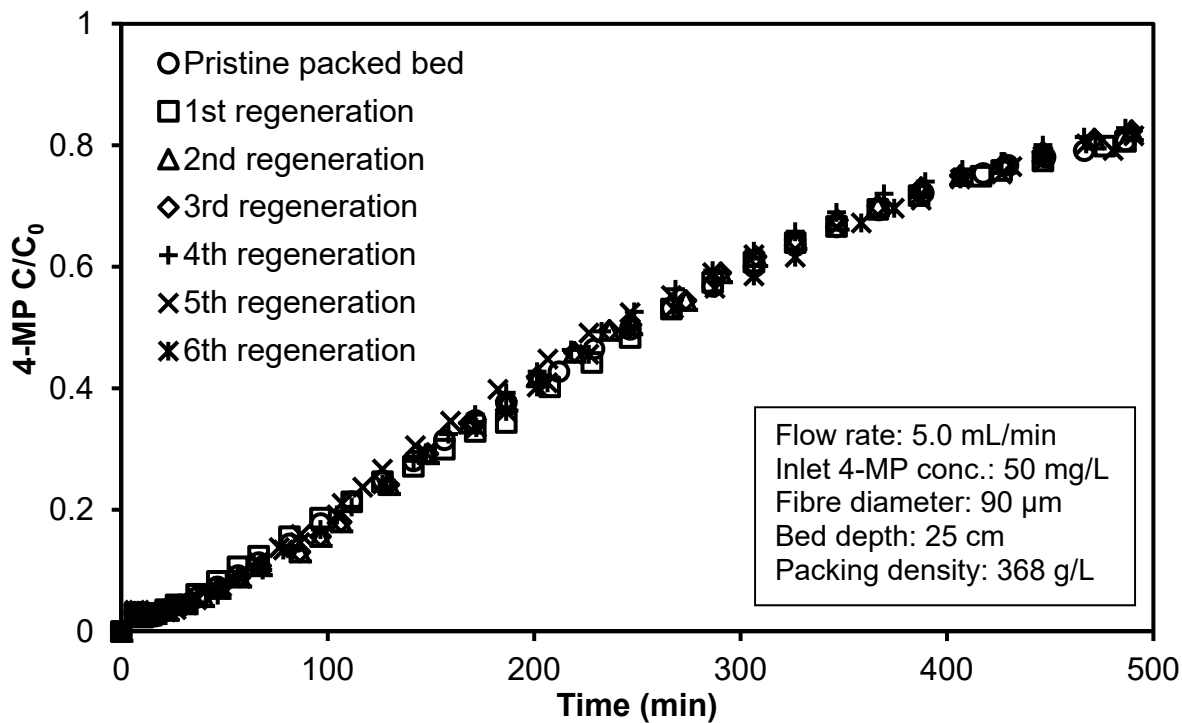
Figure 7.12(d) Sorption of 4-MP in packed PEBA columns after regeneration with NaOH
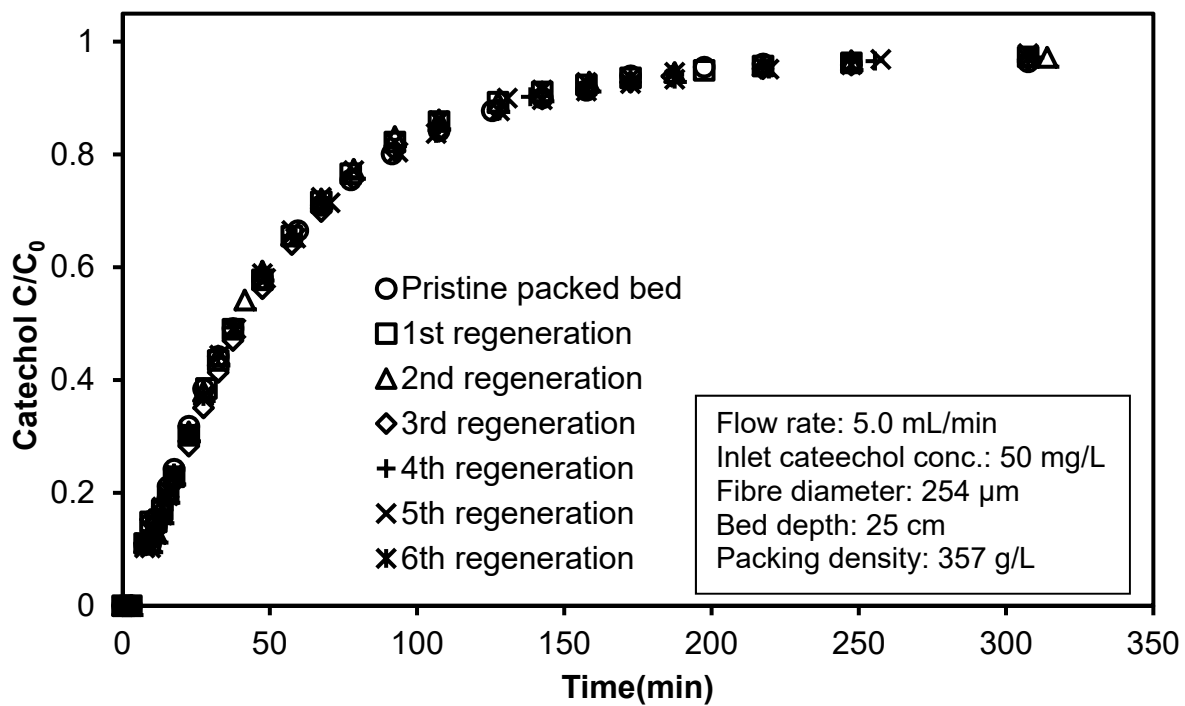
Figure 7.12(e) Sorption of catechol in packed PEBA columns after regeneration with NaOH

Flow rate: 5.0 mL/min
Inlet cateechol conc.: 50 mg/L
Fibre diameter: 254 μm
Bed depth: 25 cm
Packing density: 357 g/L

○ Pristine packed bed
□ 1st regeneration
△ 2nd regeneration
◇ 3rd regeneration
+ 4th regeneration
✕ 5th regeneration
✳ 6th regeneration

7.4 Conclusions

1. The breakthrough time for sorption of phenol, 4-CP, 4-NP, 4-MP and catechol in packed fibre column decreased with an increase in the inlet solute concentration, feed flow rate and fibre diameter.

2. In the region of ($C/C_0<0.15$), the sorption of phenol, 4-CP, 4-NP, 4-MP and catechol in the packed fibre column could be described by the BDST model; in the region of ($0.08<C/C_0<0.99$), the Clark model seemed to fit the experimental data better than the Yoon-Nelson model.

3. Sorption capacities of phenolic compounds in packed fibre columns were close to that obtained from batch operations.

4. Complete regeneration of the packed fibre column was achieved with NaOH solution. The regenerated column showed essentially the same breakthrough as the fresh column for the sorption of the phenolic compounds from water.

Chapter 8

General conclusions, original contributions, and recommendations

8.1 General conclusions from the original research

The sorption of phenol, 4-chlorophenol, 4-nitrophenol, 4-methylphenol and catechol in the PEBA sorbent was studied using batch operation and packed bed column operation. The sorption isotherms and kinetics were investigated for feed solutions with single solute and multi-solutes. The regeneration of the exhausted PEBA sorbent was also studied. PEBA was shown to be a promising sorbent for removal of phenolic compounds from wastewater. The general conclusions drawn from this study are as follows:

8.1.1 Batch sorption of phenols in PEBA for single-solute systems

(1) The sorption capacity of phenol, 4-chlorophenol, 4-nitrophenol, 4-methylphenol and catechol in PEBA was in the order of: 4-chlorophenol>4-nitrophenol>4-methylphenol>phenol>catechol. The sorption capacity of phenolic compounds in PEBA was affected by their solubility in the solution and their substituent group.

(2) The uptake of phenolic compounds in PEBA 2533 was a sorption process into the bulk of the sorbent, rather than surface-based adsorption. The sorption occurred at the surface of PEBA, followed by diffusion of the sorbed molecules into the bulk of the sorbent.

(3) The widely used data treatment for the pseudo-second order model was revisited and an oversight in considering constant Q_e during the batch sorption was corrected.

243

8.1.2 Sorption of multi phenolic solutes in PEBA

(1) The presence of strongly sorbed solutes tended to reduce the sorption capacity of the weakly sorbed solute in most binary solute systems. The competitive Freundlich model was suitable to represent the sorption isotherm of a phenolic solute by PEBA in binary solute systems.

(2) The sorption competition in the quinary solute system was more significant than that in binary solute systems. The effects of sorption competition on the uptake capacity depended on the molecular size of the solute, its affinity to the sorbent, and the concentration of the solute in the feed solution.

(3) Although sorption competition was observed in some multi-solute systems, the overall sorption capacity and sorption rate were greater than the sorption capacity and sorption rate of individual solute in single-solute solutions.

8.1.3 Regeneration of the PEBA sorbent

(1) The PEBA sorbent exhausted with phenolic compounds could be regenerated by using NaOH solution, methanol and ethanol.

(2) Thermal regeneration at a relatively low temperature ($\leq 120°C$) could be used to regenerate PEBA sorbent exhausted with phenol, 4-chlorophenol and 4-methylphenol. When the PEBA sorbent was exhausted with 4-methylphenol, vacuum assisted thermal regeneration could be used.

(3) The regenerated PEBA sorbent exhibited the same sorption characteristics as pristine PEBA sorbent.

8.1.4 Sorption of phenolic compounds by PEBA in packed bed columns

(1) The PEBA sorbent could be immobilized in a packed bed operation in the form of fibre bundles.

(2) The breakthrough characteristics of sorption of phenolic compounds in the packed column were affected by the inlet solute concentration, feed flow rate and fibre diameter.

(3) The sorption of phenolic compounds in the packed PEBA bed column can be described by the BDST model at a low concentration range, and the Clark model could describe the sorption at a broader concentration range.

8.2 Contributions to the original research

(1) The mechanism of sorption of phenolic compounds in the PEBA sorbent was revealed by a proper experimental design. The sorption of phenolic compounds occurred at the surface of the PEBA sorbent, followed by diffusion of solute molecules into the sorbent bulk. The Freundlich model was suitable to represent the sorption isotherms of phenolic compounds by PEBA in single-solute systems. The sorption isotherms of a phenolic compound by PEBA in binary-solute systems could be described by the competitive Freundlich model.

(2) The sorption kinetics of phenolic compounds in PEBA could be described by the pseudo-second order model and the internal diffusion model mathematically, but the sorption rate was not controlled by the surface reaction or the internal diffusion alone. An oversight in data fitting with the pseudo-second order model was corrected and validated with experimental data.

(3) The PEBA sorbent was immobilized in the form of fine fibres to reduce the internal mass transfer resistance in the PEBA sorbent for the packed bed operations. The sorption of phenolic compounds in the packed fibre column can be represented by the BDST model and the Clark model at a certain concentration range.

(4) Regeneration of the PEBA sorbent exhausted with phenolic compounds was achieved by using different methods. The regenerated PEBA sorbent exhibited the same sorption characteristics as the pristine sorbent.

8.3 Recommendations for the future work

(1) The currently available sorption kinetics models are generally developed based on only one rate-controlling step (surface reaction or diffusion). However, the sorption kinetics results in this thesis show that the sorption of phenolic compounds in PEBA is neither solely controlled by the surface reaction, nor solely controlled by the internal diffusion. An integrated model which incorporates the effects of both the surface reaction and internal diffusion may be developed in the future.

(2) In the equilibrium sorption study of the quinary solute system, neither the competitive Freundlich model nor the IAST model could provide a good prediction of sorption uptake. The deviation in the competitive Freundlich model prediction was due to the fact that the competition coefficients in binary solute systems are different from those in quinary solute systems, while the non-ideality of the sorbent phase causes the IAST model to deviate from the experimental data. Therefore, it will be of interest to modify the existing models or develop new models to analyze the sorption isotherm data in multi-solute systems.

(3) A pervaporation-crystallization coupling process has been proposed recently to recover phenol from dilute aqueous solutions [190]. Due to the high melting point of phenol, phenol can be crystallized in the first-stage condenser at− 15⁰C, and the remaining permeate vapour (phenol and water) can be obtained in the second-stage cold trap. The melting points of 4-chlorophenol and 4-methylphenol are 42-45 and 31-37⁰C, respectively. The vacuum-assisted thermal regeneration of PEBA sorbent exhausted with 4-chlorphenol and 4-methylphenol suggests the feasibility of recovering the sorbate in the form of crystals using two stages of cold traps. This may be investigated further.

(4) Few attempts have been made to investigate the competitive sorption of phenolic compounds in the packed bed column operation. Sulaymon and Ahmed [231] developed a mathematical model which includes axial dispersion, film mass transfer, pore diffusion and sorption isotherms to describe the competitive sorption of furfural and phenolic compounds on activated carbon in fixed bed columns. The competitive sorption of phenolic compounds in the packed PEBA columns can be investigated in the future, the competitive sorption on the sorption breakthrough can be studied, and new mathematical models can be developed to describe the sorption breakthrough of phenolic compounds in the fixed bed column for multi-solute systems.

(5) For the regeneration of PEBA sorbent with NaOH, ethanol and methanol, desorption kinetics of phenolic compounds may be examined to elucidate the desorption mechanism and to quantify the desorption rate of phenolic compounds from the PEBA sorbent. Proper models (e.g. the first-order kinetic model or the pore diffusion model) can be used to represent the kinetic desorption data of phenolic compounds [232]. In addition, in order to optimize the operating conditions of chemical regeneration of the PEBA sorbent,

the effects of desorption time, desorption temperature, the concentration of NaOH solution, and the amount of eluting reagents (i.e., NaOH solution, ethanol or methanol) on desorption efficiency can be evaluated.

(6) The PEBA 2533 sorbent may be further modified to improve the sorptive performance. For instance, introducing micro porosity to the sorbent can be used to improve the sorption rate. It has been reported that a variety of microporous structures were achievable for some commercially available polymers through thermally-induced solid-liquid phase separation [233] . In addition, selective sorption is of particular interest in industrial application, incorporating proper functional groups into PEBA sorbent may be used to improve the sorption selectivity of the sorbent over a particular solute component.

(7) Two packed bed columns are recommended to be used in continuous sorption-regeneration processes: one for sorption and the other one for regeneration. Other components present in industrial wastewater such as microorganisms and heavy metals may also affect the sorption process, thus the biodegradability of the PEBA sorbent and the sorption of heavy metals in the PEBA sorbent may be examined in the future.

References

[1]   S. Mohammadi, A. Kargari, H. Sanaeepur, K. Abbassian, A. Najafi, and E. Mofarrah, *Phenol removal from industrial wastewaters: a short review.* Desalination and Water Treatment, 2014. 53(8):1-20.

[2]   N. Hosseinzadeh, A. Kargari, M. Soleimani, K. Abbassian, and M. Fallahi. *Evaluation of 4-chlorophenol extraction from aqueous solution by kerosene.* in *The Seventh International Chemical Engineering Congress and Exhibition, Kish Island, Iran.* 2011.

[3]   H. Amiri, N. Jaafarzadeh, M. Ahmadi, and S.S. Martínez, *Application of LECA modified with Fenton in arsenite and arsenate removal as an adsorbent.* Desalination, 2011. **272**(1):212-217.

[4]   M. Tobajas, V.M. Monsalvo, A.F. Mohedano, and J.J. Rodriguez, *Enhancement of cometabolic biodegradation of 4-chlorophenol induced with phenol and glucose as carbon sources by Comamonas testosteroni.* Journal of environmental management, 2012. **95**:S116-S121.

[5]   X. Hao, M. Pritzker, and X. Feng, *Use of pervaporation for the separation of phenol from dilute aqueous solutions.* Journal of Membrane Science, 2009. **335**(1):96-102.

[6]   W. Kujawski, A. Warszawski, W. Ratajczak, T. Porebski, W. Capała, and I. Ostrowska, *Application of pervaporation and adsorption to the phenol removal from wastewater.* Separation and Purification Technology, 2004. **40**(2):123-132.

[7]   W. Kujawski, A. Warszawski, W. Ratajczak, T. Porebski, W. Capała, and I. Ostrowska, *Removal of phenol from wastewater by different separation techniques.* Desalination, 2004. **163**(1):287-296.

[8]   K.A.G. Gusmão, L.V.A. Gurgel, T.M.S. Melo, and L.F. Gil, *Adsorption studies of methylene blue and gentian violet on sugarcane bagasse modified with EDTA dianhydride (EDTAD) in aqueous solutions: Kinetic and equilibrium aspects.* Journal of environmental management, 2013. **118**:135-143.

[9]   B. Hameed, *Equilibrium and kinetic studies of methyl violet sorption by agricultural waste.* Journal of Hazardous Materials, 2008. **154**(1):204-212.

[10]   B.H. Hameed and M.I. El-Khaiary, *Batch removal of malachite green from aqueous solutions by adsorption on oil palm trunk fibre: Equilibrium isotherms and kinetic studies.* Journal of Hazardous Materials, 2008. **154**(1–3):237-244.

[11]   Z. Reddad, C. Gerente, Y. Andres, and P. Le Cloirec, *Adsorption of Several Metal Ions onto a Low-Cost Biosorbent: Kinetic and Equilibrium Studies.* Environmental science & technology, 2002. **36**(9):2067-2073.

[12] C. Tien, *Remarks on adsorption manuscripts received and declined: An editorial.* Separation and Purification Technology, 2007. **54**(3):277-278.

[13] B. Volesky, *Sorption and biosorption*. 2003: BV Sorbex, Inc., Quebec, Canada.

[14] S. Liu, *Cooperative adsorption on solid surfaces.* Journal of Colloid and Interface Science, 2015. **450**:224-238.

[15] V.K. Gupta, S. Srivastava, and R. Tyagi, *Design parameters for the treatment of phenolic wastes by carbon columns (obtained from fertilizer waste material).* Water Research, 2000. **34**(5):1543-1550.

[16] D.O. Cooney, A. Nagerl, and A.L. Hines, *Solvent regeneration of activated carbon.* Water Research, 1983. **17**(4):403-410.

[17] T.M. Grant and C.J. King, *Mechanism of irreversible adsorption of phenolic compounds by activated carbons.* Industrial & Engineering Chemistry Research, 1990. **29**(2):264-271.

[18] C.C. Leng and N.G. Pinto, *An investigation of the mechanisms of chemical regeneration of activated carbon.* Industrial & Engineering Chemistry Research, 1996. **35**(6):2024-2031.

[19] X. Zeng, Y. Fan, G. Wu, C. Wang, and R. Shi, *Enhanced adsorption of phenol from water by a novel polar post-crosslinked polymeric adsorbent.* Journal of Hazardous Materials, 2009. **169**(1):1022-1028.

[20] Y.P. Teoh, M.A. Khan, T.S. Choong, L.C. Abdullah, and S. Hosseini, *Comparative removal of phenols and its chlorinated derivatives by carbon-coated monolith: equilibrium, kinetics and regeneration studies.* Desalination and Water Treatment, 2015. **54**(2):393-404.

[21] B. Pan, W. Du, W. Zhang, X. Zhang, Q. Zhang, B. Pan, L. Lv, Q. Zhang, and J. Chen, *Improved adsorption of 4-nitrophenol onto a novel hyper-cross-linked polymer.* Environmental science & technology, 2007. **41**(14):5057-5062.

[22] B. Özkaya, *Adsorption and desorption of phenol on activated carbon and a comparison of isotherm models.* Journal of Hazardous Materials, 2006. **129**(1):158-163.

[23] R. Berenguer, J. Marco-Lozar, C. Quijada, D. Cazorla-Amorós, and E. Morallón, *Comparison among chemical, thermal, and electrochemical regeneration of phenol-saturated activated carbon†.* Energy & Fuels, 2010. **24**(6):3366-3372.

[24] C. Ania, J. Menéndez, J. Parra, and J. Pis, *Microwave-induced regeneration of activated carbons polluted with phenol. A comparison with conventional thermal regeneration.* Carbon, 2004. **42**(7):1383-1387.

[25]   P. Alvarez, F. Beltran, V. Gomez-Serrano, J. Jaramillo, and E. Rodrıguez, *Comparison between thermal and ozone regenerations of spent activated carbon exhausted with phenol.* Water Research, 2004. **38**(8):2155-2165.

[26]   C. Zidi, R. Tayeb, M.B.S. Ali, and M. Dhahbi, *Liquid–liquid extraction and transport across supported liquid membrane of phenol using tributyl phosphate.* Journal of Membrane Science, 2010. **360**(1–2):334-340.

[27]   G. Busca, S. Berardinelli, C. Resini, and L. Arrighi, *Technologies for the removal of phenol from fluid streams: A short review of recent developments.* Journal of Hazardous Materials, 2008. **160**(2):265-288.

[28]   O. Abdelwahab, N. Amin, and E. El-Ashtoukhy, *Electrochemical removal of phenol from oil refinery wastewater.* Journal of Hazardous Materials, 2009. **163**(2):711-716.

[29]   K. Turhan and S. Uzman, *Removal of phenol from water using ozone.* Desalination, 2008. **229**(1):257-263.

[30]   D. Manojlovic, D. Ostojic, B. Obradovic, M. Kuraica, V. Krsmanovic, and J. Puric, *Removal of phenol and chlorophenols from water by new ozone generator.* Desalination, 2007. **213**(1):116-122.

[31]   L. Chu, J. Wang, J. Dong, H. Liu, and X. Sun, *Treatment of coking wastewater by an advanced Fenton oxidation process using iron powder and hydrogen peroxide.* Chemosphere, 2012. **86**(4):409-414.

[32]   E.I. García-Peña, P. Zarate-Segura, P. Guerra-Blanco, T. Poznyak, and I. Chairez, *Enhanced phenol and chlorinated phenols removal by combining ozonation and biodegradation.* Water, Air, & Soil Pollution, 2012. **223**(7):4047-4064.

[33]   L. Xu and J. Wang, *A heterogeneous Fenton-like system with nanoparticulate zero-valent iron for removal of 4-chloro-3-methyl phenol.* Journal of Hazardous Materials, 2011. **186**(1):256-264.

[34]   Z. Zeng, H. Zou, X. Li, M. Arowo, B. Sun, J. Chen, G. Chu, and L. Shao, *Degradation of phenol by ozone in the presence of Fenton reagent in a rotating packed bed.* Chemical Engineering Journal, 2013. **229**:404-411.

[35]   M. Minella, G. Marchetti, E. De Laurentiis, M. Malandrino, V. Maurino, C. Minero, D. Vione, and K. Hanna, *Photo-Fenton oxidation of phenol with magnetite as iron source.* Applied Catalysis B: Environmental, 2014. **154**:102-109.

[36]   C. Comninellis and C. Pulgarin, *Electrochemical oxidation of phenol for wastewater treatment using SnO2, anodes.* Journal of Applied Electrochemistry, 1993. **23**(2):108-112.

[37]   M. Pimentel, N. Oturan, M. Dezotti, and M.A. Oturan, *Phenol degradation by advanced electrochemical oxidation process electro-Fenton using a carbon felt cathode.* Applied Catalysis B: Environmental, 2008. **83**(1):140-149.

[38]   A. Dixit, A. Mungray, and M. Chakraborty, *Photochemical oxidation of phenolic wastewaters and its kinetic study.* Desalination and Water Treatment, 2012. **40**(1-3):56-62.

[39]   F. Tumakaka, I.V. Prikhodko, and G. Sadowski, *Modeling of solid–liquid equilibria for systems with solid-complex phase formation.* Fluid Phase Equilibria, 2007. **260**(1):98-104.

[40]   S. Ghizellaoui and A.H. Meniai, *Experimental study and modeling of the salt effect on phase equilibria for binary hydroxylic liquid systems.* Desalination, 2005. **185**(1–3):457-472.

[41]   H. Jiang, Y. Fang, Y. Fu, and Q.X. Guo, *Studies on the extraction of phenol in wastewater.* Journal of Hazardous Materials, 2003. **101**(2):179-190.

[42]   A.M. Urtiaga and I. Ortiz, *Extraction of phenol using trialkylphosphine oxides (Cyanex 923) in kerosene.* Separation science and technology, 1997. **32**(6):1157-1162.

[43]   Š. Schlosser, I. Rothová, and H. Frianová, *Hollow-fibre pertractor with bulk liquid membrane.* Journal of Membrane Science, 1993. **80**(1):99-106.

[44]   Y. Park, A.H.P. Skelland, L.J. Forney, and J.-H. Kim, *Removal of phenol and substituted phenols by newly developed emulsion liquid membrane process.* Water Research, 2006. **40**(9):1763-1772.

[45]   M. Peng, L.M. Vane, and S.X. Liu, *Recent advances in VOCs removal from water by pervaporation.* Journal of Hazardous Materials, 2003. **98**(1):69-90.

[46]   C. Pereira, J. Rufino, A. Habert, R. Nobrega, L. Cabral, and C. Borges, *Aroma compounds recovery of tropical fruit juice by pervaporation: membrane material selection and process evaluation.* Journal of food engineering, 2005. **66**(1):77-87.

[47]   V. Cunha, M. Paredes, C. Borges, A. Habert, and R. Nobrega, *Removal of aromatics from multicomponent organic mixtures by pervaporation using polyurethane membranes: experimental and modeling.* Journal of Membrane Science, 2002. **206**(1):277-290.

[48]   P. Wu, R.W. Field, R. England, and B.J. Brisdon, *A fundamental study of organofunctionalised PDMS membranes for the pervaporative recovery of phenolic compounds from aqueous streams.* Journal of Membrane Science, 2001. **190**(2):147-157.

[49]   W. Kujawski, A. Warszawski, W. Ratajczak, T. Porębski, W. Capała, and I. Ostrowska, *Application of pervaporation and adsorption to the phenol removal from wastewater.* Separation and Purification Technology, 2004. **40**(2):123-132.

[50]   K.W. Böddeker, G. Bengtson, and E. Bode, *Pervaporation of low volatility aromatics from water.* Journal of Membrane Science, 1990. **53**(1):143-158.

[51] M. Streat, J.W. Patrick, and M.J.C. Perez, *Sorption of phenol and para-chlorophenol from water using conventional and novel activated carbons.* Water Research, 1995. **29**(2):467-472.

[52] M. Ahmaruzzaman, *Adsorption of phenolic compounds on low-cost adsorbents: a review.* Advances in Colloid and Interface Science, 2008. **143**(1):48-67.

[53] B. Hameed, L. Chin, and S. Rengaraj, *Adsorption of 4-chlorophenol onto activated carbon prepared from rattan sawdust.* Desalination, 2008. **225**(1):185-198.

[54] D. Kalderis, D. Koutoulakis, P. Paraskeva, E. Diamadopoulos, E. Otal, J.O.d. Valle, and C. Fernández-Pereira, *Adsorption of polluting substances on activated carbons prepared from rice husk and sugarcane bagasse.* Chemical Engineering Journal, 2008. **144**(1):42-50.

[55] V.M. Monsalvo, A.F. Mohedano, and J.J. Rodriguez, *Adsorption of 4-chlorophenol by inexpensive sewage sludge-based adsorbents.* Chemical Engineering Research and Design, 2012. **90**(11):1807-1814.

[56] A. Aygün, S. Yenisoy-Karakaş, and I. Duman, *Production of granular activated carbon from fruit stones and nutshells and evaluation of their physical, chemical and adsorption properties.* Microporous and Mesoporous Materials, 2003. **66**(2):189-195.

[57] S. Babel and T.A. Kurniawan, *Low-cost adsorbents for heavy metals uptake from contaminated water: a review.* Journal of Hazardous Materials, 2003. **97**(1–3):219-243.

[58] P.X. Wu, Z.W. Liao, H.F. Zhang, and J.G. Guo, *Adsorption of phenol on inorganic–organic pillared montmorillonite in polluted water.* Environment International, 2001. **26**(5–6):401-407.

[59] H. Koyuncu, N. Yıldız, U. Salgın, F. Köroğlu, and A. Çalımlı, *Adsorption of o-, m- and p-nitrophenols onto organically modified bentonites.* Journal of Hazardous Materials, 2011. **185**(2):1332-1339.

[60] K. Shakir, H.F. Ghoneimy, A. Elkafrawy, S.G. Beheir, and M. Refaat, *Removal of catechol from aqueous solutions by adsorption onto organophilic-bentonite.* Journal of Hazardous Materials, 2008. **150**(3):765-773.

[61] M. Khalid, G. Joly, A. Renaud, and P. Magnoux, *Removal of Phenol from Water by Adsorption Using Zeolites.* Industrial & Engineering Chemistry Research, 2004. **43**(17):5275-5280.

[62] F. Su, L. Lv, T.M. Hui, and X.S. Zhao, *Phenol adsorption on zeolite-templated carbons with different structural and surface properties.* Carbon, 2005. **43**(6):1156-1164.

[63] A. Kuleyin, *Removal of phenol and 4-chlorophenol by surfactant-modified natural zeolite.* Journal of Hazardous Materials, 2007. **144**(1–2):307-315.

[64]   R. Marouf, N. Khelifa, K. Marouf-Khelifa, J. Schott, and A. Khelifa, *Removal of pentachlorophenol from aqueous solutions by dolomitic sorbents.* Journal of Colloid and Interface Science, 2006. **297**(1):45-53.

[65]   N.S. Kumar, M. Suguna, M.V. Subbaiah, A.S. Reddy, N.P. Kumar, and A. Krishnaiah, *Adsorption of phenolic compounds from aqueous solutions onto chitosan-coated perlite beads as biosorbent.* Industrial & Engineering Chemistry Research, 2010. **49**(19):9238-9247.

[66]   F.S. Mohamed, W.A. Khater, and M.R. Mostafa, *Characterization and phenols sorptive properties of carbons activated by sulphuric acid.* Chemical Engineering Journal, 2006. **116**(1):47-52.

[67]   S. Dutta, J.K. Basu, and R.N. Ghar, *Studies on adsorption of p-nitrophenol on charred saw-dust.* Separation and Purification Technology, 2001. **21**(3):227-235.

[68]   G. Vázquez, J. González-Álvarez, A.I. García, M.S. Freire, and G. Antorrena, *Adsorption of phenol on formaldehyde-pretreated Pinus pinaster bark: Equilibrium and kinetics.* Bioresource technology, 2007. **98**(8):1535-1540.

[69]   N. Chaudhary and C. Balomajumder, *Optimization study of adsorption parameters for removal of phenol on aluminum impregnated fly ash using response surface methodology.* Journal of the Taiwan Institute of Chemical Engineers, 2014. **45**(3):852-859.

[70]   A. Tor, Y. Cengeloglu, M.E. Aydin, and M. Ersoz, *Removal of phenol from aqueous phase by using neutralized red mud.* Journal of Colloid and Interface Science, 2006. **300**(2):498-503.

[71]   A. Tor, Y. Cengeloglu, and M. Ersoz, *Increasing the phenol adsorption capacity of neutralized red mud by application of acid activation procedure.* Desalination, 2009. **242**(1–3):19-28.

[72]   V.M. Monsalvo, A.F. Mohedano, and J.J. Rodriguez, *Activated carbons from sewage sludge: Application to aqueous-phase adsorption of 4-chlorophenol.* Desalination, 2011. **277**(1–3):377-382.

[73]   J.M. Li, X.G. Meng, C.W. Hu, and J. Du, *Adsorption of phenol, p-chlorophenol and p-nitrophenol onto functional chitosan.* Bioresource technology, 2009. **100**(3):1168-1173.

[74]   A.E. Navarro, R.F. Portales, M.R. Sun-Kou, and B.P. Llanos, *Effect of pH on phenol biosorption by marine seaweeds.* Journal of Hazardous Materials, 2008. **156**(1–3):405-411.

[75]   J. Wu and H.Q. Yu, *Biosorption of phenol and chlorophenols from aqueous solutions by fungal mycelia.* Process Biochemistry, 2006. **41**(1):44-49.

[76]   V. Farkas, A. Felinger, A. Hegedűsova, I. Dékány, and T. Pernyeszi, *Comparative study of the kinetics and equilibrium of phenol biosorption on immobilized white-rot*

fungus Phanerochaete chrysosporium from aqueous solution. Colloids and Surfaces B: Biointerfaces, 2013. **103**:381-390.

[77] J.R. Rao and T. Viraraghavan, *Biosorption of phenol from an aqueous solution by Aspergillus niger biomass.* Bioresource technology, 2002. **85**(2):165-171.

[78] E. Rubín, P. Rodríguez, R. Herrero, S. de Vicente, and E. Manuel, *Biosorption of phenolic compounds by the brown alga Sargassum muticum.* Journal of Chemical Technology and Biotechnology, 2006. **81**(7):1093-1099.

[79] B. Antizar-Ladislao and N. Galil, *Biosorption of phenol and chlorophenols by acclimated residential biomass under bioremediation conditions in a sandy aquifer.* Water Research, 2004. **38**(2):267-276.

[80] A.a.H. Al-Muhtaseb, K.A. Ibrahim, A.B. Albadarin, O. Ali-Khashman, G.M. Walker, and M.N. Ahmad, *Remediation of phenol-contaminated water by adsorption using poly (methyl methacrylate)(PMMA).* Chemical Engineering Journal, 2011. **168**(2):691-699.

[81] A. Li, Q. Zhang, J. Chen, Z. Fei, C. Long, and W. Li, *Adsorption of phenolic compounds on Amberlite XAD-4 and its acetylated derivative MX-4.* Reactive and Functional Polymers, 2001. **49**(3):225-233.

[82] M.S. Bilgili, *Adsorption of 4-chlorophenol from aqueous solutions by xad-4 resin: isotherm, kinetic, and thermodynamic analysis.* Journal of Hazardous Materials, 2006. **137**(1):157-164.

[83] A. Li, Q. Zhang, G. Zhang, J. Chen, Z. Fei, and F. Liu, *Adsorption of phenolic compounds from aqueous solutions by a water-compatible hypercrosslinked polymeric adsorbent.* Chemosphere, 2002. **47**(9):981-989.

[84] Y. Sun, J. Chen, A. Li, F. Liu, and Q. Zhang, *Adsorption of resorcinol and catechol from aqueous solution by aminated hypercrosslinked polymers.* Reactive and Functional Polymers, 2005. **64**(2):63-73.

[85] I. Langmuir, *The constitution and fundamental properties of solids and liquids. Part I. Solids.* Journal of the American Chemical Society, 1916. **38**(11):2221-2295.

[86] C. Tien, *Adsorption calculations and modeling.* 1994. Butterworth-Heinemann, Massachusetts, United States.

[87] A. Kumar, S. Kumar, S. Kumar, and D.V. Gupta, *Adsorption of phenol and 4-nitrophenol on granular activated carbon in basal salt medium: equilibrium and kinetics.* Journal of Hazardous Materials, 2007. **147**(1):155-166.

[88] Ö. Aktaş and F. Çeçen, *Adsorption, desorption and bioregeneration in the treatment of 2-chlorophenol with activated carbon.* Journal of Hazardous Materials, 2007. **141**(3):769-777.

[89]   A. Kumar, S. Kumar, and S. Kumar, *Adsorption of resorcinol and catechol on granular activated carbon: Equilibrium and kinetics.* Carbon, 2003. **41**(15):3015-3025.

[90]   S. Nouri, F. Haghseresht, and G.M. Lu, *Comparison of adsorption capacity of p-cresol & p-nitrophenol by activated carbon in single and double solute.* Adsorption, 2002. **8**(3):215-223.

[91]   H. Hadjar, B. Hamdi, and C. Ania, *Adsorption of p-cresol on novel diatomite/carbon composites.* Journal of Hazardous Materials, 2011. **188**(1):304-310.

[92]   F. Banat, B. Al-Bashir, S. Al-Asheh, and O. Hayajneh, *Adsorption of phenol by bentonite.* Environmental pollution, 2000. **107**(3):391-398.

[93]   B. Koumanova and P. Peeva-Antova, *Adsorption of p-chlorophenol from aqueous solutions on bentonite and perlite.* Journal of Hazardous Materials, 2002. **90**(3):229-234.

[94]   L. S and M. A-H, *The use of sawdust as by product adsorbent of organic pollutant from wastewater: Adsorption of Phenol.* Energy Procedia, 2012. **18**:905-914.

[95]   J. Huang, *Treatment of phenol and p-cresol in aqueous solution by adsorption using a carbonylated hypercrosslinked polymeric adsorbent.* Journal of Hazardous Materials, 2009. **168**(2–3):1028-1034.

[96]   Y. Liu, *Is the free energy change of adsorption correctly calculated?* Journal of Chemical & Engineering Data, 2009. **54**(7):1981-1985.

[97]   R.I. Yousef, B. El-Eswed, and A.a.H. Al-Muhtaseb, *Adsorption characteristics of natural zeolites as solid adsorbents for phenol removal from aqueous solutions: Kinetics, mechanism, and thermodynamics studies.* Chemical Engineering Journal, 2011. **171**(3):1143-1149.

[98]   Q.S. Liu, T. Zheng, P. Wang, J.P. Jiang, and N. Li, *Adsorption isotherm, kinetic and mechanism studies of some substituted phenols on activated carbon fibers.* Chemical Engineering Journal, 2010. **157**(2–3):348-356.

[99]   C. Bertagnolli, M.G.C. da Silva, and E. Guibal, *Chromium biosorption using the residue of alginate extraction from Sargassum filipendula.* Chemical Engineering Journal, 2014. **237**:362-371.

[100]   I.I. Fasfous and J.N. Dawoud, *Uranium (VI) sorption by multiwalled carbon nanotubes from aqueous solution.* Applied Surface Science, 2012. **259**:433-440.

[101]   A. Marsal, F. Maldonado, S. Cuadros, M. Elena Bautista, and A.M. Manich, *Adsorption isotherm, thermodynamic and kinetics studies of polyphenols onto tannery shavings.* Chemical Engineering Journal, 2012. **183**:21-29.

[102]   H.M. Zalloum, B. El-Eswed, R.M. Zalloum, and M.S. Mubarak, *The effect of crosslinking on the adsorption behavior of copper (II) onto poly(2-hydroxy-4-*

256

acryloyloxybenzophenone). Journal of Applied Polymer Science, 2012. **126**(3):1008-1015.

[103] Q. Zhang, L. Zhao, Y.h. Dong, and G.y. Huang, *Sorption of norfloxacin onto humic acid extracted from weathered coal.* Journal of environmental management, 2012. **102**:165-172.

[104] J. Kong, Q. Yue, S. Sun, B. Gao, Y. Kan, Q. Li, and Y. Wang, *Adsorption of Pb(II) from aqueous solution using keratin waste – hide waste: Equilibrium, kinetic and thermodynamic modeling studies.* Chemical Engineering Journal, 2014. **241**:339-400.

[105] C. Ouellet-Plamondon, R. Lynch, and A. Al-Tabbaa, *Metal Retention Experiments for the Design of Soil-Mix Technology Permeable Reactive Barriers.* Clean–Soil, Air, Water, 2011. **39**(9):844-852.

[106] S.K. Milonjić, *A consideration of the correct calculation of thermodynamic parameters of adsorption.* Journal of the Serbian Chemical Society, 2007. **72**(12):1363-1367.

[107] A. Halajnia, S. Oustan, N. Najafi, A.R. Khataee, and A. Lakzian, *Adsorption–desorption characteristics of nitrate, phosphate and sulfate on Mg–Al layered double hydroxide.* Applied Clay Science, 2013. **80–81**:305-312.

[108] I.A.A. Hamza, B.S. Martincigh, J.C. Ngila, and V.O. Nyamori, *Adsorption studies of aqueous Pb(II) onto a sugarcane bagasse/multi-walled carbon nanotube composite.* Physics and Chemistry of the Earth, Parts A/B/C, 2013. **66**:157-166.

[109] J. Sarma and S. Mahiuddin, *Comparative adsorption involving ortho- and para-hydroxybenzoic acids in mixed-adsorbate mode onto α-alumina surface: Effect of molecular structure.* Journal of Environmental Chemical Engineering, 2014. **2**(1):90-99.

[110] Q. Zhou, W. Gong, C. Xie, D. Yang, X. Ling, X. Yuan, S. Chen, and X. Liu, *Removal of Neutral Red from aqueous solution by adsorption on spent cottonseed hull substrate.* Journal of Hazardous Materials, 2011. **185**(1):502-506.

[111] R. Otero, J.M. Fernández, M.A. Ulibarri, R. Celis, and F. Bruna, *Adsorption of non-ionic pesticide S-Metolachlor on layered double hydroxides intercalated with dodecylsulfate and tetradecanedioate anions.* Applied Clay Science, 2012. **65–66**:72-79.

[112] J. Biggar and M. Cheung, *Adsorption of picloram (4-amino-3,5,6-trichloropicolinic acid) on Panoche, Ephrata, and Palouse soils: a thermodynamic approach to the adsorption mechanism.* Soil Science Society of America Journal, 1973. **37**(6):863-868.

[113] G. Zhao, J. Li, and X. Wang, *Kinetic and thermodynamic study of 1-naphthol adsorption from aqueous solution to sulfonated graphene nanosheets.* Chemical Engineering Journal, 2011. **173**(1):185-190.

[114] L. Fan, M. Li, Z. Lv, M. Sun, C. Luo, F. Lu, and H. Qiu, *Fabrication of magnetic chitosan nanoparticles grafted with β-cyclodextrin as effective adsorbents toward hydroquinol.* Colloids and Surfaces B: Biointerfaces, 2012. **95**(0):42-49.

[115] I.I. Fasfous, E.S. Radwan, and J.N. Dawoud, *Kinetics, equilibrium and thermodynamics of the sorption of tetrabromobisphenol A on multiwalled carbon nanotubes.* Applied Surface Science, 2010. **256**(23):7246-7252.

[116] X. Sun, L. Yang, H. Xing, J. Zhao, X. Li, Y. Huang, and H. Liu, *Synthesis of polyethylenimine-functionalized poly(glycidyl methacrylate) magnetic microspheres and their excellent Cr(VI) ion removal properties.* Chemical Engineering Journal, 2013. **234**:338-345.

[117] Z. Al-Qodah, W.K. Lafi, Z. Al-Anber, M. Al-Shannag, and A. Harahsheh, *Adsorption of methylene blue by acid and heat treated diatomaceous silica.* Desalination, 2007. **217**(1–3):212-224.

[118] B.A. Olasumbo, *Kinetic, isotherm and thermodynamic studies of the biosorption of zinc (II) from solution by maize wrapper.* International Journal of Physical Sciences, 2008. **3**(2):50-55.

[119] A. Bhattacharya, T. Naiya, S. Mandal, and S. Das, *Adsorption, kinetics and equilibrium studies on removal of Cr (VI) from aqueous solutions using different low-cost adsorbents.* Chemical Engineering Journal, 2008. **137**(3):529-541.

[120] R. Han, H. Li, Y. Li, J. Zhang, H. Xiao, and J. Shi, *Biosorption of copper and lead ions by waste beer yeast.* Journal of Hazardous Materials, 2006. **137**(3):1569-1576.

[121] S.Lagergren, *Zur theorie der sogenannten adsorption geluster stoffe.* KSven VetenskapsakadHandl, 1898. **24**:1-39.

[122] Y. Ho, *Review of second-order models for adsorption systems.* Journal of Hazardous Materials, 2006. **136**(3):681-689.

[123] Y. Ho and G. McKay, *A comparison of chemisorption kinetic models applied to pollutant removal on various sorbents.* Process Safety and Environmental Protection, 1998. **76**(4):332-340.

[124] W. Weber and J. Morris. *Advances in water pollution research. in Proceedings of the First International Conference on Water Pollution Research.* 1962. Pergamon Press Oxford.

[125] Q. Lu and G.A. Sorial, *The role of adsorbent pore size distribution in multicomponent adsorption on activated carbon.* Carbon, 2004. **42**(15):3133-3142.

[126] R. Mihalache, I. Peleanu, I. Meghea, and A. Tudorache, *Competitive adsorption models of organic pollutants from bi-and tri-solute systems on activated carbon.* Journal of radioanalytical and nuclear chemistry, 1998. **229**(1-2):B133-138.

[127] J. HUH, D. SONG, and Y. Jeon, *Sorption of phenol and alkylphenols from aqueous solution onto organically modified montmorillonite and applications of dual-mode sorption model.* Separation science and technology, 2000. **35**(2):243-259.

[128] S. Srivastava and R. Tyagi, *Competitive adsorption of substituted phenols by activated carbon developed from the fertilizer waste slurry.* Water Research, 1995. **29**(2):483-488.

[129] K. Abburi, *Adsorption of phenol and p-chlorophenol from their single and bisolute aqueous solutions on Amberlite XAD-16 resin.* Journal of Hazardous Materials, 2003. **105**(1):143-156.

[130] A. Khan, T. Al-Bahri, and A. Al-Haddad, *Adsorption of phenol based organic pollutants on activated carbon from multi-component dilute aqueous solutions.* Water Research, 1997. **31**(8):2102-2112.

[131] J. Garcia-Araya, F. Beltran, P. Alvarez, and F. Masa, *Activated carbon adsorption of some phenolic compounds present in agroindustrial wastewater.* Adsorption, 2003. **9**(2):107-115.

[132] R. Juang, S. Lin, and K. Tsao, *Mechanism of sorption of phenols from aqueous solutions onto surfactant-modified montmorillonite.* Journal of Colloid and Interface Science, 2002. **254**(2):234-241.

[133] Q. Wei and T. Nakato, *Competitive adsorption of phenols on organically modified layered hexaniobate $K_4Nb_6O_{17}$.* Microporous and Mesoporous Materials, 2006. **96**(1):84-92.

[134] J. Butler and C. Ockrent, *Studies in electrocapillarity. III.* The Journal of Physical Chemistry, 1930. **34**(12):2841-2859.

[135] J.S. Jain and V.L. Snoeyink, *Adsorption from bisolute systems on active carbon.* Journal (Water Pollution Control Federation), 1973:2463-2479.

[136] C. Sheindorf, M. Rebhun, and M. Sheintuch, *A Freundlich-type multicomponent isotherm.* Journal of Colloid and Interface Science, 1981. **79**(1):136-142.

[137] N. Abdehagh, F.H. Tezel, and J. Thibault, *Multicomponent adsorption modeling: isotherms for ABE model solutions using activated carbon F-400.* Adsorption, 2016. **22**(3):357-370.

[138] V.C. Srivastava, I.D. Mall, and I.M. Mishra, *Antagonistic competitive equilibrium modeling for the adsorption of ternary metal ion mixtures from aqueous solution onto bagasse fly ash.* Industrial & Engineering Chemistry Research, 2008. **47**(9):3129-3137.

[139] A. Myers and J.M. Prausnitz, *Thermodynamics of mixed-gas adsorption.* AIChE Journal, 1965. **11**(1):121-127.

[140]   C. Radke and J. Prausnitz, *Adsorption of organic solutes from dilute aqueous solution of activated carbon.* Industrial & Engineering Chemistry Fundamentals, 1972. **11**(4):445-451.

[141]   K.K. Choy, J.F. Porter, and G. McKay, *Single and multicomponent equilibrium studies for the adsorption of acidic dyes on carbon from effluents.* Langmuir, 2004. **20**(22):9646-9656.

[142]   R. Aghav, S. Kumar, and S. Mukherjee, *Artificial neural network modeling in competitive adsorption of phenol and resorcinol from water environment using some carbonaceous adsorbents.* Journal of Hazardous Materials, 2011. **188**(1):67-77.

[143]   Y.S Kim, D.I. Song, Y.W. Jeon, and S.J. Choi, *Adsorption of organic phenols onto hexadecyltrimethylammonium-treated montmorillonite.* Separation science and technology, 1996. **31**(20):2815-2830.

[144]   A. Torrents, R. Damera, and O.J. Hao, *Low-temperature thermal desorption of aromatic compounds from activated carbon.* Journal of Hazardous Materials, 1997. **54**(3):141-153.

[145]   P. Magne and P. Walker, *Phenol adsorption on activated carbons: application to the regeneration of activated carbons polluted with phenol.* Carbon, 1986. **24**(2):101-107.

[146]   C. Moreno-Castilla, J. Rivera-Utrilla, J. Joly, M. Lopez-Ramon, M. Ferro-Garcia, and F. Carrasco-Marin, *Thermal regeneration of an activated carbon exhausted with different substituted phenols.* Carbon, 1995. **33**(10):1417-1423.

[147]   E. Sabio, E. González, J. González, C. González-Garcıa, A. Ramiro, and J. Ganan, *Thermal regeneration of activated carbon saturated with p-nitrophenol.* Carbon, 2004. **42**(11):2285-2293.

[148]   S. Lin and M. Cheng, *Adsorption of phenol and m-chlorophenol on organobentonites and repeated thermal regeneration.* Waste Management, 2002. **22**(6):595-603.

[149]   N. Roostaei and F.H. Tezel, *Removal of phenol from aqueous solutions by adsorption.* Journal of environmental management, 2004. **70**(2):157-164.

[150]   S. Rengaraj, S.-H. Moon, R. Sivabalan, B. Arabindoo, and V. Murugesan, *Removal of phenol from aqueous solution and resin manufacturing industry wastewater using an agricultural waste: rubber seed coat.* Journal of Hazardous Materials, 2002. **89**(2):185-196.

[151]   M. Ghasemi, A.R. Keshtkar, R. Dabbagh, and S.J. Safdari, *Biosorption of uranium (VI) from aqueous solutions by Ca-pretreated Cystoseira indica alga: breakthrough curves studies and modeling.* Journal of Hazardous Materials, 2011. **189**(1):141-149.

[152]   F. An, R. Du, X. Wang, M. Wan, X. Dai, and J. Gao, *Adsorption of phenolic compounds from aqueous solution using salicylic acid type adsorbent.* Journal of Hazardous Materials, 2012. **201**:74-81.

[153] V. Gupta, I. Tyagi, S. Agarwal, R. Singh, M. Chaudhary, A. Harit, and S. Kushwaha, *Column operation studies for the removal of dyes and phenols using a low cost adsorbent.* Global Journal of Environmental Science and Management, 2016. **2**(1):1-10.

[154] V.V. Goud, K. Mohanty, M. Rao, and N. Jayakumar, *Phenol removal from aqueous solutions by tamarind nutshell activated carbon: batch and column studies.* Chemical engineering & technology, 2005. **28**(7):814-821.

[155] H. Karunarathne and B. Amarasinghe, *Fixed bed adsorption column studies for the removal of aqueous phenol from activated carbon prepared from sugarcane bagasse.* Energy Procedia, 2013. **34**:83-90.

[156] M. Abdelkreem, *Adsorption of phenol from industrial wastewater using olive mill waste.* APCBEE Procedia, 2013. **5**:349-357.

[157] M.F.F. Sze and G. McKay, *Enhanced mitigation of para-chlorophenol using stratified activated carbon adsorption columns.* Water Research, 2012. **46**(3):700-710.

[158] S. Yoshida, S. Iwamura, I. Ogino, and S.R. Mukai, *Adsorption of phenol in flow systems by a monolithic carbon cryogel with a microhoneycomb structure.* Adsorption, 2016. **22**(8):1-8.

[159] F. Oughlis-Hammache, N. Hamaidi-Maouche, F. Aissani-Benissad, and S. Bourouina-Bacha, *Central composite design for the modeling of the phenol adsorption process in a fixed-bed reactor.* Journal of Chemical & Engineering Data, 2010. **55**(7):2489-2494.

[160] Z. Xu, J. Cai, and B. Pan, *Mathematically modeling fixed-bed adsorption in aqueous systems.* Journal of Zhejiang University Science A, 2013. **14**(3):155-176.

[161] Z. Aksu, *Determination of the equilibrium, kinetic and thermodynamic parameters of the batch biosorption of nickel(II) ions onto Chlorella vulgaris.* Process Biochemistry, 2002. **38**(1):89-99.

[162] G. Bohart and E. Adams, *Some aspects of the behavior of charcoal with respect to chlorine. 1.* Journal of the American Chemical Society, 1920. **42**(3):523-544.

[163] R. Hutchins, *New method simplifies design of activated-carbon systems.* Chemical Engineering, 1973. **80**(19):133-138.

[164] V. Srivastava, B. Prasad, I. Mishra, I. Mall, and M. Swamy, *Prediction of breakthrough curves for sorptive removal of phenol by bagasse fly ash packed bed.* Industrial & Engineering Chemistry Research, 2008. **47**(5):1603-1613.

[165] Z. Aksu and F. Gönen, *Biosorption of phenol by immobilized activated sludge in a continuous packed bed: prediction of breakthrough curves.* Process Biochemistry, 2004. **39**(5):599-613.

[166] A. Adak and A. Pal, *Removal of phenol from aquatic environment by SDS-modified alumina: Batch and fixed bed studies.* Separation and Purification Technology, 2006. **50**(2):256-262.

[167] N. Singh and C. Balomajumder, *Continuous packed bed adsorption of phenol and cyanide onto modified rice husk: an experimental and modeling study.* Desalination and Water Treatment, 2016. **57**(50):1-15.

[168] D.C. Ko, J.F. Porter, and G. McKay, *Optimised correlations for the fixed-bed adsorption of metal ions on bone char.* Chemical engineering science, 2000. **55**(23):5819-5829.

[169] A. Wolborska, *Adsorption on activated carbon of p-nitrophenol from aqueous solution.* Water Research, 1989. **23**(1):85-91.

[170] H.C. Thomas, *Heterogeneous ion exchange in a flowing system.* Journal of the American Chemical Society, 1944. **66**(10):1664-1666.

[171] H.C. Thomas, *Chromatography: a problem in kinetics.* Annals of the New York Academy of Sciences, 1948. **49**(2):161-182.

[172] R.M. Clark, *Evaluating the cost and performance of field-scale granular activated carbon systems.* Environmental science & technology, 1987. **21**(6):573-580.

[173] Y.H. Yoon and J.H. Nelson, *Application of gas adsorption kinetics I. A theoretical model for respirator cartridge service life.* The American Industrial Hygiene Association Journal, 1984. **45**(8):509-516.

[174] K. Chen, H. Lyu, S. Hao, G. Luo, S. Zhang, and J. Chen, *Separation of phenolic compounds with modified adsorption resin from aqueous phase products of hydrothermal liquefaction of rice straw.* Bioresource Technology, 2015. **182**:160-168.

[175] J. Huang, L. Yang, X. Wu, M. Xu, Y.N. Liu, and S. Deng, *Phenol adsorption on α, α'-dichloro-p-xylene (DCX) and 4,4'-bis (chloromethyl)-1,1'-biphenyl (BCMBP) modified XAD-4 resins from aqueous solutions.* Chemical Engineering Journal, 2013. **222**:1-8.

[176] G. Sangeeta, K. Deepak, and A. Jana, *Fixed bed column studies for the sorption of para-nitrophenol from aqueous solutions using corss-linked starch based polymer.* Journal of Environmental Research And Development, 2012. **7**(2A):843-850.

[177] C. Li, M. Xu, X. Sun, S. Han, X. Wu, Y.-N. Liu, J. Huang, and S. Deng, *Chemical modification of Amberlite XAD-4 by carbonyl groups for phenol adsorption from wastewater.* Chemical Engineering Journal, 2013. **229**:20-26.

[178] A. Garba, N.S. Nasri, H. Basri, R. Ismail, Z.A. Majid, U.D. Hamza, and J. Mohammed, *Adsorptive removal of phenol from aqueous solution on a modified palm shell-based carbon: fixed-bed adsorption studies.* Desalination and Water Treatment, 2016. **57**(60):1-12.

[179] C. Girish and V.R. Murty, *Adsorption of phenol from aqueous solution using Lantana camara, forest waste: packed bed studies and prediction of breakthrough curves.* Environmental Processes, 2015. **2**(4):773-796.

[180] Y.A. Alhamed, *Adsorption kinetics and performance of packed bed adsorber for phenol removal using activated carbon from dates' stones.* Journal of Hazardous Materials, 2009. **170**(2):763-770.

[181] G. Vázquez, R. Alonso, S. Freire, J. González-Álvarez, and G. Antorrena, *Uptake of phenol from aqueous solutions by adsorption in a pinus pinaster bark packed bed.* Journal of Hazardous Materials, 2006. **133**(1):61-67.

[182] J. Chern and Y. Chien, *Adsorption of nitrophenol onto activated carbon: isotherms and breakthrough curves.* Water Research, 2002. **36**(3):647-655.

[183] R. Juang, S. Lin, and K. Tsao, *Sorption of phenols from water in column systems using surfactant-modified montmorillonite.* Journal of Colloid and Interface Science, 2004. **269**(1):46-52.

[184] B. Pan, F. Meng, X. Chen, B. Pan, X. Li, W. Zhang, X. Zhang, J. Chen, Q. Zhang, and Y. Sun, *Application of an effective method in predicting breakthrough curves of fixed-bed adsorption onto resin adsorbent.* Journal of Hazardous Materials, 2005. **124**(1):74-80.

[185] D. Richard, M.D.L.D. Núñez, and D. Schweich, *Adsorption of complex phenolic compounds on active charcoal: breakthrough curves.* Chemical Engineering Journal, 2010. **158**(2):213-219.

[186] A.C. Lua and Q. Jia, *Adsorption of phenol by oil–palm-shell activated carbons in a fixed bed.* Chemical Engineering Journal, 2009. **150**(2):455-461.

[187] G.S. Kirshenbaum and R.B. Seymour, *High Performance Polymers: Their Origin and Development: Proceedings of the Symposium on the History of High Performance Polymers at the American Chemical Society Meeting Held in New York, April 15-18,* 1986, Elsevier.

[188] A. Groß and A. Heintz, *Diffusion coefficients of aromatics in nonporous PEBA membranes.* Journal of Membrane Science, 2000. **168**(1):233-242.

[189] C. Ding, X. Zhang, C. Li, X. Hao, Y. Wang, and G. Guan, *ZIF-8 incorporated polyether block amide membrane for phenol permselective pervaporation with high efficiency.* Separation and Purification Technology, 2016. **166**:252-261.

[190] C. Li, X. Zhang, X. Hao, X. Feng, X. Pang, and H. Zhang, *Thermodynamic and mechanistic studies on recovering phenol crystals from dilute aqueous solutions using pervaporation–crystallization coupling (PVCC) system.* Chemical Engineering Science, 2015. **127**:106-114.

[191] I. Souchon, J. Rojas, A. Voilley, and G. Grevillot, *Trapping of aromatic compounds by adsorption on hydrophobic sorbents.* Separation Science and Technology, 1996. **31**(18):2473-2491.

[192] C. Moreno-Castilla, J. Rivera-Utrilla, and M. Lopez-Ramon, *Adsorption of some substituted phenols on activated carbons from a bituminous coal.* Carbon, 1995. **33**(6):845-851.

[193] H. Qiu, L. Lv, B. Pan, Q. Zhang, W. Zhang, and Q. Zhang, *Critical review in adsorption kinetic models.* Journal of Zhejiang University Science A, 2009. **10**(5):716-724.

[194] S. Lagergren, *Zur Theorie der Sogenannten Absorption gelöster Stoffe*. 1898: PA Norstedt & söner.

[195] S. Azizian, *Kinetic models of sorption: a theoretical analysis.* Journal of Colloid and Interface Science, 2004. **276**(1):47-52.

[196] Y. Ho and G. McKay, *Sorption of dye from aqueous solution by peat.* Chemical Engineering Journal, 1998. **70**(2):115-124.

[197] G. McKay, M. Otterburn, and A. Sweeney, *The removal of colour from effluent using various adsorbents—III. Silica: rate processes.* Water Research, 1980. **14**(1):15-20.

[198] W. Plazinski, W. Rudzinski, and A. Plazinska, *Theoretical models of sorption kinetics including a surface reaction mechanism: A review.* Advances in Colloid and Interface Science, 2009. **152**(1–2):2-13.

[199] V.C. Taty-Costodes, H. Fauduet, C. Porte, and A. Delacroix, *Removal of Cd (II) and Pb (II) ions, from aqueous solutions, by adsorption onto sawdust of pinus sylvestris.* Journal of Hazardous Materials, 2003. **105**(1):121-142.

[200] C. Namasivayam and D. Kavitha, *Adsorptive removal of 2,4-dichlorophenol from aqueous solution by low-cost carbon from an agricultural solid waste: coconut coir pith.* Separation Science and Technology, 2005. **39**(6):1407-1425.

[201] B. Acemioğlu, *Batch kinetic study of sorption of methylene blue by perlite.* Chemical Engineering Journal, 2005. **106**(1):73-81.

[202] M. Basso, E. Cerrella, and A. Cukierman, *Activated carbons developed from a rapidly renewable biosource for removal of cadmium (II) and nickel (II) ions from dilute aqueous solutions.* Industrial & Engineering Chemistry Research, 2002. **41**(2):180-189.

[203] M.X. Loukidou, A.I. Zouboulis, T.D. Karapantsios, and K.A. Matis, *Equilibrium and kinetic modeling of chromium(VI) biosorption by Aeromonas caviae.* Colloids and Surfaces A: Physicochemical and Engineering Aspects, 2004. **242**(1–3):93-104.

[204] S. Singh, B.N. Rai, and L.C. Rai, *Ni (II) and Cr (VI) sorption kinetics by Microcystis in single and multimetallic system.* Process Biochemistry, 2001. **36**(12):1205-1213.

[205]   Z. Aksu and E. Kabasakal, *Batch adsorption of 2,4-dichlorophenoxy-acetic acid (2,4-D) from aqueous solution by granular activated carbon.* Separation and Purification Technology, 2004. **35**(3):223-240.

[206]   Y. Liu and L. Shen, *From Langmuir kinetics to first-and second-order rate equations for adsorption.* Langmuir, 2008. **24**(20):11625-11630.

[207]   W. Rudzinski and W. Plazinski, *Kinetics of solute adsorption at solid/solution interfaces: a theoretical development of the empirical pseudo-first and pseudo-second order kinetic rate equations, based on applying the statistical rate theory of interfacial transport.* The Journal of Physical Chemistry B, 2006. **110**(33):16514-16525.

[208]   C. Namasivayam and D. Kavitha, *Removal of Congo Red from water by adsorption onto activated carbon prepared from coir pith, an agricultural solid waste.* Dyes and Pigments, 2002. **54**(1):47-58.

[209]   B. Acemioğlu, *Adsorption of Congo red from aqueous solution onto calcium-rich fly ash.* Journal of Colloid and Interface Science, 2004. **274**(2):371-379.

[210]   T.S. Anirudhan and P.G. Radhakrishnan, *Thermodynamics and kinetics of adsorption of Cu(II) from aqueous solutions onto a new cation exchanger derived from tamarind fruit shell.* The Journal of Chemical Thermodynamics, 2008. **40**(4):702-709.

[211]   W. Cheng, S.G. Wang, L. Lu, W.X. Gong, X.W. Liu, B.Y. Gao, and H.Y. Zhang, *Removal of malachite green (MG) from aqueous solutions by native and heat-treated anaerobic granular sludge.* Biochemical Engineering Journal, 2008. **39**(3):538-546.

[212]   D.M. Ruthven, *Principles of adsorption and adsorption processes.* 1984. Elsevier. Amsterdam, Netherlands.

[213]   W.J. Weber and J.C. Morris, *Adsorption in heterogeneous aqueous systems.* Journal of American Water Works Association, 1964. **56**(4):447-456.

[214]   Y. Ho, D.J. Wase, and C. Forster, *Kinetic studies of competitive heavy metal adsorption by sphagnum moss peat.* Environmental Technology, 1996. **17**(1):71-77.

[215]   S.A. Boyd, S. Sun, J. Lee, and M.M. Mortland, *Pentachlorophenol sorption by organo-clays.* Clays Clay Miner, 1988. **36**(2):125-130.

[216]   J.A. Smith, P.R. Jaffe, and C.T. Chiou, *Effect of ten quaternary ammonium cations on tetrachloromethane sorption to clay from water.* Environmental Science & Technology, 1990. **24**(8):1167-1172.

[217]   G. Sheng, S. Xu, and S.A. Boyd, *Cosorption of organic contaminants from water by hexadecyltrimethylammonium-exchanged clays.* Water Research, 1996. **30**(6):1483-1489.

[218] H. Cho, K. Baek, H. Lee, S. Lee, and J. Yang, *Competitive extraction of multi-component contaminants in water by carboxen–polydimethylsiloxane fiber during solid-phase microextraction.* Journal of Chromatography A, 2003. **988**(2):177-184.

[219] C. Radke and J. Prausnitz, *Thermodynamics of multi-solute adsorption from dilute liquid solutions.* AIChE Journal, 1972. **18**(4):761-768.

[220] W. Tanthapanichakoon, P. Ariyadejwanich, P. Japthong, K. Nakagawa, S. Mukai, and H. Tamon, *Adsorption–desorption characteristics of phenol and reactive dyes from aqueous solution on mesoporous activated carbon prepared from waste tires.* Water Research, 2005. **39**(7):1347-1353.

[221] M. Ahmaruzzaman and D. Sharma, *Adsorption of phenols from wastewater.* Journal of Colloid and Interface Science, 2005. **287**(1):14-24.

[222] D.P. Mungasavalli, T. Viraraghavan, and Y. Jin, *Biosorption of chromium from aqueous solutions by pretreated Aspergillus niger: batch and column studies.* Colloids and Surfaces A: Physicochemical and Engineering Aspects, 2007. **301**(1):214-223.

[223] X. Feng and D. Lawless, *Modulated Bundle Element*. US Patent 20080303125 A1, 2008.

[224] S. Kundu, S.S. Kavalakatt, A. Pal, S.K. Ghosh, M. Mandal, and T. Pal, *Removal of arsenic using hardened paste of Portland cement: batch adsorption and column study.* Water Research, 2004. **38**(17):3780-3790.

[225] F.G. Helfferich, *Ion exchange,* 1962. Dover publications, Inc., New York, United States

[226] A. Garcia-Mendieta, M. Solache-Rios, and M. Olguin, *Comparison of phenol and 4-chlorophenol adsorption in activated carbon with different physical properties.* Separation Science and Technology, 2003. **38**(11):2549-2564.

[227] M. Solache-Ríos, M. Olguín, I. García-Sosa, and J. Jiménez-Becerril, *Evaluation of the sorption properties of a Mexican organo clinoptilolite-rich tuff for phenol and 4-chlorophenol.* Environmental Technology, 2004. **25**(7):819-824.

[228] J.S. Zogorski, S.D. Faust, and J.H. Haas, *The kinetics of adsorption of phenols by granular activated carbon.* Journal of Colloid and Interface Science, 1976. **55**(2):329-341.

[229] M.L. Brusseau, P. Rao, R. Jessup, and J. Davidson, *Flow interruption: A method for investigating sorption nonequilibrium.* Journal of Contaminant Hydrology, 1989. **4**(3):223-240.

[230] M.K. Mandal and P.K. Bhattacharya, *Poly(ether-block-amide) membrane for pervaporative separation of pyridine present in low concentration in aqueous solution.* Journal of Membrane Science, 2006. **286**(1–2):115-124.

[231] A.H. Sulaymon and K.W. Ahmed, *Competitive adsorption of furfural and phenolic compounds onto activated carbon in fixed bed column.* Environmental Science & Technology, 2008. **42**(2):392-397.

[232] B. Özkaya, *Adsorption and desorption of phenol on activated carbon and a comparison of isotherm models.* Journal of Hazardous Materials, 2006. **129**(1–3):158-163.

[233] D.R. Lloyd, K.E. Kinzer, and H.S. Tseng, *Microporous membrane formation via thermally induced phase separation. I. Solid-liquid phase separation.* Journal of Membrane Science, 1990. **52**(3):239-261.

[234] M.U. Farooq, *Separation of heavy metals from water using fibroin as adsorbent. (Docoral Thesis) 2014. University of Waterloo. Retrieved from UW Space.*

Appendix I

I.1 Fortran Programming for calculation of k_2 in the modified pseudo-second order equation

In this study, the k_2 in the modified pseudo-second order equation was solved by the "The non-dominated sorting genetic algorithm technique", which has been introduced in an earlier study in our research group [234] . The computational algorithm for calculation of k_2 using this technique was demonstrated in Figure I.1 and the values of parameters used in this technique was listed in Table I.1.

Table I.1 Computational parameters used in the Non-dominated Sorting Genetic Algorithm[234]

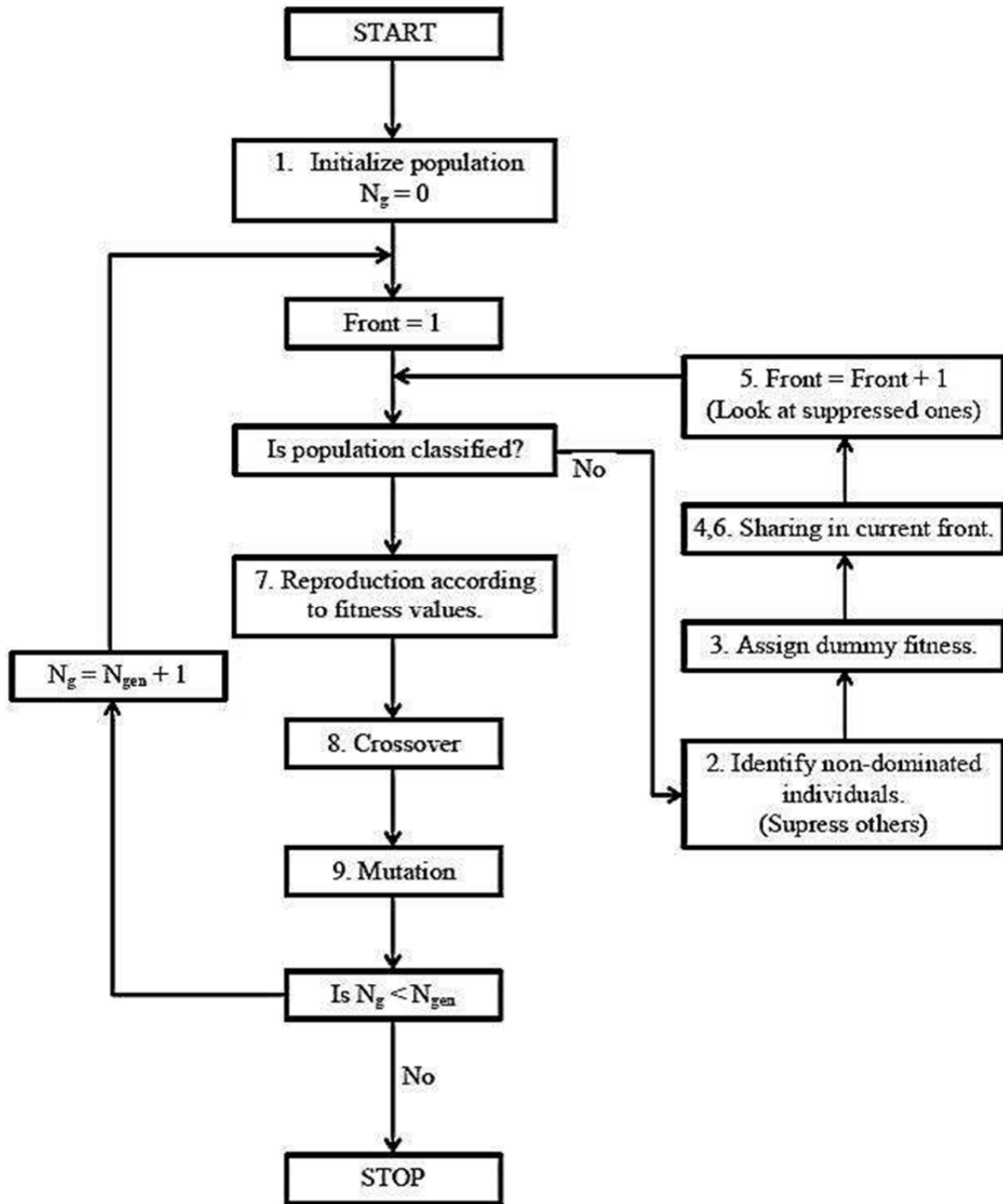| Parameters	Notation	Values
Sub-string length coding for each decision variable	l_{substr}	32
Number of generations	N_{gen}	50
Population size	N_{pop}	50
Crossover probability	P_{cross}	0.7
Mutation Probability	P_{mute}	0.005
Jumping jene probability	P_{jump}	0.15
Seed for random number generator	S_r	0.45

Figure I.1 Computational algorithm for calculation of k_2 in the modified pseudo-second order equation [234]

```fortran
      Program main
      PARAMETER (NDATA=100)
      integer ipopsize, lchrom, maxgen, ncross, nmute, nparam
      integer lsubstr(10)
      integer I, NEXPERIMENT
      double precision pcross, pmute, pjump
      double precision alow(10),ahigh(10),factor(10)
      common/sgaparam/ipopsize,lchrom,maxgen,ncross,nmute,nparam
      common/sgaparam1/pcross,pmute,pjump
      DOUBLE PRECISION K2, Kf, onebyn, Co, m, V
      DOUBLE PRECISION TEXP, CCEXP
      DIMENSION TEXP(NDATA), CCEXP(NDATA)
      COMMON /GA1/ TEXP, CCEXP
      COMMON /GA2/ TS
      COMMON /GA3/ K2, Kf, onebyn, Co, m, V
      COMMON /GA7/ NEXPERIMENT
      EXTERNAL nsga2
      OPEN(unit=20, FILE='ads.txt')
      OPEN(unit=10, FILE='ads-res.res')
          READ(20, *) alow(1), ahigh(1)
           READ(20, *) Kf, onebyn, Co, m, V
           READ(20, *) TS, NEXPERIMENT
           DO I=1, NDATA
           TEXP(I) = 0.0D0
           CCEXP(I) = 0.0D0
      ENDDO
      DO 27 I=1, NEXPERIMENT
      READ(20, *) TEXP(I), CCEXP(I)
27    CONTINUE
      ipopsize=50                   ! number of generations, decrease it to get quick result
      maxgen=50
      pcross=0.7d0
      pmute=0.005
      pjump=0.15d0
      nmute=0
      ncross=0
      lchrom=0.
      DO 2 i=1, nparam
      lsubstr(i)=10
      lchrom=lchrom+lsubstr(i)
      factor (i)=2.0**float(lsubstr(i))-1.0
2     continue
!     alow(1)=0.0010d0
!     alow(2)=30.0d0
!     alow(3)=0.4d0
!     alow(4)=0.15d0
```

```fortran
!    ahigh(1)=1.00d0
!    ahigh(2)=100.0d0
!    ahigh(3)=0.8d0
!    ahigh(4)=0.35d0
     write (10, 100) maxgen, ipopsize, nparam
     write (10, 200) pcross, pmute, pjump, lchrom
     Do 3 i=1, nparam
     write(10, 300) i, lsubstr(i), alow(i), ahigh(i)
3    continue
     write(10, *)
     write(10,350)
     call nsga2 (alow, ahigh, lsubstr, factor)
100  format(1x, 'No. of Generations=',I3,3X,'No. of population=',& I3,3X,'No. of
     Variables=',I3,3X,'No. of objectives=1',I3)
200  format(1x,'crossover=',F5.3,3X,'mutation=',F6.4,3X,'jumping genes=',F5.3,&
     3X,'chromosome length=',I3)
300  format(1x, 'variable No.',I3,3X,'stringlength=',I3,3X,&
     'lowlimit=',F14.6,3X,'highlimit=',F14.6)
350  format(15X,'X(1)',8X,'simulout(1)',8X,'F')
     end
         subroutine simul(nparam,x,simulout)
           IMPLICIT double precision (A-H,O-Z)
                parameter (ndatas=10, NDATA=100)
                integer ipopsize,lchrom,maxgen,ncross,nmute,nparamm,igen,nobjfn, I, J
     double precision x(nparam),simulout(ndatas),pen,pcross, pmute,pjump
     double precision F
     double precision TEXP, CCEXP, CCAL
     dimension TEXP(NDATA)
     dimension CCEXP(NDATA), CCAL(NDATA)
     common/sgaparam/ipopsize,lchrom,maxgen,ncross,nmute,nparamm
     common/sgaparam1/pcross,pmute,pjump
     common/statist/igen            !avg,amax,aminO,sumfitness
     common/GA1/ TEXP, CCEXP
       COMMON /GA7/ NEXPERIMENT
       EXTERNAL Isosimul
     call Isosimul(X, NDATA, TEXP, CCAL)
 ! Define the objective
     F=0.0d0
     DO 111 J=1, NEXPERIMENT
     F=F+ (CCEXP (J)-CCAL (J)) **2.0
!              Print*, CCEXP, CCAL
!              Pause
111     CONTINUE
     simulout(1)=1.0/(1.0+F)
!    simulout(2)=1.0/(1.0+F)
     if(mod(igen,1) .eq. 0) then
```

```
        write(10,100) X, simulout(1), F
        end if
100   format(8X, 3F14.6)
        return
        end
      Subroutine Isosimul(X, NDATA, TEXP, CCAL)
      INTEGER MXPARM, N, NDATA, I, J
      PARAMETER (MXPARM=50, N=1)
      INTEGER MABSE, MBDF
      PARAMETER (MABSE=1, MBDF=2)
      INTEGER IDO, NOUT, ISTEP, TOTSTEP
      DOUBLE PRECISION A (1, 1), PARAM (MXPARM), T, TEND, TT, TOL
      DOUBLE PRECISION Y, X
      DOUBLE PRECISION TEXP, CCAL
      DOUBLE PRECISION K2, Kf, onebyn, Co, m, V
      DIMENSION Y(N),X(10),TEXP(NDATA), CCAL(NDATA)
      EXTERNAL DIVPAG, SSET, UMACH
      EXTERNAL FCN, FCNJ
      COMMON /GA2/ TS
      COMMON /GA3/ K2, Kf, onebyn, Co, m, V
      COMMON /GA7/ NEXPERIMENT
      K2=X (1)

!        Q=6.138735421d0

!        b=0.00825437d0

!        CO=150.0d0

!        m=1.0d0

!        V=0.08d0

!        TS=300.0d0

      CALL UMACH (2, NOUT)
      CALL SSET (MXPARM, 0.0, PARAM, 1)
      PARAM (4) =100000000
      PARAM (10) =MABSE
      PARAM (12) =MBDF
      TOL=1.0E-8
      DO 56 I=1, N
          Y (I) =1.0E-08
56    CONTINUE
      T=0.0
      IDO=1
```

```fortran
      ISTEP=1
          TOTSTEP = TS*100.0
      DO 20 WHILE (ISTEP .LE. TOTSTEP+1)
      IF (ISTEP .EQ. TOTSTEP+1) IDO=3
!     IF (ISTEP .GT. 60000) KZF=0.0! Use the KZF value to initiate the rectangular pulse
injection
      TEND=TS*ISTEP/TOTSTEP
      TT=TEND
      CALL DIVPAG (IDO, N, FCN, FCNJ, A, T, TEND, TOL, PARAM, Y)! This function
is used to solve the ODE
      DO 30 J=1, NEXPERIMENT
      IF (TT .EQ. TEXP (J)) THEN
      CCAL (J) =Y (N)
      END IF
 30   CONTINUE
      ISTEP=ISTEP+1
 20    CONTINUE
      RETURN
      END
      SUBROUTINE FCN (N, T, Y, YPRIME)
      INTEGER I, N
      DOUBLE PRECISION T, Y (N), YPRIME (N)
      DOUBLE PRECISION K2, Kf, onebyn, Co, m, V
      DOUBLE PRECISION A1, A2, A3, A4, A5
      COMMON /GA3/ K2, Kf, onebyn, Co, m, V
YPRIME(1)=K1*(((Qm/(1+(1/(Ke*(CO-((m*Y(1))/V))))))-Y(1))**2.0)    ! Pseudo 2nd
order model!     Freundlich Model
      A1 = m/V
      A2 = (Co-Y (1)*A1)
      A3 = A2** (onebyn)
      A4 = Kf*A3
      A5 = (A4-Y (1)) **2.0
      YPRIME (1) = K2*A5
      RETURN
      END
```

Appendix II

Model fitting to kinetic sorption data of phenolic compounds in single and multi-solute systems

II.1 Data fitting based on the modified pseudo-second order equation
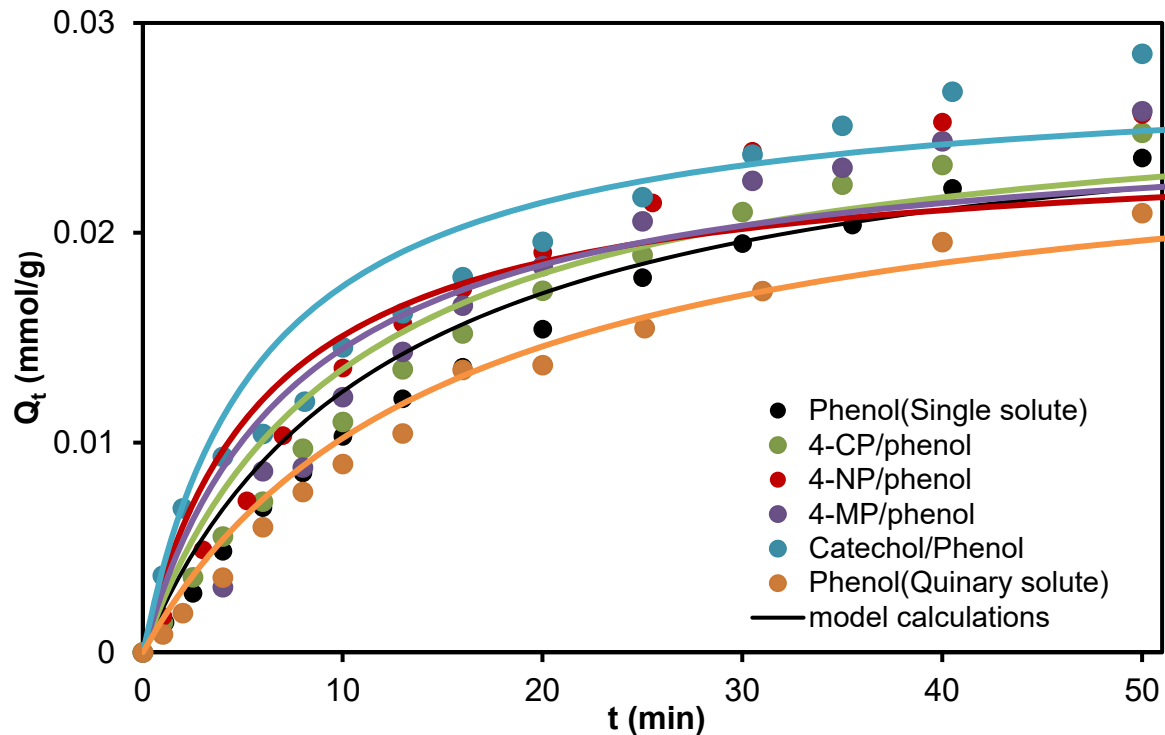
Figure II.1(a) Comparison of experimental data and model calculations for sorption kinetics of phenol by PEBA in single- and multi- solute systems based on the modified pseudo-second order equation
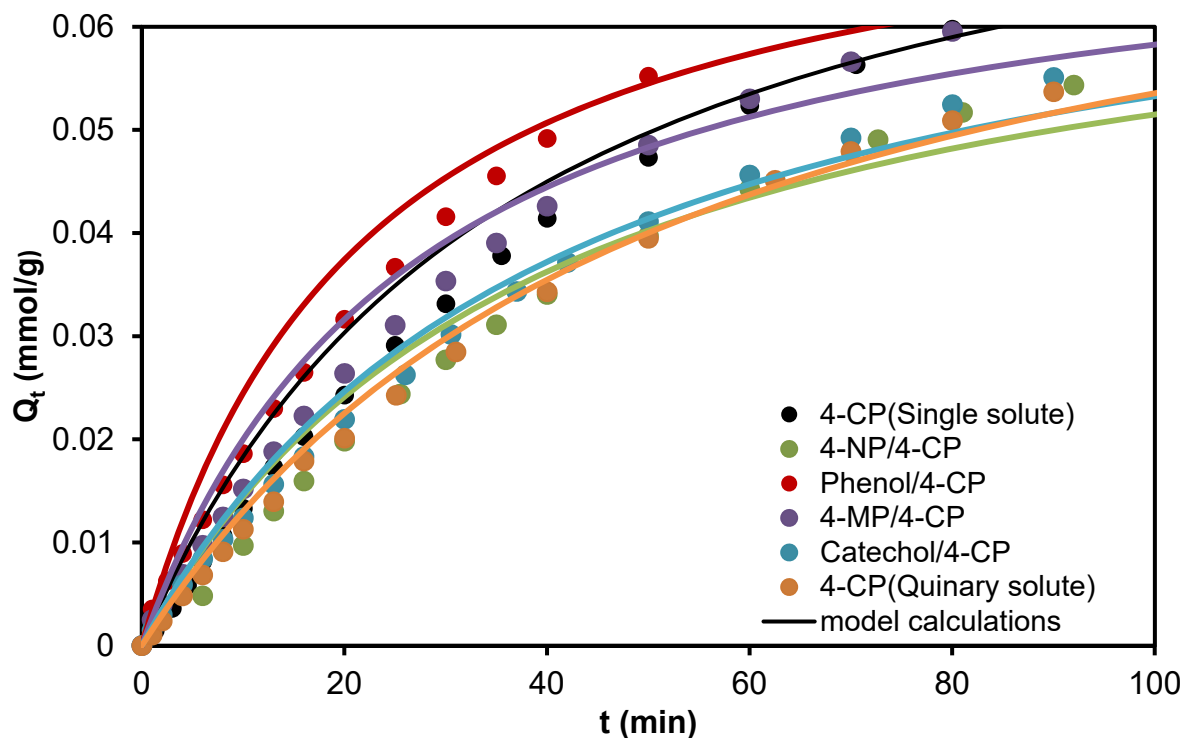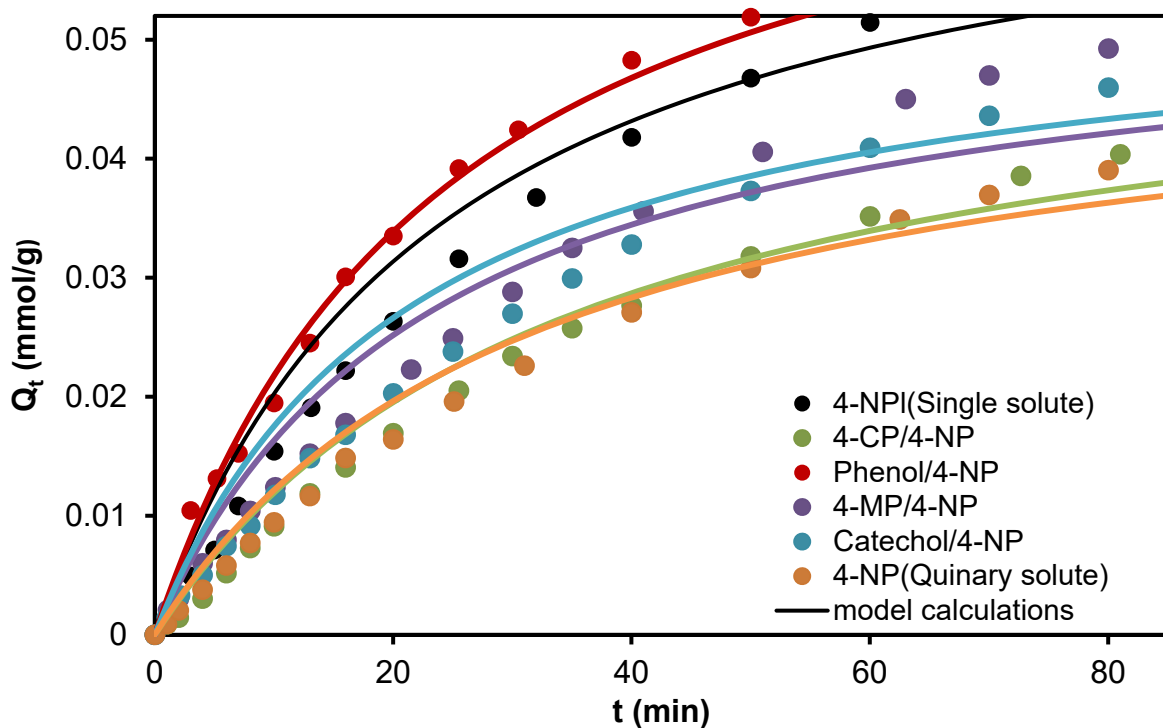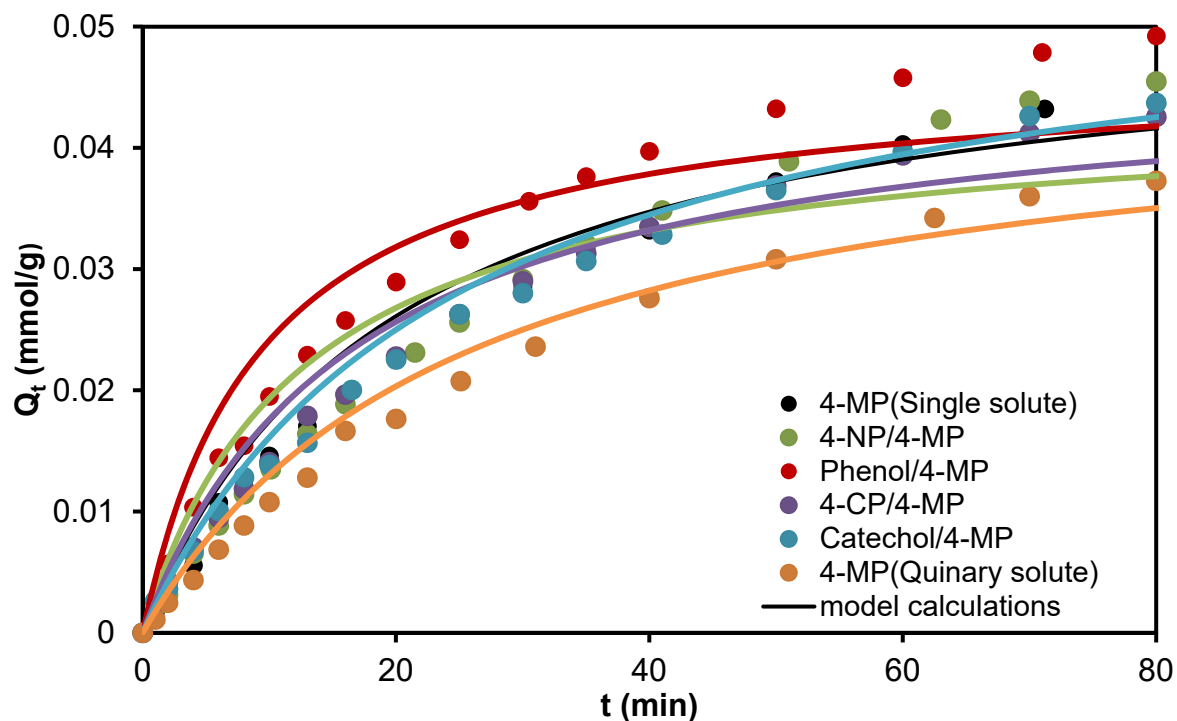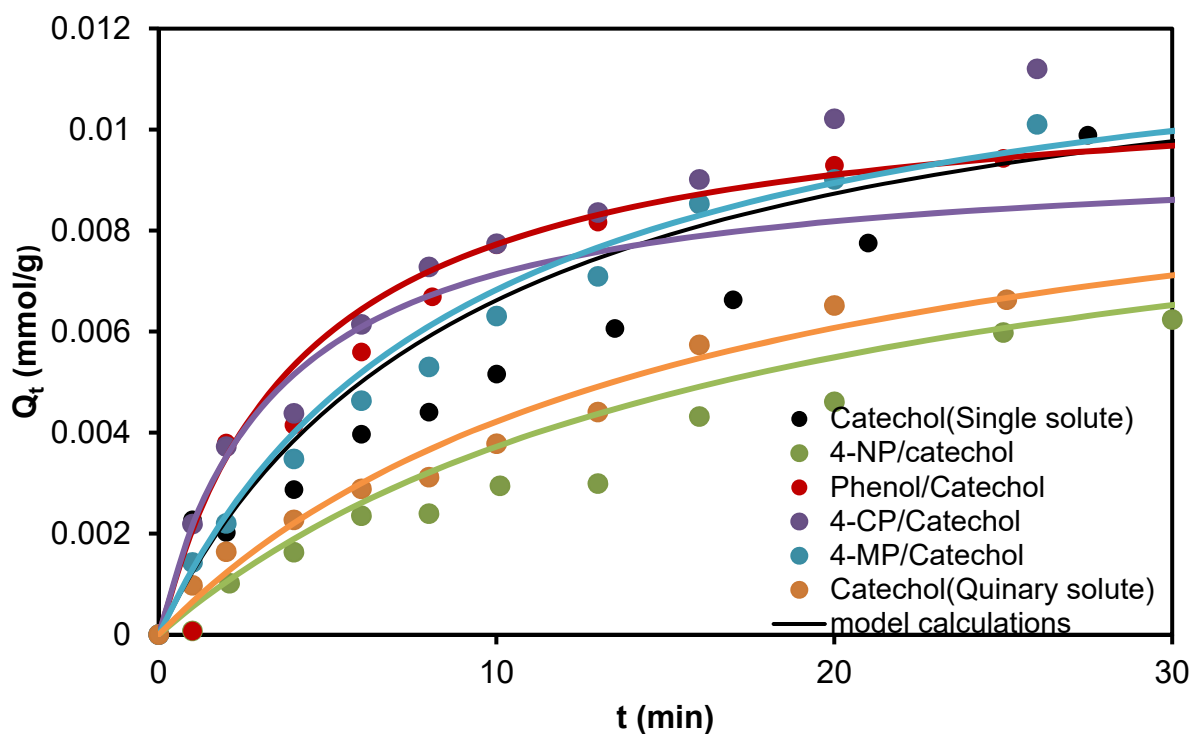
Figure II.1(b) Comparison of experimental data and model calculations for sorption kinetics of 4-CP by PEBA in single- and multi- solute systems based on the modified pseudo-second order equation

Figure II.1(c) Comparison of experimental data and model calculations for sorption kinetics of 4-NP by PEBA in single- and multi- solute systems based on the modified pseudo-second order equation

Figure II.1(d) Comparison of experimental data and model calculations for sorption kinetics of 4-MP by PEBA in single- and multi- solute systems based on the modified pseudo-second order equation

Figure II.1(e) Comparison of experimental data and model calculations for sorption kinetics of catechol by PEBA in single- and multi- solute systems based on the modified pseudo-second order equation

276

II.2 Data fitting based on the internal diffusion model (Eq. (4.7))
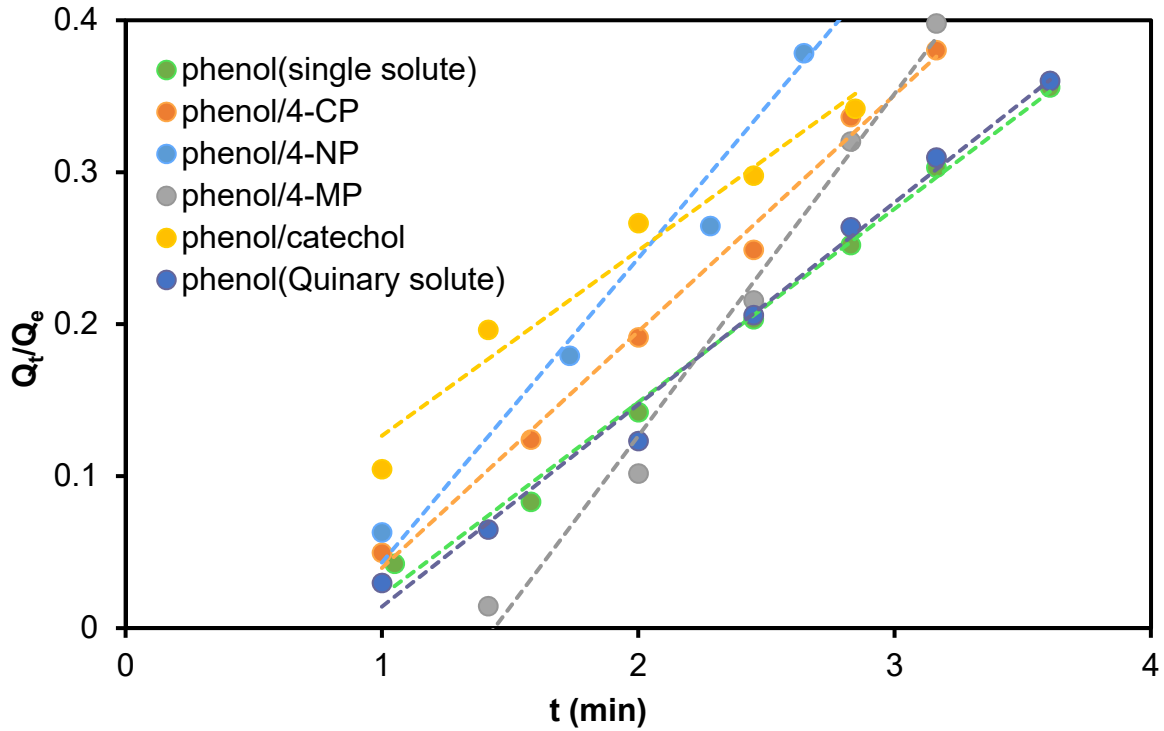
Figure II.2(a) Plots of Q_t/Q_e vs. t for sorption of phenol by PEBA in single- and multi-solute systems
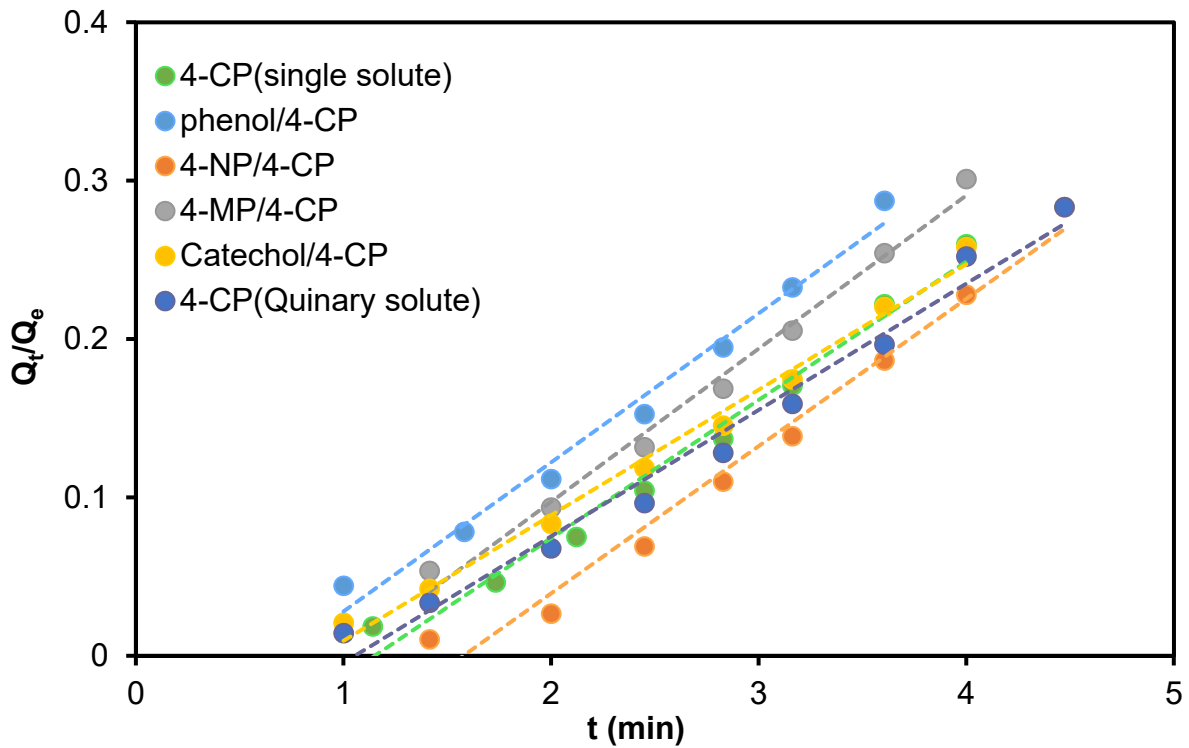
Figure II.2(b) Plots of Q_t/Q_e vs. t for sorption of 4-CP by PEBA in single- and multi-solute systems
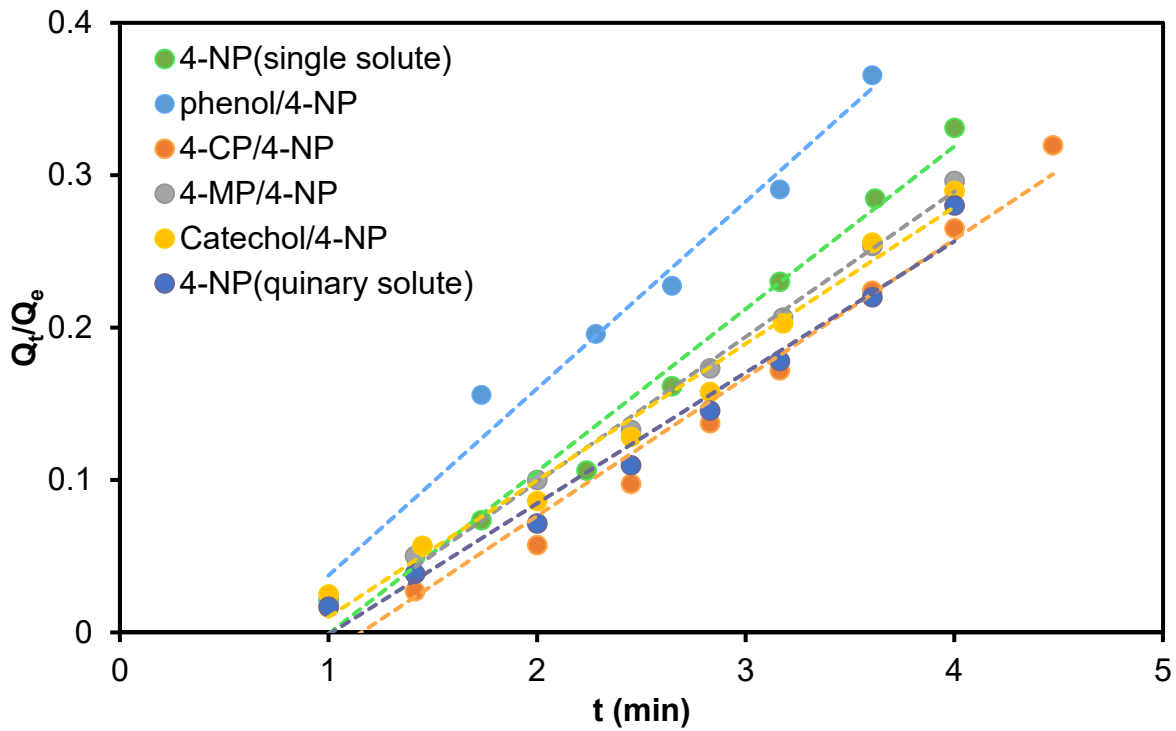
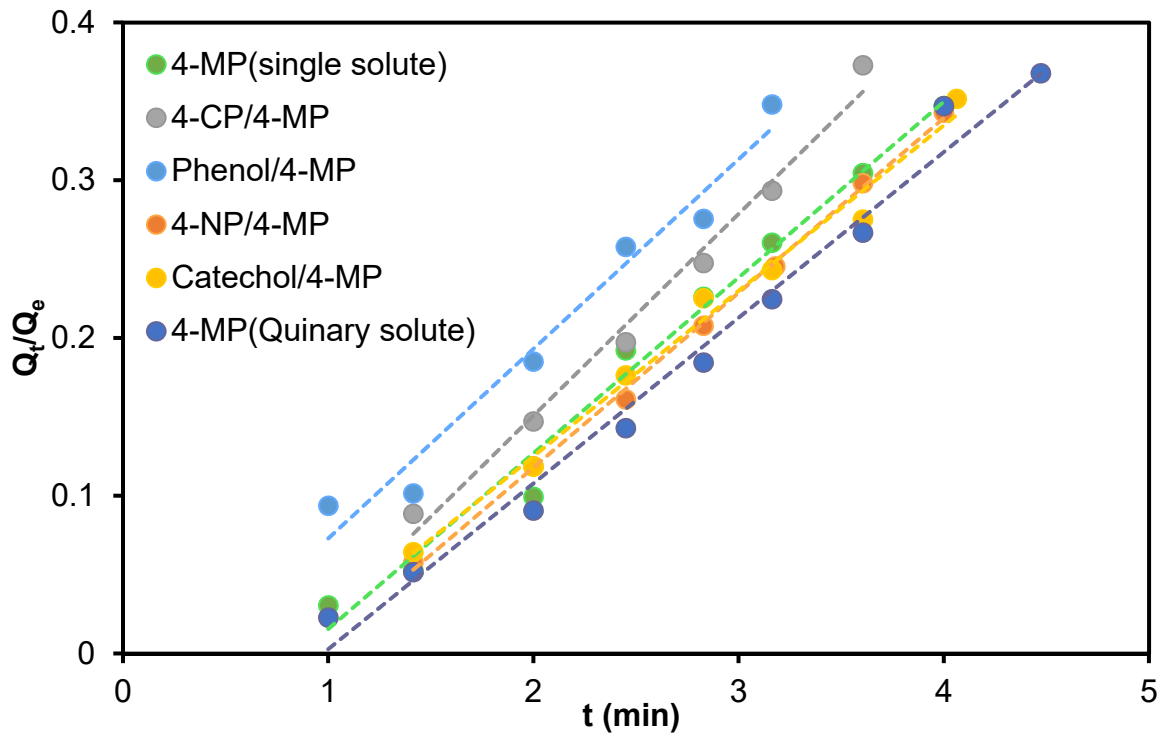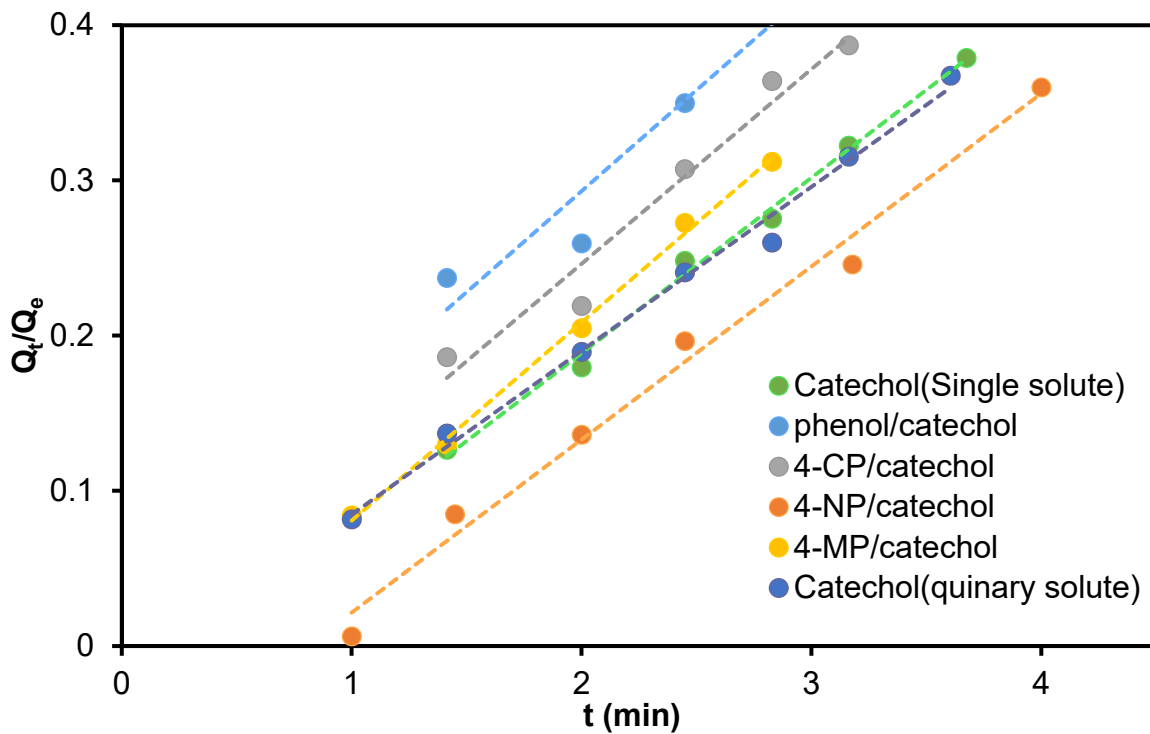Figure II.2(c) Plots of Q_t/Q_e vs. t for sorption of 4-NP by PEBA in single- and multi-solute systems

Figure II.2(d) Plots of Q_t/Q_e vs. t for sorption of 4-MP by PEBA in single- and multi-solute systems

Figure II.2 (e) Plots of Q_t/Q_e vs. t for sorption of catechol by PEBA in single- and multi-solute systems
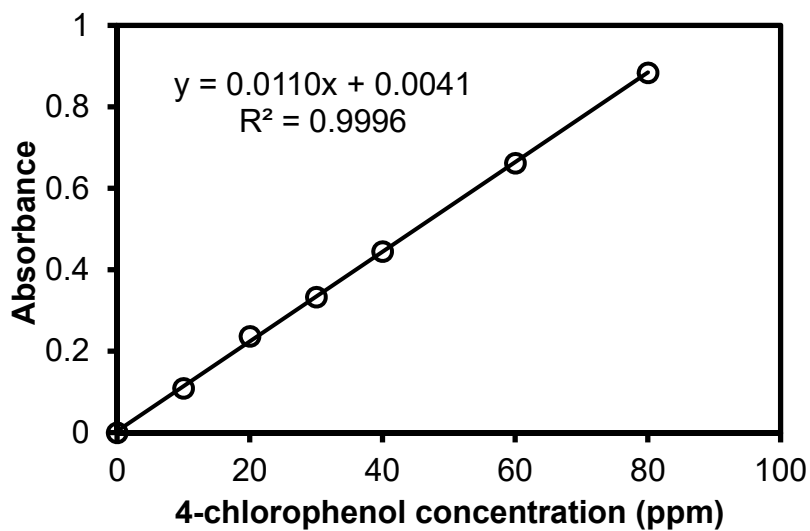
Appendix III

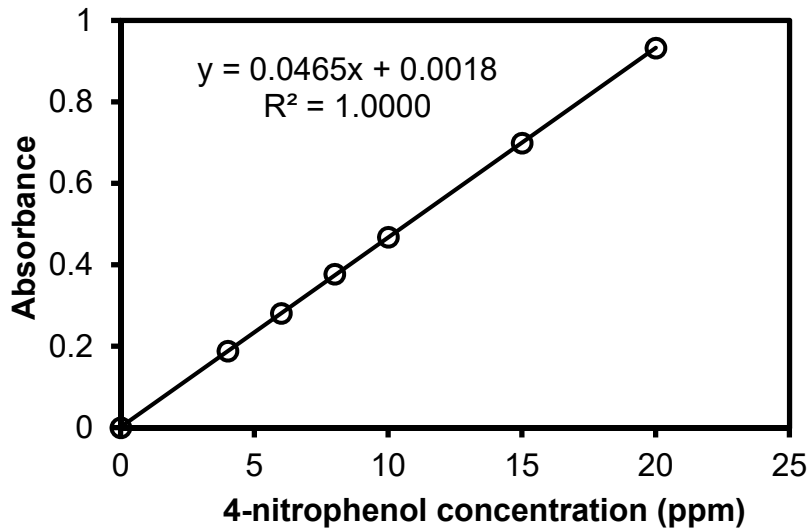# Calibration curves for determining concentration of phenolic compounds in water
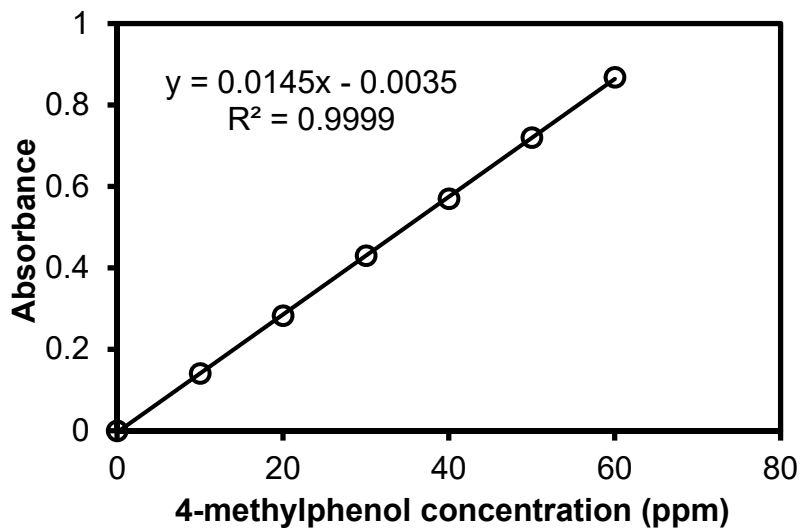
Calibration of phenol standard aqueous solutions

Plot of Absorbance vs Phenol concentration (ppm). $y = 0.0143x - 0.0070$, $R^2 = 0.9996$
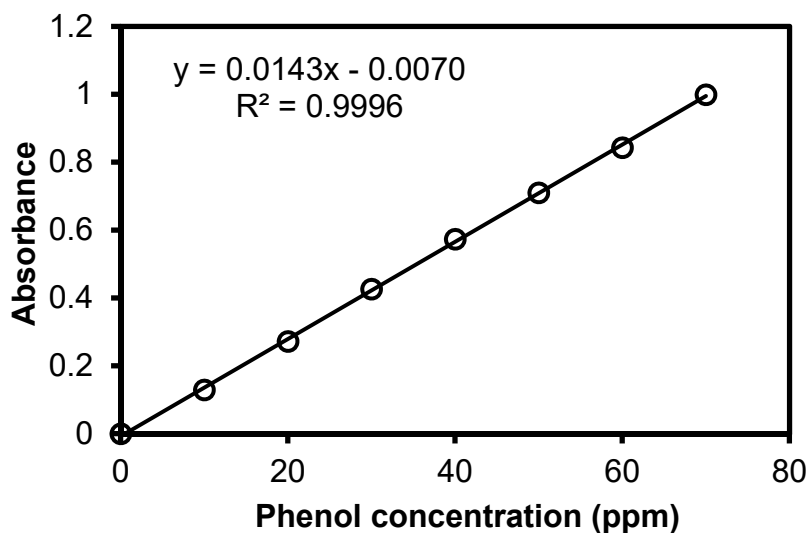
Calibration of 4-chlorophenol standard aqueous solutions

Plot of Absorbance vs 4-chlorophenol concentration (ppm). $y = 0.0110x + 0.0041$, $R^2 = 0.9996$

Calibration of 4-nitrophenol standard aqueous solutions

$y = 0.0465x + 0.0018$
$R^2 = 1.0000$

(Absorbance vs. 4-nitrophenol concentration (ppm))

Calibration of 4-methylphenol standard aqueous solutions

$y = 0.0145x - 0.0035$
$R^2 = 0.9999$

(Absorbance vs. 4-methylphenol concentration (ppm))

Calibration of catechol standard aqueous solutions

$y = 0.0198x - 0.0095$
$R^2 = 0.9995$

Absorbance

Catechol concentration (ppm)
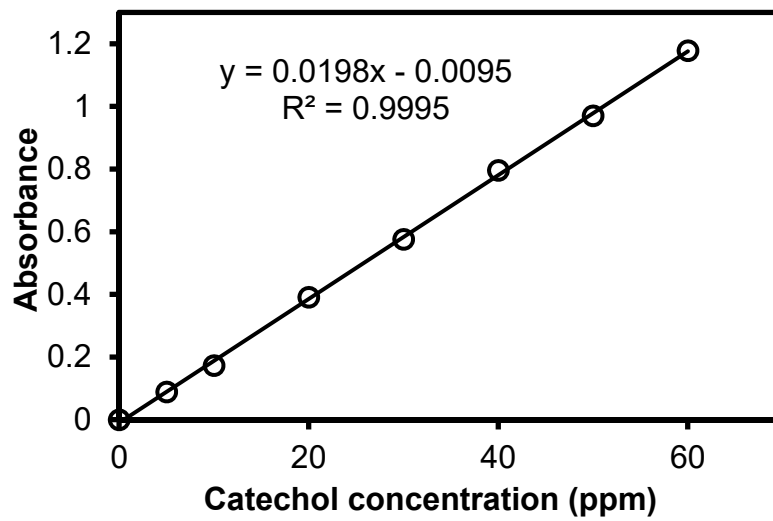
Appendix IV

An example of HPLC chromatogram of multi-phenolic compounds in liquid solutions
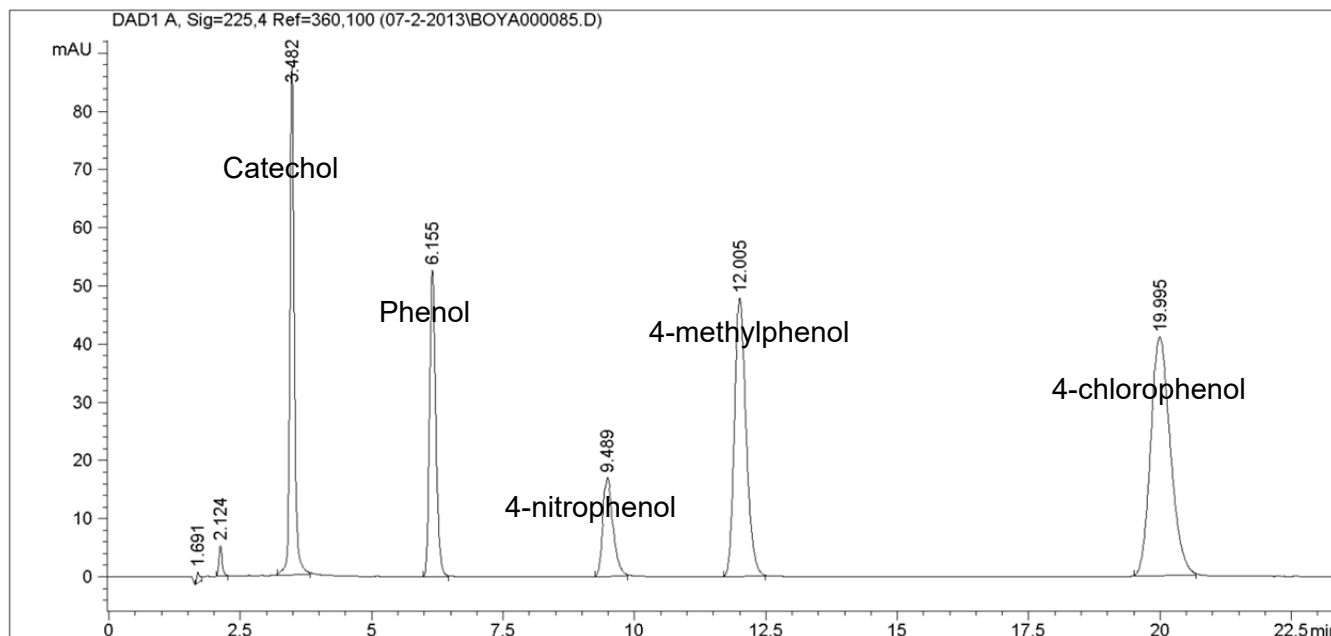
Operating conditions:

Mobile phase: 40% methanol and 60% water

Flow rate: 1.0 mL/min

Sample volume: 5 μL

Column temperature: 22°C

The detector wavelength: 225 nm.

Concentration of each phenolic compound in the solution: 100 ppm